NI

NASA CR- 165166

EDR 10361

EXPERIMENTAL DETERMINATION OF UNSTEADY BLADE ELEMENT AERODYNAMICS IN CASCADES

TRANSLATION MODE CASCADE FINAL REPORT
VOLUME II

By
R.E. Riffel and M.D. Rothrock

DETROIT DIESEL ALLISON
DIVISION OF GENERAL MOTORS CORPORATION
INDIANAPOLIS, INDIANA 46206

Prepared For

NATIONAL AERONAUTICS AND SPACE ADMINISTRATION

DECEMBER 1980

NASA LEWIS RESEARCH CENTER

CONTRACT: NAS3-20055

EXPERIMENTAL DETERMINATION OF UNSTEADY BLADE ELEMENT AERODYNAMICS IN CASCADES

TRANSLATIONAL MODE CASCADE FINAL REPORT
VOLUME II

By
R. E. Riffel and M. D. Rothrock

DETROIT DIESEL ALLISON
DIVISION OF GENERAL MOTORS CORPORATION
INDIANAPOLIS, INDIANA 46206

Prepared For
NATIONAL AERONAUTICS AND SPACE ADMINISTRATION

DECEMBER 1980

NASA LEWIS RESEARCH CENTER
CONTRACT: NAS3-20055

TABLE OF CONTENTS

LIST OF ILLUSTRATIONS

LIST OF ILLUSTRATIONS (continued)

LIST OF ILLUSTRATIONS (continued)

LIST OF TABLES

I. SUMMARY

A two-dimensional five bladed cascade of harmonically oscillating airfoils was designed to model a near-tip section from a rotor which was known to have experienced supersonic high back pressure bending mode flutter. This five-bladed cascade had a solidity of 1.52 and a setting angle of 0.9 rad (51.7^{0}) from axial. This report contains the documentation of the data obtained during the testing, and the correlation of the time unsteady data with an appropriate state-of-the-art analysis. A description of the aerodynamic and mechanical design of the research hardware is also included.

The translational mode cascade airfoil was modeled from the 86.3% span section of the second stage of the NASA Two-Stage Fan. The cascade was tested over a range of static pressure ratios between 1.065 and 1.680:1. These pressure ratios approximated the blade element operating conditions of the rotor along a constant speed line, which penetrated the torsional flutter boundary. The cascade inlet Mach number was 1.320.

In order to achieve the realistic reduced frequency level of 0.15, and to maximize the airfoil translational amplitude, unique airfoils were fabricated from graphite/epoxy composite material, with hollow steel trunnions attached at the 50% chord location. Translational excitation forces were imparted to tuned spring bars via computer-controlled electromagnetic drivers. These spring bars were attached to both of the airfoil's trunnions to ensure a two-dimensional mode shape.

Each test program involved three distinct phases during which the center airfoil was replaced with a particular instrumented airfoil. The first or steady-state aerodynamic phase utilized a static pressure tap airfoil. This was followed by the time variant aerodynamic testing with an airfoil instrumented Kulite dynamic pressure transducers. The third and final phase involved studying the regions of flow separation on the airfoil using surface-mounted heated film gages.

This report completes the experimental test program for the NASA II translation cascade as described under Task II of Contract NAS3-20055. The results of this program are summarized in the following:

- Provided fundamental quantitative time variant data at realistic reduced frequency levels for cascade being driven in the translational mode

- Examined effect of cascade loading on unsteady aerodynamic data

- Provided cascade stability plots over a range of back pressures

- Verified usage of DDA's in-house supersonic flutter analysis at low back pressures

- Verified usage of NASA strong in-passage shock unsteady flow code at high back pressures

II. INTRODUCTION

The advent of the high speed turbofan engine led to the discovery of a new type of blading instability--supersonic flutter. This instability is a self-excited vibration of the airfoils, which are operating in a uniform supersonic relative inlet flow field. At these high operating speeds a region of supersonic unstalled torsional flutter is encountered in the low back pressure portion of the compressor map. In addition, a region of supersonic high back pressure bending flutter is found in the moderate to high back pressure portion of the compressor map. To avoid these instabilities during the design phase it becomes necessary to calculate the time-variant pressure distributions on harmonically oscillating airfoils. The designer can use this information combined with structural damping to accurately predict the flutter boundaries. The generally used calculation procedure assumes an inviscid supersonic flow with a subsonic axial component through a differential radial height fan stage. This differential fan stage is then developed into a two-dimensional rectilinear cascade of zero thickness flat plates executing small harmonic oscillations.

DDA has pioneered the concept of investigating fundamental blade instability mechanisms through the use of computer-controlled, time-variant, supersonic, rectilinear cascades to obtain time unsteady pressure data. These data have provided a reference for correlation studies using appropriate state-of-the-art analyses, and have pointed out necessary refinements to the analyses. This program has made use of the aforementioned experience to provide time variant cascade aeroelastic data pertaining to supersonic flutter at reduced frequencies and aerodynamic loading levels in both the torsional and the translational mode of vibration.

III. HARDWARE DESCRIPTION

CASCADE AIRFOIL DESIGN

The translational mode cascade airfoil was modeled from a multiple circular arc blade element located at 83.3% span on the second stage rotor of the NASA Two-Stage Fan[(1)*]. The reference blade element was modified geometrically to account for the lack of radius change and streamline convergence in the two dimensional cascade test section. This geometric modification has been previously described in the torsional mode final report[(2)]. The blade element section and the resulting cascade airfoil section data comparison is included in Table I. The cascade airfoil has a 7.62 cm (3.00 in.) chord and a 7.62 cm (3.00 in.) span, and its profile is illustrated in Figure 1.

The requirement for the translational mode cascade harmonic oscillation was such that its reduced frequency value, k ($k = wc/2v$, where w is the frequency of oscillation, c is the airfoil chord, and v is the inlet relative velocity) be approximately equal to that exhibited by the subject rotor. The rotor test value of reduced frequency was 0.15 during supersonic high back pressure bending mode flutter. The requirements of the translational mode drive system was that it be capable of producing a two-dimensional rigid body motion, while forcing the airfoil at the specified frequency over a range of interblade phase angles. The system was also to produce reasonable amplitudes so that measurable time unsteady pressure would be created. A composite graphite/epoxy material was selected for airfoil fabrication to meet these requirements. The material features included low inertia, high modulus to density (E/ρ) ratio, and also the capability to embed the appropriate aerodynamic instrumentation into the surface during fabrication.

---

*Numbers are references which are listed at the end of this volume.

Table I.

Design data comparison between NASA Two-Stage Fan second stage rotor blade element and resulting cascade airfoil.

Velocity Diagram Data

	Rotor	Cascade
Inlet Mach	1.245	1.245
Exit Mach	0.744	0.744
Inlet Air Angle, rad	1.023 (58.61^{o})	.995 (57.05^{o})
Exit Air Angle, rad	.891 (51.06^{o})	.928 (53.15^{o})
Diffusion Factor	0.465	0.455
$\Delta P_S/Q$	0.411	0.411
Turning	.132 (7.55^{o})	.068 (3.90^{o})

Blading Design Data

	Rotor	Cascade
Inlet Metal Angle, rad	.961 (55.05^{o})	.933 (53.44^{o})
Exit Metal Angle, rad	.778 (44.58^{o})	.821 (47.05^{o})
Inflection Angle, rad	.936 (53.63^{o})	.933 (53.43^{o})
Net Camber, rad	.183 (10.47^{o})	.112 (6.39^{o})
Forward Camber, rad	.025 (1.42^{o})	.0001 (0.01^{o})
Rear Camber, rad	.158 (9.05^{o})	.111 (6.38^{o})
Meanline Incidence, rad	.056 (3.20^{o})	.063 (3.59^{o})
Suction Surface Incidence, rad	.028 (1.60^{o})	.029 (1.68^{o})
Meanline Deviation, rad	.107 (6.10^{o})	.107 (6.10^{o})
Setting Angle, rad	.899 (51.50^{o})	.902 (51.70^{o})
Solidity	1.512	1.516
Chord	2.10	3.00
Thickness/Chord	.0376	.0376
LER/Chord	.0028	.0028
TER/Chord	.0028	.0028
TMAX/Chord	.602	.602
Inflection Location	.451	.451
Min A/A*	1.037	1.037

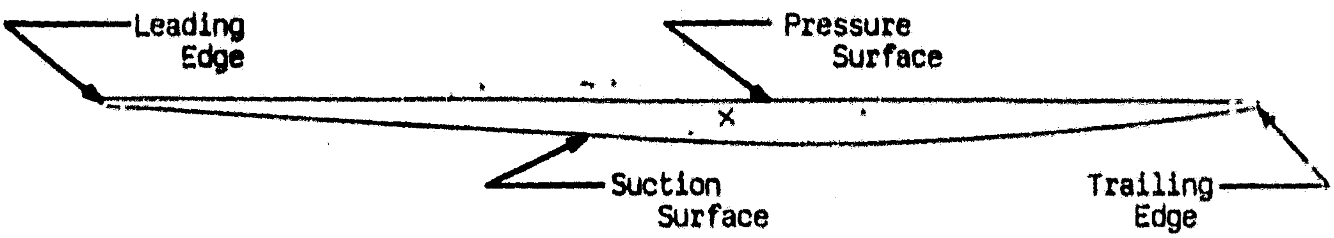

Figure 1. NASA II translation airfoil profile schematic.

The airfoils were fabricated from Hercules 3501-AS-5 pre-impregnated graphite tape wrapped with an outer layer of Kevlar cloth, and injected with an epoxy resin under pressure into a booking mold. The graphite fiber orientation was controlled to bext meet stress requirements while maintaining a low density and a high modulus of elasticity. The orientations used for fabrication were alternating layers of 0 rad, $\pi/2$ rad and $\pm\ \pi/4$ rad (0^0, 90^0, and $\pm 45^0$) to the torsional axis of the airfoil. Hollow steel (AMS 5643) trunnions were attached to the composite airfoils at mid-chord. Graphite chips and an epoxy fill were used in the trunnion caps to provide strength at the airfoil-trunnion interface. The splines located on the trunnion were used for mounting and to resist torsional displacement.

In order to maintain the composite material properties and airfoil surface contour, the use of nonconventional instrumentation techniques were employed during airfoil fabrication. Twenty 0.041 cm (0.016 in.) diameter hypodermic tubes with 0.010 cm (0.004 in.) wall thickness were embedded in the steady-state airfoil by relieving the laminate during layup. Wiring harnesses to accommodate twelve dynamic pressure transducers and ten heated film gages were also embedded into their respective airfoils during fabrication. The ends of the lead wires were exposed during installation of the respective sensor by local spot-facing of the airfoil surface.

TRANSLATIONAL MODE DRIVE SYSTEM DESIGN

The desired frequency of oscillation for equal values of reduced frequency between the cascade and the rotor was 250 Hz. A translational mode drive system incorporating parallel spring bars was tuned to this frequency utilizing the bench rig shown in Figure 2. The airfoil was positioned with the two flexible spring bars via a "squirrel cage" support, which was attached to splines on the airfoil trunnion. The splines ensured torsional restraint with no slippage of airfoil setting angle. The airfoil trunnion splines were positioned axially by the driver arm which is piloted and clamped to the trunnion with an attached spacer tube. Translational excitation forces were supplied to each trunnion through the driver arms from the computer controlled electromagnets. The electromagnets were excited at the airfoil drive system natural frequency. Strain gages mounted on the spring bars exhibited excellent sensitivity to the translational displacement. Five of these blade driver systems were then mounted in plexiglas windows for schlieren flow visualization and the entire assembly in- stalled in the cascade test section.

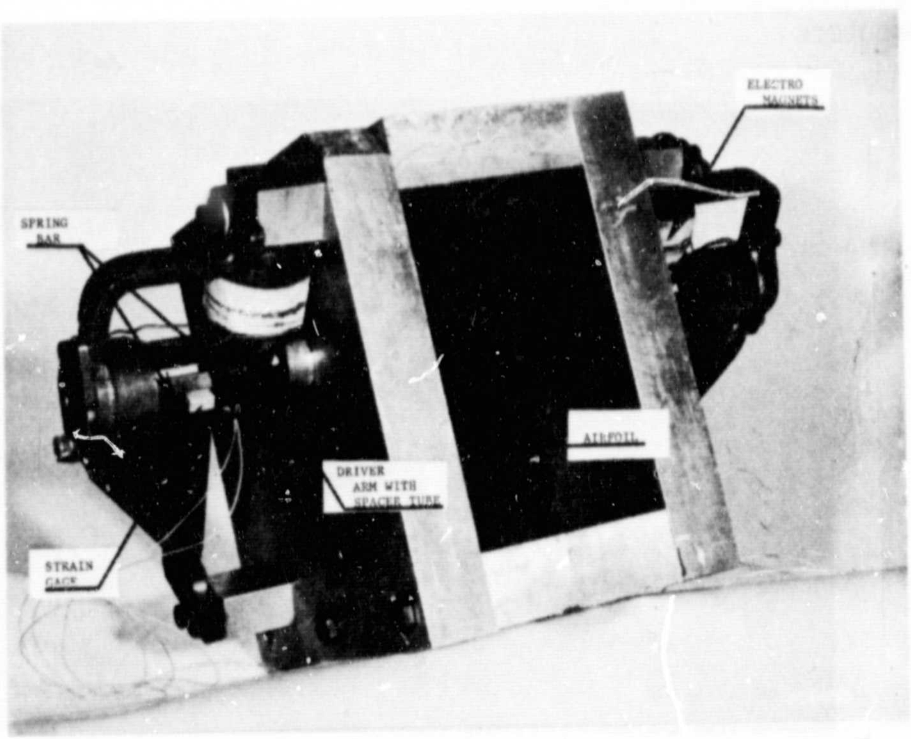

Figure 2. Translational mode drive system bench rig.

IV. TEST FACILITY

The DDA rectilinear cascade facility shown in Figure 3 was conceived and built as a research tool to evaluate the aerodynamic characteristics of compressor and turbine blade sections. The facility is a continuous flow, nonreturn, pressure-vacuum type wind tunnel with the test section evacuated by means of two primary steam ejectors. Up to 4.54 kg/s (10 lbm/sec) of filtered, dried, and temperature-controlled air can be supplied. A more detailed description of the cascade facility is included in the torsional mode final report(2).

Major features of the rectilinear cascade facility include:

- o Continuous operation for extended time periods
- o Mechanized test section for rotating a cascade of airfoils with the tunnel in operation
- o Schlieren optical system for visual observation and photography of the cascade in operation
- o Endwall and sidewall boundary layer control systems
- o Sophisticated instrumentation system centered on laboratory-size digital computers

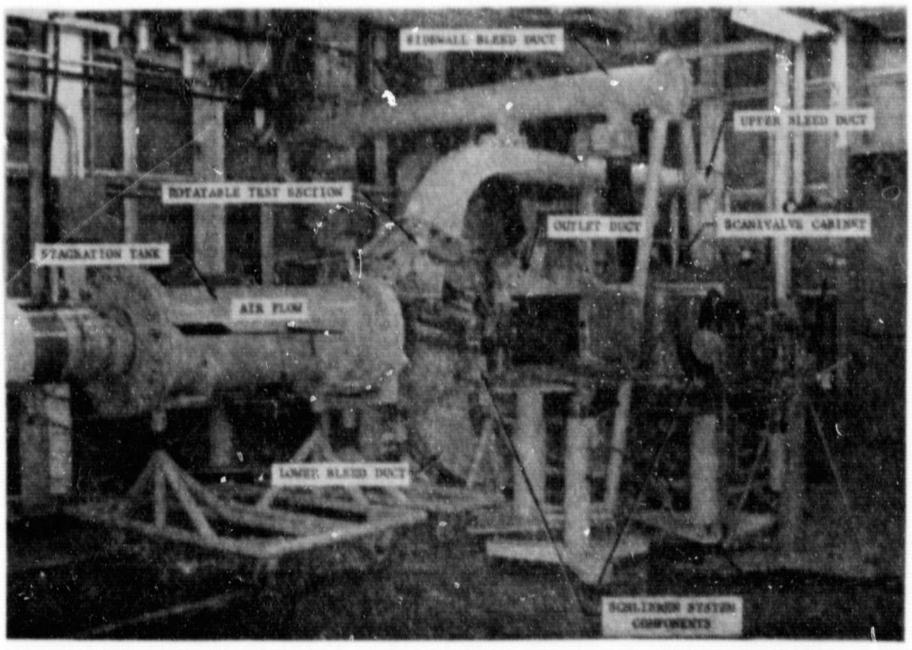

Figure 3. DDA rectilinear cascade facility.

The NASA translation cascade, including the boundary layer control system, is shown schematically in Figure 4. The cascade was equipped with adjustable upper and lower exit tailboards, which were porous with a 50% open area. These tailboards were open to the exit plenum pressure level. The setting of the upper tailboard in conjunction with the application of atmospheric bleed in the upper splitter aft cavity was critical in setting the exit periodicity. The object was to produce an endwall which simulates the streamline of an infinite cascade at the operating pressure ratio.

The wind tunnel facility was equipped with a sophisticated instrumentation system centered around laboratory-size digital computers to provide rapid on-line data acquisition and reduction. The computer was used for control of instrumentation during both steady-state and dynamic testing, data acquisition, and data reduction. Peripheral equipment included a CRT terminal, an 80-column line printer, high-speed punch, high-speed punched-tape reader, X-Y digital plotter, magnetic disk storage unit with 2.5 x 10^6 word capacity, and 16-channel-100KHz analog to digital converter.

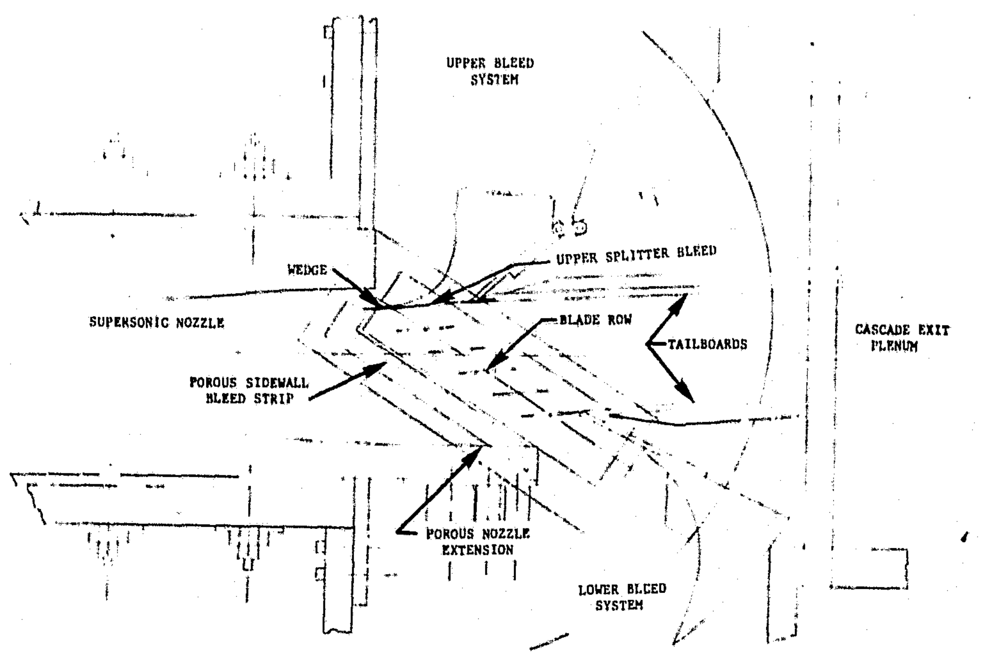

Figure 4. Schematic of cascade facility with NASA II translational cascade installed.

V. INSTRUMENTATION AND CALIBRATION

The instrumentation for this unsteady blade element cascade aerodynamics program was of prime concern. To make the proposed experiments meaningful, it was necessary to accurately measure in detail both time-steady and time-unsteady cascade flow parameters. In general, the instrumentation was selected to:

- o Define the steady cascade inlet and exit aerodynamics
- o Establish the airfoil surface steady pressure distributions
- o Establish the airfoil surface unsteady pressure distributions
- o Define the steady and unsteady shock wave patterns
- o Define regions of flow separation

This instrumentation is divided into the following two functional areas, with some overlap.

- o Steady-state aerodynamics instrumentation
- o Unsteady aerodynamics instrumentation

All instrumentation was designed and distributed in such a manner as to obtain meaningful data and minimize aerodynamic interference. Detailed calibrations were performed on the instrumentation to assure the attainment of exact quantitative data.

STEADY-STATE AERODYNAMIC INSTRUMENTATION

The objective of the steady-state testing was to quantitatively determine the details of the cascade steady flow field. The instrumentation was selected to accurately determine the cascade inlet and exit pressure, flow angle, and Mach number distributions as well as the blade surface static pressure distributions. The steady-state instrumentation was concerned with three basic flow regions: cascade inlet, cascade exit, and airfoil surface. A discussion of each region follows.

In the DDA rectilinear cascade facility, the cascade inlet flow field was established by means of a sharp-edged wedge positioned upstream of the cascade at the exit of the calibrated 1.3 Mach nozzle. The inlet flow direction was determined by the orientation of this wedge with respect to the nozzle exit flow field. The wedge boundary layer profile has been established experimentally and was accounted for in defining the inlet flow direction. Changes of the inlet flow field are made by rotating the cascade with respect to the fixed nozzle blocks. The inlet Mach number was established by expansion (Prandtl-Meyer) of the nozzle flow about the wedge. Using this procedure, the inlet flow field was defined employing the following instrumentation techniques.

The cascade inlet total temperature and total pressure were defined, based on measurements in the facility low velocity stagnation tank. The inlet flow angle was determined by the orientation of the wedge with respect to the nozzle flow, with the wedge boundary layer profile taken into account. The inlet Mach number was calculated based on the degree of expansion of the flow. The inlet static pressure was based on the isentropic flow relations. Cascade sidewall static pressure taps were located immediately upstream of the leading edge of each airfoil in the cascade and were used to verify the cascade inlet flow field and to quantitatively aid in establishing the cascade steady-state periodicity.

The cascade exit flow field properties were measured by means of a five-port conical probe. The probe had been previously calibrated over a range of Mach numbers between 0.35 and 1.80 at various angles of attack between ± 0.26 rad ($\pm 15^{\circ}$). The probe was mounted on a computer-controlled, three-axis traversing mechanism which was capable of traversing the complete cascade exit flow field. The tangential passage length was divided into 5% increments with discrete data taken at each increment over two complete passages downstream of airfoils #2 and #3 (instrumented airfoil). The calibrated probe performance permits the determination of flow parameters via measured pressures on the probe. A series of exit sidewall static pressure taps were located such as to

define the exit static pressure distributions across a minimum of two passages and were also located near the mid-passage position of each blade to help establish exit periodicity.

The blade surface static pressure distribution was determined during the ca cade steady-state testing phase with an airfoil instrumented with 20 surface static pressure taps - ten per surface -- as shown schematically in Figure 5. The chordwise locations are also presented in the figure. Twelve of these static taps, six per surface, were at identical locations to those of the Kulite dynamic pressure transducers.

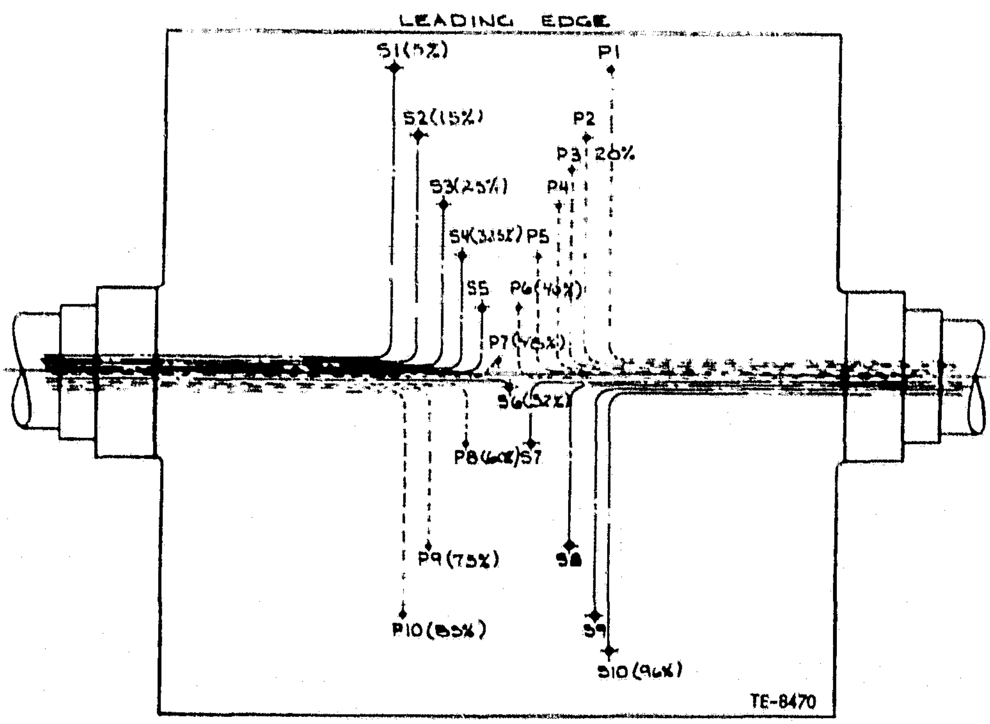

Figure 5. NASA II translation static tap airfoil schematic.

TIME VARIANT AERODYNAMIC INSTRUMENTATION

To achieve the program goal of producing fundamental experimental data to offer guidance in the development of analytical models for flutter prediction, detailed data had to be acquired and analyzed to establish the relationships existing between the airfoil motion and that of the surrounding air. The time-unsteady blade surface pressure distributions were of particular interest as they represented the physical driving force of the flutter phenomena. In addition to the unsteady pressure and blade motion measurements, instrumentation was also provided to detect such gross aerodynamic instabilities as boundary layer separation. In the following discussion, provisions for making the necessary unsteady aerodynamic measurements are outlined.

Kulite Semiconductor Products type XTL-1-190-25 thin-line design transducers were used to make the dynamic pressure measurements. Experience in the use of this type of transducer has been gained in DDA stationary and rotating cascade facilities. These high-response pressure transducers were flush mounted on the test airfoil at six chordwise locations staggered across the center 50% of the span on each surface of the airfoil. The distribution of the transducers is shown schematically in Figure 6. A thin, pliable coating of RTV over the transducer diaphragm was used to preserve the airfoil surface contour and minimize the aerodynamic disturbances.

To obtain quantitative data from the dynamic pressure measurements, it was necessary to provide not only a static calibration for the pressure transducers, but also an acceleration calibration. Both the static and acceleration calibrations were conducted with the transducers installed on the airfoil.

Prior to the actual acceleration calibration, the signal conditioners and associated electronics were calibrated at the same frequency level at which the test was conducted. The instrumented airfoil was then installed in the translational mode bench fixture, and a set of sensitivities relating amplitude to strain gage signal level were obtained for the spring bar strain gages. The

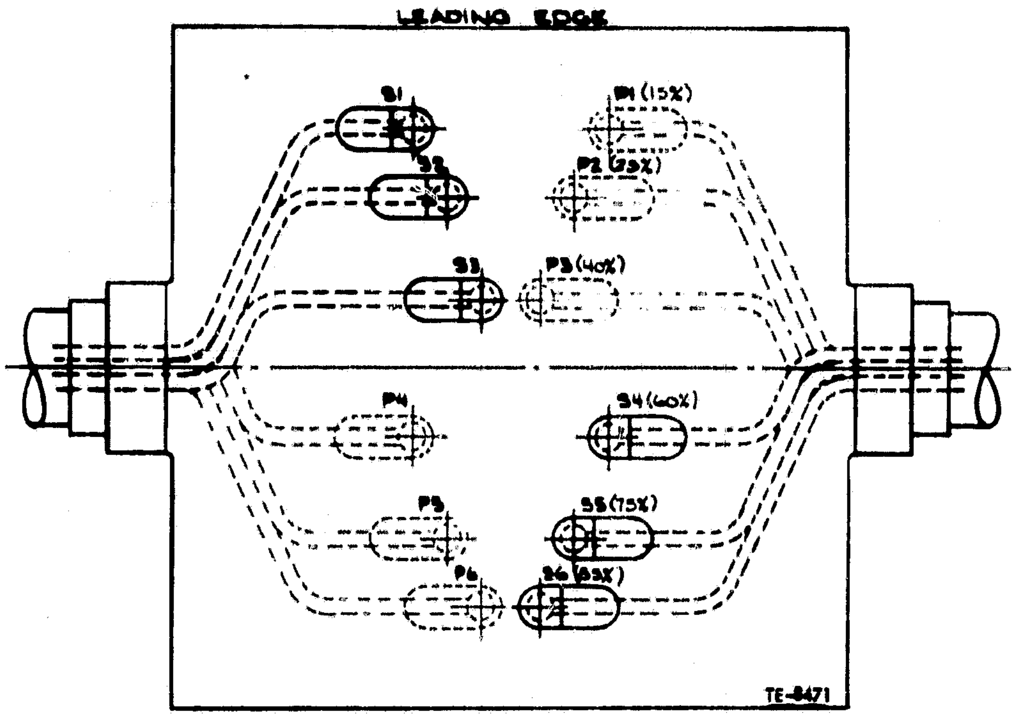

Figure 6. NASA II translation Kulite dynamic pressure instrumented airfoil schematic.

airfoil and bench rig were then installed in a controlled pressure chamber for the transducer calibrations. The Kulites were first calibrated for static pressure over a range of pressures between 2.0 and 10.0 psia, which is typical of their static operating conditions. The pressure in the vacuum chamber was controlled at a prescribed level using a Mensor quartz manometer-controller. The resulting Kulite static pressure sensitivities are presented in Table II.

Upon completion of the Kulite static calibration, the translational mode bench rig was tuned to the same frequency level as the blade experienced in cascade testing. This was done to ensure that the transducers were calibrated at the

Table II.

NASA II instrumented airfoil Kulite transducer static calibration sensitivity.

Kulite transducer	Number	Location percent chord	Sensitivity mv/kPa(mv/psi)
Pressure surface	1	15	0.645 (4.45)
	2	25	0.644 (4.44)
	3	40	0.683 (4.71)
	4	60	0.799 (5.51)
	5	75	0.666 (4.59)
	6	85	0.641 (4.42)
Suction surface	1	15	0.686 (4.73)
	2	25	0.718 (4.95)
	3	40	0.648 (4.47)
	4	60	0.580 (4.00)
	5	75	0.576 (3.97)
	6	85	0.658 (4.54)

same level of frequency and airfoil mode shape as it experienced in the cascade. The vacuum signals are then directly relatable to acceleration effects of the RTV/diaphragm or any strain related phenomena resulting from airfoil/transducer deformation. The Kulite signals were analyzed over a range of airfoil amplitudes corresponding to those encountered in testing. By knowing the translational displacement, that portion of the total signal due to acceleration/deformation was removed directly by simple vector subtraction.

As described in the Test Procedure, the time-dependent aerodynamic data was referenced to airfoil motion as determined from strain gage measurements. Blade-to-blade motion was also determined in this manner. Multiple use of strain gages provided for redundancy and the ability to check out the driver system operation. The strain gages were dynamically calibrated for blade motion using the following technique. The bench rig was assembled with a given blade, and its associated spring bar pair was instrumented with strain gages. This system was then tuned to the desired natural frequency. The computer was used to digitize and analyze the strain gage signals, printing out the peak voltage produced at each gage by the blade oscillations. The blade

amplitude was then determined using a vernier height-gage. The displacements were plotted against voltage to yield the gage factors for each strain gage.

Regions of flow separation were identified using surface-type heated film gages in conjunction with flow visualization techniques. Ten film gages were mounted at the locations shown in Figure 7. These gages were placed near mid-span in a staggered configuration to prevent aerodynamic interference with one another. The chordwise locations for these gages correspond to the chordwise locations of the first five Kulite pressure transducers. Film gage calibration was accomplished by installing the static tap instrumented airfoil in a low speed wind tunnel and mapping out the chordwise progression of the separation zone with increased incidence. This was accomplished by injecting alcohol back through the static pressure taps and observing its flow direction. Once this mapping procedure was finished the heated film airfoil was installed in the tunnel and the procedure repeated. The resulting ac and dc voltage levels of the heated film gage were recorded. For this instrumentation the voltage level is an indicator of the level of wall shear stress. The dc component is related to the mean level of wall shear stress and the fluctuating component is related to the fluctuations in the shear stress level. By assuming that a fully developed turbulent boundary layer exists, the following emperical relationship can be developed for the wall shear stress intensity parameter:

$$\frac{\sqrt{\overline{\tau'_w{}^2}}}{\tau_w} \qquad \frac{6.0E^2\sqrt{\overline{E'^2}}}{(E^2 - E_o^2)E}$$

where $\frac{\sqrt{\overline{\tau'_w{}^2}}}{\tau_w}$ = shear stress intensity parameter, E = dc voltage, E' = ac voltage, and E_o = zero flow voltage.

Flow visualization was used to aid in the evaluation of the unsteady aerodynamic data obtained throughout the test. Time-dependent schlieren flow visualization of the unsteady aerodynamic cascade phenomena was obtained with a high-speed movie camera.

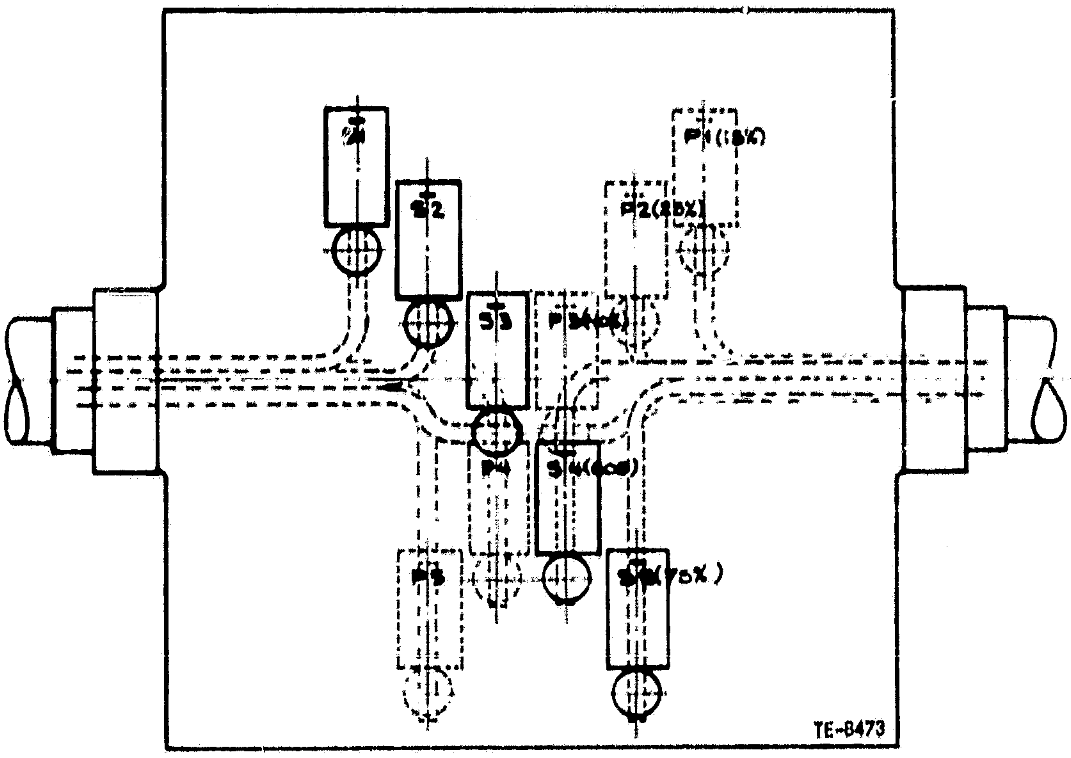

Figure 7. NASA II translation heated film gage airfoil schematic.

VI. EXPERIMENTAL TEST PROCEDURE

The translational mode cascade test procedures were designed to obtain valid two-dimensional steady and time-variant data and were based on the invaluable experience acquired by DDA in approximately seven years of time-unsteady experiments and ten years of steady flow supersonic cascade investigations. Three phases of test effort were performed for the cascade:

- o Steady state cascade investigation
- o Unsteady cascade investigation
- o Flow separation study

A description of these three phases follows:

STEADY STATE AERODYNAMIC INVESTIGATION

The objectives of the steady cascade testing were to establish a periodic steady-state cascade flow field and to obtain a complete definition of the cascade steady-state performance and the blade surface pressure distributions. The airfoil cascade was installed in the supersonic cascade facility with the airfoils in a fixed mode. The center airfoil in the cascade was instrumented with 20 static pressure taps as defined in the instrumentation plans.

Cascade periodicity was established, based on the leading edge sidewall static pressure tap measurements, the cone probe exit survey over the center two airfoil passages, and the schlieren flow visualization of the cascade operation. With the periodicity established, the steady performance of the cascade was measured at four specified steady operating points. These steady operating points were selected to best meet the test objectives of thoroughly defining the aerodynamic characteristics through the flutter boundary while maintaining a realistic distribution of cascade exit Mach number.

TIME VARIANT AERODYNAMIC INVESTIGATION

Upon completion of the steady cascade investigation for each task, the static tap instrumented airfoil (the center airfoil in the cascade) was replaced with the one instrumented with 12 flush-mounted Kulite pressure transducers. At each of the steady operating points, the cascade periodicity was reestablished. The airfoil drive systems were then made operational, and the unsteady cascade investigation initiated. Six interblade phase angle values were investigated for each steady point. For each of the unsteady data points, the motion of each airfoil in the cascade was measured, and once an interblade phase was established, the pressure signals were recorded on magnetic tape along with the reference strain gage signal. These taped pressure signals were analyzed as detailed in Data Reduction/Correlation section.

FLOW SEPARATION INVESTIGATION

The flow separation study followed the completion of the steady and unsteady cascade investigation. This involved replacing the Kulite airfoil in the cascade with the previously described heated film gage instrumented airfoil. The four other airfoils in the cascade were untouched.

With the airfoils in a stationary mode, steady operating conditions were established at the two unsteady operating points wherein the aerodynamic work per cycle had a maximum and a minimum value, determined from the previously described unsteady cascade data. At these operating points the heated-film gage signals and strain gage signals were recorded and qualitatively analyzed to determine any relationships between the boundary layer behavior and the blade motion.

VII. DATA REDUCTION/CORRELATION

Described herein are summaries of the data reduction procedures and data presentations for both the time steady and the time unsteady data. A brief discussion of the theoretical technique used for correlation purposes is also included.

STEADY-STATE AERODYNAMIC DATA

The steady state data reduction procedures which are incorporated in the DDA wind tunnel on-line instrumentation system were used to analyze data from the translational mode compressor cascade. The supersonic wind tunnel on-line instrumentation system yielded thirteen pages of computer print-out describing the cascade steady performance for each test condition. Identification of the first stage print out is shown in Figure 8. On this page of the print-out following the title lines, four entries appear which describe the test point operating conditions; cascade inlet Mach number, cascade ideal static pressure ratio, the cascade blade behind which the conical probe data was taken, and the conical probe axial location downstream of the blade row.

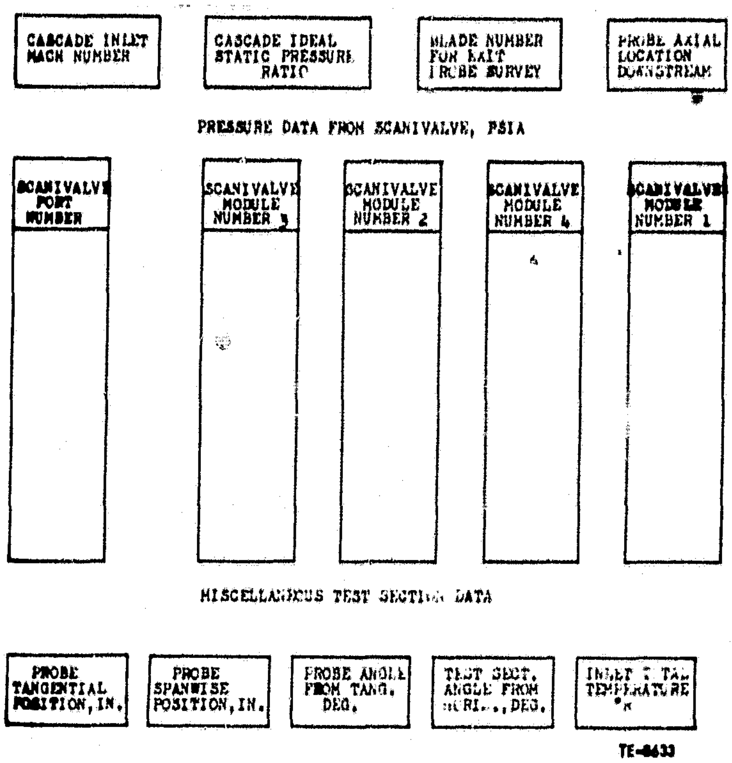

Figure 8. Computer print-out identification--Scanivalve pressure data.

The second entry on the first page of print-out presents a listing of the pressures measured on the four Scanivalves. The first seven ports of each Scanivalve are used for reference calibration pressures with alternate ports thereafter connected to a vacuum source to eliminate transducer hysteresis and minimize pneumatic settling time. From these pressures, the cascade performance is determined.

The last entry on the first page of the print-out presents miscellaneous test section data including the conical probe position in the exit flow field, test section angular position, and the wind tunnel total temperature.

The first entry on the second page of the print-out presents the nozzle exit flow field properties.

The second entry on the second page is the wedge and blade inlet flow parameters determined from the sidewall static pressure taps located in the sidewall ahead of the wedge and each blade.

The last entry on the second page describes the flow properties across the sharp leading edge wedge which is used to expand or compress the nozzle exit flow to establish the cascade inlet Mach number and flow direction.

The first entry on the third page of the print-out consists of two lines describing the cascade physical design parameters.

The last entry on the third page describes the cascade inlet flow field conditions. Identification of the cascade inlet parameters is presented in Figure 9.

The entry on the fourth page of the computer print-out as identified in Figure 10 is the cascade ideal performance based on sidewall static pressures. Included is a listing of the pressures presented on the first page of the print-out for the sidewall static pressure taps. From these pressures, a mean

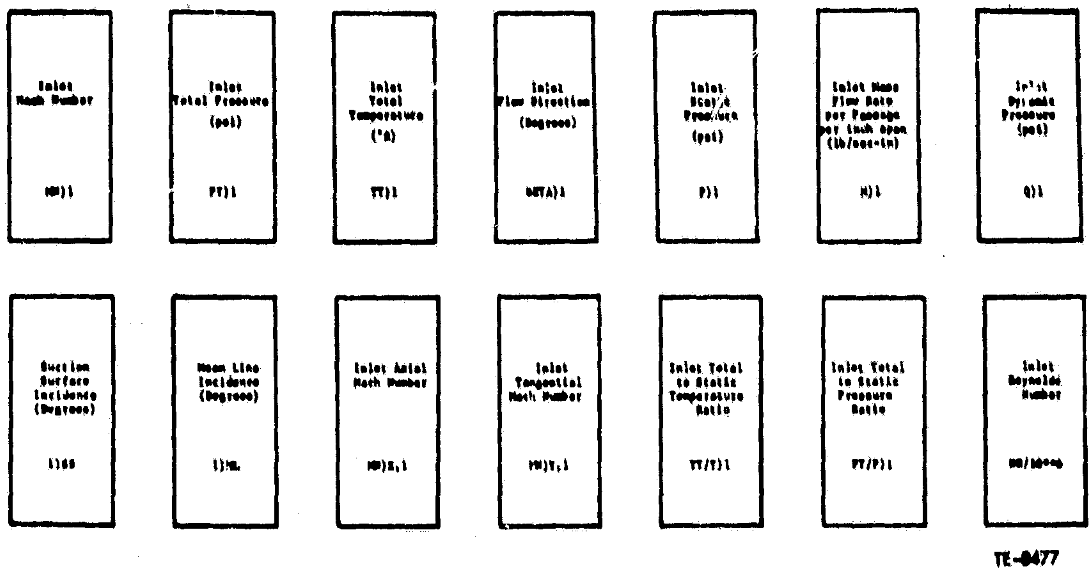

Figure 9. Computer print-out identification - cascade inlet conditions.

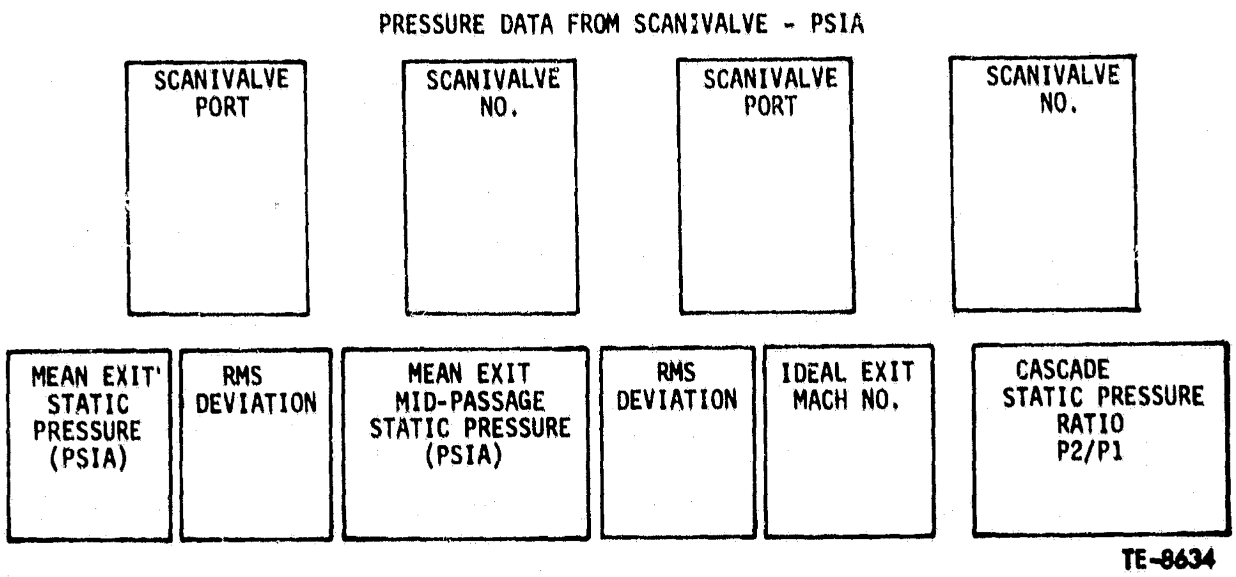

Figure 10. Computer print-out identification - cascade ideal performance.

exit static pressure and RMS deviation are calculated along with the same parameters for the mid-passage static pressure taps. The cascade ideal exit Mach number and ideal static pressure ratio are determined from the mean exit static pressure.

The fifth page of the computer print-out describes the instrumented blade parameters. The first entry presents the surface static pressure distribution on the airfoil along with associated columns describing local performance characteristics and static tap locations in terms of percent chord. Figure 11 provides identification of the entries on the fifth page.

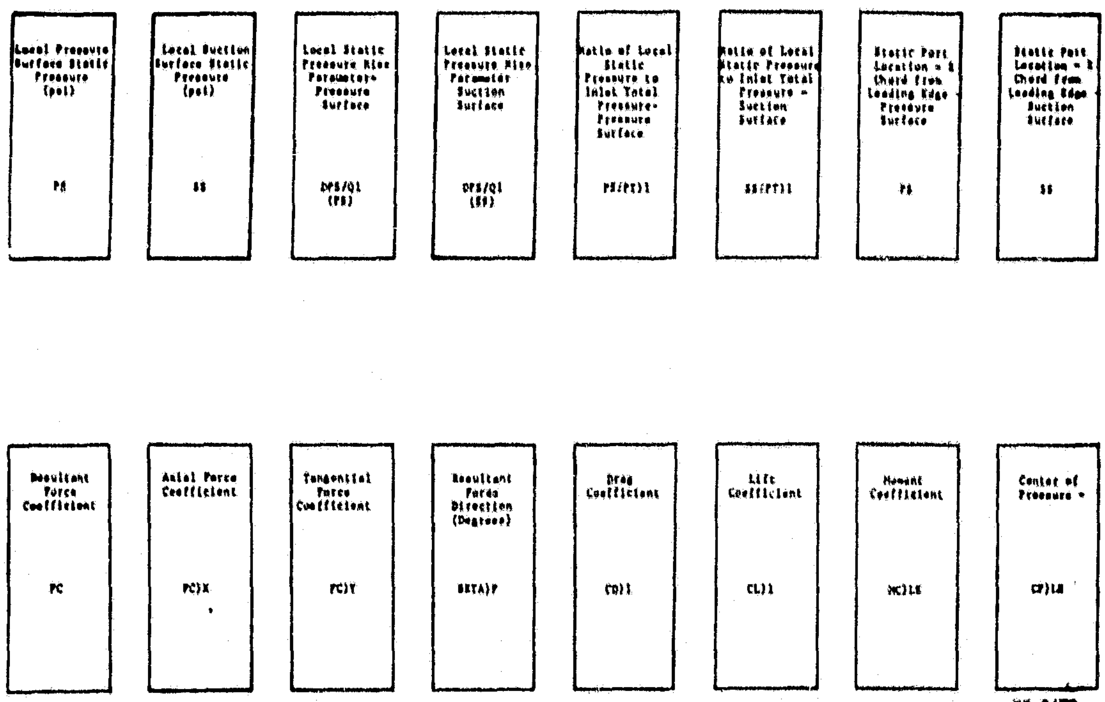

TE-8478

Figure 11. Computer print-out identification - instrumented blade parameters.

The local cascade exit performance was determined by utilizing a conical probe to measure Mach number, flow angle, and total pressure at twenty discrete points across one passage of the cascade. The probe was positioned at the center of cascade passage number 2 and measurements taken in five percent steps to the center of passage number 4 (data obtained behind blade number 3). The sixth through eleventh pages of the computer print-out present the local exit performance characteristics of the cascade. Figure 12 provides the identification for the parameters presented on these pages.

The cascade exit flow field properties are determined by mass-averaging and mixing to an uniform flow the local exit parameters. Identification of the exit flow field parameters on the twelth page of the computer print-out is present- ed in Figure 13.

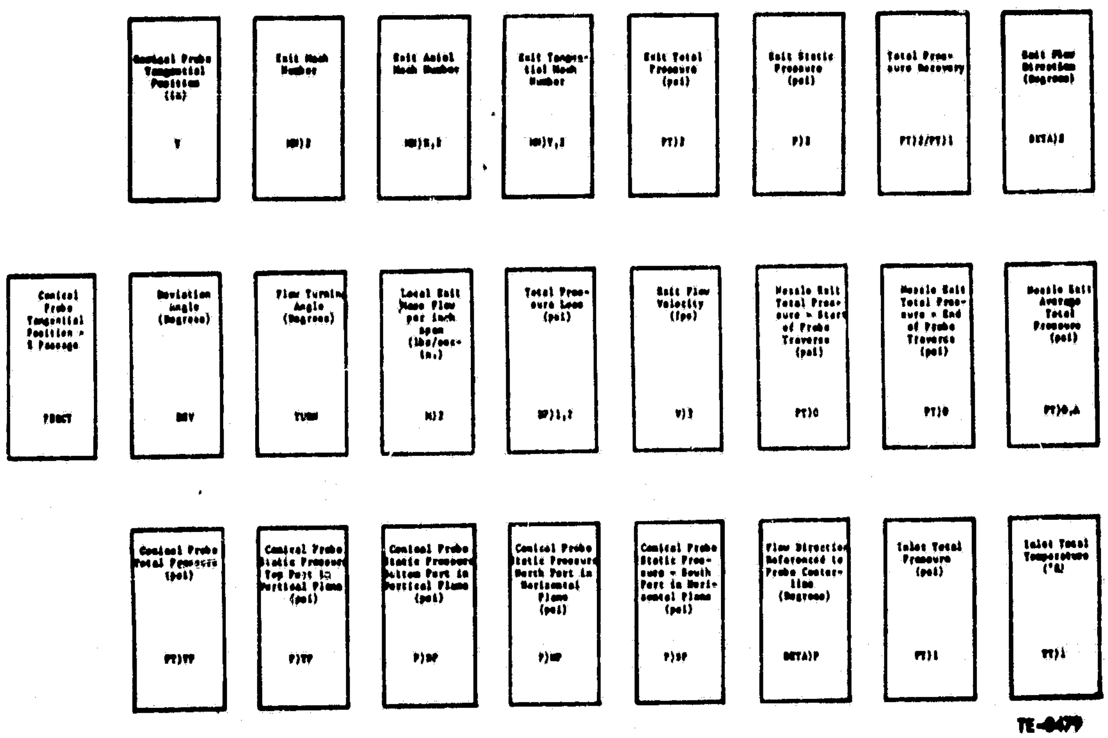

Figure 12. Computer print-out identification - local cascade exit performance.

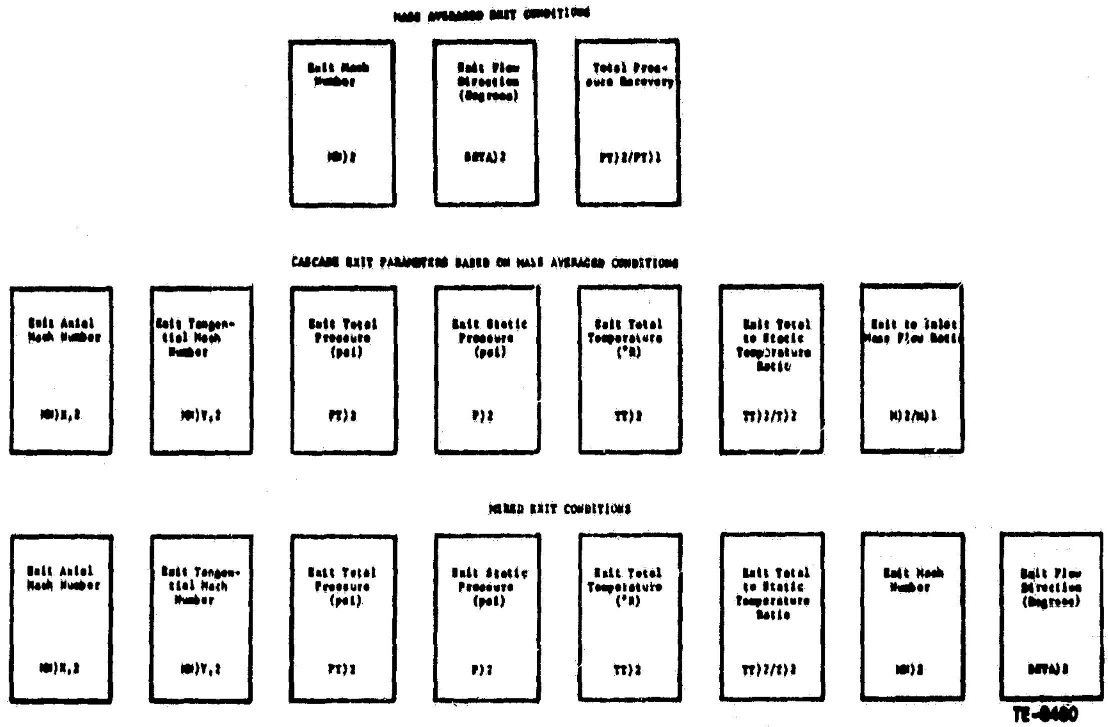

Figure 13. Computer print-out identification - mass averaged and mixed exit conditions.

The cascade overall performance characteristics relating the inlet and exit properties are presented on the thirteenth page of the computer print-out and are identified in Figure 14.

A sample of the computer print outs for a typical data set is included in Appendix A.

TIME VARIANT AERODYNAMIC DATA

The fundamental time-unsteady data of interest is the complex airfoil surface chordwise pressure distribution. This data, together with the airfoil motion data, determines the aerodynamic stability. The unsteady force (lift) and moment on the airfoil are calculated from this pressure and airfoil motion data.

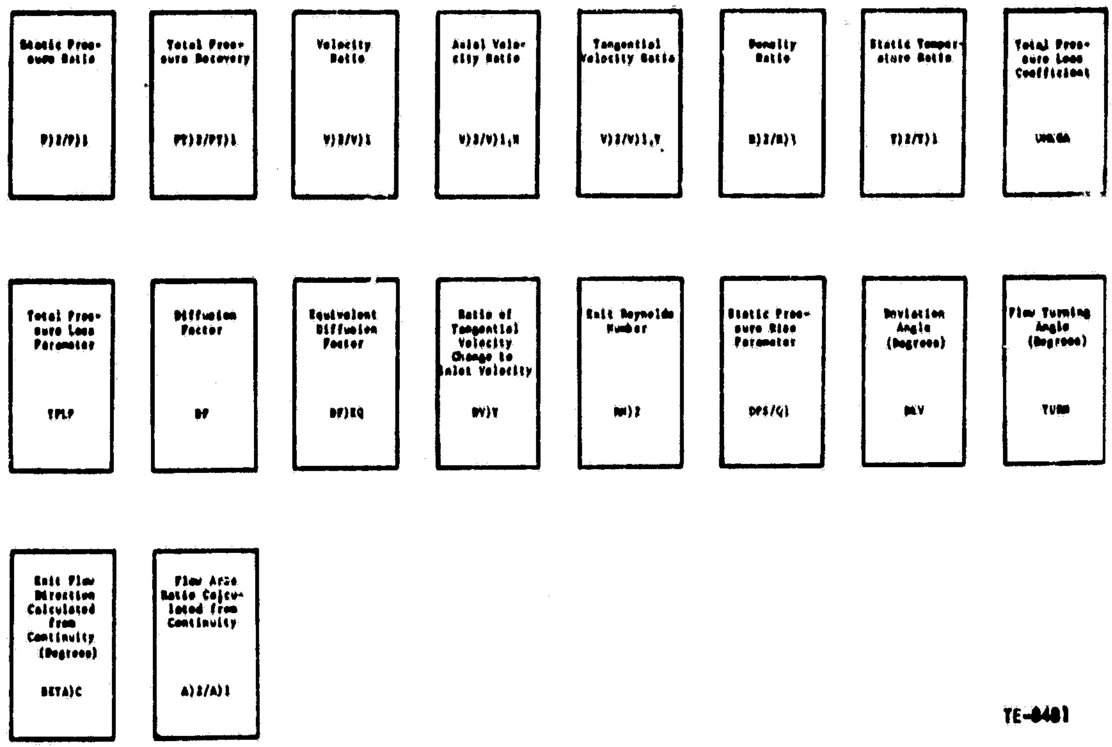

Figure 14. Computer print-out identification overall performance.

The instrumentation used to acquire the unsteady data included the following.

- o Strain Gages - Two per airfoil with one on either side of the tunnel.
- o Kulite Pressure Transducers - Six flush-mounted per surface on the center airfoil of the cascade (a total of twelve transducers on blade 3).
- o Heated Film Gages - Five surface-mounted per surface (a total of ten) on the center airfoil of the cascade.

The heated film gages were used to qualitatively examine the transition and flow separation phenomena on the airfoil surfaces for the conditions where the measured unsteady work per cycle attains its maximum and minimum values. The dynamic characteristic of each heated film gage at a particular operating point were determined from the taped oscilloscope traces of the blade motion as defined by the signals from the strain gage and the particular heated film gage. In addition, for the conditions of maximum and minimum unsteady work per cycle, high speed schlieren movies were taken.

The strain gage and pressure transducer data was acquired simultaneously. The on-line analysis was performed on the strain gage signals concurrent with the magnetic tape recording of the signals from the instrumented blade's strain gage and pressure transducers. The on-line analysis involved ten channels of strain gage data; two per airfoil. The twelve surface dynamic pressure sig nals, six from the pressure surface and six from the suction surface, along with the reference strain gage signal from the instrumented blade were taped for each data point.

In this investigation an analog-to-digital converter having a rate of 100,000 points per second was used. Data, either real time or taped, was digitized and stored on a magnetic disc for evaluation. An "n" cycle data averaging technique was adapted early in the test program to eliminate background noise from the unsteady pressure signal. This technique is currently used at DDA to reduce data from a low speed, single-stage compressor facility. The data is sampled at a preset time, triggered by a square wave pulse supplied by the airfoil drive system computer. The analog-to-digital converter is triggered by the positive voltage at the leading edge of the pulse, initiating the acquisition of the unsteady pressure data. The data can be sampled for "m" ensembles and "n" cycles and an average data set obtained. The results of this technique can best be presented with the aid of Figure 15, which represents the output signal of the first pressure surface pressure transducer obtained when 100 ensembles of 5 cycles were averaged.

The data analysis comprised the following three techniques:

- o Amplitude calculation
- o Frequency calculation
- o Phase calculation

In the amplitude calculation, a second order least square fit of the data on the positive and negative sides of the time axis was made for each half cycle of motion. The signal amplitude becomes the average of the positive peaks minus the average of the negative peaks.

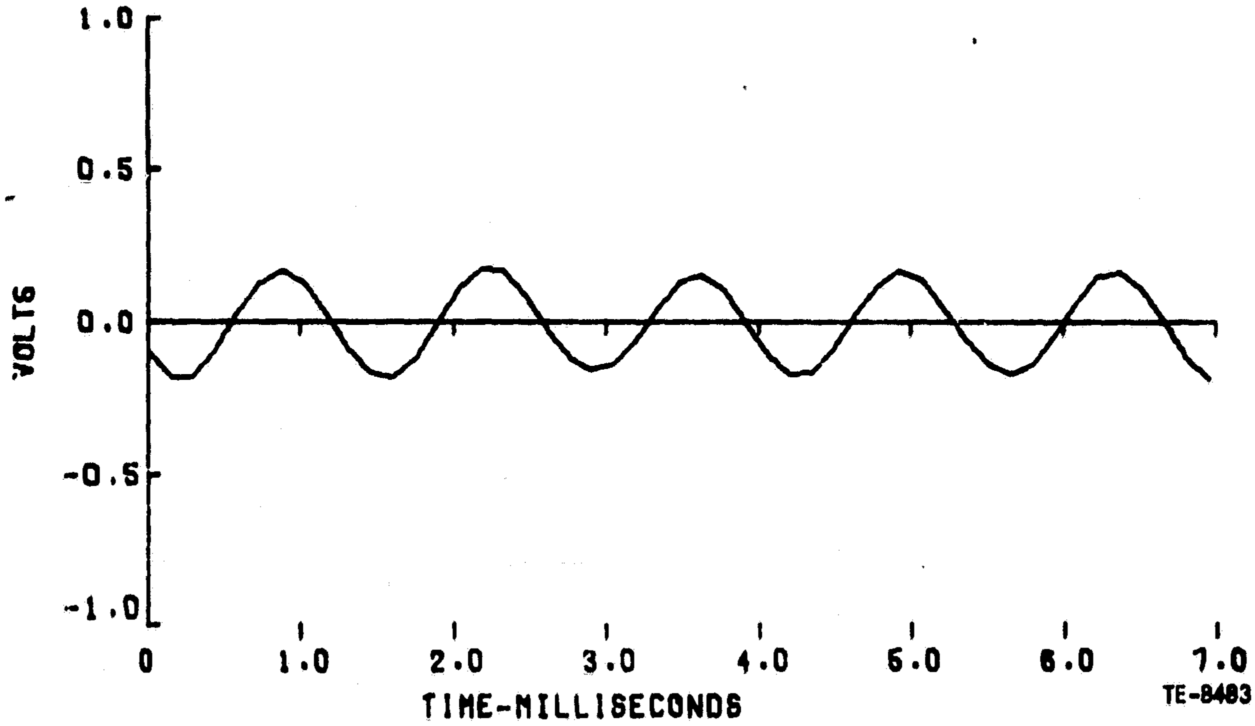

Figure 15. "N" - cycle averaging technique results for first pressure surface Kulite signal.

The frequency of the time-dependent digital data was determined through the autocorrelation function. This function describes the dependence on the values of the data at one time, X_i, on the values at another time, X_{i+r}. The lag time, ΔT, is inversely proportional to the rate at which the data are digitized. An autocorrelogram of the digitized data exhibits the features of a sine wave plus random noise. A second order least square fit function was fit to the data depicting the second positive peak of the autocorrelogram. The inverse of the time at which this least square function is a maximum is equal to the frequency, f, of the time-dependent data. Additionally, the frequency is known from the computer commanded input and an on-line, electronic counter.

The phase difference between the time-variant digitized signals was calculated through the cross-correlation function. This function, for two sets of data, X_i, Y_i, describes the dependence of the values of one set of data on the

other. As in the frequency calculation, a second order least square curve was fit to the data in the nearest to zero time positive peak of the cross-correlogram. The time, t_p, at which this least square function is a maximum was analytically determined. The phase difference, in degrees, was calculated as

$$\theta_p = t_p f \, 360$$

where f is the frequency calculated for the airfoil motion from the strain gage data.

The reference signal for all of the phase angle determinations was a strain gage signal from the instrumented airfoil. This signal was common in both the on- and the off-line data acquisition.

Figures 16 through 22 present the on-line and off-line unsteady data formats. A summary chart listing the steady aerodynamic operating characteristics of the cascade together with the desired frequency, interblade phase angle, reduced frequency, and multiplexer rate, was printed on the first page, as indicated in Figure 16.

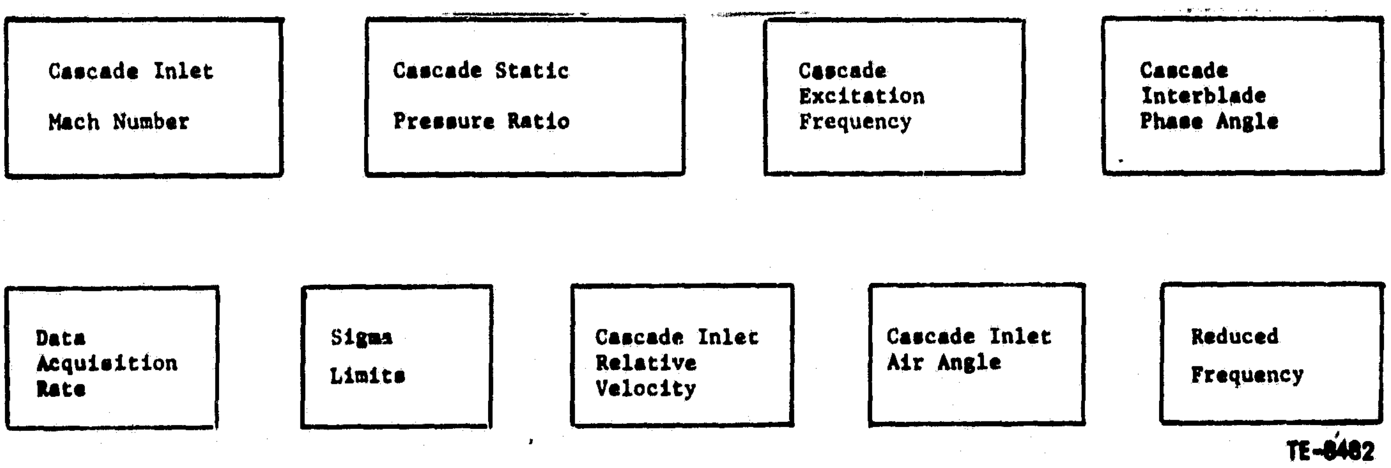

Figure 16. Unsteady data output format page 1.

The next pages, indicated in Figures 17 and 18, present the cyclic summaries of the positive and negative peaks of the signals, respectively.

Cycle	Signal 1		Signal 2		Signal 3		Signal 4		Signal 5	
	Time	Amplitude	Time	Amplitude	Time	Amplitude	Time	Amplitude	Time	Amplitude

TE-8484

Figure 17. Unsteady data output format page 2.

Cycle	Signal 1		Signal 2		Signal 3		Signal 4		Signal 5	
	Time	Amplitude	Time	Amplitude	Time	Amplitude	Time	Amplitude	Time	Amplitude

TE-8485

Figure 18. Unsteady data output format page 3.

The auto and cross-correlation results are presented on the following pages, as indicated in Figures 19 and 20.

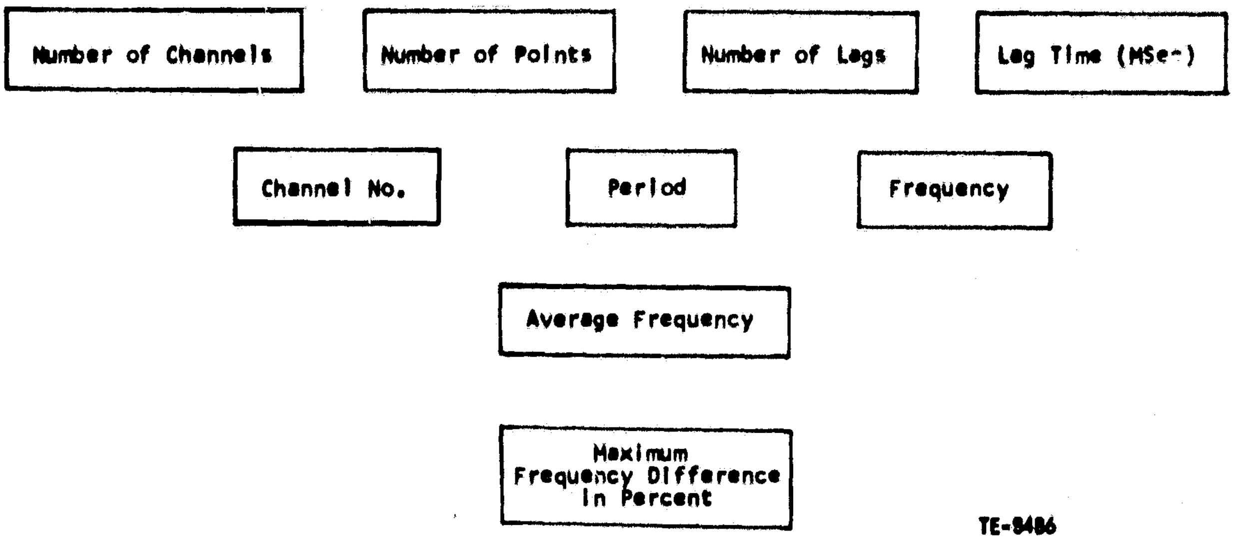

Figure 19. Unsteady data output format page 4.

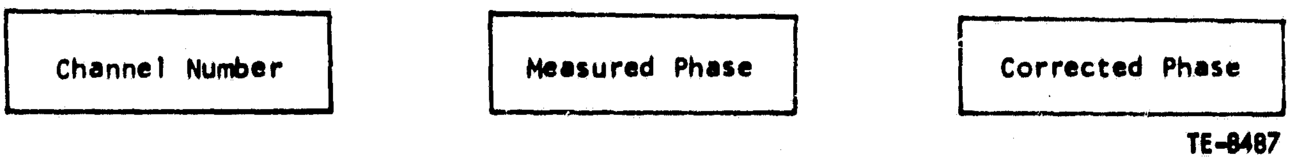

Figure 20. Unsteady data output format page 5.

Figure 21 shows a summary of the dynamic pressure transducer data. Included herein are the raw values of phase (after electronic calibration) and unsteady pressure, as well as the corresponding values after correction for acceleration effects.

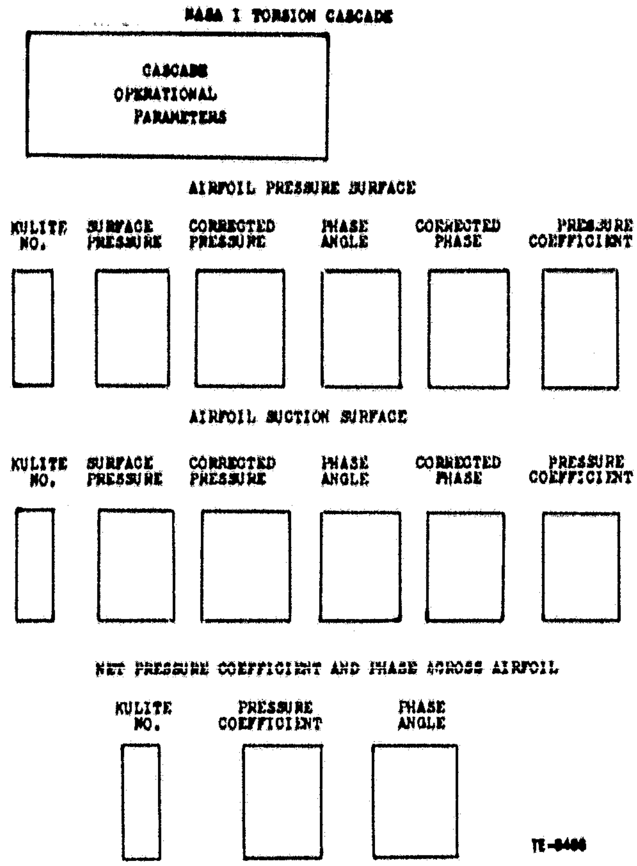

Figure 21. Unsteady data output format page 6.

Figure 22 depicts the last page of the time variant data set. This includes the airfoil surface unsteady pressure distributions, as well as the resultant real and imaginary parts of the lift and moment coefficients.

A sample of the aforementioned data sheets for a typical data set is included in Appendix B.

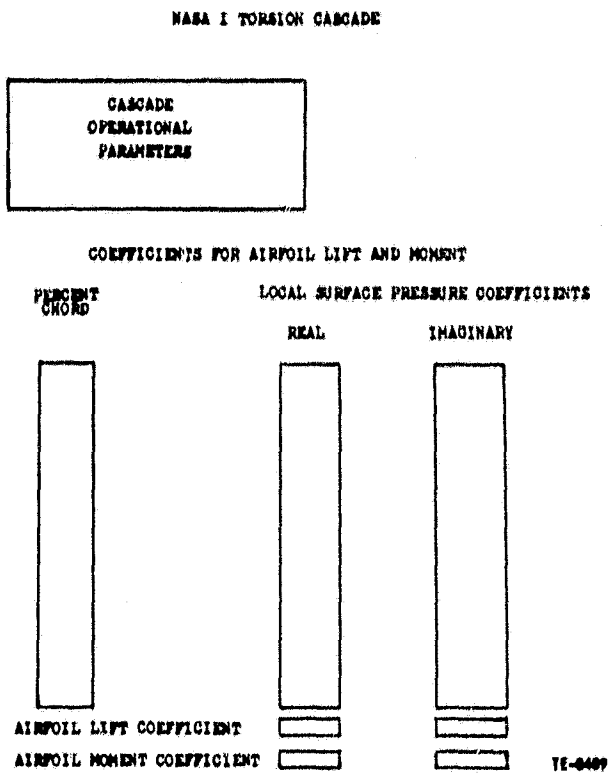

Figure 22. Unsteady data output format page 7.

The time-variant aerodynamic data are correlated against the DDA in-house developed method for a supersonic cascade utilizing a finite-difference/pressure-amplitude-function technique. This technique was further modified[3] to allow for variable blade-to-blade amplitudes of harmonic oscillation. The flow model is inviscid and assumes an operating pressure ratio of unity. The airfoils are assumed to be zero camber, zero thickness, flat plates. The theoretical results obtained from this numerical method have been compared to the published results of Garrick and Rubinow[4], Chalkley[5], Verdon and McCune[6] and Platzer and Brix[7] in the Ph. D. Thesis of John Caruthers at Georgia Institute of Technology[8]. All of the torsional mode cascade time-variant data was correlated against the analysis.

VIII. RESULTS AND DISCUSSION

The steady stat aerodynamics computer print-outs for the translational mode cascade tests are included in the Supplement to Volume II, and a sample is included in Appendix A. The time variant aerodynamics computer print outs are also included in the Supplement to Volume II and a sample is included in Appendix B. Included herein are the associated data plots and schlieren photographs for each cascade operating point.

The overall steady state performance results are summarized in Table III.

Table III. Translational Mode Cascade Steady-State Performance Summary

	Far Away from Flutter	Near Boundary Outside	Near Boundary Inside	Deep into Flutter
Inlet Mach Number	1.32	1.32	1.32	1.32
Mass Averaged Static Pressure Ratio	1.065	1.304	1.475	1.680
Mass Averaged Exit Mach Number	1.229	1.063	0.950	0.850
Mass Averaged Exit Air Angle, rad	0.95 (54.7^{o})	0.94 (53.7^{o})	0.90 (51.3^{o})	0.89 (50.8^{o})
Mass Averaged Total Pressure Loss, Dimensionless	0.090	.099	.115	.084

The translation cascade steady state flow field is described by the schlieren photographs included in Figures 23 through 26. These schlierens correspond to cascade mass averaged pressure ratios of 1.065, 1.304, 1.475 and 1.680:1 respectively. Because of the high solidity level of the cascade, the mounting hardware obscures a significant portion of the field of view. As the cascade is back-pressured the shock system moves up into the airfoil passage, until at the 1.68:1 condition the passage starts to become subcritical.

Figure 23. NASA II translation cascade schlieren at 1.065:1 mass average pressure ratio

Figure 24. NASA II translation cascade schlieren at 1.304:1 mass average pressure ratio

Figure 25. NASA II translation cascade schlieren at 1.475:1 mass average pressure ratio

ORIGINAL PAGE IS
OF POOR QUALITY

Figure 26. NASA II translation cascade schlieren at 1.680:1 mass average pressure ratio

Cascade periodicity is a measure of the uniformity of the blade-to-blade flow. Figures 27 through 30 are the translational mode cascade inlet and exit periodicity plots based on sidewall static pressure measurements normalized to the inlet total pressure. As can be seen from these plots the cascade periodicity was excellent for the four steady state operating points. A possible exception to this might be the 100% exit location static pressure for the 1.304:1 pressure ratio, which is plotted as an open symbol. However, this localized static pressure decrease was not evident at the 140% location which is plotted as a solid symbol.

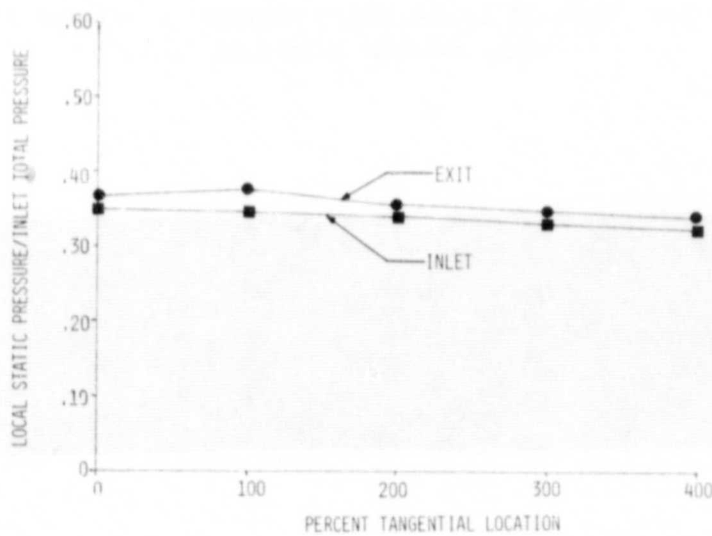

Figure 27. Translation cascade sidewall static periodicity plots at 1.065 pressure ratio

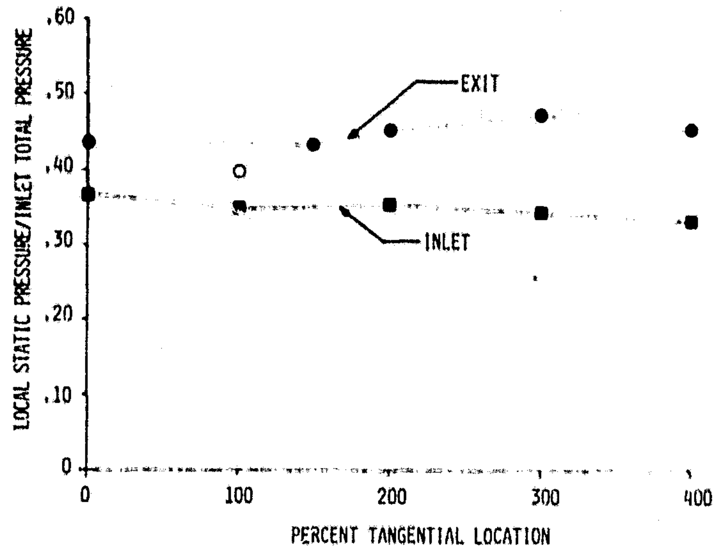

Figure 28. Translation cascade sidewall static periodicity plots at 1.304:1 pressure ratio

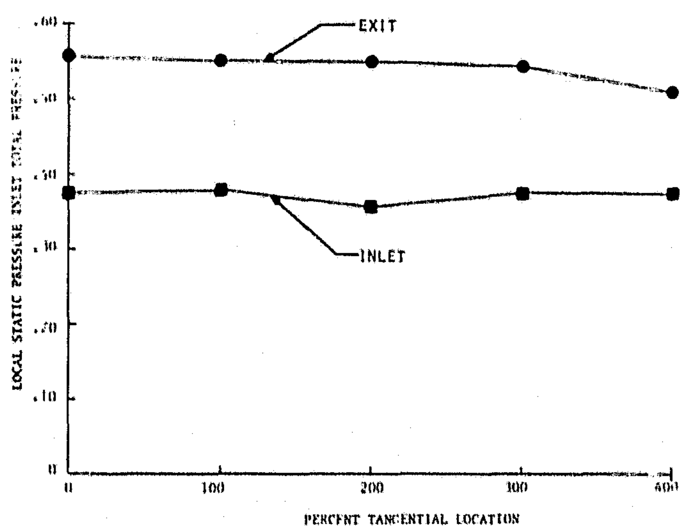

Figure 29. Translation cascade sidewall static periodicity plots at 1.475:1 pressure ratio

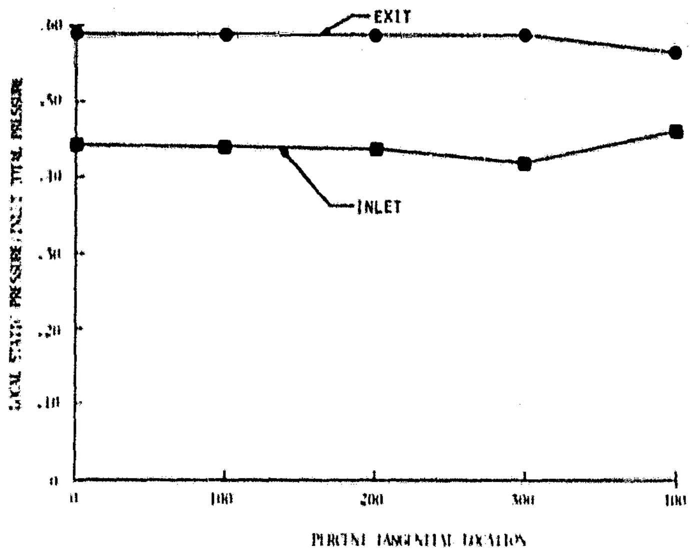

Figure 30. Translation cascade sidewall static periodicity plots at 1.680:1 pressure ratio

The uniformity of the exit flow field is further qualified by the cascade exit wake surveys presented in Figures 31 through 34. These data result from the cone probe survey downstream of the second and third (instrumented) cascade airfoils. The measured local value of total pressure is normalized to the cascade inlet total pressure.

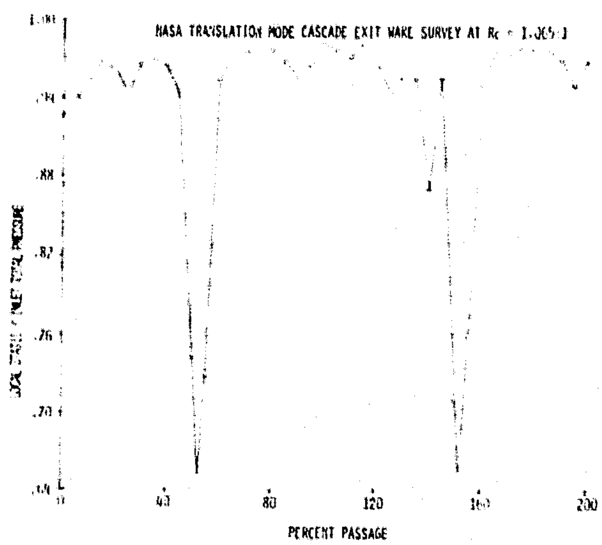

Figure 31. Translation cascade exit survey at 1.065:1

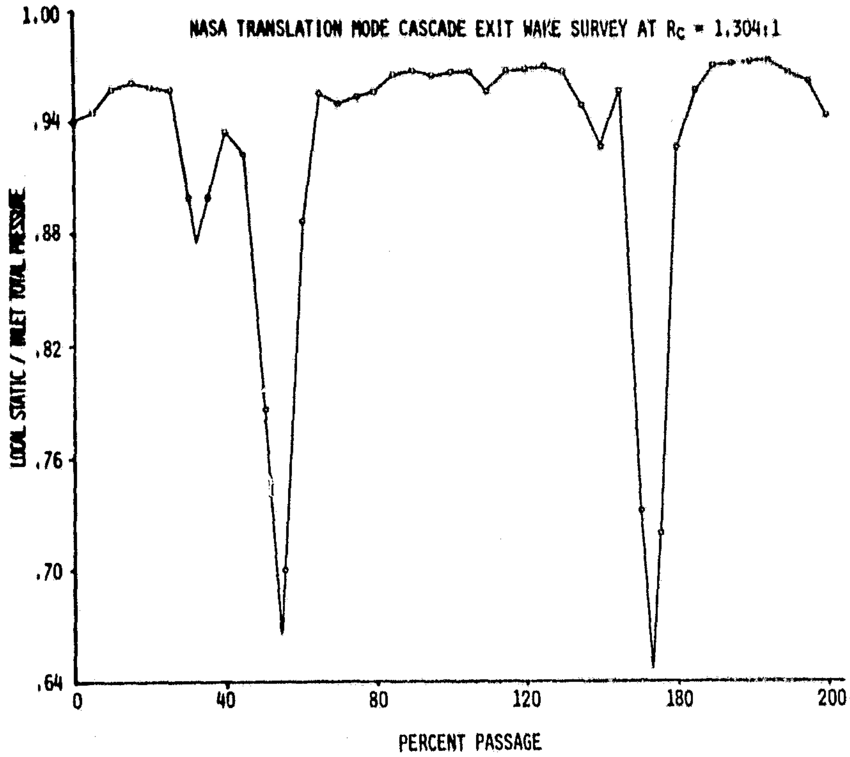

Figure 32. Translation cascade exit survey at 1.304:1

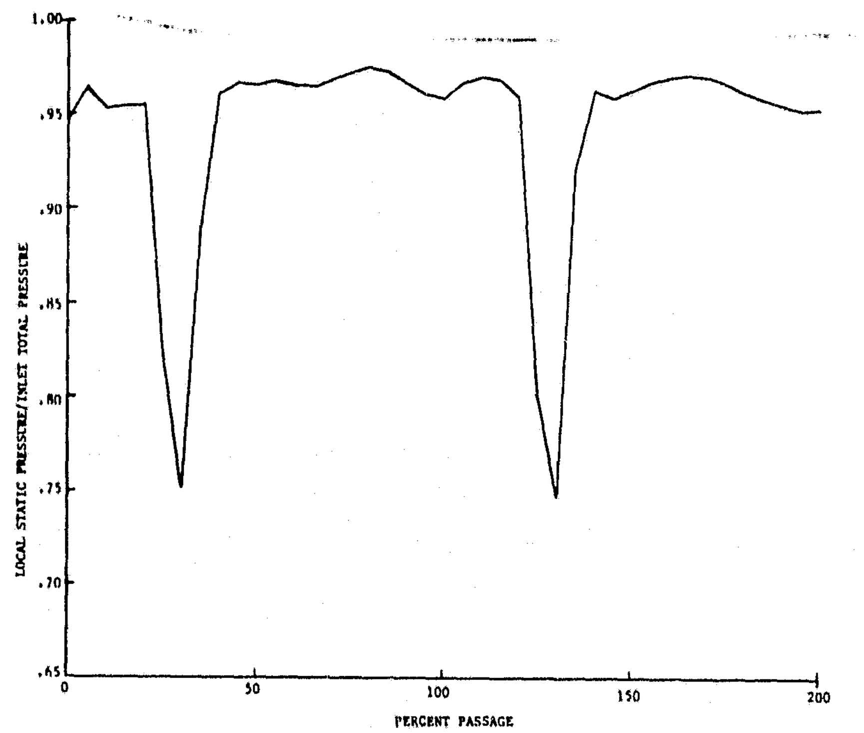

Figure 33. Translation cascade exit survey at 1.475:1

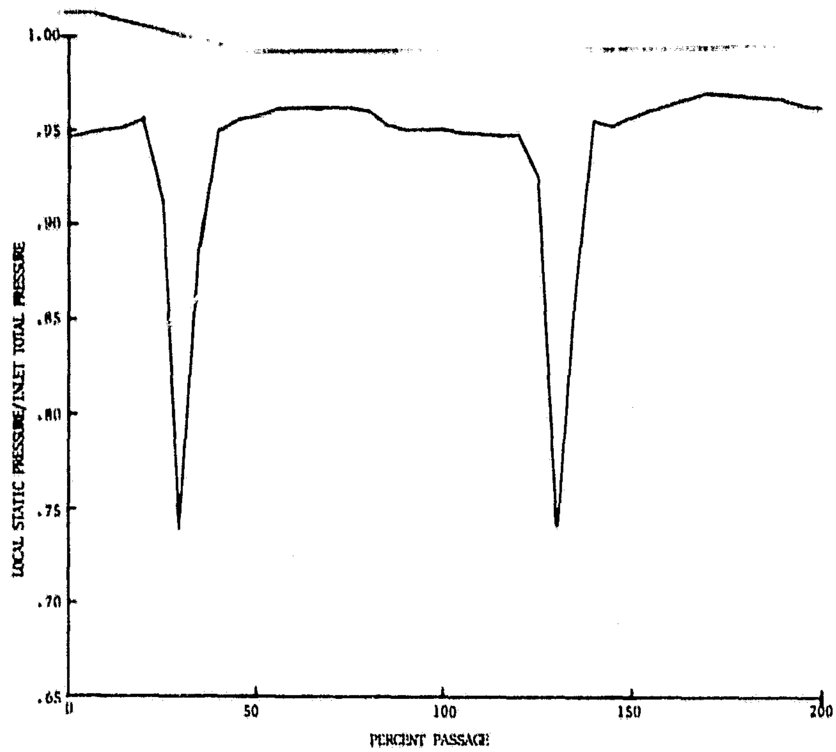

Figure 34. Translation cascade exit survey at R_c = 1.680:1

Figures 35 through 38 are the static tap instrumented airfoil surface pressure distributions normalized to the inlet total pressure. These data plots correspond to static pressure ratios of 1.065, 1.304, 1.475 and 1.680:1 repsectively. The instrumented airfoils' pressure surface 5 percent chord location static tap was inopearative during part of the testing. The data plotted as an open symbol at this location was obtained from combined analytical results and earlier test data.

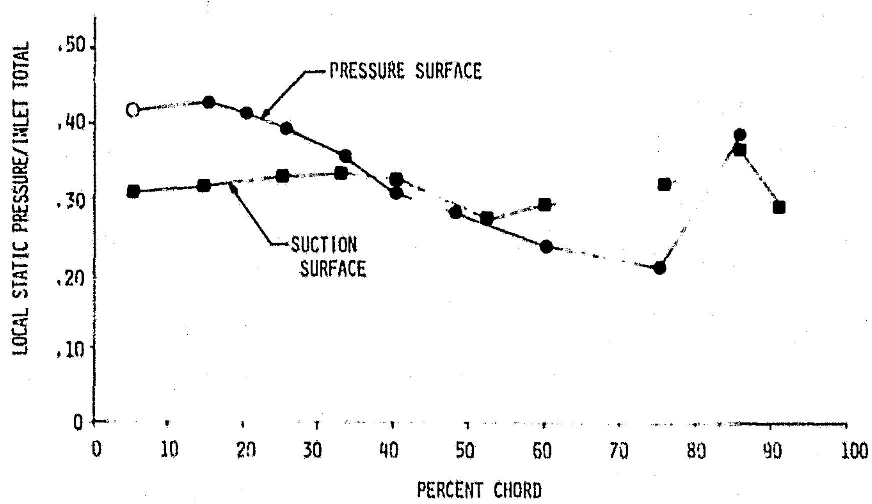

Figure 35. Translation cascade instrumented airfoil static pressure distribution at 1.065:1

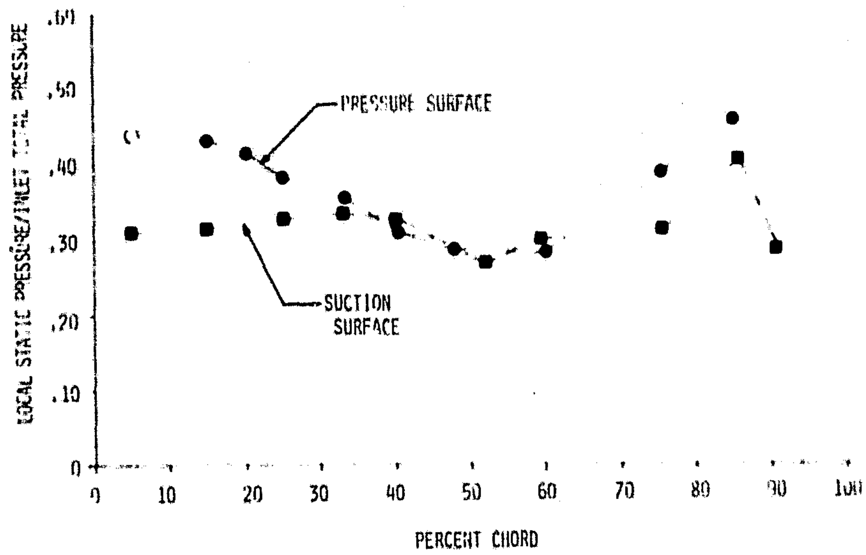

Figure 36. Translation cascade instrumented airfoil static pressure distribution at 1.304:1

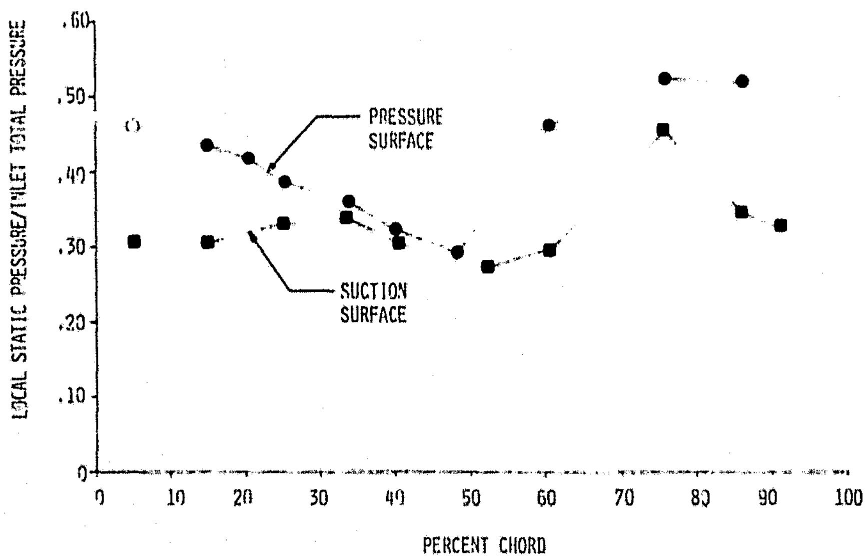

Figure 37. Translation cascade instrumented airfoil static pressure distribution at 1.475:1

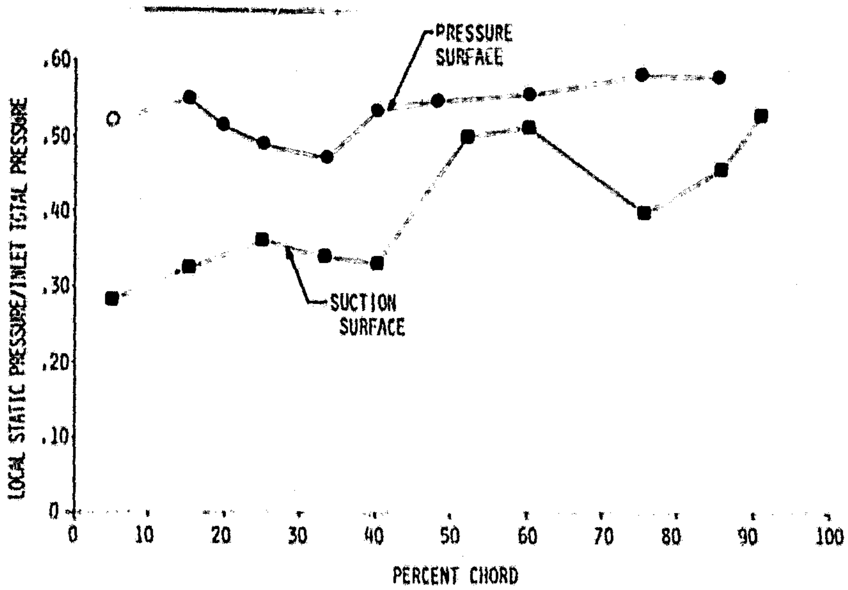

Figure 38. Translation cascade instrumented airfoil static pressure distribution at 1.680:1

An alcohol injection tchnique was used to identify regions of flow separation. This involves injecting alcohol back through the static pressure taps on the instrumented airfoil. The only region of flow separation evident during the testing was located on the suction surface near the trailing edge. This condition was observed over a range of static pressure ratios between 1.35 - 1.68:1. The action of the fluid was not nearly as violent as that observed during the baseline torsional mode cascade.

After completion of the steady-state testing, the static tap airfoil was removed and the Kulite instrumented airfoil was installed. The time variant aerodynamic computer output data sheets for the translation mode cascades are included in the supplement and a sample data set is included in Appendix B. This includes the print-out of the raw and corrected data. Plots of the chordwise variation of the measured surface unsteady pressure and the corresponding phase lag are included in Appendix C. These data plots also include the correlation with the aforementioned variable amplitude analysis. All pressure surface data is plotted as a solid symbol and the corresponding variable amplitude theory is represented by a solid line. All suction surface data is plotted as an open symbol and the theory is a dashed line.

At each steady state cascade operating point a total of six interblade phase angles between +3.14 rad (+180°) and -3.14 rad (-180°) were tested. A tabulation of the test phase angles along with other pertinent operational characteristics are included in Table IV. The first column in the figure is the average test interblade phase angle to the nearest 0.09 rad (5.$^{\circ}$). Positive phase angles means that the first airfoil, leads the second airfoil, leads the third airfoil, etc., and is equivalent to a backward traveling wave. The static pressure ratios in the table are cascade mass averaged values.

Table IV.

Translation mode cascade time variant testing results summary.

TABLE IV.

NASA II TRANSLATION CASCADE TIME-VARIANT TESTS SUMMARY

PHASE RAD	CASCADE STATIC PRESSURE RATIO	INTERBLADE PHASE ANGLE, RAD ϕ_{1-2}	ϕ_{2-3}	ϕ_{3-4}	ϕ_{4-5}	MEAN PHASE ϕ	σ_ϕ	AIRFOIL TRANSLATIONAL AMPLITUDES, cm δ_1	δ_3/δ_1	δ_2/δ_1	δ_4/δ_1	δ_5/δ_1	FREQUENCY f	k
3.14	1.065:1	3.12	3.16	3.10	3.01	3.11	±0.03	.013	1.500	1.000	0.500	1.000	218	.142
1.57	↓	1.56	1.57	1.47	1.77	1.59	±0.12	.020	0.875	0.938	0.313	0.250	218	.142
1.05		1.08	0.99	0.97	1.12	1.04	±0.07	.020	0.938	0.875	0.563	1.000	218	.142
0.0		0.05	0.01	0.01	-0.05	0.01	±0.04	.018	0.857	1.857	0.714	0.571	218	.142
-1.05		-1.09	-1.10	-0.98	-1.10	-1.07	±0.06	.020	1.375	1.438	0.688	0.625	218	.142
-1.57		-1.61	-1.52	-1.65	-1.42	-1.55	±0.10	.023	1.111	1.111	0.111	0.556	218	.142
3.14	1.304:1	3.14	3.10	3.18	2.97	3.10	±0.09	.008	2.667	1.333	1.000	3.333	218	.142
0.52	↓	0.59	0.51	0.52	0.60	0.56	±0.05	.018	1.000	0.929	0.643	0.357	218	.142
0.0		-0.03	0.04	0.04	0.03	0.02	±0.03	.020	1.125	1.000	0.625	0.125	218	.142
-0.52		-0.58	-0.56	-0.56	-0.45	-0.54	±0.06	.015	1.167	1.583	0.583	0.333	242	.144
-1.05		-1.02	-1.05	-0.98	-1.04	-1.03	±0.04	.015	1.667	1.333	0.583	0.333	242	.144
-1.57		-1.54	-1.64	-1.66	-1.56	-1.60	±0.06	.013	1.800	1.300	0.700	0.300	242	.144
3.14	1.475:1	3.23	3.09	3.12	3.10	3.14	±0.07	.010	1.750	1.000	1.125	0.500	242	.144
1.57	↓	1.55	1.55	1.52	1.66	1.57	±0.06	.015	1.167	0.667	1.083	0.333	242	.144
1.05		-1.08	1.04	1.04	1.02	1.05	±0.03	.018	0.571	0.785	0.714	0.571	242	.144
0.0		0.01	0.00	0.00	0.03	0.01	±0.02	.018	0.786	1.205	0.786	0.429	242	.144
-1.05		-1.08	-1.01	-1.05	-1.03	-1.04	±0.03	.018	1.071	1.071	0.714	0.357	242	.144
-1.57		-1.65	-1.53	-1.56	-1.40	-1.53	±0.10	.020	1.000	1.063	0.500	0.375	242	.144
3.14	1.680:1	3.12	3.07	3.14	3.27	3.15	±0.08	.005	1.000	1.000	2.500	1.500	242	.144
1.57	↓	1.49	1.50	1.62	1.52	1.53	±0.06	.015	0.667	0.583	0.667	0.333	242	.144
0.79		0.80	0.80	0.87	0.64	0.78	±0.10	.018	1.929	0.571	0.929	0.714	242	.144
0.0		0.03	-0.01	0.06	-0.02	0.02	±0.04	.018	1.857	0.357	1.000	0.429	242	.144
-0.79		-0.82	-0.81	-0.73	-0.89	-0.81	±0.07	.018	1.071	1.143	0.714	0.500	242	.144
-1.57		-1.56	-1.58	-1.60	-1.53	-1.57	±0.03	.018	1.714	0.643	0.500	0.571	242	.144

The individual phase angles ($\phi_{1-2}, \phi_{2-3}, \phi_{3-4}$, and ϕ_{4-5}) tabulated are the measured blade-to-blade test values. The mean phase tabulation includes the mean of the four individual phases and the deviation ($\pm \sigma_{\phi}$) from this mean. The blade amplitude tabulation includes the instrumented (third) airfoil zero-to-peak amplitude (δ_3), and the amplitudes of airfoils 1, 2, 4 and 5 as normalized to the instrumented airfoil. Test frequencies are tabulated with their respective reduced frequency value (k).

Figures 39 through 42 are plots of the chordwise variation of the unsteady pressures and their corresponding phase lags at the low (1.065:1) static pressure ratio and a 0.0 rad interblade phase angle. These data are correlated against the DDA unsteady supersonic cascade flow analysis for both the constant and the variable airfoil amplitude results.

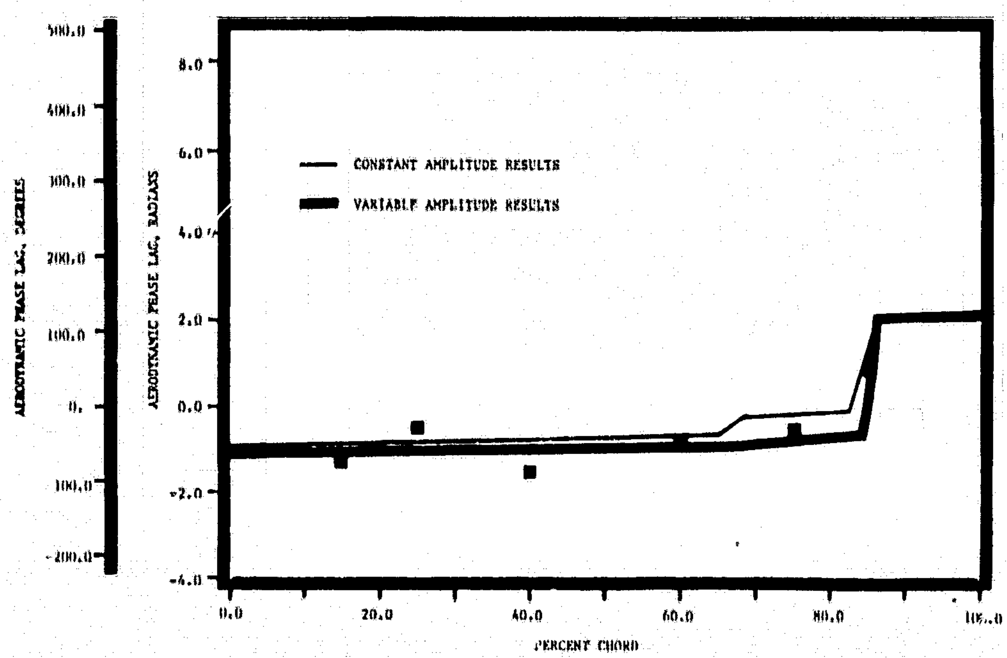

Figure 39. Translation cascade pressure surface phase lag distribution at 1.065:1 and 0.0 rad interblade phade angle

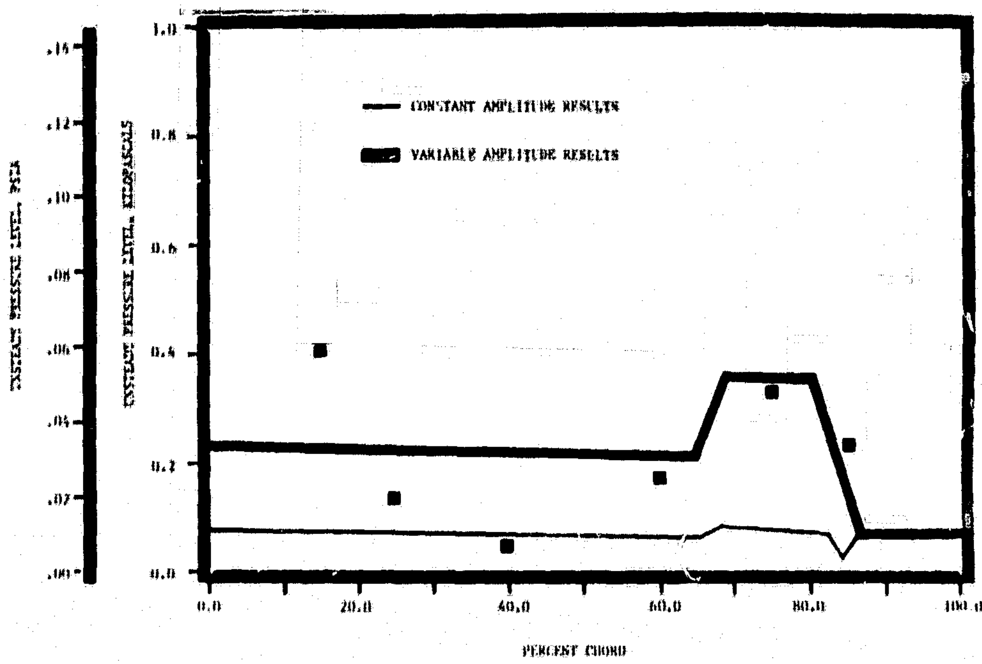

Figure 40. Translation cascade pressure surface unsteady pressure distribution at 1.065:1 and 0.0 rad interblade system angle

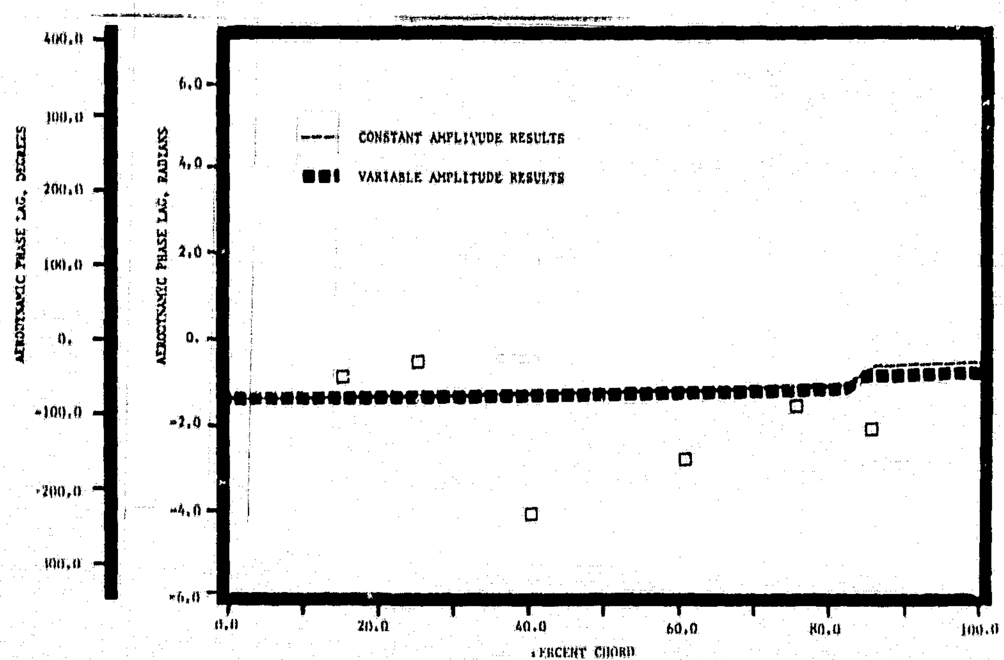

Figure 41. Translation cascade suction surface phase lag distribution at 1.065:1 and 0.0 rad interblade phase angle

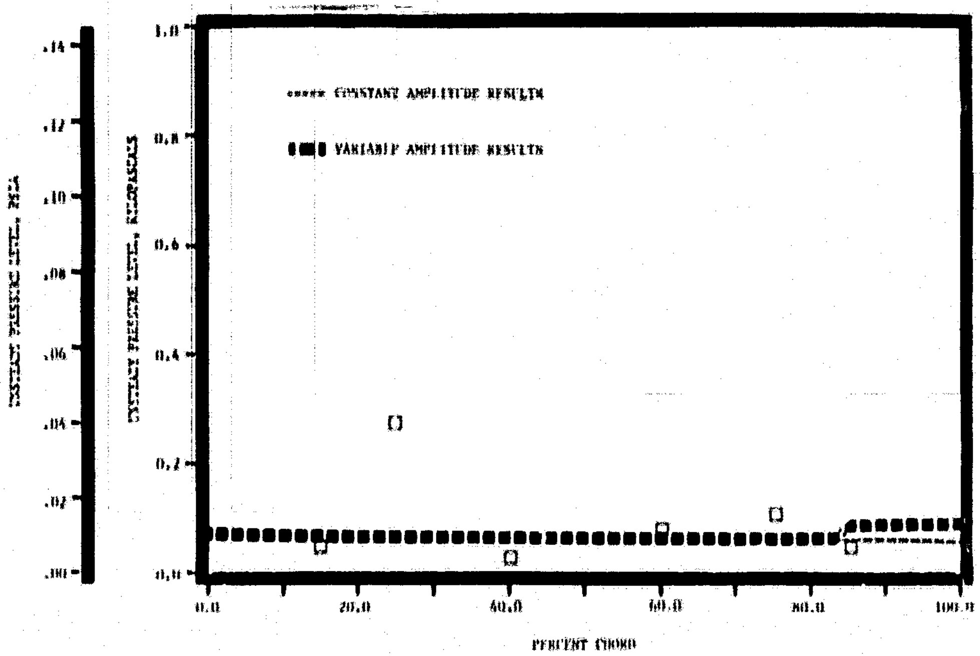

Figure 42. Translation cascade suction surface unsteady pressure distribution at 1.065:1 and 0.0 rad interblade phase angle

As can be seen from Figure 39 the pressure surface chordwise phase lag data/theory correlation is excellent. The corresponding pressure surface unsteady pressure level is presented in Figure 40. This correlation is also excellent, with the exception of the leading edge region where the 15 percent transducer indicates a higher level of unsteady pressure.

The suction surface phase lag data as presented in Figure 41 is in good agreement with theory, except near the 40 percent chord location. At this location the measured phase lag was significantly lower than the theory predicted. This trend was noticed at other cascade pressure ratios and interblade phase angles. The suction surface unsteady pressure level data/theory correlation is shown in Figure 42 and in general exhibits excellent agreement. The measured pressure level at the 25 percent chord location was however significantly higher than theory.

Figures 43 through 46 are plots of the chordwise variation in the unsteady pressures and phase lags at the highest (1.68:1) static pressure ratio and 0.0 rad interblade phase angle. These data are correlated against the DDA variable amplitude analysis and a NASA strong in-passage shock unsteady flow code[9]. The cascade shock system at the 1.68:1 pressure ratio was such that the inlet wave was nearly normal in the passage. These flow conditions are more closely modeled by the NASA strong shock code. As can be seen from the data/theory correlation, the NASA code more accurately predicts the phase lag levels on both the pressure and the suction surface of the airfoil. However, the measured level of the unsteady pressure is higher than the calculated values over both surfaces.

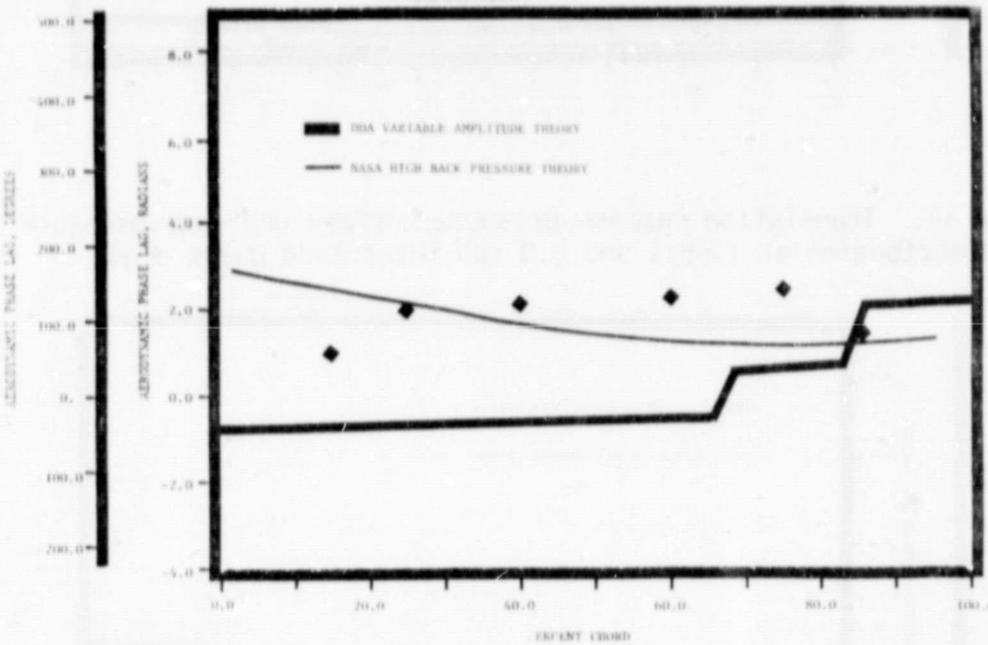

Figure 43. Translation cascade pressure surface phase lag distribution at 1.68:1 and 0.0 rad interblade phase angle

The appropriate unsteady lift and moment coefficients were calculated from the measured blade amplitude and the unsteady pressure coefficient and its phase relative to the blade motion. A linear interpolation was assumed between Kulite locations. The leading edge and trailing edge values were obtained by extrapolating the 15% and 85% chord data.

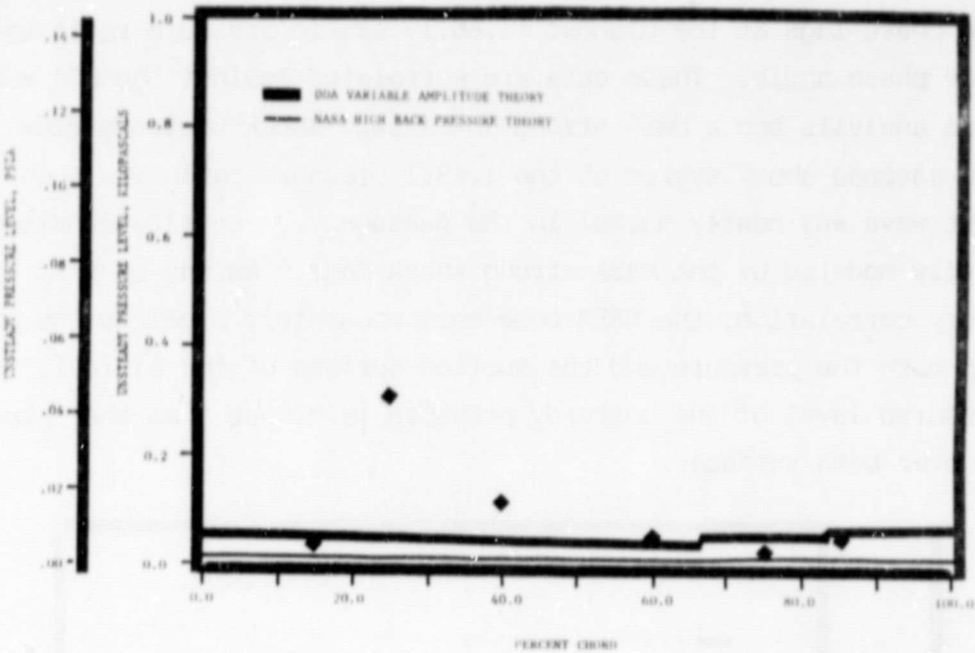

Figure 44. Translation cascade pressure surface unsteady pressure distribution at 1.68:1 and 0.0 rad interblade phase angle

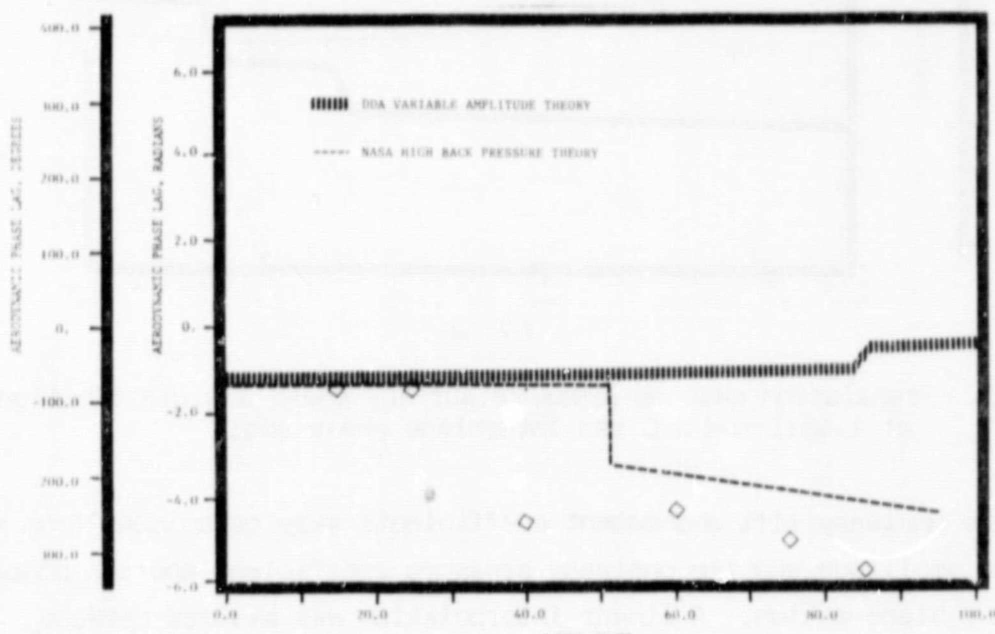

Figure 45. Translation cascade suction surface phase lag distribution at 1.68:1 and 0.0 rad interblade phase lag

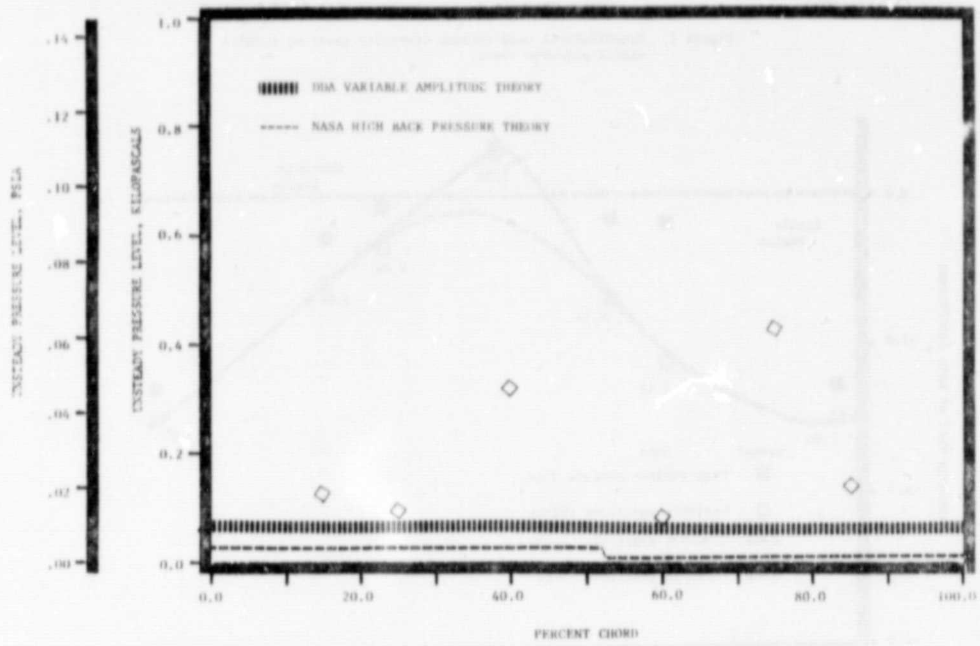

Figure 46. Translation cascade suction surface unsteady pressure distribution at 1.68:1 and 0.0 rad interblade phase angle

The unsteady lift coefficient components were obtained by direct integration of the resulting real and imaginary distributions. The unsteady moment coefficient was obtained by applying the appropriate moement arm to the data.

The cascade stability is related to the imaginary part of the unsteady lift coefficient (CL_i). As this value increases into the positive regime the airfoil damping becomes insufficient and the airstream imparts energy into the airfoil resulting in an aeroelastic instability. Figures 47 through 50 are the stability plots obtained at the four static pressure ratios over the range of interblade phase angles tested. Each data plot has the variable amplitude theory line for comparative purposes.

As can be seen from Figure 47, the 0.0 rad phase angle data point was unstable at the low pressure ratio of 1.065:1. This is in disagreement with the flutter map. However, it is felt that this stability was influenced by the high amplitude of the second cascade airfoil, which was almost twice that of the

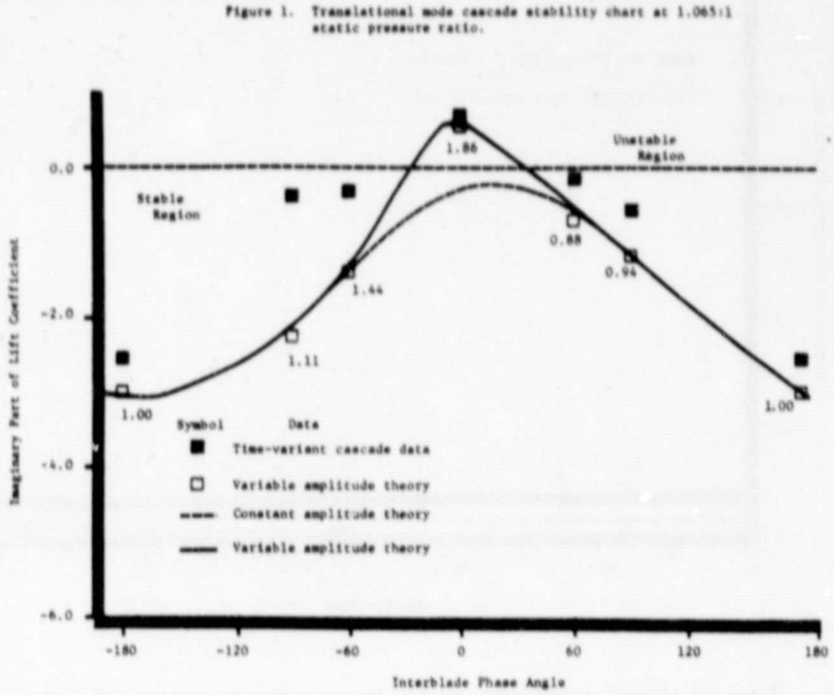

Figure 47. Translation cascade stability curve at 1.065:1 static pressure ratio

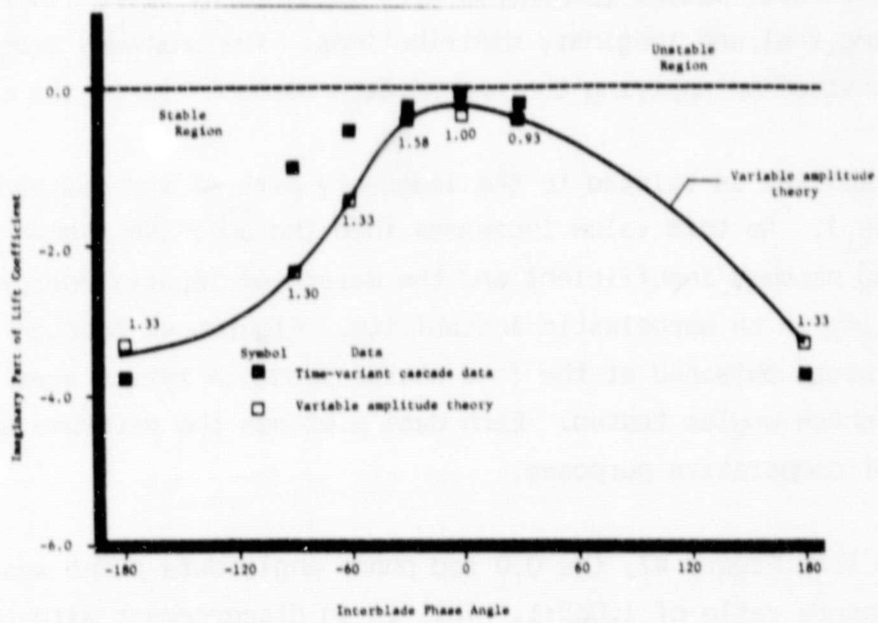

Figure 48. Translation cascade stability curve at 2.304:1 static pressure ratio

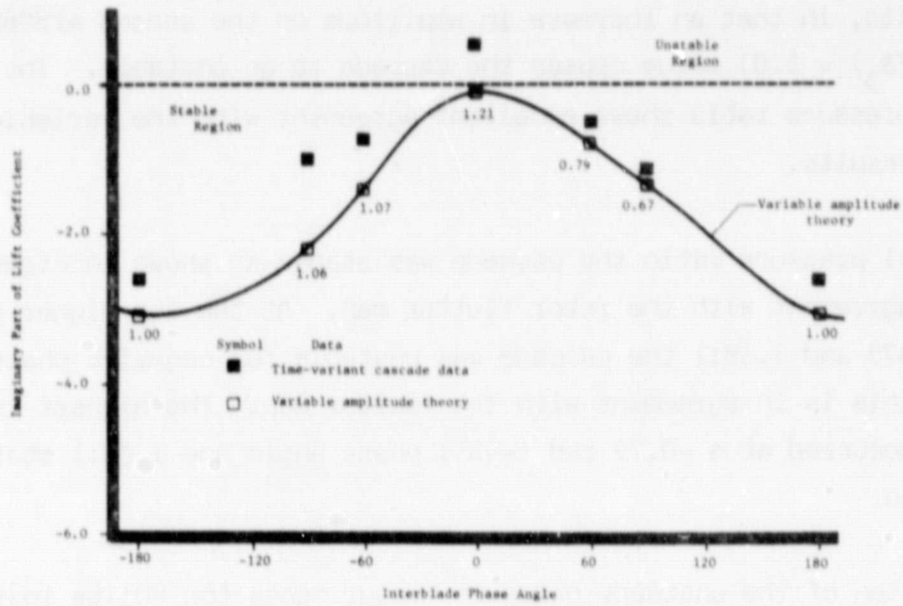

Figure 49. Translation cascade stability curve at 1.475:1 static pressure ratio

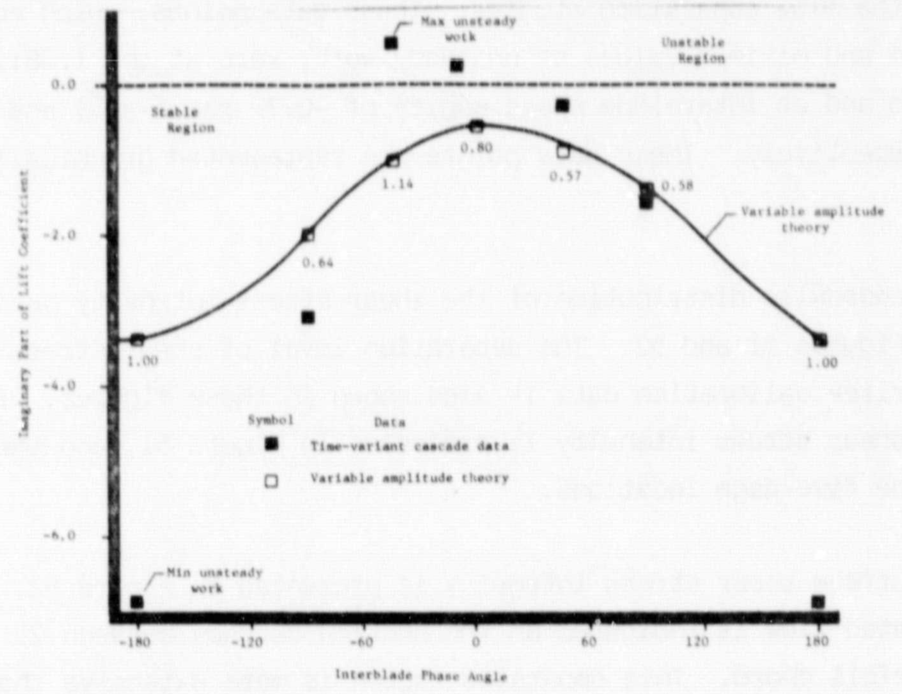

Figure 50. Translation cascade stability curve at 1.680:1 static pressure ratio

instrumented airfoil (δ_2/δ_3 = 1.86). This is substantiated by the theoretical results, in that an increase in amplitude on the second airfoil from a constant (δ_2/δ_3) = 1.0) value causes the cascade to go unstable. The data at this low pressure ratio shows excellent agreement with the variable amplitude theory results.

At the 1.304:1 pressure ratio the cascade was stable as shown in Figure 48, which is in agreement with the rotor flutter map. At the two higher pressure ratios of 1.475 and 1.68:1 the cascade was unstable for negative phase angles near zero. This is in agreement with the flutter map. The highest level of instability occurred at a -0.79 rad (-45^{o}) phase angle and 1.68:1 static pressure ratio.

After completion of the unsteady pressure measurements the Kulite instrumented airfoil was replaced with the heated film gage instrumented airfoil. Based on the results of the previously discussed stability plots, two data points were selected for the flow separation studies. These data points, which correspond to the maximum and minimum values of unsteady work, were at the 1.68:1 static pressure ratio and at interblade phase angles of -0.79 rad (-45^{o}) and 3.14 rad (180^{o}) respectively. These data points are represented graphically in Figure 50.

The measured chordwise distribution of the shear stress intensity parameter is presented in Figures 51 and 52. The separation level of shear stress as determined from earlier calibration data is also shown in these figures. The pressure surface shear stress intensity is presented in Figure 51, and the flow is attached at the five gage locations.

The suction surface shear stress intensity is presented in Figure 52. A region of separated flow is indicated on the suction surface between 25 and 60 percent of airfoil chord. This separated region is more extensive than that indicated by the alcohol injection flow visualization tests. During the alcohol injection tests the separated region was only observed near the airfoils trailing edge region. This separated region on the suction surface may explain the data/theory variations indicated at the 25 and 40 percent chord locations.

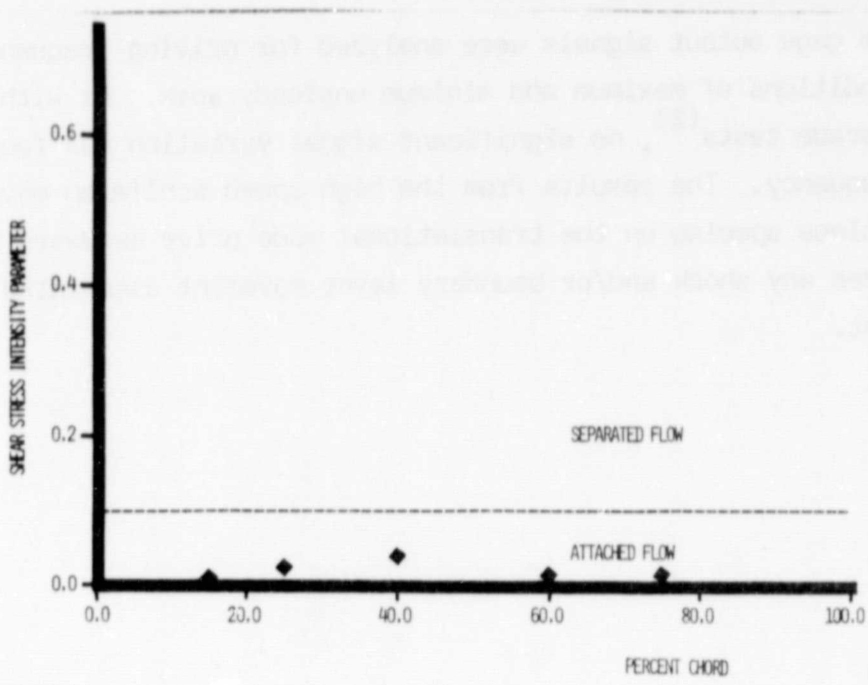

Figure 51. Translation cascade pressure surface chordwise distribution of shear stress intensity parameter

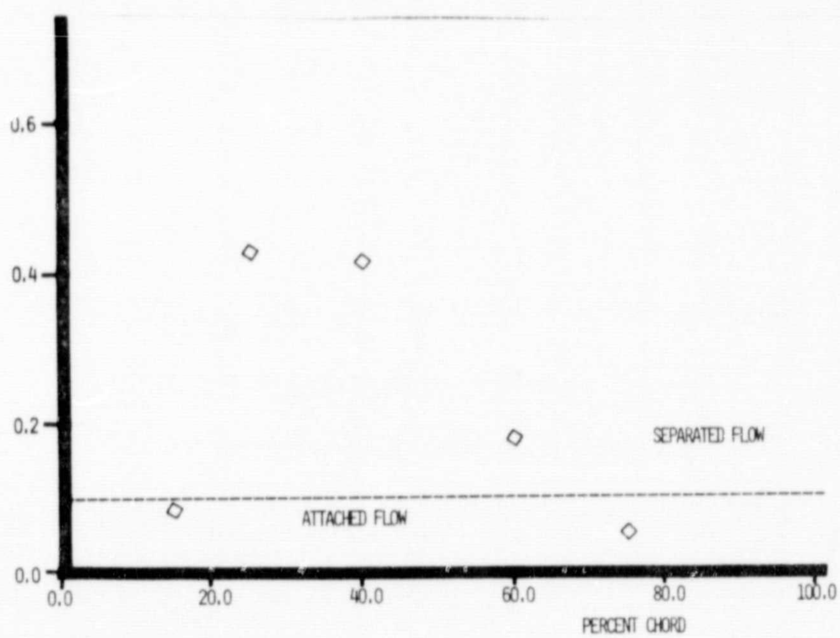

Figure 52. Translation cascade suction surface chordwise distribution of shear stress intensity parameter

The heated film gage output signals were analyzed for driving frequency content at the conditions of maximum and minimum unsteady work. As with the torsional mode cascade tests[2], no significant signal variation was found at the driving frequency. The results from the high speed schlieren movies were masked by the close spacing on the translational mode drive hardware making it impossible to see any shock and/or boundary layer movement associated with the airfoil movement.

APPENDIX A

Sample of Steady State Aerodynamics Computer Print Out
Refer to Section VII for item identification and explanation of meanings.

SUPERSONIC COMPRESSOR CASCADE
NASA TRANSLATION CASCADE

DATA SET NO. 1

CASCADE INLET MACH NUMBER	CASCADE IDEAL STATIC PRESSURE RATIO	PROBE DATA TAKEN BEHIND BLADE	PROBE AXIAL LOCATION (IN.)
1.320	.464	3	.550

PRESSURE DATA FROM SCANIVALVE - PSIA

SCANIVALVE PORT #	SCANIVALVE NO. 3	SCANIVALVE NO. 2	SCANIVALVE NO. 4	SCANIVALVE NO. 1
9	15.575	15.567	15.570	15.580
11	14.674	5.634	6.460	4.818
13	7.212	5.054	6.631	4.884
15	7.294	5.210	6.430	5.285
17	7.295	5.569	5.946	5.201
19	7.285	5.011	5.521	4.883
21	15.537	5.227	4.814	4.168
23	5.411	5.563	4.430	4.457
25	5.225	5.712	3.714	4.943
27	5.436	5.560	3.239	5.745
29	5.255	5.430	5.988	4.456
31	5.438	5.412	15.577	15.589
33	5.768	5.300	1.679	1.729
35	5.911	5.080	5.278	5.047
37	5.618	5.332	4.536	4.570
39	5.452	5.387	5.487	5.244
41	5.413	5.343	14.276	14.285
43	5.261	5.330	5.279	5.437
45	4.191	3.853	5.706	14.285
47	15.608	15.572	15.585	15.587

MISCELLANEOUS TEST SECTION DATA

PROBE TANGENTIAL POSITION (IN.)	PROBE SPANWISE POSITION (IN.)	PROBE ANGLE (REF. TANG.) (DEG.)	TEST SECTION ANGLE (REF. HORIZ) (DEG.)	TUNNEL TOTAL TEMPERATURE (DEG.R)
7.166	.907	35.737	31.510	554.528

ORIGINAL PAGE IS
OF POOR QUALITY

SUPERSONIC COMPRESSOR CASCADE
NASA TRANSLATION CASCADE

NOZZLE EXIT CONDITIONS

MN1C	PT1C	TT1C	M1C	BETA1C
1.300	15.573	554.528	7.290	58.490

TEST SECTION AND CASCADE INLET PERFORMANCE
BASED ON SIDEWALL STATIC PRESSURES

	SCANIVALVE PORT #	SCANIVALVE NO. 2	MACH NUMBER
BLADE	27	5.550	1.309
BLADE	29	5.430	1.325
BLADE	31	5.412	1.328
BLADE	33	5.300	1.343
BLADE	35	5.082	1.373

SUPERSONIC FLOW PROPERTIES ACROSS LEADING WEDGE

WEDGE UPSTREAM MACH NO.	+ COMPRESSION - EXPANSION OF FLOW	WAVE ANGLE	DOWNSTREAM MACH NUMBER	TOTAL PRESSURE RATIO	STATIC PRESSURE RATIO
1.300	-.540	49.271	1.320	1.000	.974

SUPERSONIC COMPRESSOR CASCADE
NASA TRANSLATION CASCADE

CASCADE PHYSICAL DESIGN PARAMETERS

STAGGER ANGLE (DEG)	CHORD (IN)	BLADE SPACING (IN)	T/C RATIO	EXIT TO INLET SPAN RATIO (BLADE EXIT)	EXIT TO INLET SPAN RATIO (PROBE MEASURING PLANE)
51.700	3.000	1.979	.038	1.000	1.000

INLET METAL ANGLE PS (DEGREES)	INLET METAL ANGLE SS (DEGREES)	INLET METAL ANGLE ML (DEGREES)	EXIT METAL ANGLE ML (DEG.)
51.350	55.350	53.440	47.050

CASCADE INLET CONDITIONS

M)1	PT)1	TT)1	BETA)1	P)1	R)1	Q)1
1.390	15.573	554.528	57.940	5.472	.344	6.670

T)SS	I)ML	MN)X,1	MN)Y,1	TT/T)1	PT/P)1	RE/10**6
2.5[illegible]	4.500	.700	1.118	1.348	2.846	1.167

ORIGINAL PAGE IS OF POOR QUALITY

SUPERSONIC COMPRESSOR CASCADE
NASA TRANSLATION CASCADE

CASCADE IDEAL PERFORMANCE
BASED ON SIDEWALL STATIC PRESSURES

PRESSURE DATA FROM SCANIVALVE - PSIA

SCANIVALVE PORT #	SCANIVALVE NO. 3	SCANIVALVE PORT #	SCANIVALVE NO. 3
23	5.411	33	5.768
25	5.225	35	5.911
27	5.036	37	5.618
29	5.255	39	5.452
31	5.438	41	5.413

MEAN EXIT STATIC PRESSURE (PSIA)	RMS DEVIATION	MEAN EXIT MID-PASSAGE STATIC PRESSURE (PSIA)	RMS DEVIATION	IDEAL EXIT MACH NO.	CASCADE IDEAL STATIC PRESSURE RATIO (P)2/(P)1
5.273	.145	5.632	.188	1.347	.964

SUPERSONIC COMPRESSOR CASCADE
NASA TRANSLATION CASCADE

INSTRUMENTED BLADE PARAMETERS

	PRESSURE SURFACE (PS)	SUCTION SURFACE (SS)	DPS/Q1 (PS)	DSS/Q1 (SS)	PS/PT)1	SS/PT)1	PERCENT CHORD (PS)	PERCENT CHORD (SS)
11	6.460	4.818	.148	-.096	.415	.339	5.00	4.99
13	6.631	4.684	.174	-.088	.425	.314	15.08	15.01
15	6.430	5.085	.144	-.056	.413	.326	20.06	25.01
17	5.946	5.201	.071	-.041	.382	.334	25.07	33.30
19	5.521	4.883	.007	-.088	.355	.314	33.44	40.01
21	4.814	4.168	-.299	-.196	.309	.268	40.16	52.12
23	4.430	4.457	-.156	-.152	.284	.286	48.18	60.26
25	3.714	4.943	-.264	-.079	.238	.317	60.24	75.53
27	3.239	5.745	-.335	.041	.208	.369	75.37	85.66
29	5.988	4.456	.077	-.152	.385	.286	85.43	90.76

FC	FC)X	FC)Y	BETA)F	CD)1	CL)1	MC)LE	CP)LE
.012	.012	.006	1.943	-.008	.009	-.044	-368.889

SUPERSONIC COMPRESSOR CASCADE
NASA TRANSLATION CASCADE

LOCAL CASCADE EXIT PERFORMANCE

PERCT	Y DEV PT)YP	MA)2 TURN P)TP	MA)X,2 M)2 P)PP	MA)Y,2 P)2/P)1 P)NP	PT)2 V)2 P)SP	P)2 PT)C BETA)P	PT)2/PT)1 PT)C PT)1	BETA)2 PT)0,A TT)1
	3.231	1.206	.716	.971	14.405	5.893	.925	53.582
.00	6.532	4.358	.000	1.077	1225.333	15.573	15.533	15.553
	14.291	7.528	7.650	7.716	7.493	-.688	15.553	554.872
	3.330	1.165	.647	.968	14.614	6.306	.938	56.244
5.07	9.194	1.696	.018	1.152	1192.415	15.573	15.551	15.562
	14.540	8.331	7.981	7.552	8.278	1.974	15.562	553.148
	3.429	1.103	.587	.934	14.848	6.926	.953	57.844
10.01	10.794	.096	.018	1.266	1141.812	15.573	15.537	15.555
	14.822	8.901	8.280	8.542	8.783	3.574	15.555	553.493
	3.528	1.138	.507	.962	15.065	6.728	.967	57.753
15.01	10.723	.187	.018	1.229	1170.448	15.573	15.549	15.561
	15.017	8.785	8.158	8.403	8.689	3.483	15.561	554.528
	3.627	.953	.573	.762	14.947	8.328	.960	53.074
20.01	6.024	4.866	.019	1.522	1011.914	15.573	15.539	15.556
	14.944	9.290	9.275	9.121	9.375	-1.196	15.556	552.803
	3.726	.944	.543	.772	14.680	8.263	.943	54.910
25.01	7.860	3.032	.019	1.510	1003.824	15.573	15.543	15.558
	14.676	9.101	9.005	8.934	9.304	.640	15.558	553.493
	3.825	1.291	.603	.909	15.020	7.109	.964	56.429
30.02	9.379	1.511	.019	1.299	1131.977	15.573	15.546	15.560
	15.021	8.942	8.564	8.614	9.008	2.159	15.560	553.148

SUPERSONIC COMPRESSOR CASCADE
NASA TRANSLATION CASCADE

LOCAL CASCADE EXIT PERFORMANCE

PERCT	Y DEV PT)YP	MN)2 TURN P)TP	MN)X,2 M)2 P)RP	MN)Y,2 P)2/P)1 P)NP	PT)2 V)2 P)SP	P)2 PT)0 BETA)P	PT)2/PT)1 PT)C PT)1	BETA)2 PT)C,A TT)1
	3.924	1.150	.619	.969	15.977	6.632	.968	57.433
35.02	14.383	.507	.018	1.212	1182.238	15.573	15.547	15.560
	15.216	8.650	8.076	8.208	8.733	3.163	15.560	554.528
	4.023	1.190	.628	1.011	15.016	6.273	.964	58.125
40.02	11.075	-.185	.018	1.146	1212.529	15.573	15.546	15.560
	14.929	8.324	7.812	7.854	8.370	3.855	15.560	554.872
	4.122	1.207	.625	1.733	14.568	5.992	.942	58.843
45.03	11.793	-.423	.017	1.095	1226.158	15.573	15.558	15.566
	14.535	8.044	7.216	7.464	8.041	4.573	15.566	554.528
	4.221	.884	.443	.765	11.526	6.928	.740	59.941
50.03	12.891	-2.201	.015	1.266	949.256	15.573	15.561	15.567
	11.500	7.717	7.088	7.104	7.455	5.671	15.567	554.183
	4.320	.911	.527	.743	11.322	6.610	.727	54.639
55.03	7.589	3.301	.014	1.208	973.783	15.573	15.558	15.566
	11.322	7.229	7.187	7.035	7.082	.369	15.566	554.183
	4.419	1.288	.754	1.042	14.837	5.465	.953	54.092
60.03	7.042	3.846	.016	.999	1266.771	15.573	15.549	15.561
	14.567	7.093	7.126	7.266	7.109	-.178	15.561	554.872
	4.518	1.366	.722	1.092	15.136	5.394	.972	56.528
65.04	9.478	1.412	.018	.986	1304.264	15.573	15.541	15.557
	14.796	7.246	6.822	7.209	7.059	2.258	15.557	553.838

ORIGINAL PAGE IS
OF POOR QUALITY

SUPERSONIC COMPRESSOR CASCADE
NASA TRANSLATION CASCADE

LOCAL CASCADE EXIT PERFORMANCE

PERCT	Y	MN)2	MN)X,2	MN)Y,2	FT)2	P)2	PT)2/PT)1	BETA)2
	DEV	TURN	M)2	P)2/P)1	V)2	PT)0	PT)C	PT)0,A
	PT)YP	F)TP	P)BP	P)NP	F)SP	BETA)P	PT)1	TT)1
	4.617	1.313	.705	1.107	15.170	5.382	.974	57.495
70.04	10.445	.445	.017	.984	1306.673	15.573	15.536	15.555
	14.817	7.339	6.733	7.037	7.167	3.225	15.555	554.183
	4.716	1.346	.719	1.138	15.230	5.162	.978	57.721
75.04	10.671	.219	.017	.943	1331.042	15.573	15.536	15.555
	14.776	7.150	6.501	6.759	6.886	3.451	15.555	553.838
	4.815	1.336	.736	1.115	15.178	5.214	.975	56.579
80.04	9.529	1.361	.017	.953	1324.003	15.573	15.549	15.561
	14.759	7.134	6.701	6.710	6.985	2.309	15.561	553.838
	4.914	1.292	.773	1.035	15.040	5.489	.966	53.273
85.05	6.223	4.667	.018	1.003	1291.185	15.573	15.548	15.561
	14.750	7.193	7.379	7.120	7.065	-.997	15.561	553.838
	5.013	1.131	.711	.879	14.866	6.697	.955	51.040
90.05	3.990	6.906	.020	1.224	1164.812	15.573	15.548	15.561
	14.826	8.143	8.715	8.515	8.447	-3.230	15.561	554.528
	5.112	1.184	.695	.958	14.987	6.310	.962	54.039
95.05	6.989	3.901	.028	1.153	1207.815	15.573	15.566	15.569
	14.899	8.278	8.121	7.969	8.238	-.231	15.569	554.872
	5.211	1.246	.723	1.014	15.267	5.931	.980	54.509
100.06	7.459	3.431	.019	1.084	1256.032	15.573	15.546	15.560
	15.078	7.712	7.566	7.604	7.836	.239	15.560	553.493

SUPERSONIC COMPRESSOR CASCADE
NASA TRANSLATION CASCADE

LOCAL CASCADE EXIT PERFORMANCE

PERCT	Y DEV PT)YP	MN)2 TURN P)TP	MN)X,2 M)2 P)RP	MN)Y,2 P)2/P)1 P)KP	FT)2 V)2 P)SP	P)2 PT)C BETA)P	PT)2/PT)1 PT)C PT)1	BETA)2 PT)C,A TT)1
	5.310	1.256	.747	1.209	15.184	5.821	.975	53.492
105.06	6.442	4.446	.019	1.264	1263.644	15.573	15.540	15.556
	14.976	7.486	7.634	7.485	7.697	-.778	15.556	554.528
	5.409	1.272	.738	1.036	15.105	5.669	.970	54.558
110.06	7.5[illegible]8	3.382	.019	1.036	1276.085	15.573	15.538	15.556
	14.861	7.365	7.331	7.332	7.543	.288	15.556	554.183
	5.[illegible]	1.333	.721	1.121	15.252	5.264	.979	57.232
115.06	10.192	.718	.018	.962	1321.457	15.573	15.547	15.560
	14.860	7.155	6.596	6.924	7.097	2.962	15.560	553.148
	5.6[illegible]7	1.289	.824	.991	15.039	5.516	.966	50.264
120.07	3.214	7.676	.019	1.006	1289.126	15.573	15.526	15.550
	14.749	6.815	7.567	7.177	7.258	-4.006	15.550	554.183
	5.766	1.256	.753	1.005	14.669	5.623	.942	53.179
125.07	6.129	4.761	.020	1.028	1263.752	15.573	15.545	15.559
	14.468	7.199	7.398	7.266	7.408	-1.091	15.559	554.528
	5.805	1.269	.774	1.006	14.869	5.598	.955	52.437
130.07	5.387	5.503	.019	1.023	1274.306	15.573	15.553	15.563
	14.631	7.128	7.466	7.113	7.478	-1.933	15.563	555.562
	5.[illegible]4	1.246	.755	1.042	14.834	5.461	.953	54.087
135.06	7.037	3.653	.019	.958	1287.118	15.573	15.550	15.562
	14.561	7.261	7.305	7.039	7.368	-.183	15.562	554.528

SUPERSONIC COMPRESSOR CASCADE
NASA TRANSLATION CASCADE

LOCAL CASCADE EXIT PERFORMANCE

PERCT	Y DEV PT)YP	MN)2 TURN P)TP	MN)X,2 M)2 P)BP	MN)Y,2 P)2/P)1 P)NP	PT)2 V)2 P)SP	P)2 PT)0 BETA)P	PT)2/PT)1 PT)0 PT)1	BETA)2 PT)0,A T)1
	6.003	1.235	.723	.996	13.536	5.364	.869	54.029
142.08	6.979	3.911	.918	.980	1244.289	15.573	15.543	15.558
	13.492	6.914	6.958	6.783	7.133	-.241	15.558	553.838
	6.102	1.332	.759	1.095	14.863	5.134	.954	55.262
145.08	8.212	2.678	.917	.938	1321.051	15.573	15.542	15.557
	14.456	6.759	6.577	6.710	7.052	.992	15.557	552.803
	6.231	1.214	.591	.824	11.046	5.735	.709	54.342
151.75	7.232	3.598	.915	1.048	1065.847	15.573	15.545	15.559
	11.041	6.731	6.722	6.379	6.792	.072	15.559	555.562
	6.300	1.135	.728	.871	11.790	5.282	.757	50.090
155.09	3.240	7.850	.916	.965	1168.317	15.573	15.544	15.558
	11.752	6.466	7.053	6.491	6.671	-4.180	15.558	554.528
	6.349	1.332	.819	1.051	14.761	5.097	.948	52.057
162.09	5.027	5.883	.918	.932	1321.180	15.573	15.546	15.560
	14.355	6.473	6.877	6.756	6.797	-2.213	15.560	554.528
	6.498	1.362	.831	1.079	15.191	5.035	.975	52.377
165.09	5.327	5.503	.919	.920	1342.639	15.573	15.539	15.556
	14.691	6.456	5.810	6.659	6.802	-1.893	15.556	554.872
	6.547	1.371	.802	1.112	15.147	4.957	.973	54.192
170.09	7.142	3.748	.918	.906	1349.245	15.573	15.553	15.563
	14.619	6.556	5.584	6.544	6.672	-.078	15.563	553.493

SUPERSONIC COMPRESSOR CASCADE
NASA TRANSLATION CASCADE

LOCAL CASCADE EXIT PERFORMANCE

PERC1	Y DEV PT1YP	MN2 TURN P1TP	MN1X,2 M2 P1BP	MN1Y,2 P2/P11 P1AP	PT2 V2 P1SP	P2 PT1O BETA1P	PT2/PT11 PT1C FT1	BETA2 PT1O,A TT1
175.10	6.696 7.566 14.615	1.390 3.292 6.481	.804 .018 6.410	1.133 .886 6.416	15.212 1362.421 6.570	4.851 15.573 .378	.977 15.540 15.556	54.648 15.556 554.528
180.10	6.795 7.822 14.589	1.399 3.268 6.423	.805 .018 6.311	1.144 .875 6.351	15.223 1369.195 6.501	4.788 15.573 .602	.978 15.537 15.555	54.872 15.555 553.493
185.10	6.894 7.740 14.554	1.401 3.150 6.384	.808 .018 6.287	1.144 .872 6.339	15.192 1370.182 6.480	4.769 15.573 .520	.976 15.538 15.556	54.790 15.556 554.528
190.11	6.993 5.665 14.519	1.378 5.025 6.403	.831 .018 6.653	1.100 .892 6.481	15.070 1354.329 6.460	4.883 15.573 -1.355	.968 15.545 15.559	52.915 15.559 554.528
195.11	7.092 4.556 14.519	1.282 6.334 6.878	.796 .019 7.367	1.004 1.001 7.404	14.786 1283.433 6.948	5.478 15.573 -2.664	.949 15.544 15.559	51.606 15.559 555.217
200.11	7.191 7.235 14.791	1.298 3.605 7.209	.753 .019 7.205	1.048 1.008 7.224	15.077 1297.270 7.244	5.514 15.573 .015	.968 15.542 15.557	54.285 15.557 554.528

SUPERSONIC COMPRESSOR CASCADE
NASA TRANSLATION CASCADE

MASS AVERAGED EXIT CONDITIONS

MN)2	BETA)2	PT)2/PT)1
1.229	54.656	.942

CASCADE EXIT PARAMETERS
BASED ON MASS AVERAGED CONDITIONS

MN)X,2	MN)Y,2	PT)2	P)2	TT)2	TT)2/T)2	M)2/M)1
.711	1.003	14.667	5.820	554.528	1.302	1.041

MIXED EXIT CONDITIONS

MN)X,2	MN)Y,2	PT)2	P)2	TT)2	TT)2/T)2	MN)2	BETA)2
.685	.994	14.569	5.940	554.528	1.292	1.207	55.442

ORIGINAL PAGE IS
OF POOR QUALITY

SUPERSONIC COMPRESSOR CASCADE
NASA TRANSLATION CASCADE

OVERALL PERFORMANCE

MASS AVERAGED EXIT CONDITIONS

P)2/P)1	PT)2/PT)1	V)2/V)1	V)2/V)1,X	V)2/V)1,Y	R)2/R)1	T)2/T)1	OMEGA
TPLP	DF	DF)EQ	DV)Y	RN)2	DPS/Q1	DEV	TURN
BETA)C	A)2/A)1						
1.003	.942	.948	1.033	.912	1.027	1.035	.090
.017	.077	1.198	.074	1.107	.052	7.606	3.284
56.966	.942						

OVERALL PERFORMANCE

MIXED EXIT CONDITIONS

P)2/P)1	PT)2/PT)1	V)2/V)1	V)2/V)1,X	V)2/V)1,Y	R)2/R)1	T)2/T)1	OMEGA
TPLP	DF	DF)EQ	DV)Y	RN)2	DPS/Q1	DEV	TURN
BETA)C	A)2/A)1						
1.087	.935	.935	.990	.908	1.041	1.044	.099
[illegible]	.091	1.216	.078	1.100	.072	8.392	2.498
[illegible]	.961						

SUPERSONIC COMPRESSOR CASCADE
NASA-II TRANSLATION MODE CASCADE

FILE NAME NAS01

CASCADE INLET MACH NUMBER	CASCADE IDEAL STATIC PRESSURE RATIO	CASCADE EXCITATION FREQUENCY	INTERBLADE PHASE ANGLE
1.32	1.065	238	0°

DATA AQUISITION RATE PER CHANNEL (PTS/SEC)	SIGMA LIMITS	RELATIVE VELOCITY (FT/SEC)	INLET AIR ANGLE	REDUCED FREQUENCY
6923	2.00	1318	57.94	.142

APPENDIX B

Sample of Time Variant Aerodynamics Computer Print Out

Refer to Section VII for item identification and explanation of meanings.

DATA ANALYSIS OF POSITIVE PEAK

	1		2		3		4		5		6	
1	.7	.006	-.2	.064	.5	.038	.3	.025	.3	.052	.4	.078
2	4.9	.006	4.1	.062	4.7	.037	4.4	.024	4.6	.053	4.6	.078
3	9.1	.006	8.3	.063	8.9	.034	8.6	.024	8.8	.053	8.7	.076
4	13.3	.006	12.4	.058	13.1	.040	12.8	.025	12.9	.052	12.9	.077
5	17.4	.006	16.7	.060	17.3	.037	17.0	.024	17.2	.051	17.1	.079
6	21.6	.006	20.9	.059	21.5	.034	21.2	.023	21.4	.052	21.3	.077
7	25.8	.006	25.1	.058	25.7	.036	25.4	.022	25.6	.051	25.5	.078
8	30.0	.006	29.3	.058	29.9	.036	29.6	.022	29.7	.050	29.7	.079
UNCORR MEAN		.006		.060		.036		.024		.052		.078
CORR MEAN		.006		.060		.036		.024		.052		.078
WITHIN 2.0 SIGMA	8		8		8		8		8		8	

	7a	7b	8a	8b	9a	9b	10a	10b	11a	11b	12a	12b
1	1.0	.056	2.8	.014	.1	.018	2.4	.015	2.9	.017	1.9	-.024
2	5.2	.057	7.1	.016	4.2	.025	6.6	.017	7.1	.019	3.3	.030
3	9.4	.061	11.2	.016	8.4	.025	10.8	.017	11.2	.016	7.5	.029
4	13.6	.056	15.4	.014	12.5	.022	15.0	.016	15.4	.018	11.7	.031
5	17.8	.056	19.6	.015	16.8	.021	19.1	.018	19.7	.019	15.9	.031
6	22.0	.065	23.8	.014	20.9	.027	23.2	.015	23.9	.015	20.0	.028
7	26.1	.062	28.0	.013	25.1	.030	27.6	.020	28.1	.016	24.3	.029
8	30.3	.061	32.2	.013	29.3	.027	31.8	.019	32.2	.014	28.4	.030
UNCORR MEAN		.059		.014		.024		.017		.017		.023
CORR MEAN		.059		.014		.024		.017		.017		.030
WITHIN 2.0 SIGMA		8		8		8		8		8		7

		13
1	2.9	.025
2	7.1	.024
3	11.3	.024
4	15.5	.024
5	19.6	.022
6	23.9	.020
7	28.1	.022
8	32.2	.024

UNCORR
MEAN .023

CORR
MEAN .024

WITHIN
2.0 SIGMA 7

DATA ANALYSIS OF NEGATIVE PEAK

	1		2		3		4		5		6	
1	2.8	.007	2.0	.065	2.5	.036	2.4	.019	2.5	.036	2.4	.070
2	7.0	.007	6.2	.062	6.8	.037	6.6	.020	6.7	.033	6.6	.071
3	11.2	.007	10.4	.064	10.9	.038	10.7	.021	10.9	.037	10.8	.070
4	15.3	.007	14.5	.063	15.1	.037	14.9	.019	15.1	.034	15.0	.070
5	19.5	.007	18.8	.065	19.4	.039	19.2	.021	19.2	.035	19.2	.070
6	23.7	.007	23.0	.066	23.6	.039	23.3	.021	23.4	.034	23.4	.068
7	27.9	.007	27.2	.065	27.7	.037	27.5	.020	27.6	.035	27.6	.072
8	32.1	.007	31.4	.067	31.9	.034	31.7	.020	31.8	.035	31.8	.072
UNCORR MEAN		.007		.065		.037		.020		.035		.070
CORR MEAN		.007		.065		.037		.020		.035		.070
WITHIN 2.0 SIGMA		7		8		8		8		8		8

AVERAGE OF POSITIVE AND NEGATIVE PEAKS

	1	2	3	4	5	6
UNCORR AVG	.006	.062	.037	.022	.043	.074
CORR AVG	.006	.062	.037	.022	.043	.074

		7		8		9		10		11		12
1	3.1	.072	.7	.019	2.2	.027	.6	.019	.8	.028	1.3	.010
2	7.3	.069	4.9	.019	6.3	.025	4.7	.018	5.1	.028	5.5	.012
3	11.5	.071	9.1	.021	10.6	.023	8.8	.024	9.2	.028	9.7	.014
4	15.7	.071	13.3	.020	14.8	.024	13.1	.019	13.4	.027	13.9	.012
5	19.8	.065	17.5	.018	18.8	.026	17.2	.021	17.6	.027	18.1	.011
6	24.0	.066	21.7	.020	23.1	.023	21.4	.022	21.8	.028	22.1	.020
7	28.2	.069	25.9	.020	27.4	.026	25.7	.018	26.0	.029	26.4	.014
8	32.4	.072	30.0	.021	31.6	.025	29.8	.019	30.1	.028	30.5	.011
UNCORR MEAN		.069		.020		.025		.020		.028		.013
CORR MEAN		.069		.020		.025		.020		.028		.012
WITHIN 2.0 SIGMA		8		8		8		8		7		7

AVERAGE OF POSITIVE AND NEGATIVE PEAKS

UNCORR AVG	.064	.017	.025	.019	.022	.018
CORR AVG	.064	.017	.025	.019	.022	.021

		13
1	.8	.033
2	5.0	.038
3	9.2	.036
4	13.4	.034
5	17.6	.033
6	21.7	.036
7	25.9	.038
8	30.1	.036

UNCORR
MEAN .035

CORR
MEAN .039

WITHIN
2.0 SIGMA 8

AVERAGE OF POSITIVE AND NEGATIVE PEAKS

UNCORR
AVG .029

CORR
AVG .029

AUTO-CORRELATION OF

TIME DEPENDENT DATA

NUMBER OF CHANELS	NUMBER OF POINTS	NUMBER OF LAGS	LAG TIME (MSEC)
13	230	46	.1444

CHANEL #	CYCLE TIME (MSEC)	FREQUENCY (HERTZ)
1	4.2050	237.812
2	4.1866	238.857
3	4.2050	237.815
4	4.1865	238.861
5	4.1782	239.336
6	4.1901	238.660
7	4.2072	237.689
8	4.2014	238.017
9	4.1956	238.348
10	4.1721	239.685
11	4.1936	238.460
12	4.1865	238.864
13	4.1988	238.165
MEAN		238.505
STANDARD DEVIATION		.612

CROSS CORRELATION OF

TIME DEPENDENT DATA

CHANNEL NUMBER	PHASE (DEG)	CORRECTED PHASE
2	-66.137	-55.705
3	-14.564	-14.257
4	-34.087	-23.325
5	-22.931	-22.044
6	-26.271	-15.699
7	27.665	28.567
8	185.599	196.778
9	-56.226	-55.331
10	156.084	167.318
11	192.814	195.409
12	226.061	236.861
13	192.367	193.955

NASA II TRANSLATION CASCADE

TAPE COUNT: NASAII-1,665
INLET MACH NO: 1.320
STATIC PRESSURE RATIO: 1.065
INLET STATIC PRESSURE: 5.500
FREQUENCY: 242.000
PHASE: 0
BLADE AMPLITUDE: .006

AIRFOIL PRESSURE SURFACE

KULITE NO.	SURFACE PRESSURE (PSI)	CORRECTED PRESSURE (PSI)	PHASE ANGLE (DEG)	CORRECTED PHASE (DEG)	PRESSURE COEFFICIENT
1	.0624	.0590	-55.700	-72.741	4.3954
2	.0369	.0194	-14.300	-26.373	1.4448
3	.0219	.0076	-23.300	-82.773	.5628
4	.0433	.0249	-22.000	-45.888	1.8577
5	.0740	.0480	-15.700	-30.317	3.5757
6	.0643	.0434	28.600	48.444	3.2344

AIRFOIL SUCTION SURFACE

KULITE NO.	SURFACE PRESSURE (PSI)	CORRECTED PRESSURE (PSI)	PHASE ANGLE (DEG)	CORRECTED PHASE (DEG)	PRESSURE COEFFICIENT
1	.0171	.0075	196.800	-43.498	.5558
2	.0246	.0404	-55.300	-27.862	3.0135
3	.0186	.0046	167.300	128.759	.3398
4	.0222	.0105	195.400	-158.514	.7820
5	.0208	.0158	236.900	-88.753	1.1749
6	.0293	.0078	194.000	-121.066	.5797

NET PRESSURE COEFFICIENT AND PHASE ACROSS AIRFOIL

KULITE NO	PRESSURE COEFFICIENT	PHASE ANGLE (DEG)
1	3.9199	-76.213
2	1.5697	150.767
3	.8707	-70.997
4	2.2760	-27.398
5	3.1253	-11.636
6	3.8059	50.033

COEFFICIENTS FOR AIRFOIL LIFT AND MOMENT

PERCENT CHORD	LOCAL SURFACE LIFT COEFFICIENTS REAL	LOCAL SURFACE LIFT COEFFICIENTS IMAGINARY
.0	.9009	3.8150
5.0	.9009	3.8150
10.0	.9009	3.8150
15.0	.9009	3.8150
20.0	-2.1913	1.6529
25.0	-1.3698	-.7666
30.0	-1.2793	.3874
35.0	-.5024	.9828
40.0	.2835	.8233
45.0	.6092	1.0594
50.0	1.0281	1.1910
55.0	1.5105	1.1928
60.0	2.0207	1.0474
65.0	2.3704	.9646
70.0	2.7196	.8258
75.0	3.0611	.6304
80.0	-3.0729	1.1397
85.0	2.4447	-2.9169
90.0	2.4447	-2.9169
95.0	2.4447	-2.9169
100.0	2.4447	-2.9169
AIRFOIL LIFT COEFFICIENT	.8349	.7137
AIRFOIL MOMENT COEFFICIENT	.2226	-.4684

APPENDIX C

Cascade Time Variant Data/Theory Correlation Plots

The data is correlated against the DDA variable amplitude analysis[3]. The pressure surface data is plotted as a solid symbol and the corresponding theory is plotted as a solid line. The suction surface data is plotted as an open symbol and the corresponding theory as a dashed line.

NASA II TRANSLATION CASCADE

PRESSURE SURFACE AERODYNAMIC PHASE LAG DISTRIBUTION

1.32 INLET MACH NUMBER
1.065 STATIC PRESSURE RATIO
3.14 INTERBLADE PHASE ANGLE ,rad (180°)

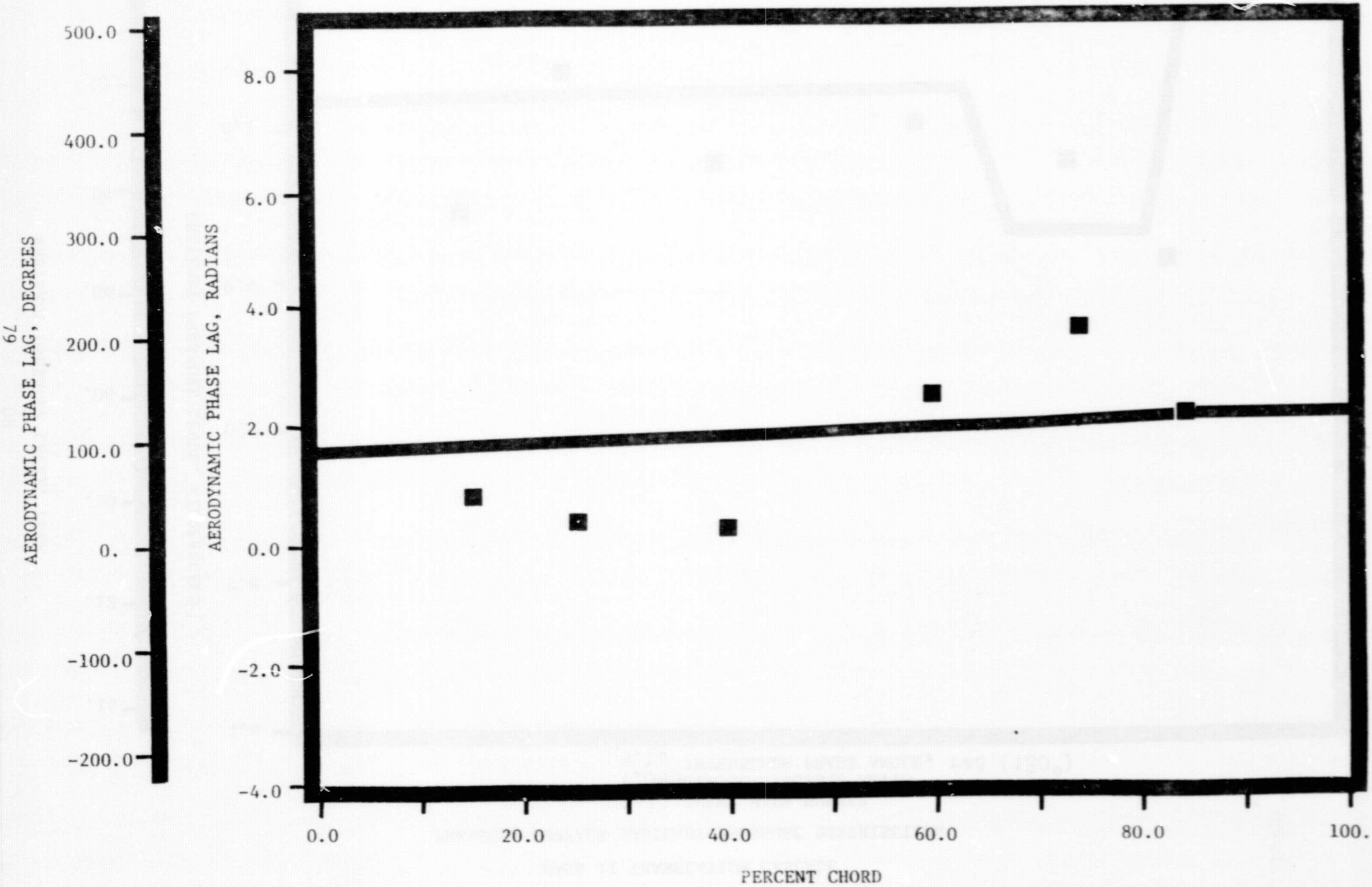

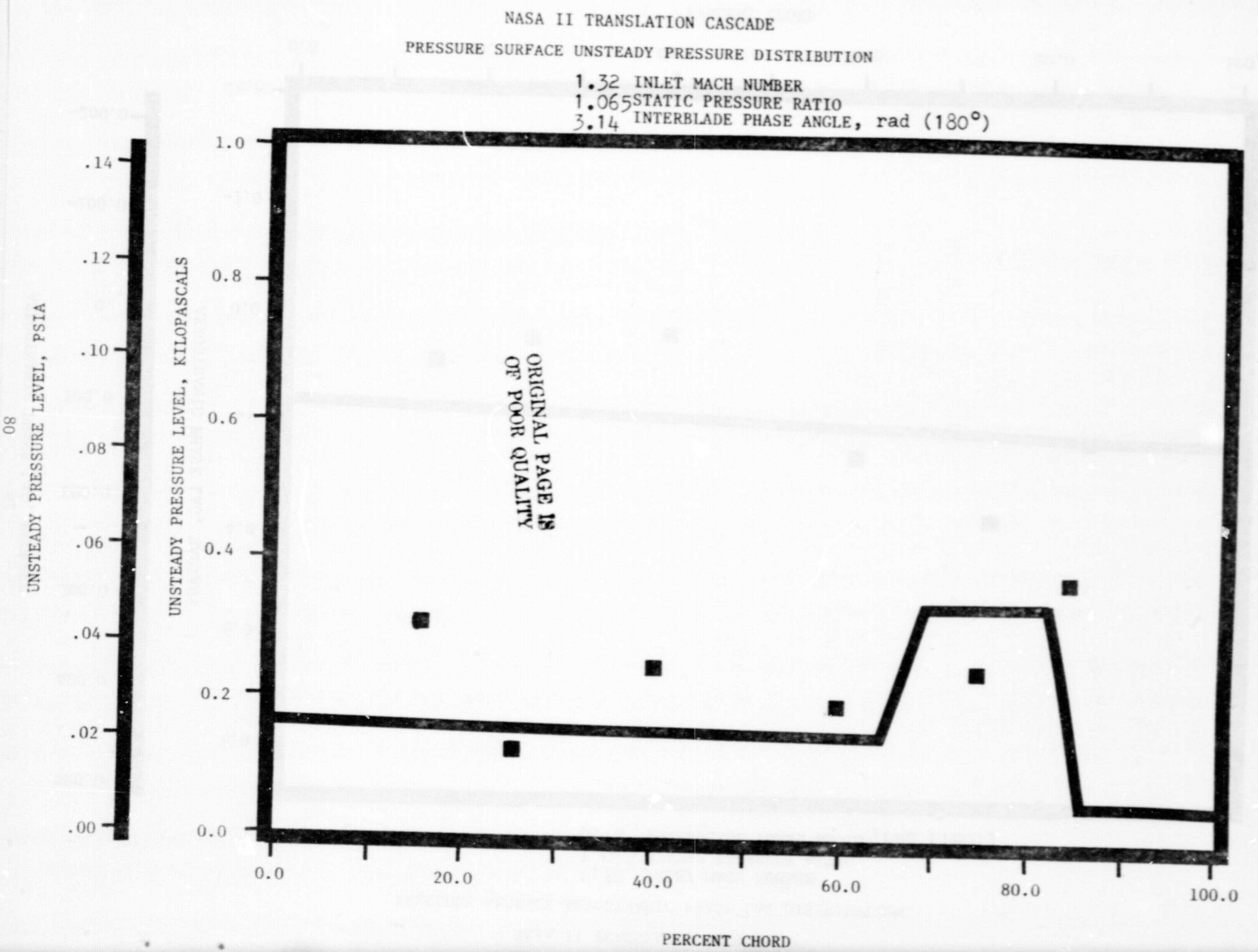

ORIGINAL PAGE IS
OF POOR QUALITY

NASA II TRANSLATION CASCADE

SUCTION SURFACE AERODYNAMIC PHASE LAG DISTRIBUTION

1.32 INLET MACH NUMBER
1.065 STATIC PRESSURE RATIO
3.14 INTERBLADE PHASE ANGLE, rad (180°)

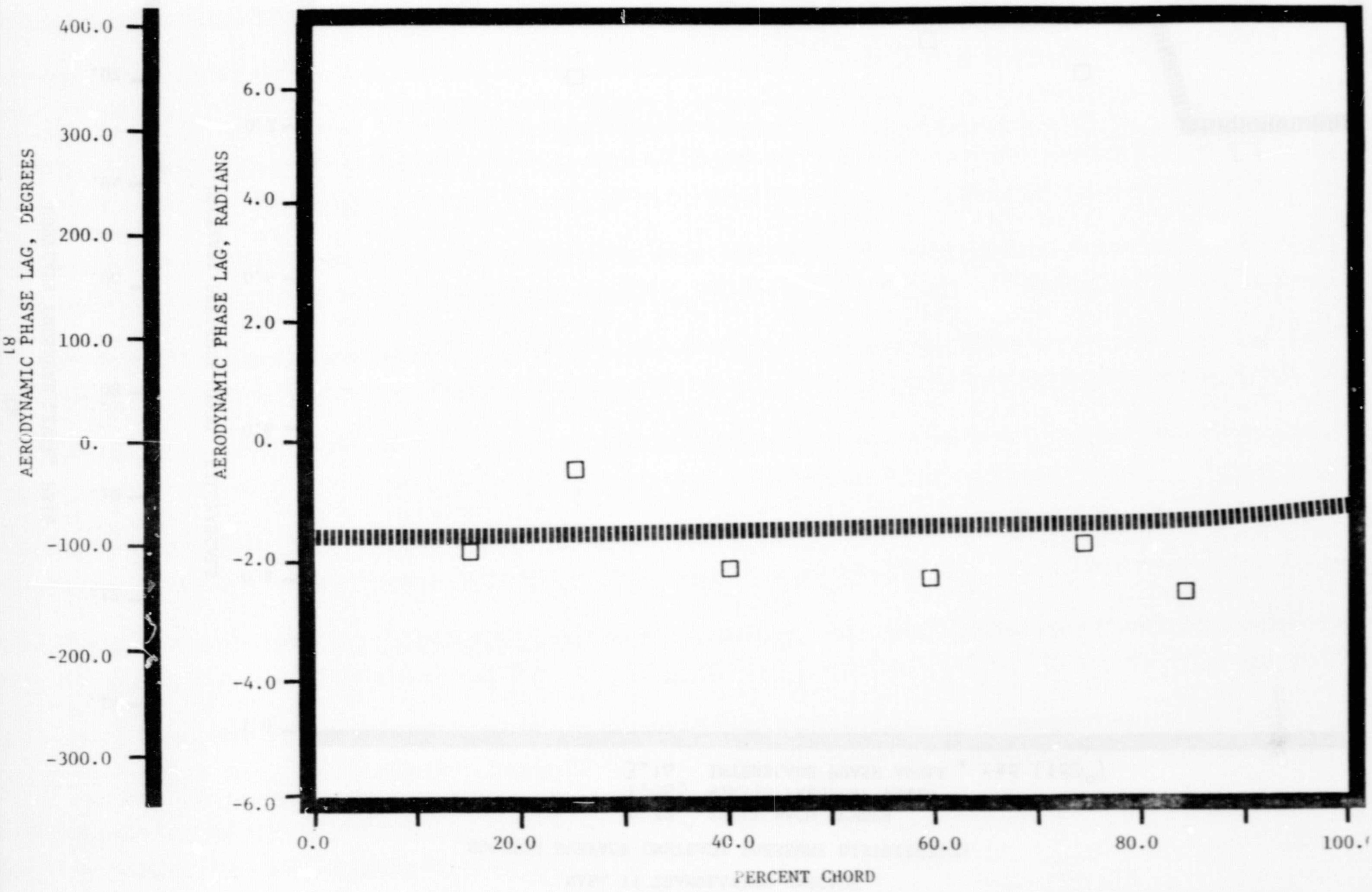

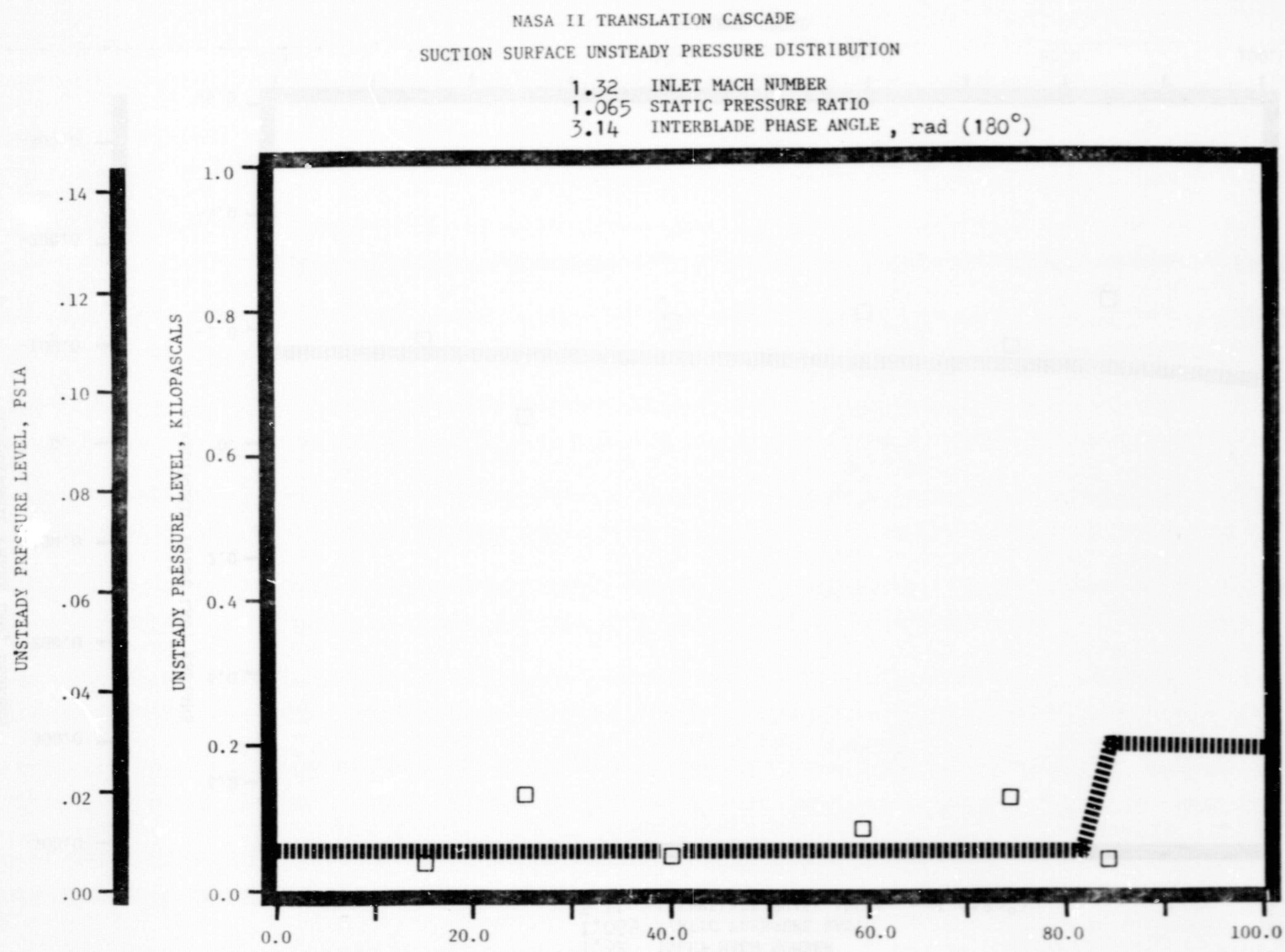

NASA II TRANSLATION CASCADE
SUCTION SURFACE UNSTEADY PRESSURE DISTRIBUTION
1.32 INLET MACH NUMBER
1.065 STATIC PRESSURE RATIO
3.14 INTERBLADE PHASE ANGLE, rad (180°)
UNSTEADY PRESSURE LEVEL, PSIA
.00
.02
.04
.06
.08
.10
.12
.14
UNSTEADY PRESSURE LEVEL, KILOPASCALS
0.0
0.2
0.4
0.6
0.8
1.0
0.0
20.0
40.0
60.0
80.0
100.0
PERCENT CHORD

NASA II TRANSLATION CASCADE

PRESSURE SURFACE AERODYNAMIC PHASE LAG DISTRIBUTION

1.32 INLET MACH NUMBER
1.065 STATIC PRESSURE RATIO
1.57 INTERBLADE PHASE ANGLE ,rad (90°)

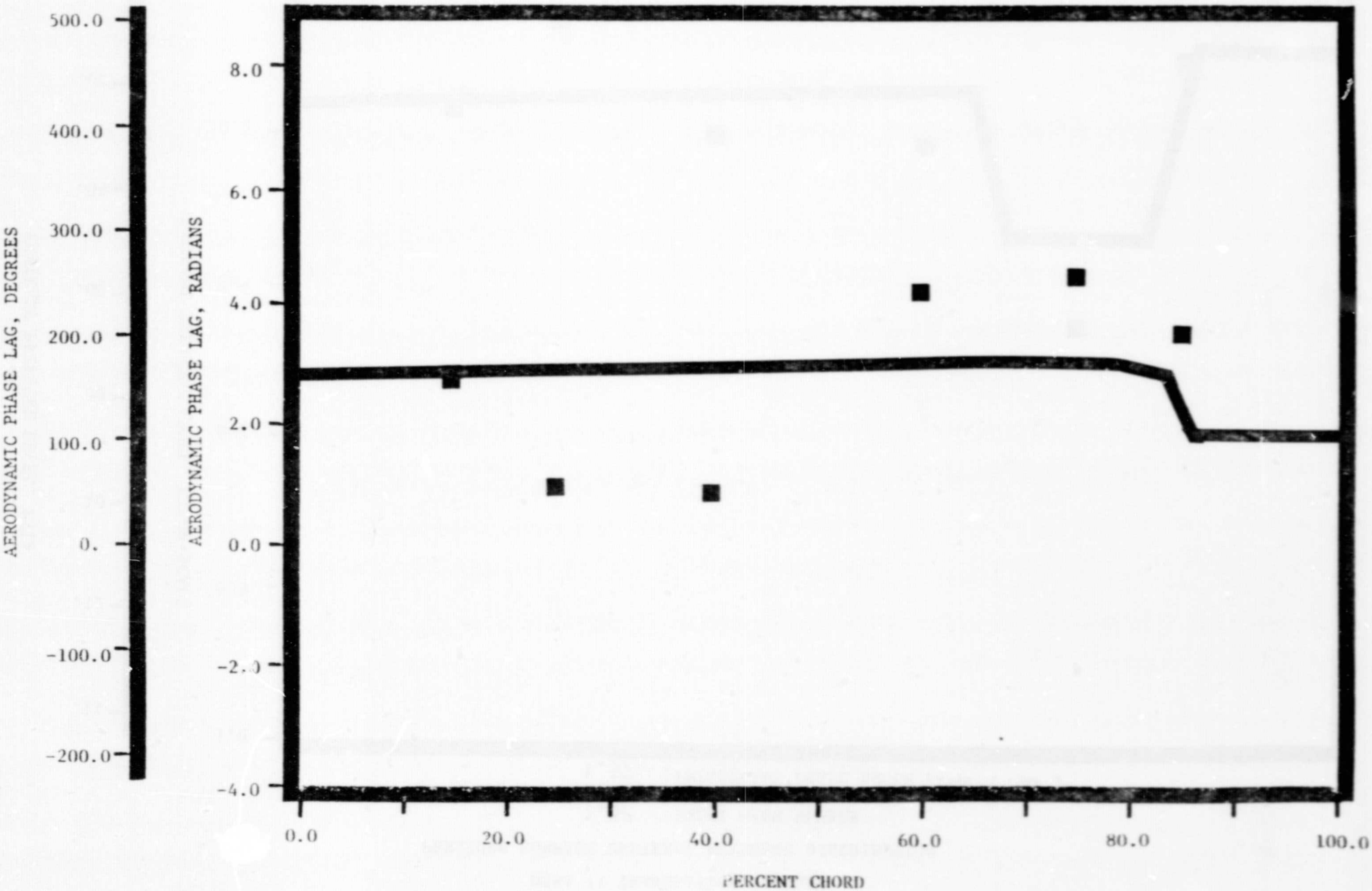

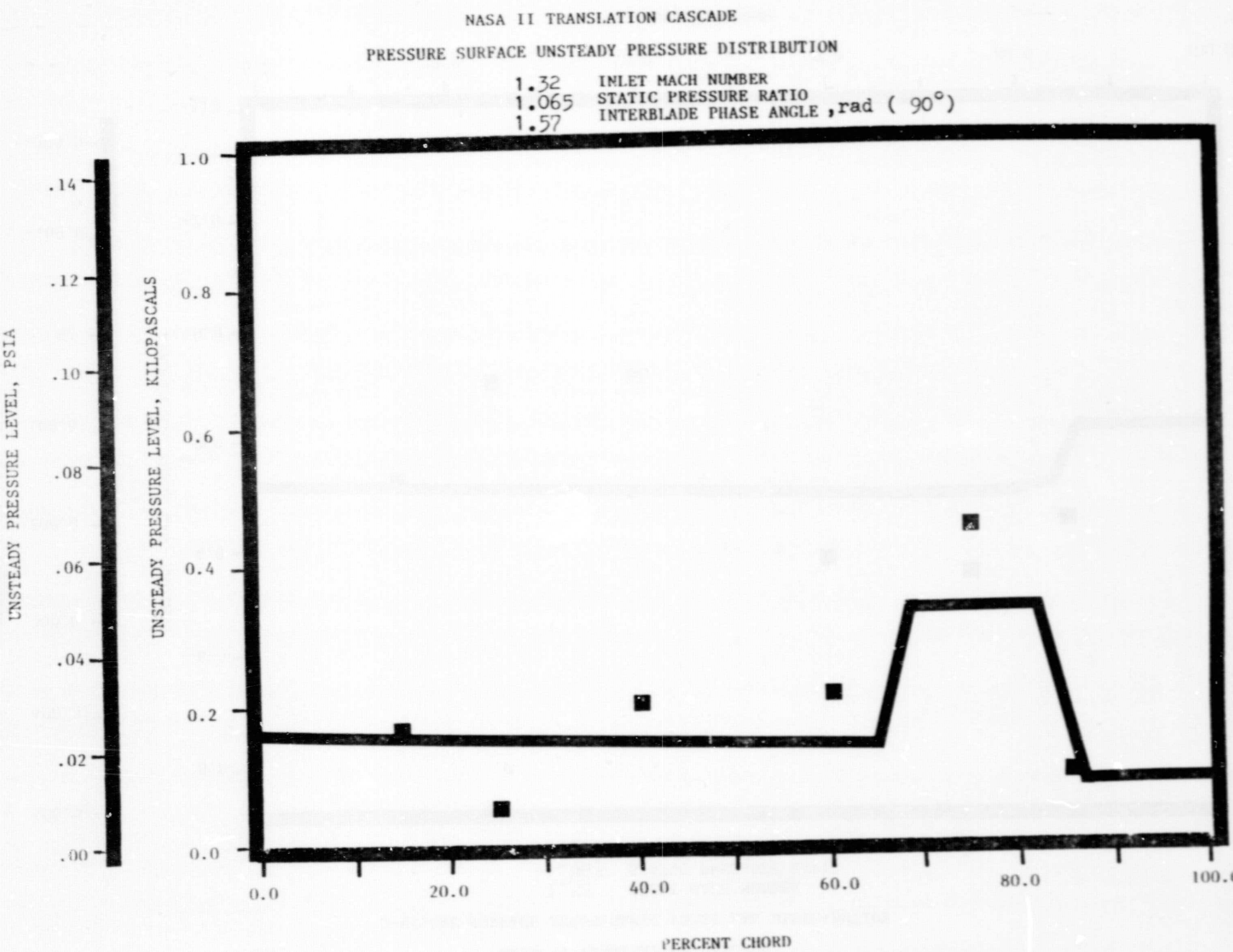
NASA II TRANSLATION CASCADE
PRESSURE SURFACE UNSTEADY PRESSURE DISTRIBUTION
1.32 INLET MACH NUMBER
1.065 STATIC PRESSURE RATIO
1.57 INTERBLADE PHASE ANGLE ,rad (90°)
UNSTEADY PRESSURE LEVEL, PSIA
.14
.12
.10
.08
.06
.04
.02
.00
UNSTEADY PRESSURE LEVEL, KILOPASCALS
1.0
0.8
0.6
0.4
0.2
0.0
0.0
20.0
40.0
60.0
80.0
100.0
PERCENT CHORD

NASA II TRANSLATION CASCADE

SUCTION SURFACE AERODYNAMIC PHASE LAG DISTRIBUTION

1.32 INLET MACH NUMBER
1.065 STATIC PRESSURE RATIO
1.57 INTERBLADE PHASE ANGLE, rad (90°)

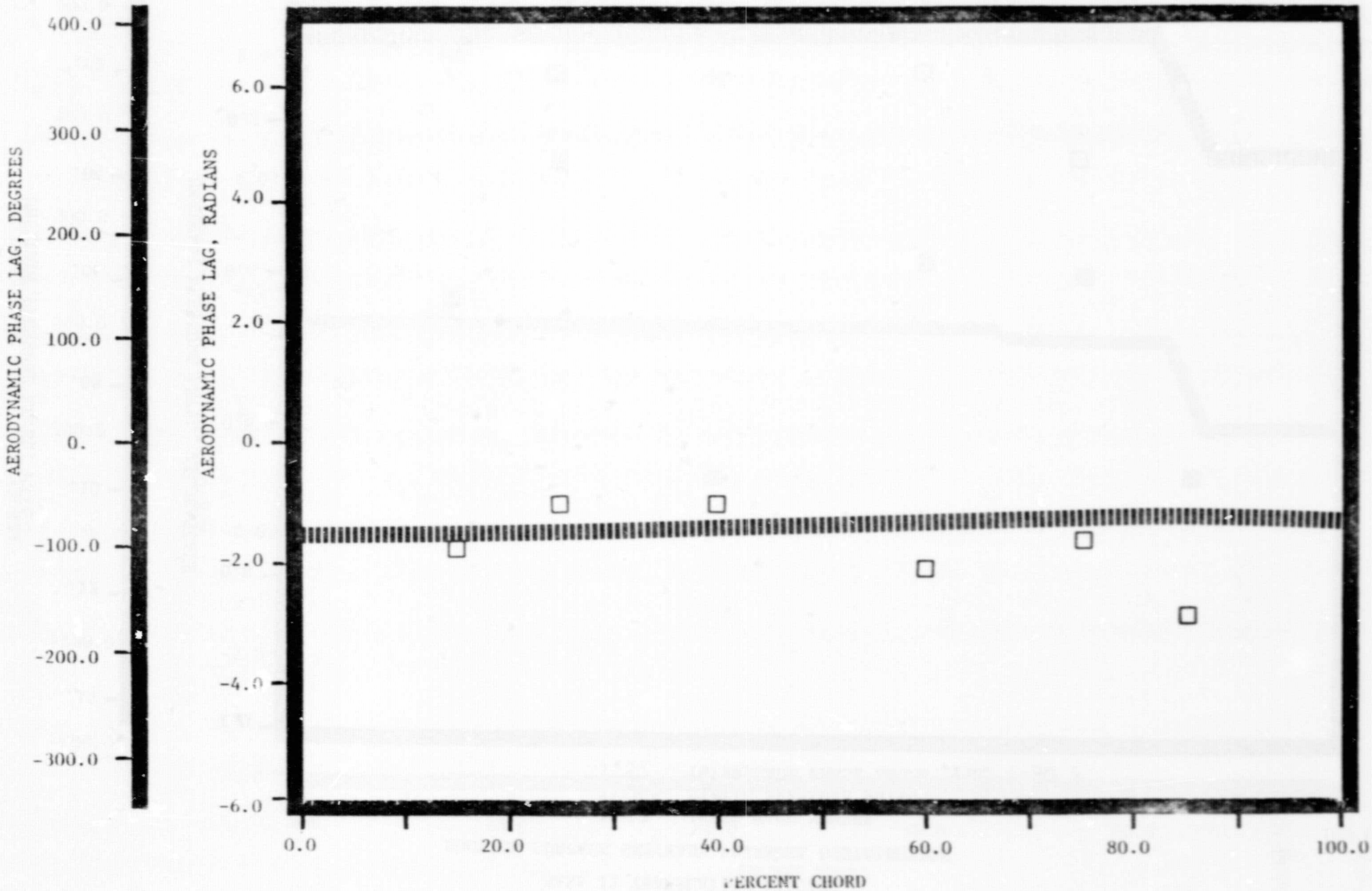

NASA II TRANSLATION CASCADE

SUCTION SURFACE UNSTEADY PRESSURE DISTRIBUTION

1.32 INLET MACH NUMBER
1.065 STATIC PRESSURE RATIO
1.57 INTERBLADE PHASE ANGLE ,rad (90°)

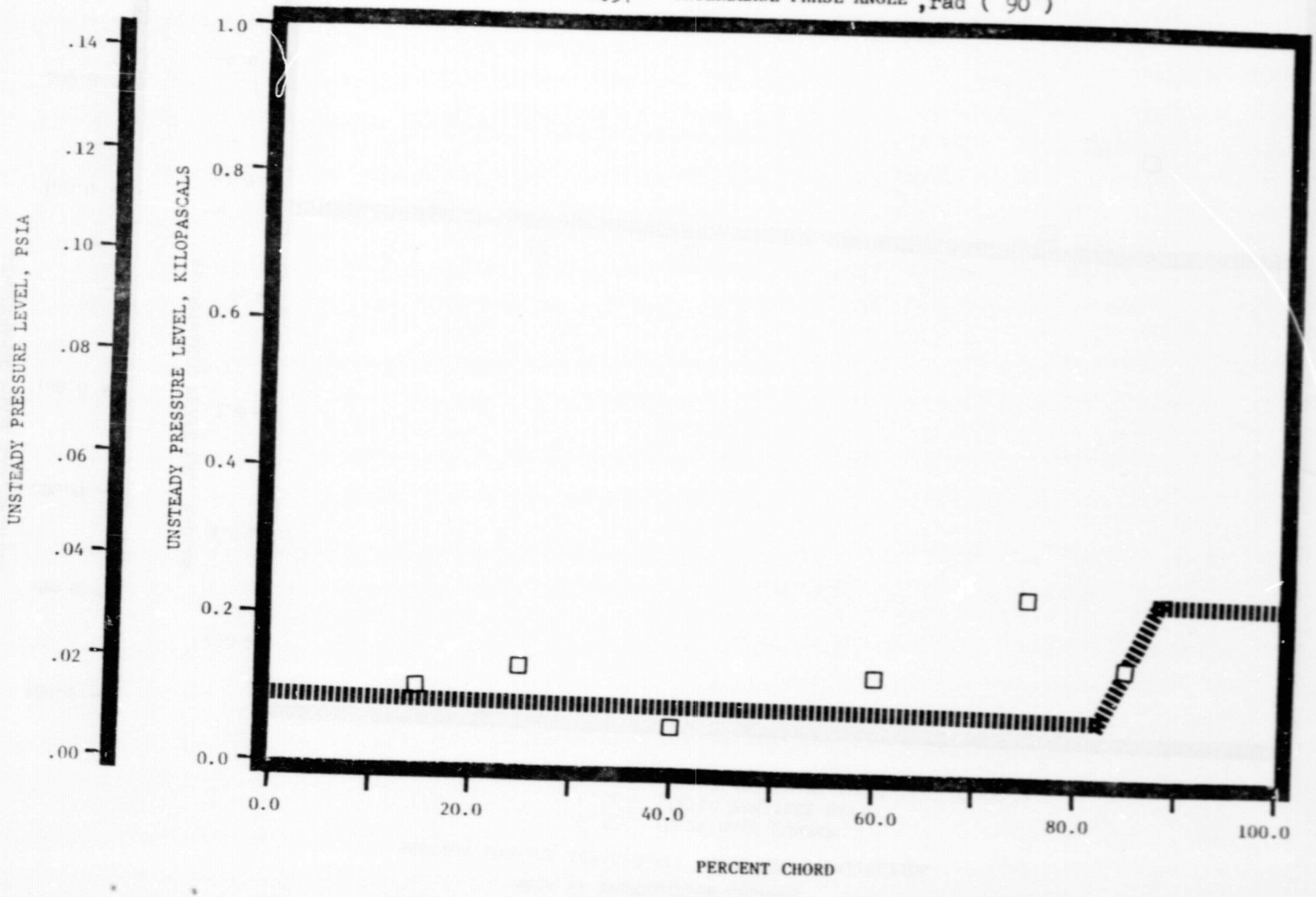

NASA II TRANSLATION CASCADE

PRESSURE SURFACE AERODYNAMIC PHASE LAG DISTRIBUTION

1.32 INLET MACH NUMBER
1.065 STATIC PRESSURE RATIO
1.05 INTERBLADE PHASE ANGLE ,rad (60°)

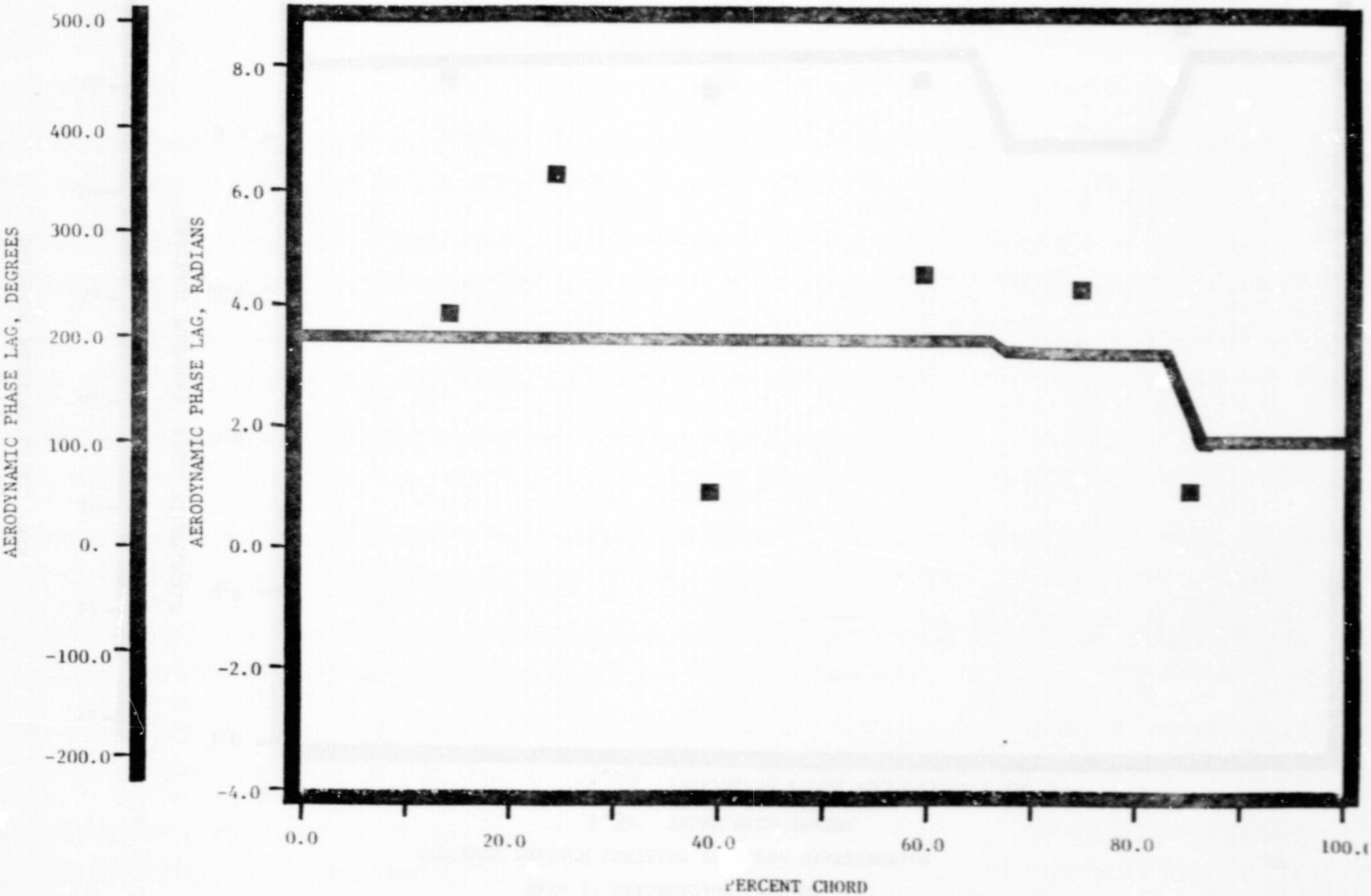

NASA II TRANSLATION CASCADE

PRESSURE SURFACE UNSTEADY PRESSURE DISTRIBUTION

1.32 INLET MACH NUMBER
1.065 STATIC PRESSURE RATIO
1.05 INTERBLADE PHASE ANGLE ,rad (60°)

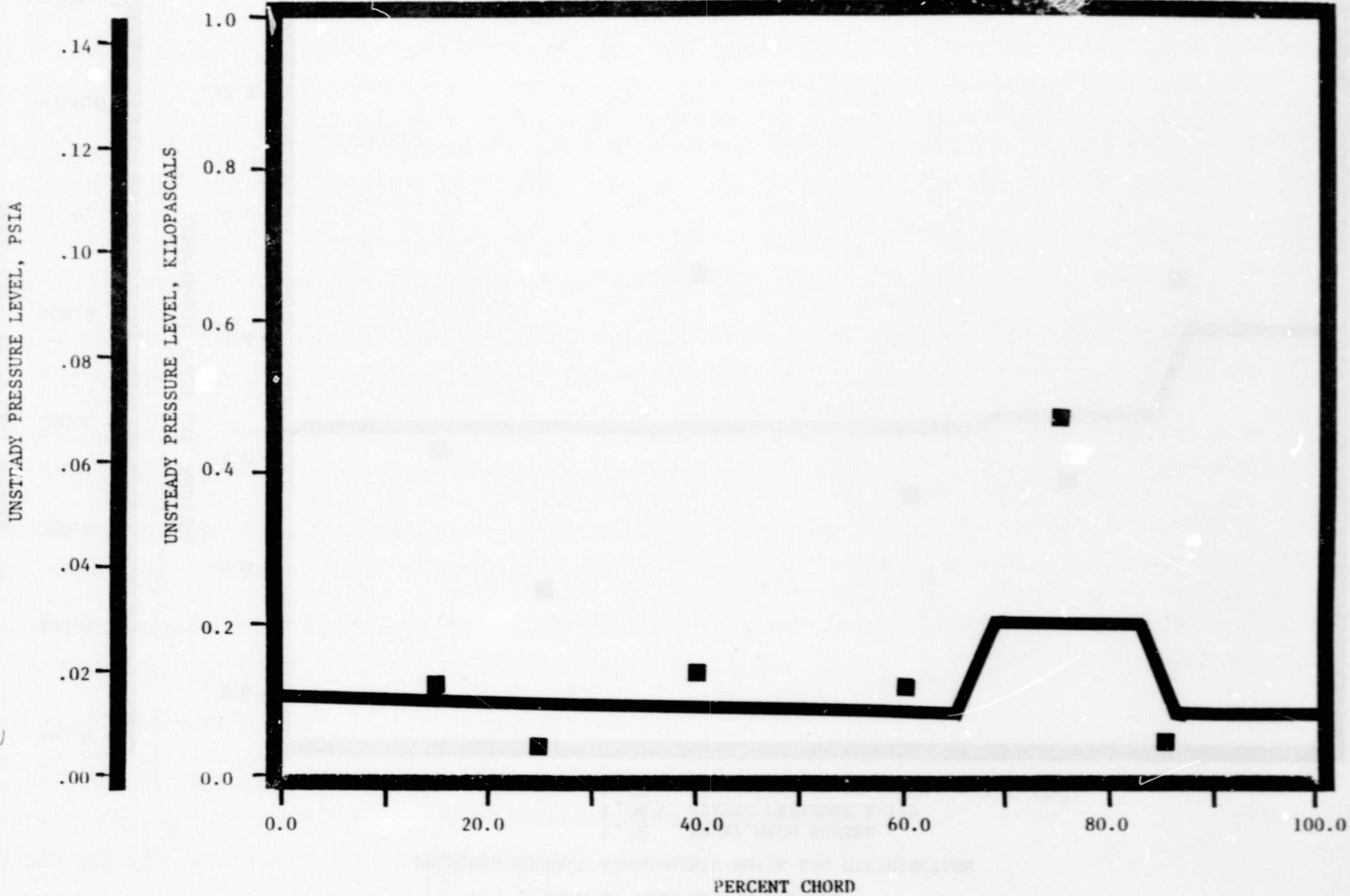

C-2

NASA II TRANSLATION CASCADE

SUCTION SURFACE AERODYNAMIC PHASE LAG DISTRIBUTION

1.32 INLET MACH NUMBER
1.065 STATIC PRESSURE RATIO
1.05 INTERBLADE PHASE ANGLE ,rad (60°)

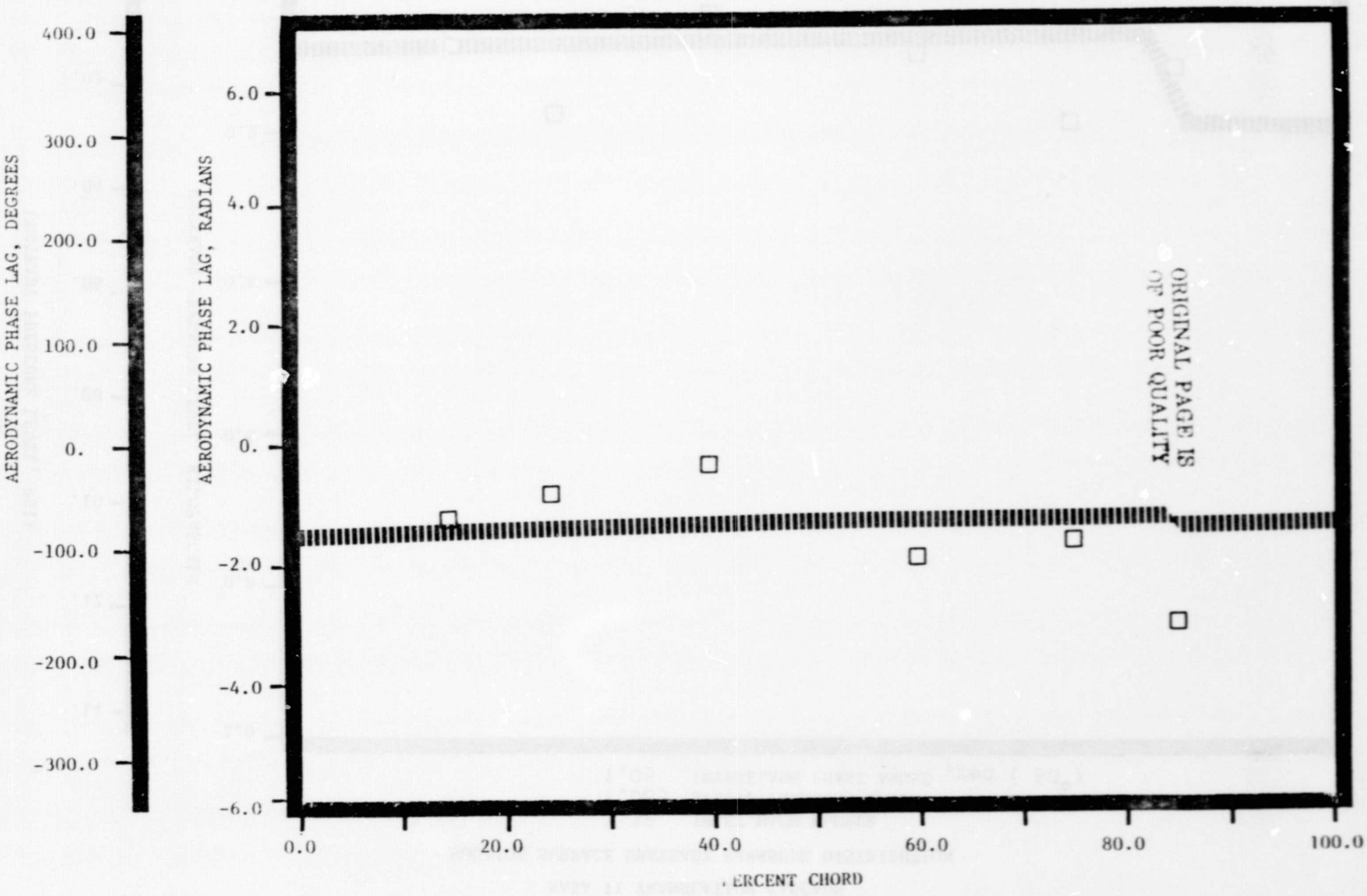

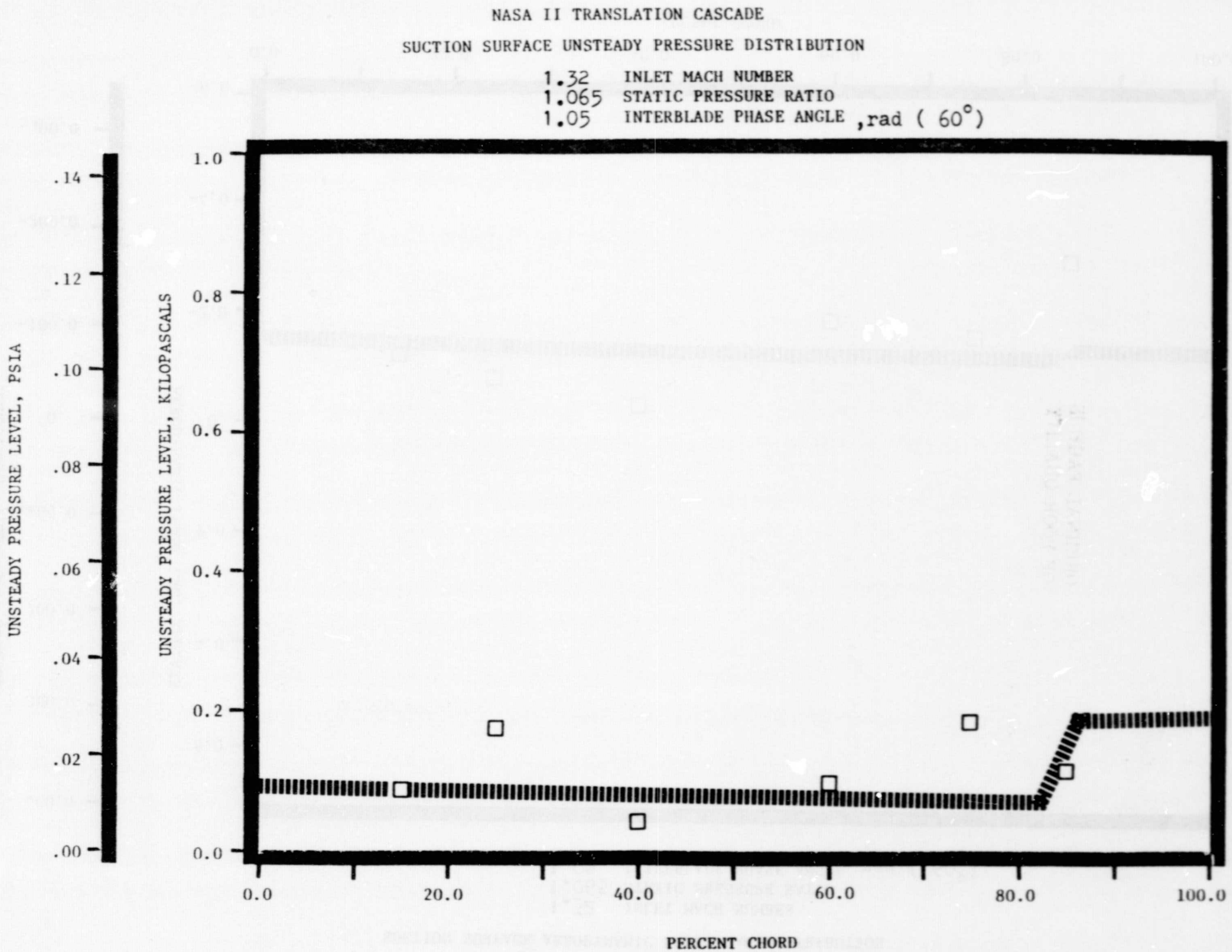
NASA II TRANSLATION CASCADE
SUCTION SURFACE UNSTEADY PRESSURE DISTRIBUTION
1.32 INLET MACH NUMBER
1.065 STATIC PRESSURE RATIO
1.05 INTERBLADE PHASE ANGLE ,rad (60°)
UNSTEADY PRESSURE LEVEL, PSIA
.14
.12
.10
.08
.06
.04
.02
.00
UNSTEADY PRESSURE LEVEL, KILOPASCALS
1.0
0.8
0.6
0.4
0.2
0.0
0.0
20.0
40.0
60.0
80.0
100.0
PERCENT CHORD

NASA II TRANSLATION CASCADE

PRESSURE SURFACE AERODYNAMIC PHASE LAG DISTRIBUTION

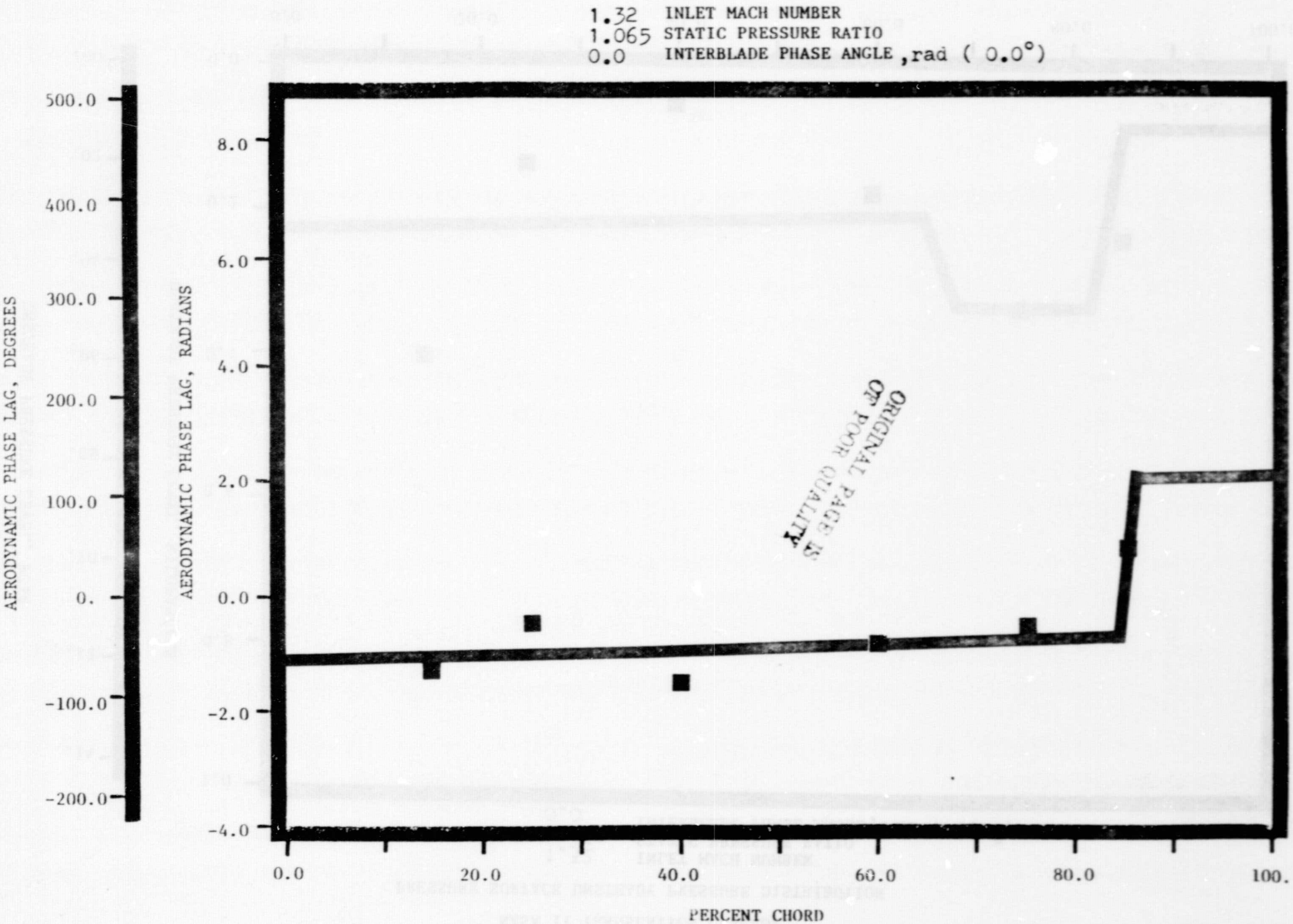

NASA II TRANSLATION CASCADE

PRESSURE SURFACE UNSTEADY PRESSURE DISTRIBUTION

1.32	INLET MACH NUMBER
1.065	STATIC PRESSURE RATIO
0.0	INTERBLADE PHASE ANGLE, rad (0.0°)

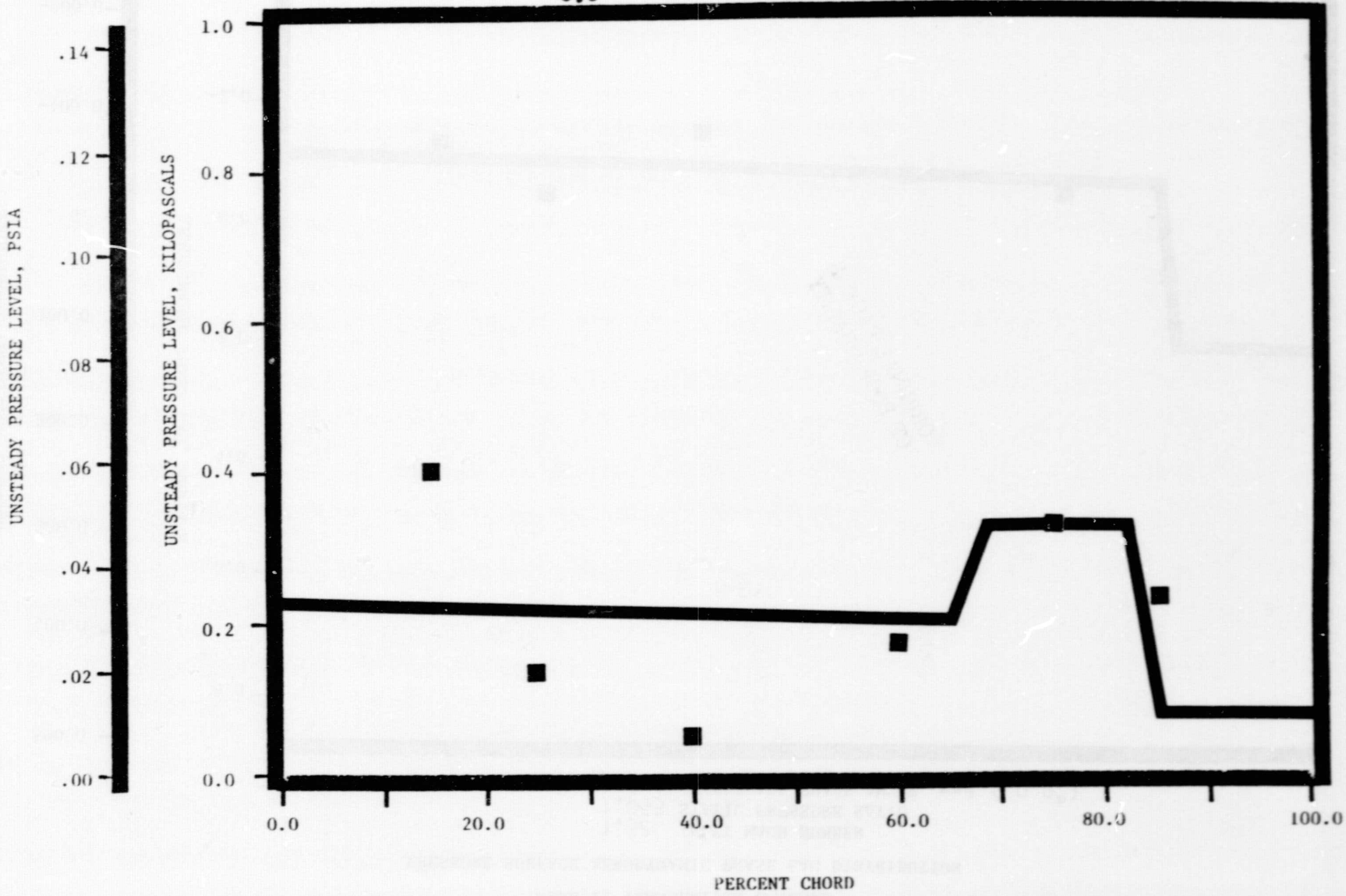

NASA II TRANSLATION CASCADE

SUCTION SURFACE AERODYNAMIC PHASE LAG DISTRIBUTION

1.32 INLET MACH NUMBER
1.065 STATIC PRESSURE RATIO
0.0 INTERBLADE PHASE ANGLE, rad (0.0°)

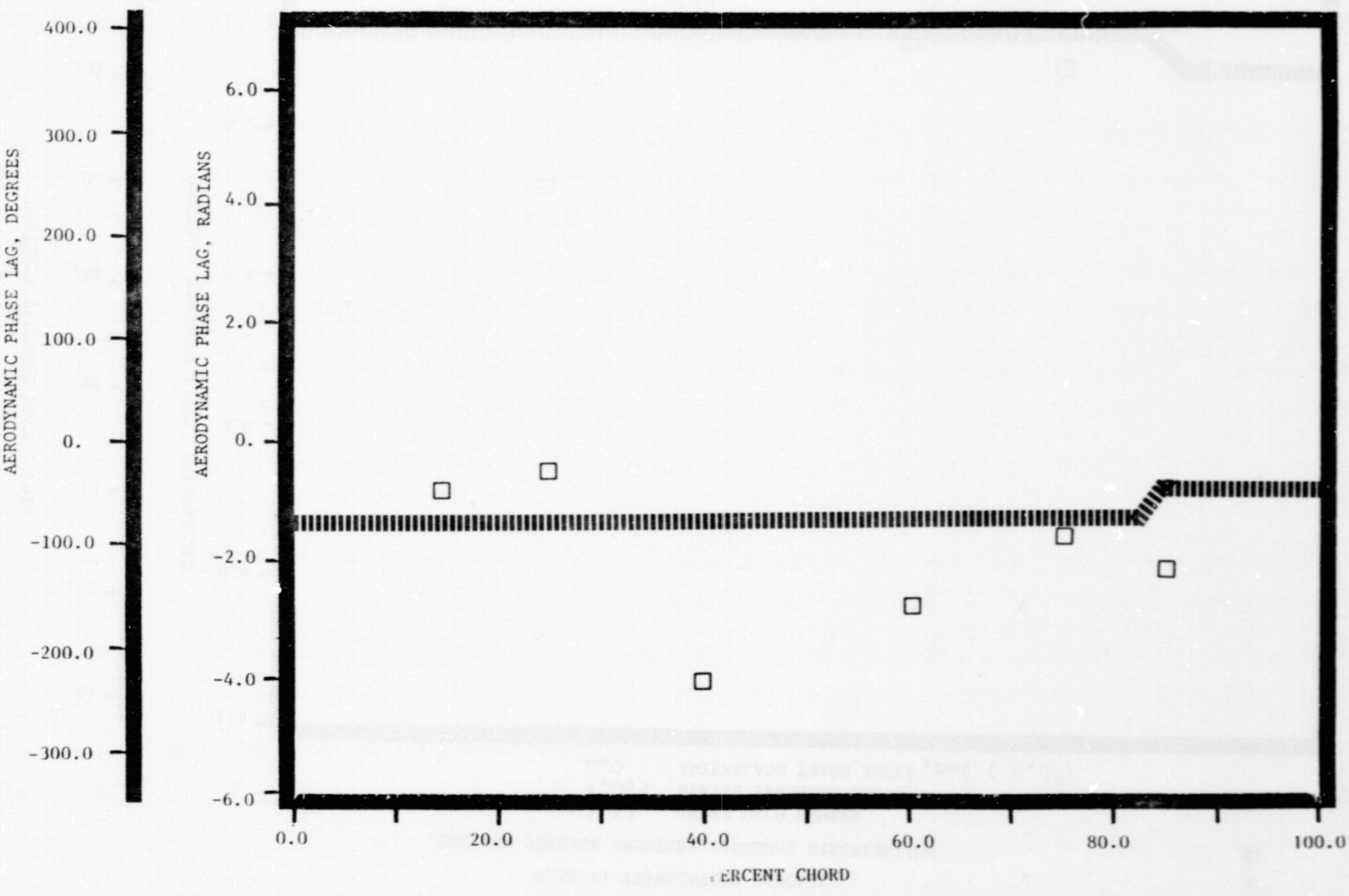

NASA II TRANSLATION CASCADE

SUCTION SURFACE UNSTEADY PRESSURE DISTRIBUTION

1.32 INLET MACH NUMBER
1.065 STATIC PRESSURE RATIO
0.0 INTERBLADE PHASE ANGLE ,rad (0.0°)

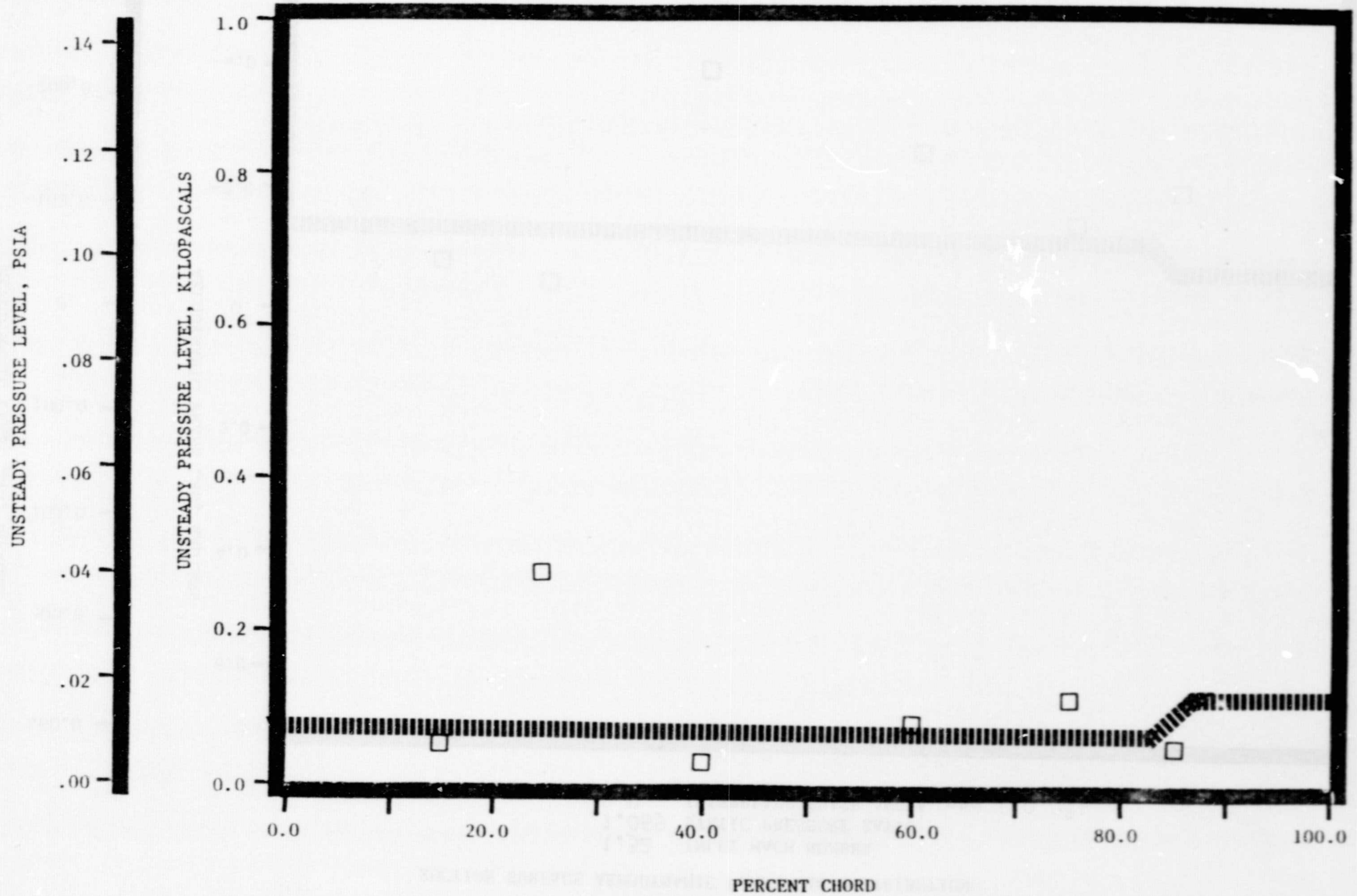

NASA II TRANSLATION CASCADE

PRESSURE SURFACE AERODYNAMIC PHASE LAG DISTRIBUTION

1.32 INLET MACH NUMBER
1.065 STATIC PRESSURE RATIO
-1.05 INTERBLADE PHASE ANGLE, rad (-60°)

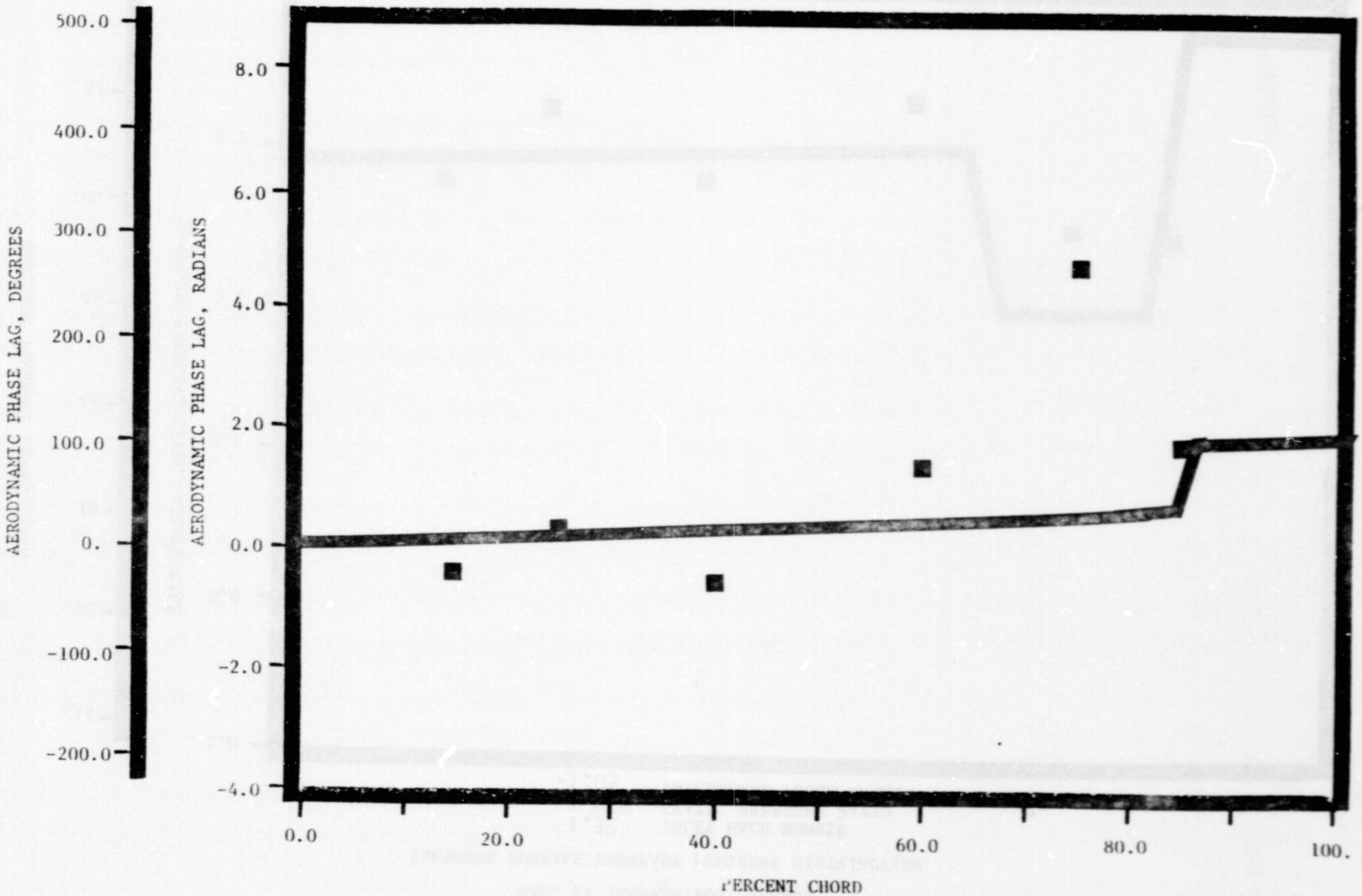

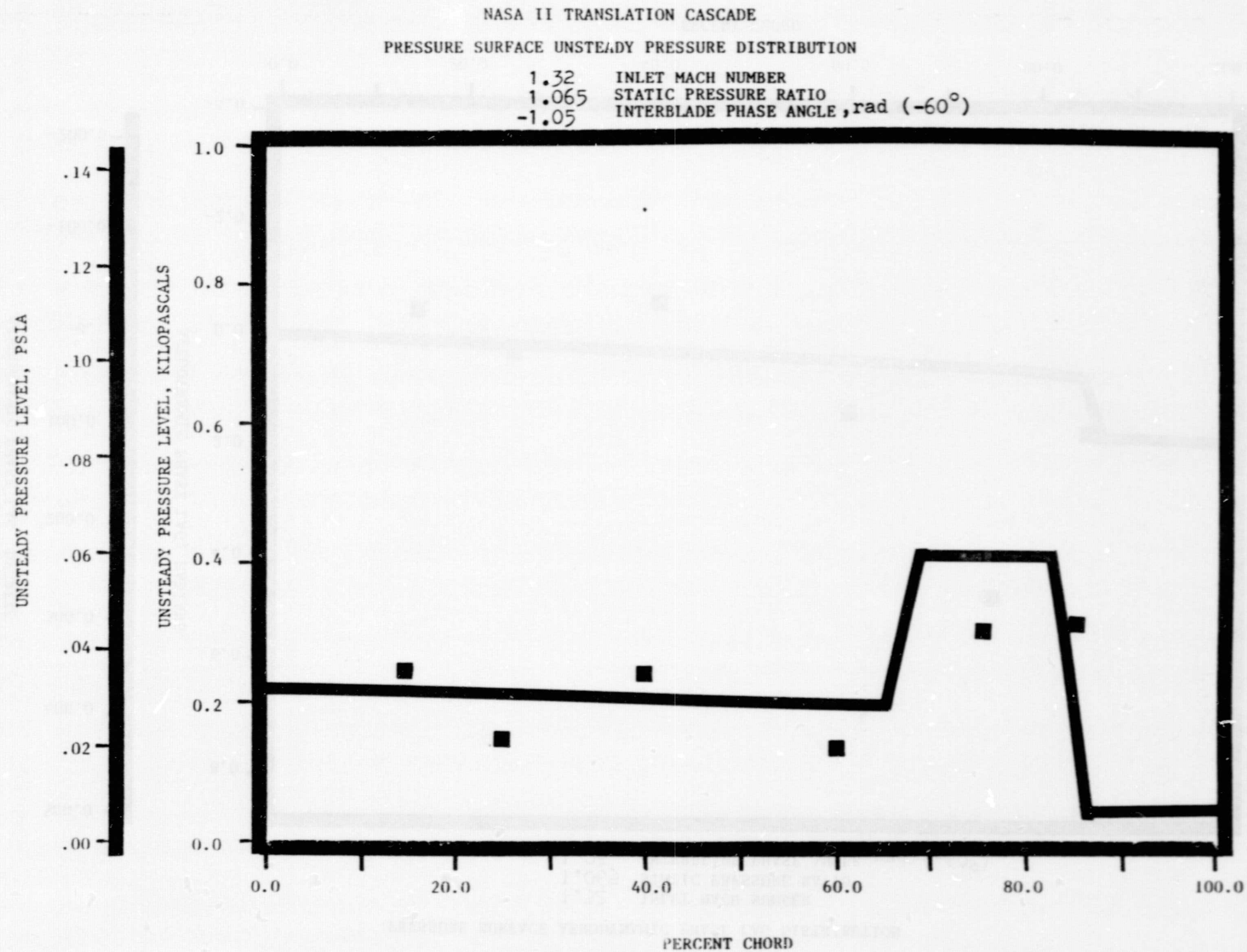

NASA II TRANSLATION CASCADE
PRESSURE SURFACE UNSTEADY PRESSURE DISTRIBUTION
1.32 INLET MACH NUMBER
1.065 STATIC PRESSURE RATIO
-1.05 INTERBLADE PHASE ANGLE, rad (-60°)
UNSTEADY PRESSURE LEVEL, PSIA
.14
.12
.10
.08
.06
.04
.02
.00
UNSTEADY PRESSURE LEVEL, KILOPASCALS
1.0
0.8
0.6
0.4
0.2
0.0
0.0
20.0
40.0
60.0
80.0
100.0
PERCENT CHORD

NASA II TRANSLATION CASCADE

SUCTION SURFACE AERODYNAMIC PHASE LAG DISTRIBUTION

1.32 INLET MACH NUMBER
1.065 STATIC PRESSURE RATIO
-1.05 INTERBLADE PHASE ANGLE, rad (-60°)

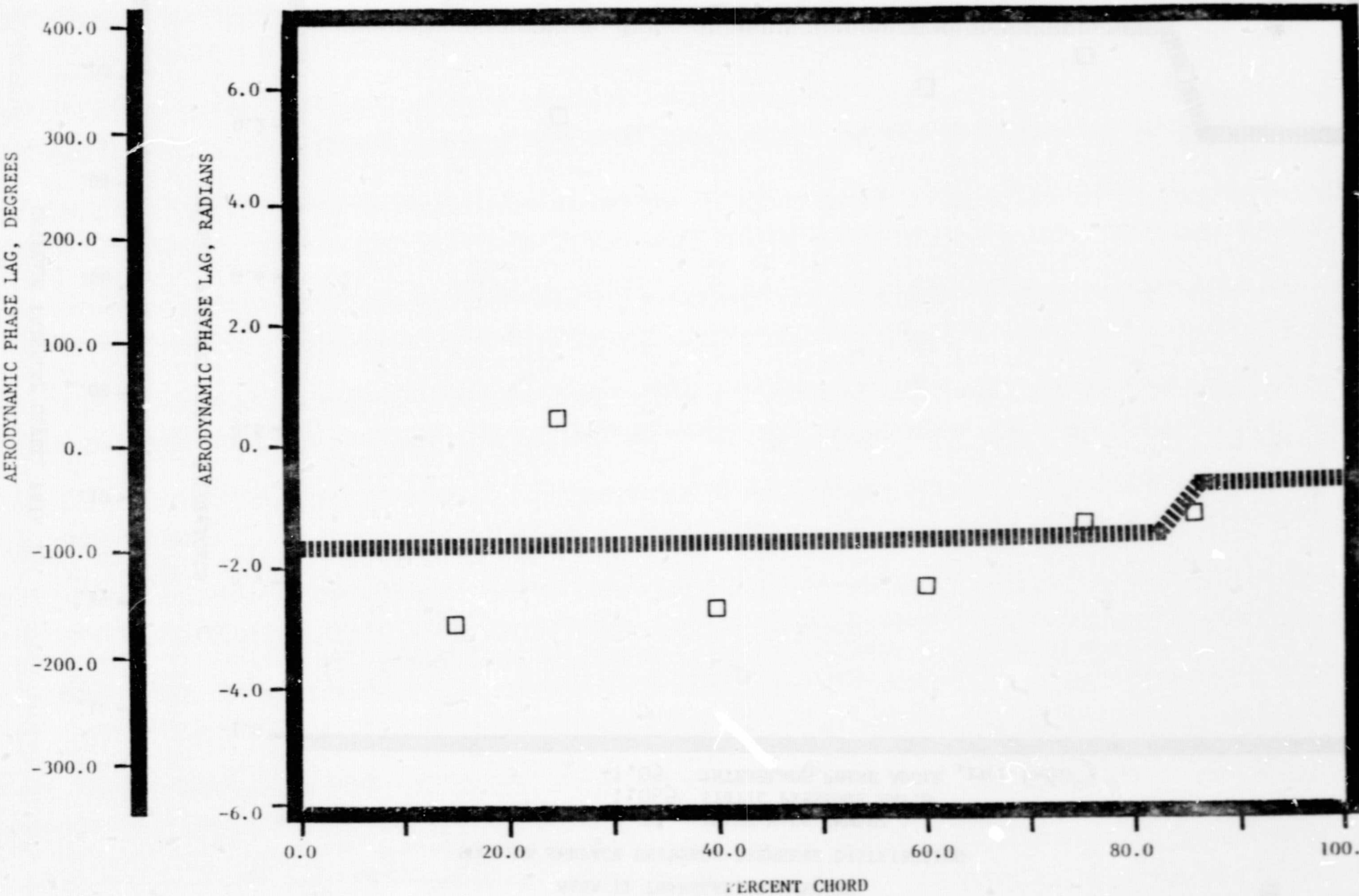

NASA II TRANSLATION CASCADE

SUCTION SURFACE UNSTEADY PRESSURE DISTRIBUTION

1.32 INLET MACH NUMBER
1.065 STATIC PRESSURE RATIO
-1.05 INTERBLADE PHASE ANGLE ,rad (-60°)

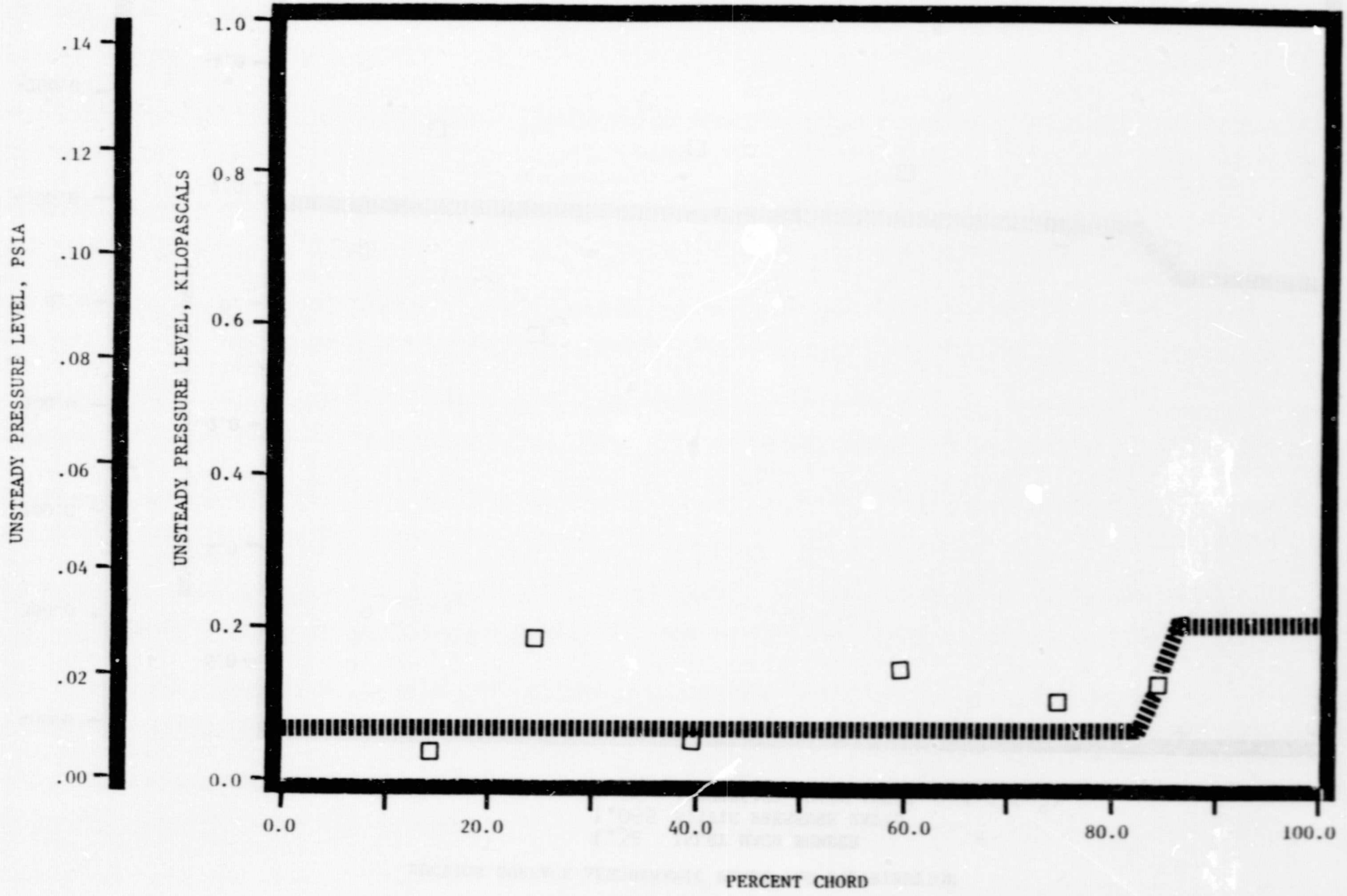

NASA II TRANSLATION CASCADE

PRESSURE SURFACE AERODYNAMIC PHASE LAG DISTRIBUTION

1.32 INLET MACH NUMBER
1.065 STATIC PRESSURE RATIO
-1.57 INTERBLADE PHASE ANGLE, rad (-90°)

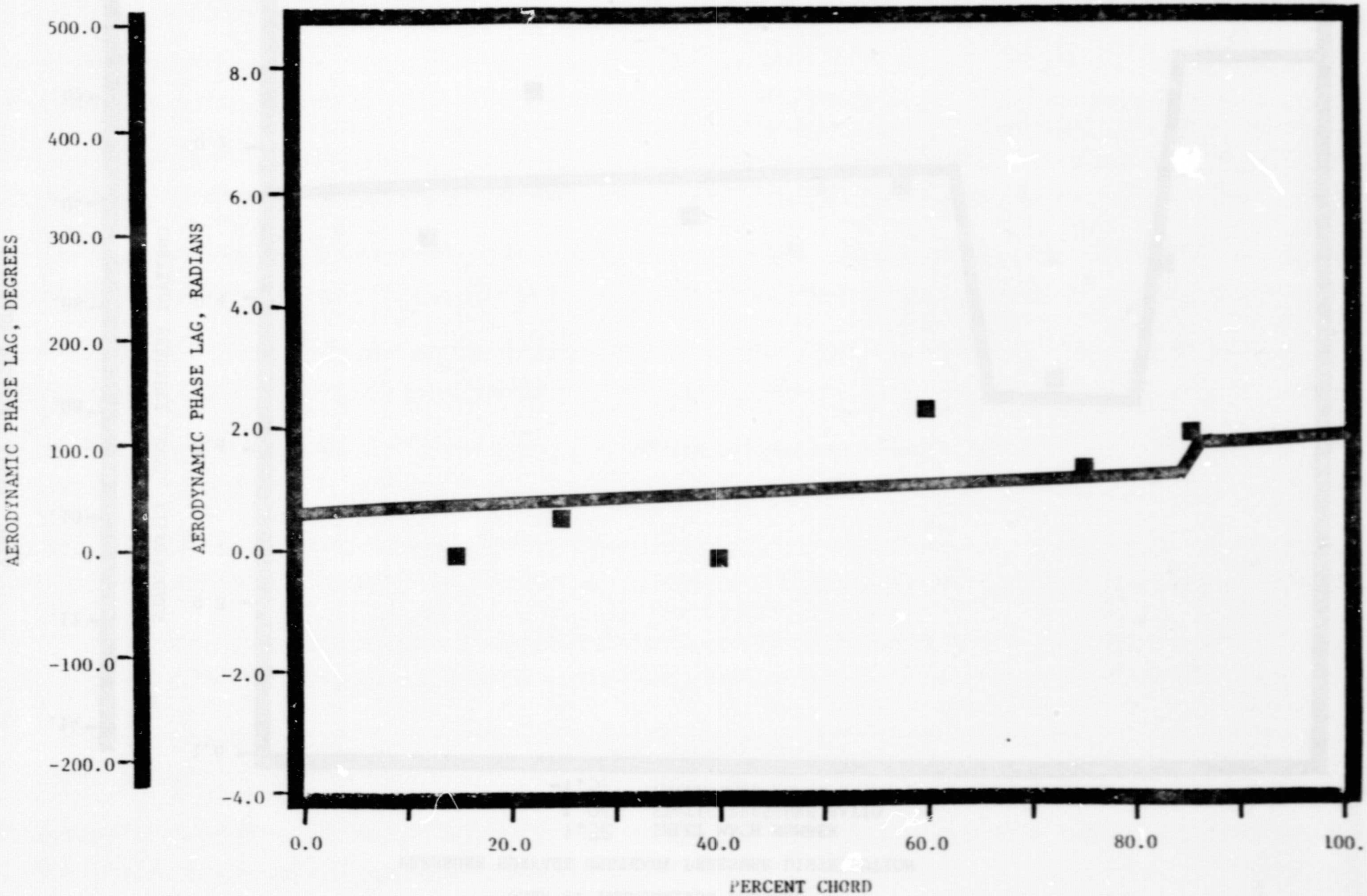

NASA II TRANSLATION CASCADE

PRESSURE SURFACE UNSTEADY PRESSURE DISTRIBUTION

1.32 INLET MACH NUMBER
1.065 STATIC PRESSURE RATIO
-1.57 INTERBLADE PHASE ANGLE ,rad (-90°)

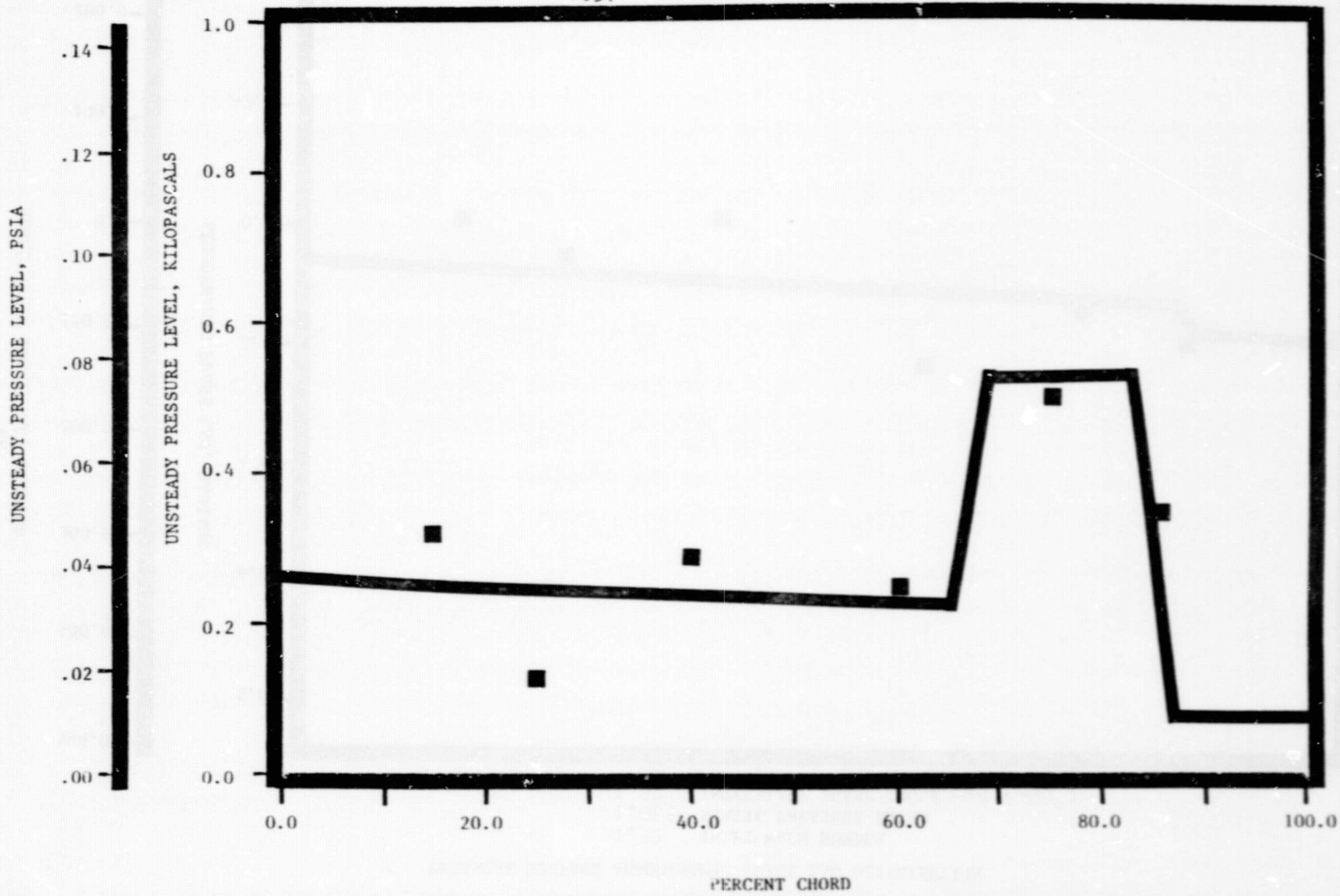

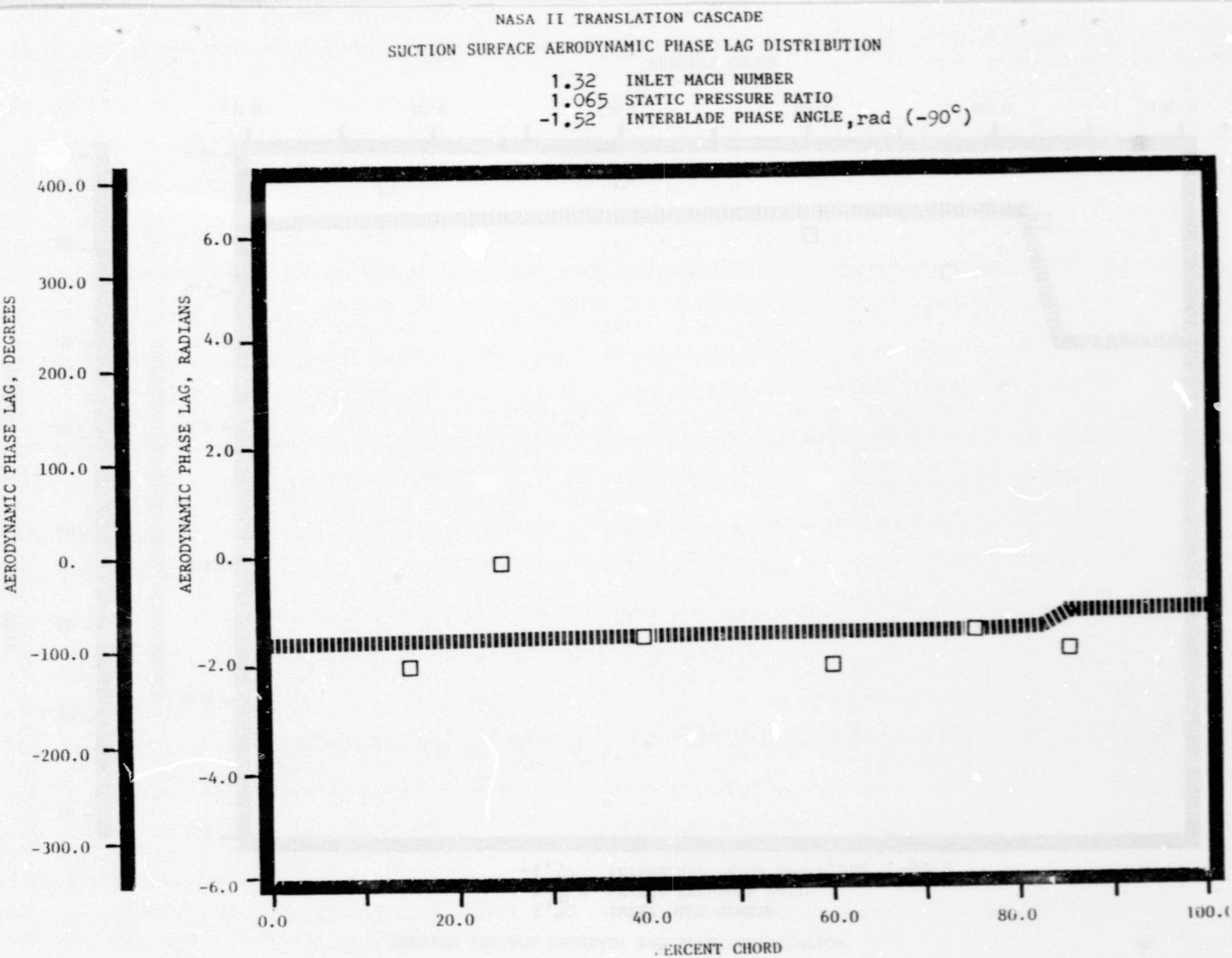
NASA II TRANSLATION CASCADE
SUCTION SURFACE AERODYNAMIC PHASE LAG DISTRIBUTION
1.32 INLET MACH NUMBER
1.065 STATIC PRESSURE RATIO
-1.52 INTERBLADE PHASE ANGLE, rad (-90°)
AERODYNAMIC PHASE LAG, DEGREES
400.0
300.0
200.0
100.0
0.
-100.0
-200.0
-300.0
AERODYNAMIC PHASE LAG, RADIANS
6.0
4.0
2.0
0.
-2.0
-4.0
-6.0
0.0
20.0
40.0
60.0
80.0
PERCENT CHORD

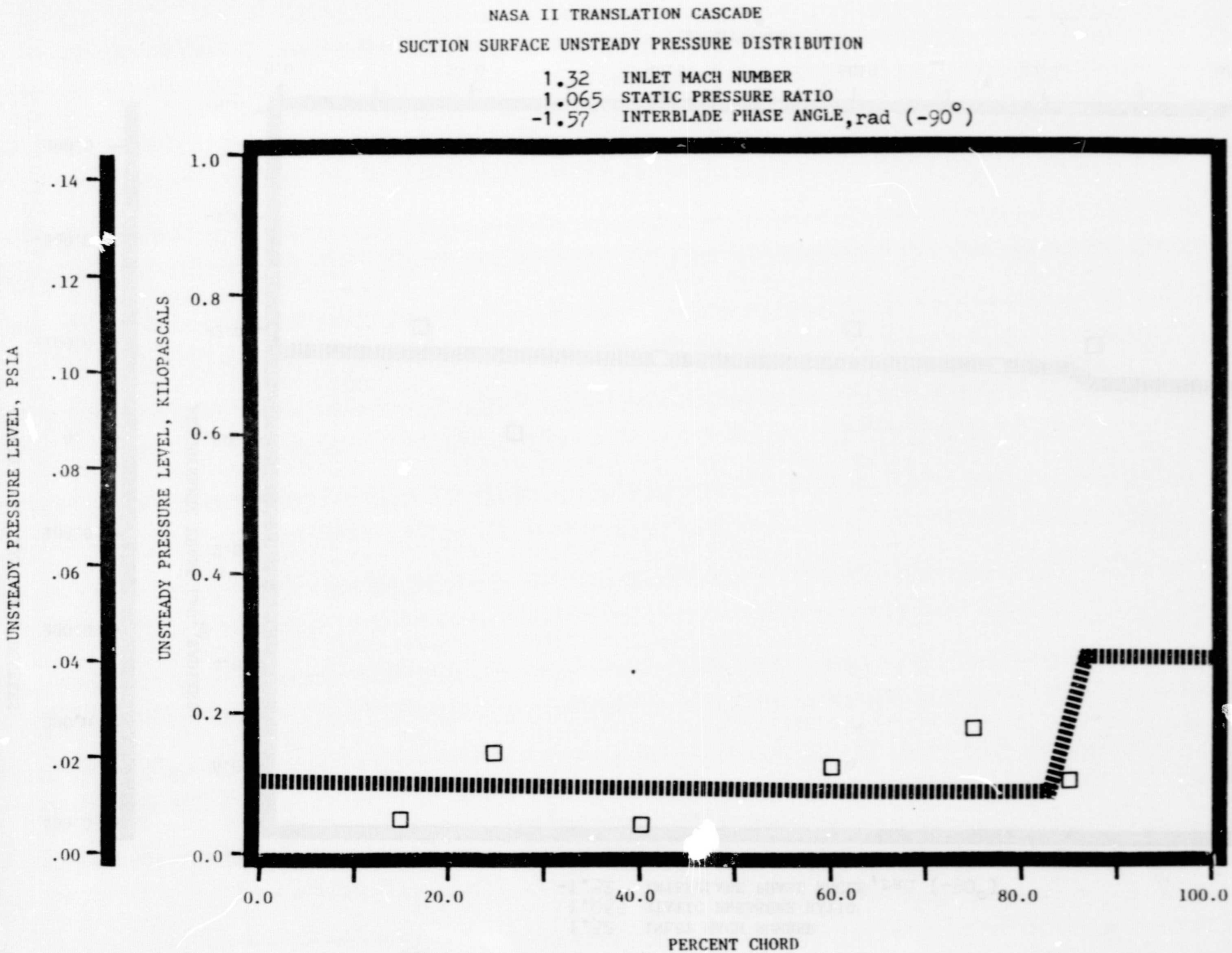

NASA II TRANSLATION CASCADE
SUCTION SURFACE UNSTEADY PRESSURE DISTRIBUTION
1.32 INLET MACH NUMBER
1.065 STATIC PRESSURE RATIO
-1.57 INTERBLADE PHASE ANGLE, rad (-90°)
UNSTEADY PRESSURE LEVEL, PSIA
.14
.12
.10
.08
.06
.04
.02
.00
UNSTEADY PRESSURE LEVEL, KILOPASCALS
1.0
0.8
0.6
0.4
0.2
0.0
0.0
20.0
40.0
60.0
80.0
100.0
PERCENT CHORD

NASA II TRANSLATION CASCADE

PRESSURE SURFACE AERODYNAMIC PHASE LAG DISTRIBUTION

1.32 INLET MACH NUMBER
1.304 STATIC PRESSURE RATIO
3.14 INTERBLADE PHASE ANGLE, rad (180°)

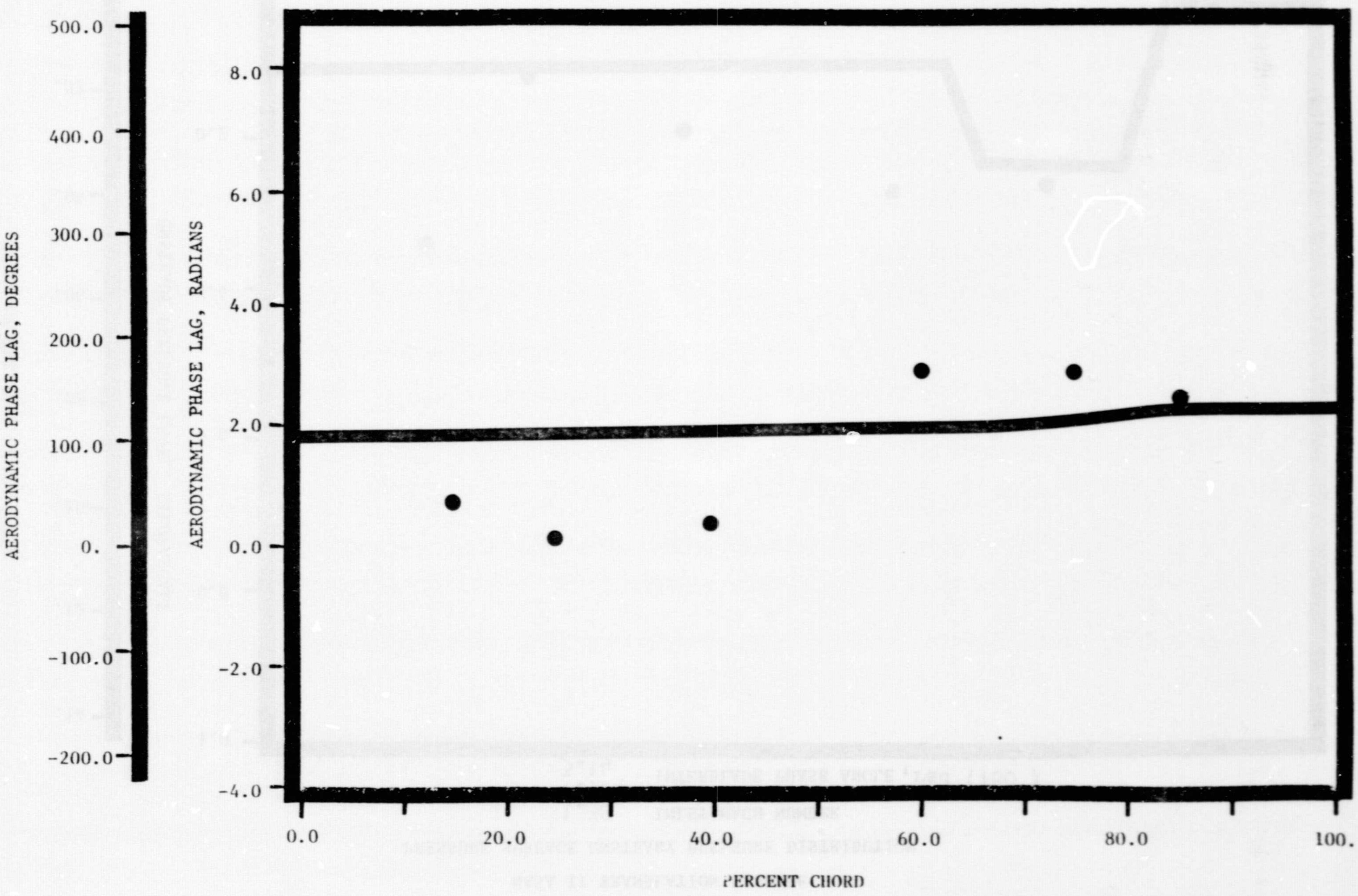

NASA II TRANSLATION CASCADE

PRESSURE SURFACE UNSTEADY PRESSURE DISTRIBUTION

1.32 INLET MACH NUMBER
1.304 STATIC PRESSURE RATIO
3.14 INTERBLADE PHASE ANGLE ,rad (180°)

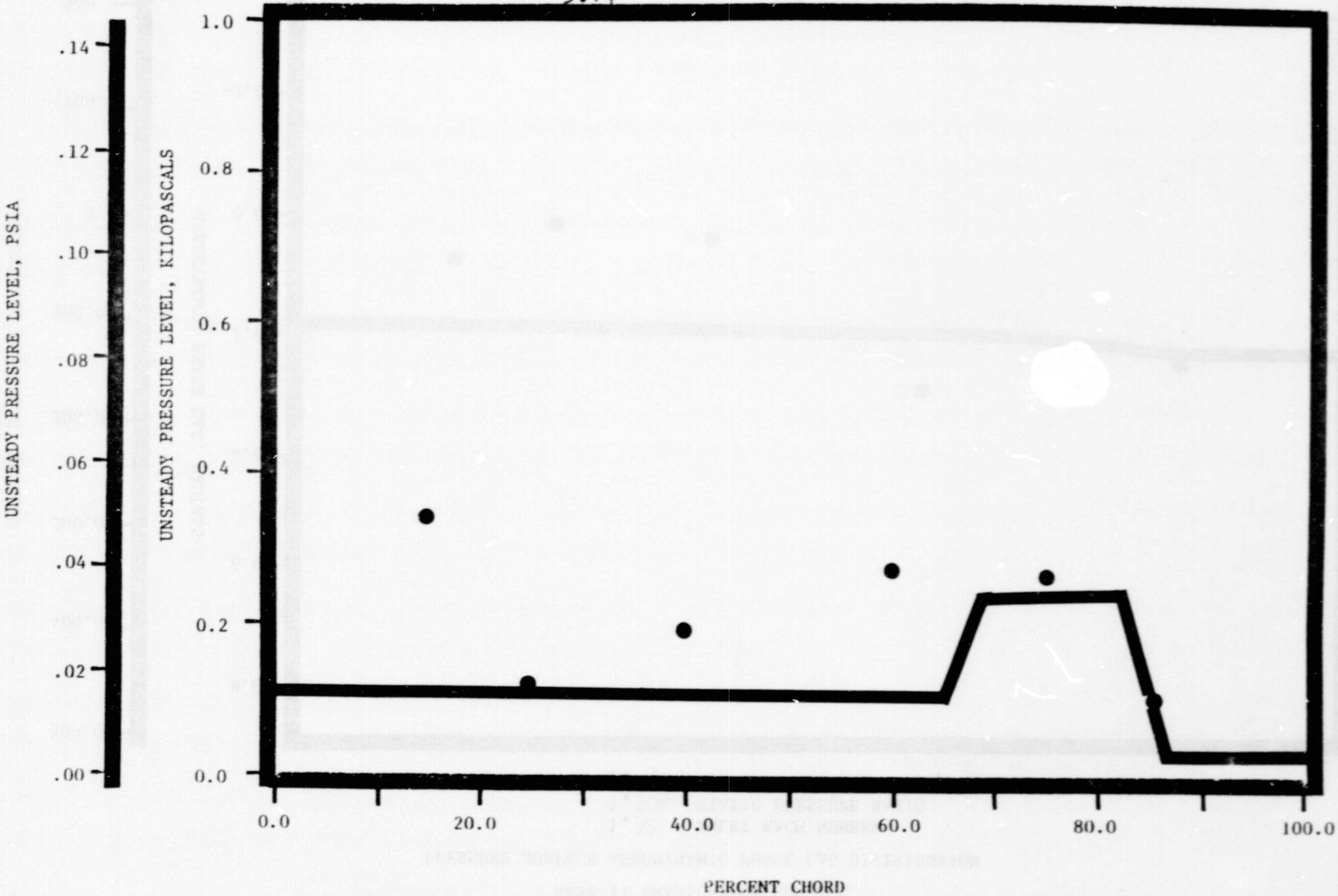

NASA II TRANSLATION CASCADE

SUCTION SURFACE AERODYNAMIC PHASE LAG DISTRIBUTION

1.32 INLET MACH NUMBER
1.304 STATIC PRESSURE RATIO
3.14 INTERBLADE PHASE ANGLE, rad (180°)

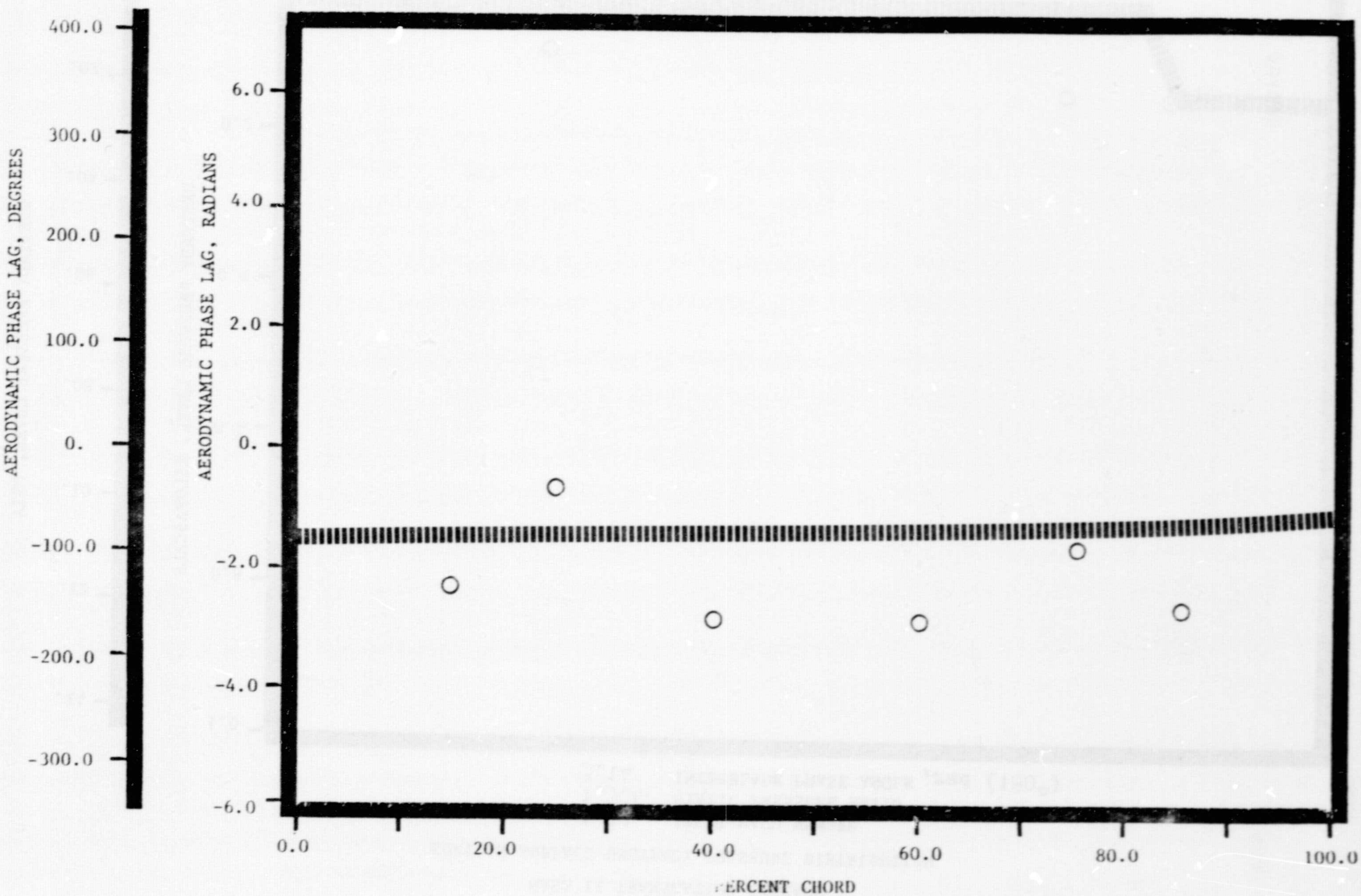

NASA II TRANSLATION CASCADE

SUCTION SURFACE UNSTEADY PRESSURE DISTRIBUTION

1.32	INLET MACH NUMBER
1.304	STATIC PRESSURE RATIO
3.14	INTERBLADE PHASE ANGLE ,rad (180°)

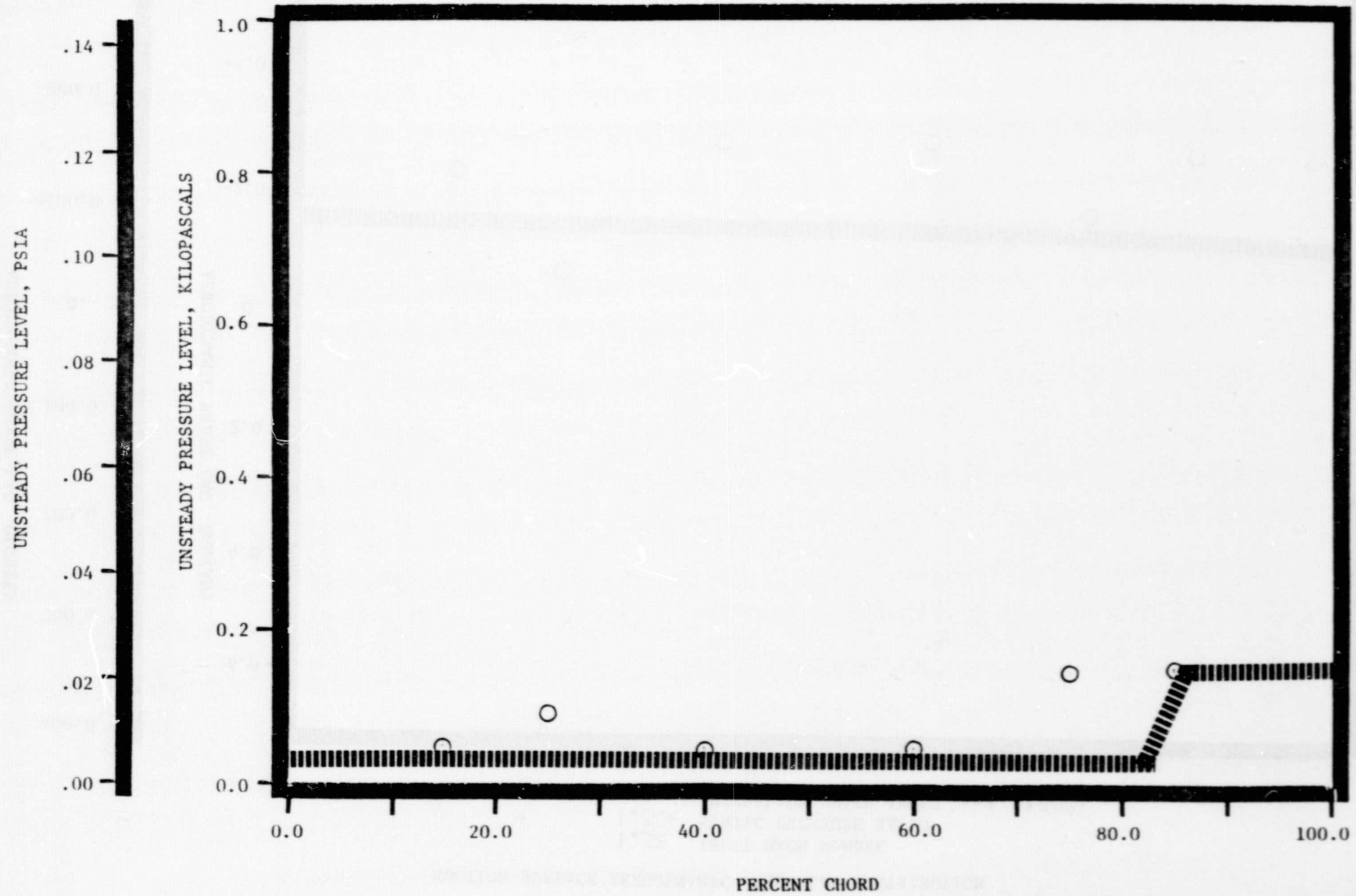

NASA II TRANSLATION CASCADE

PRESSURE SURFACE AERODYNAMIC PHASE LAG DISTRIBUTION

1.32 INLET MACH NUMBER
1.304 STATIC PRESSURE RATIO
0.52 INTERBLADE PHASE ANGLE, rad (30°)

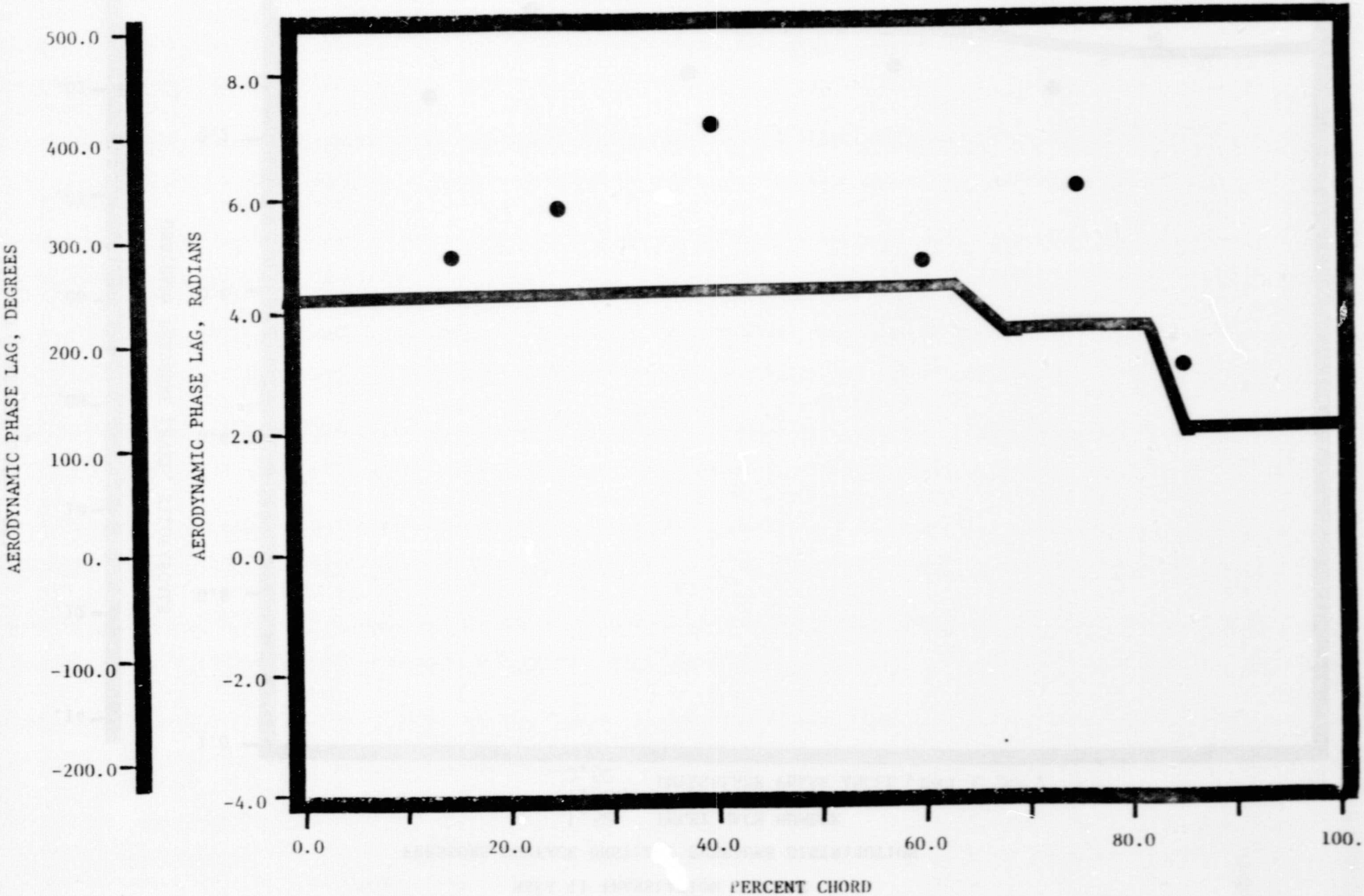

NASA II TRANSLATION CASCADE

PRESSURE SURFACE UNSTEADY PRESSURE DISTRIBUTION

1.32 INLET MACH NUMBER
1.304 STATIC PRESSURE RATIO
0.52 INTERBLADE PHASE ANGLE ,rad (30°)

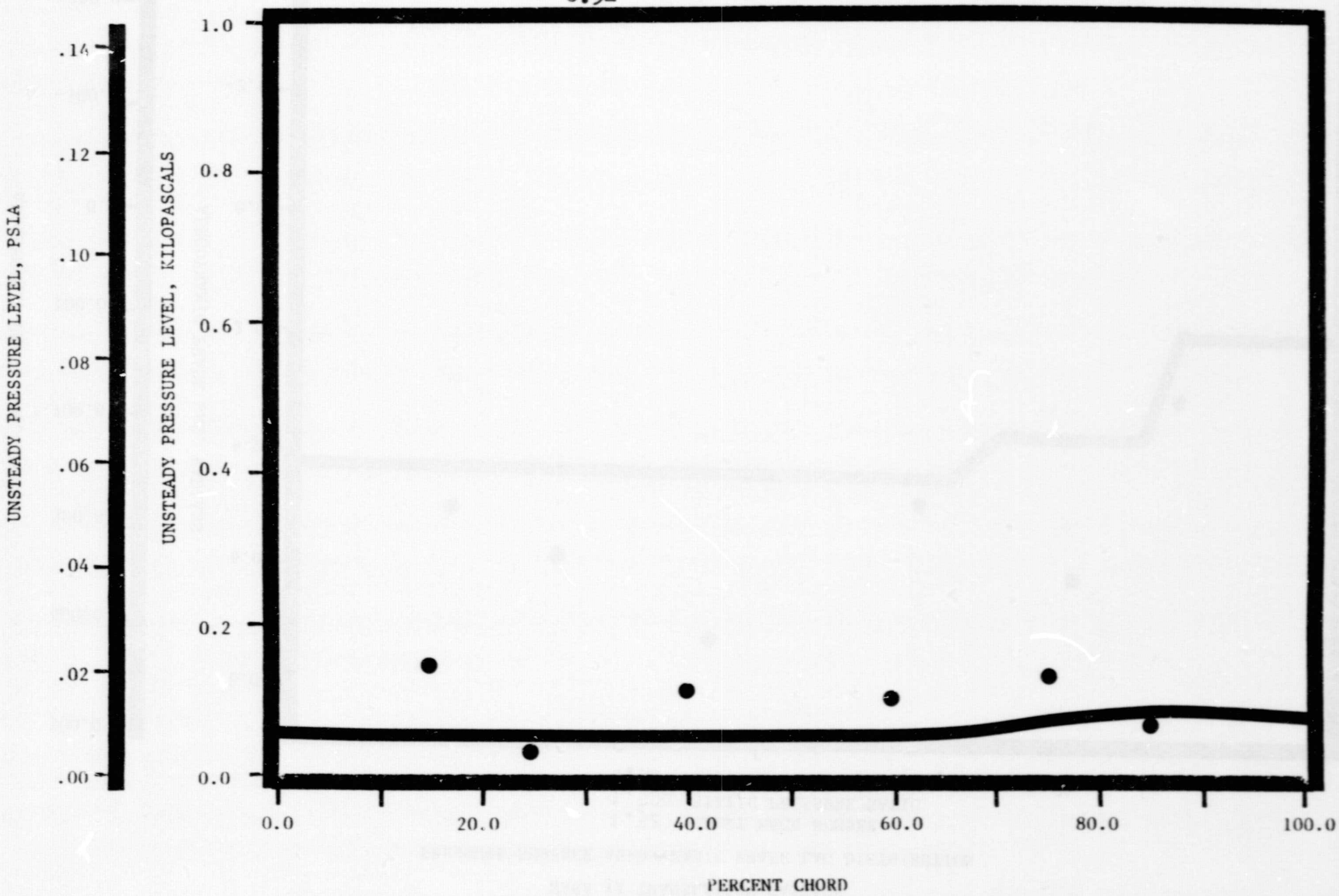

NASA II TRANSLATION CASCADE

SUCTION SURFACE AERODYNAMIC PHASE LAG DISTRIBUTION

1.32 INLET MACH NUMBER
1.304 STATIC PRESSURE RATIO
0.52 INTERBLADE PHASE ANGLE, rad (30°)

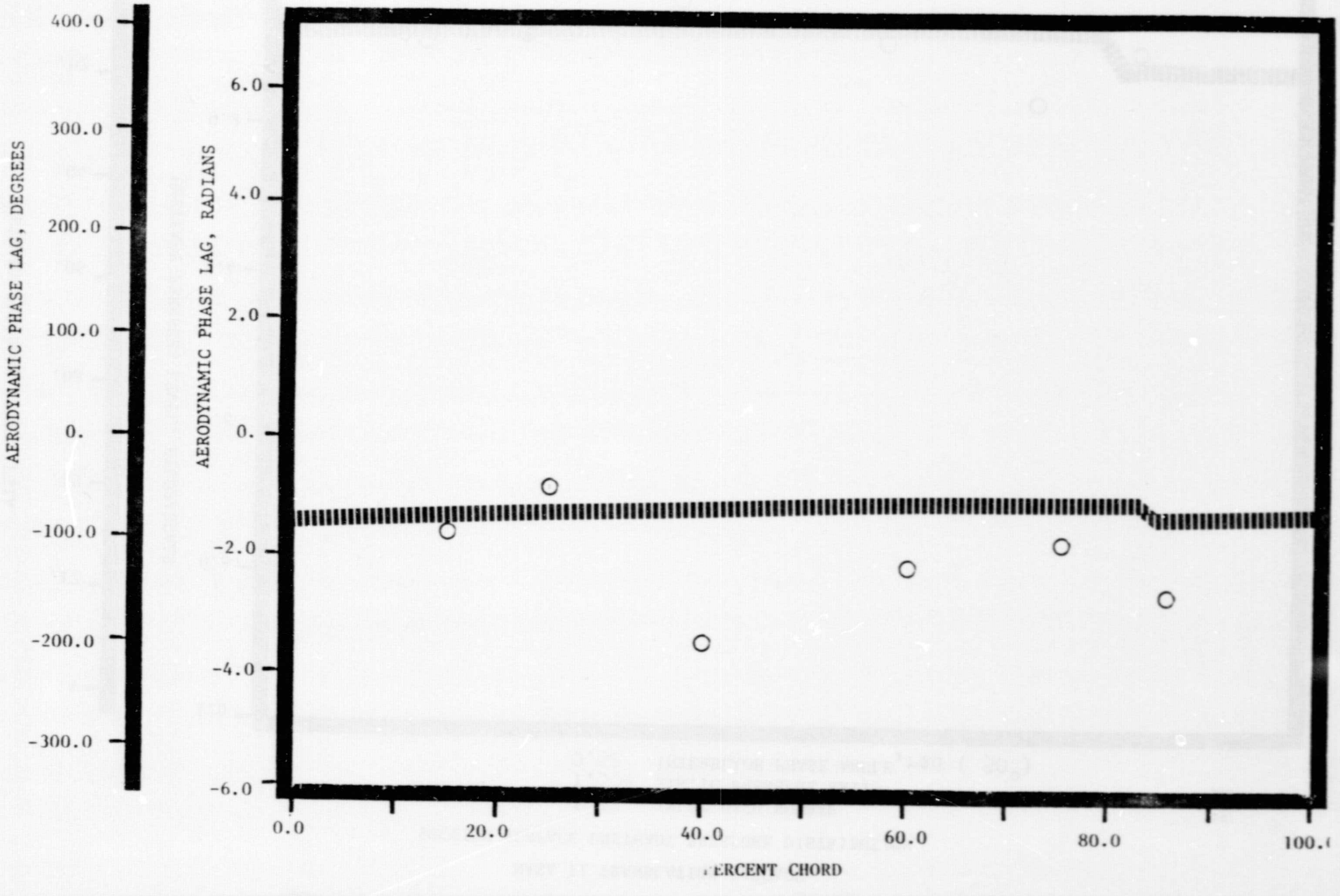

NASA II TRANSLATION CASCADE

SUCTION SURFACE UNSTEADY PRESSURE DISTRIBUTION

1.32 INLET MACH NUMBER
1.304 STATIC PRESSURE RATIO
0.52 INTERBLADE PHASE ANGLE, rad (30°)

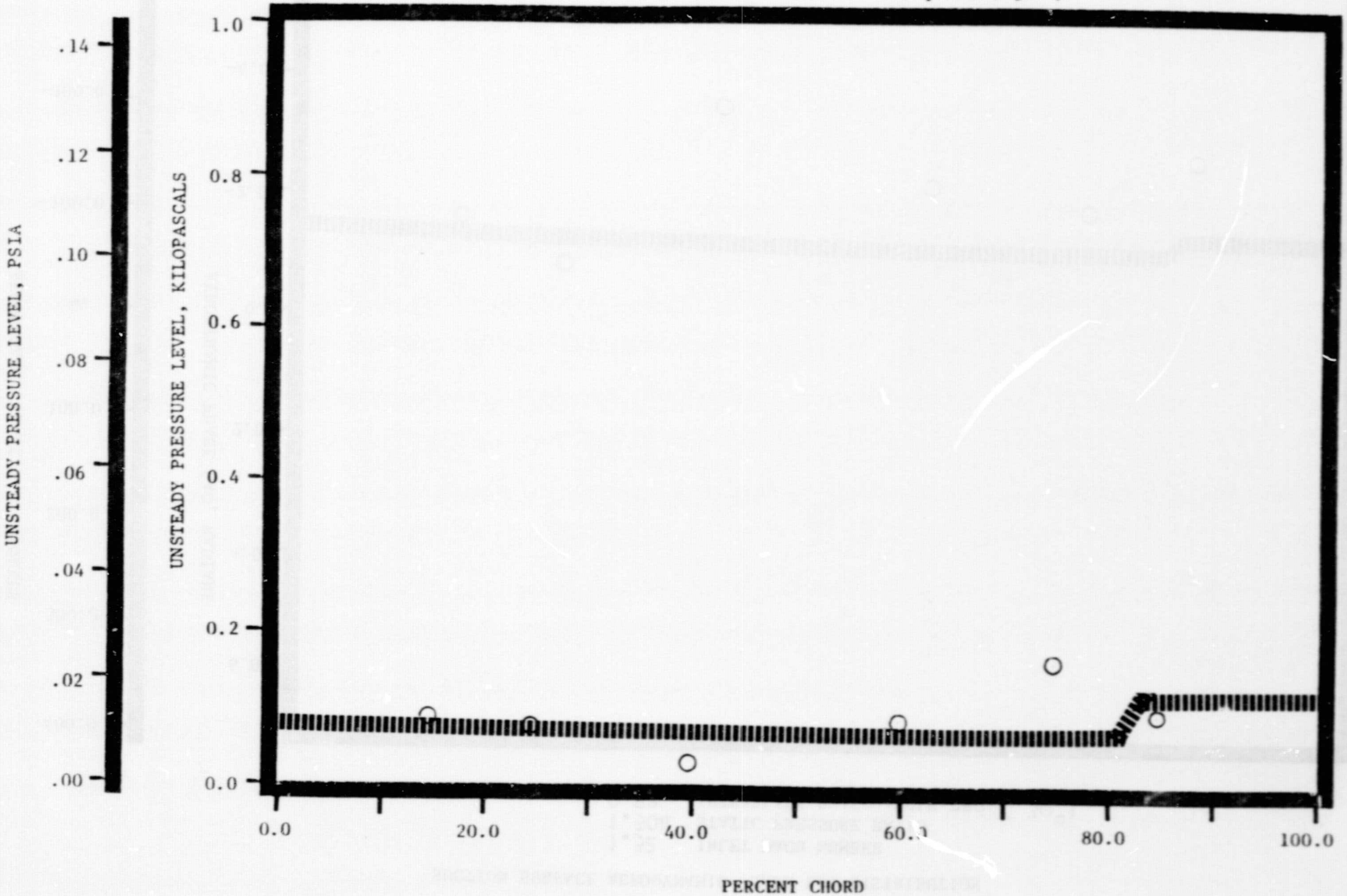

NASA II TRANSLATION CASCADE

PRESSURE SURFACE AERODYNAMIC PHASE LAG DISTRIBUTION

1.32 INLET MACH NUMBER
1.304 STATIC PRESSURE RATIO
0.0 INTERBLADE PHASE ANGLE ,rad (0.0°)

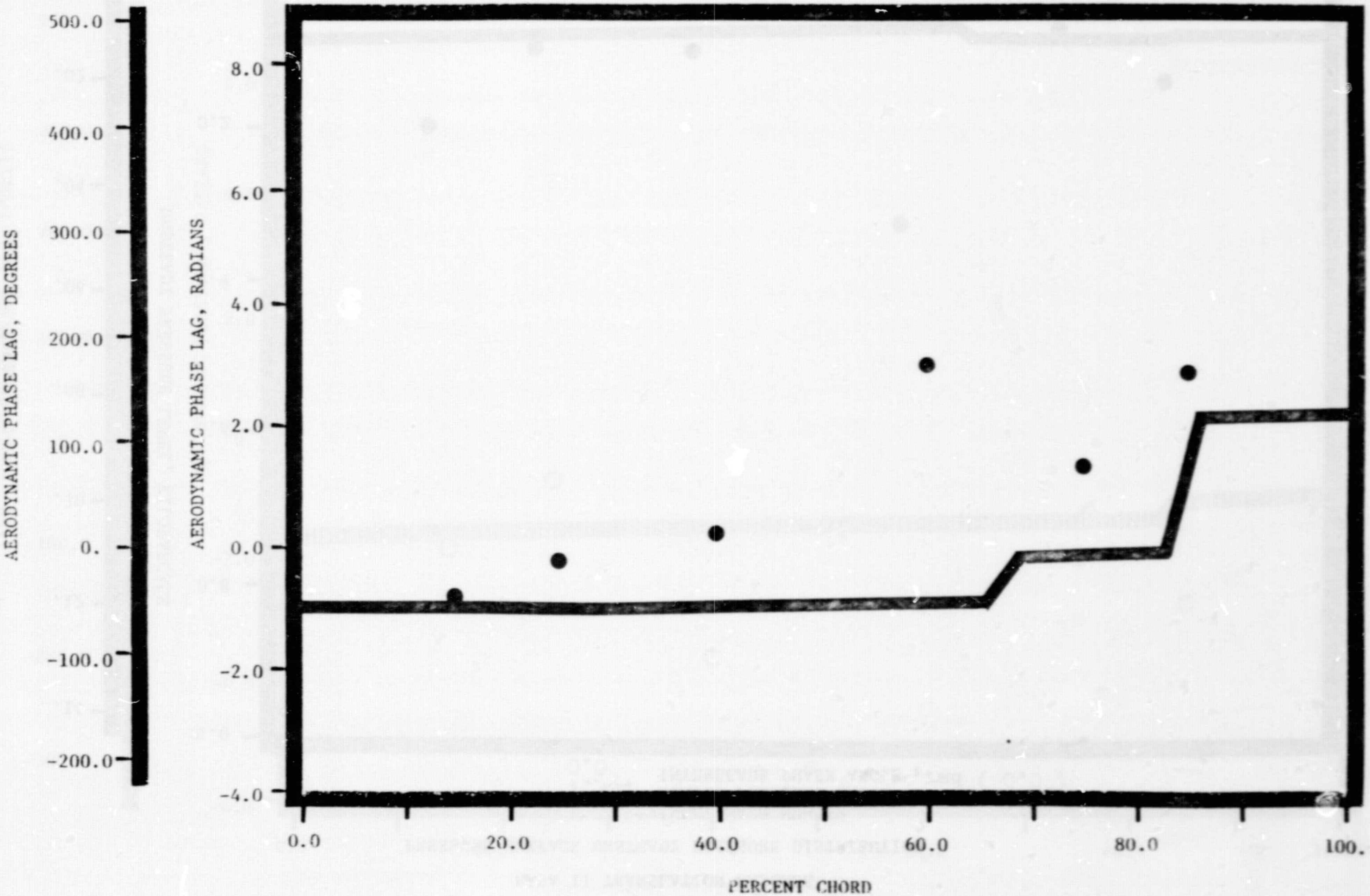

NASA II TRANSLATION CASCADE

PRESSURE SURFACE UNSTEADY PRESSURE DISTRIBUTION

1.32 INLET MACH NUMBER
1.304 STATIC PRESSURE RATIO
0.0 INTERBLADE PHASE ANGLE ,rad (0.0°)

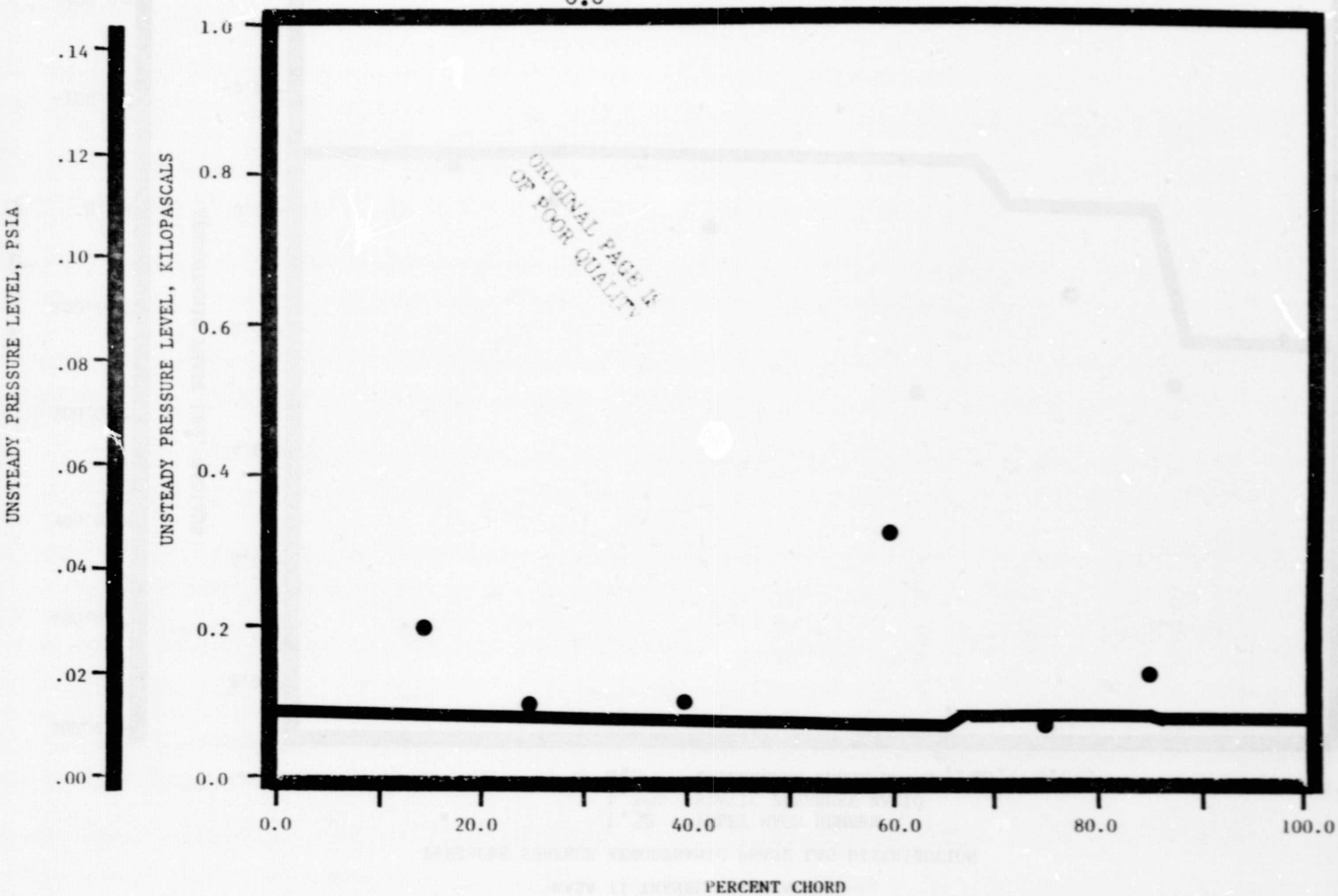

NASA II TRANSLATION CASCADE

SUCTION SURFACE AERODYNAMIC PHASE LAG DISTRIBUTION

1.32 INLET MACH NUMBER
1.304 STATIC PRESSURE RATIO
0.0 INTERBLADE PHASE ANGLE, rad (0.0°)

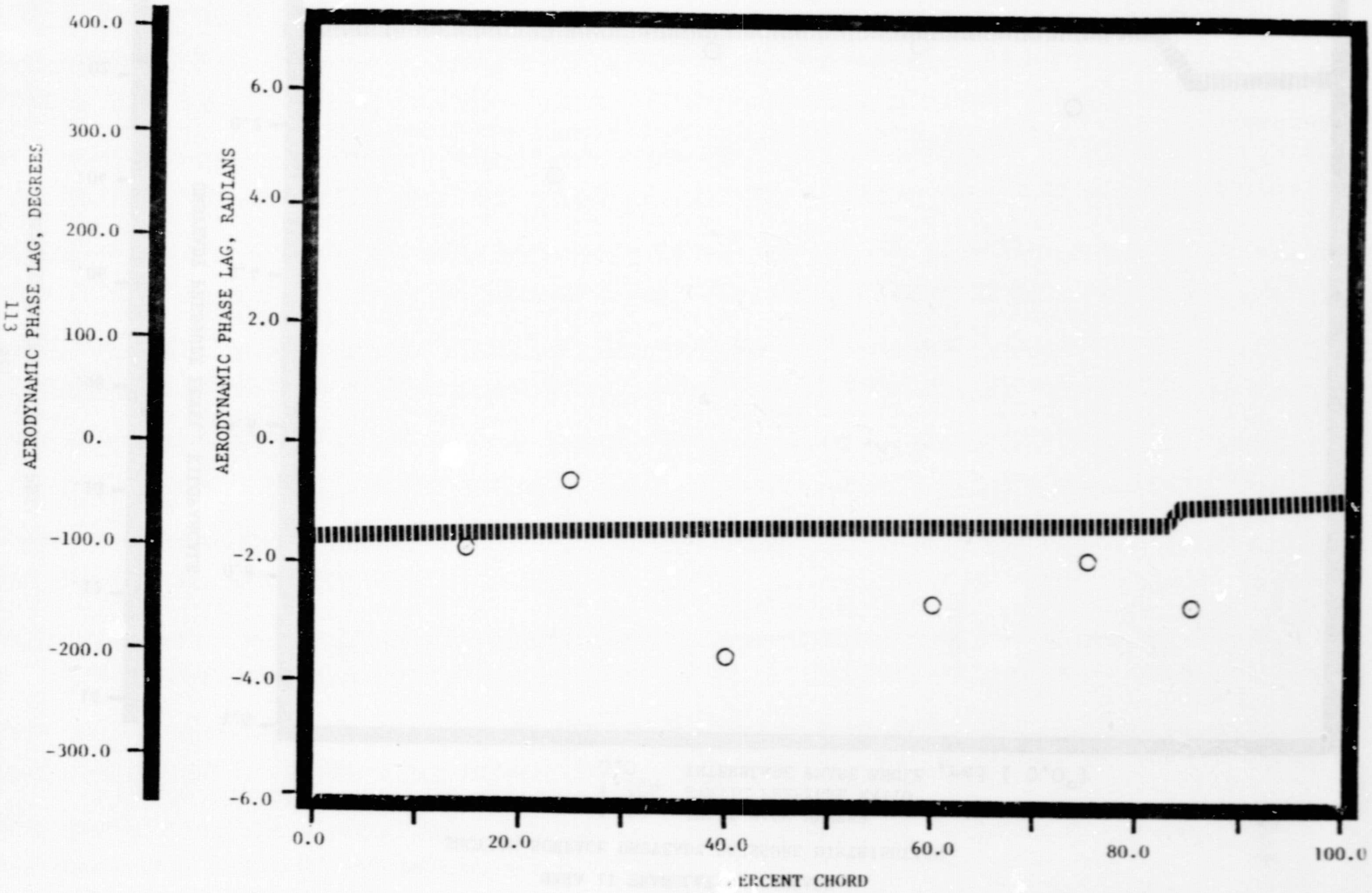

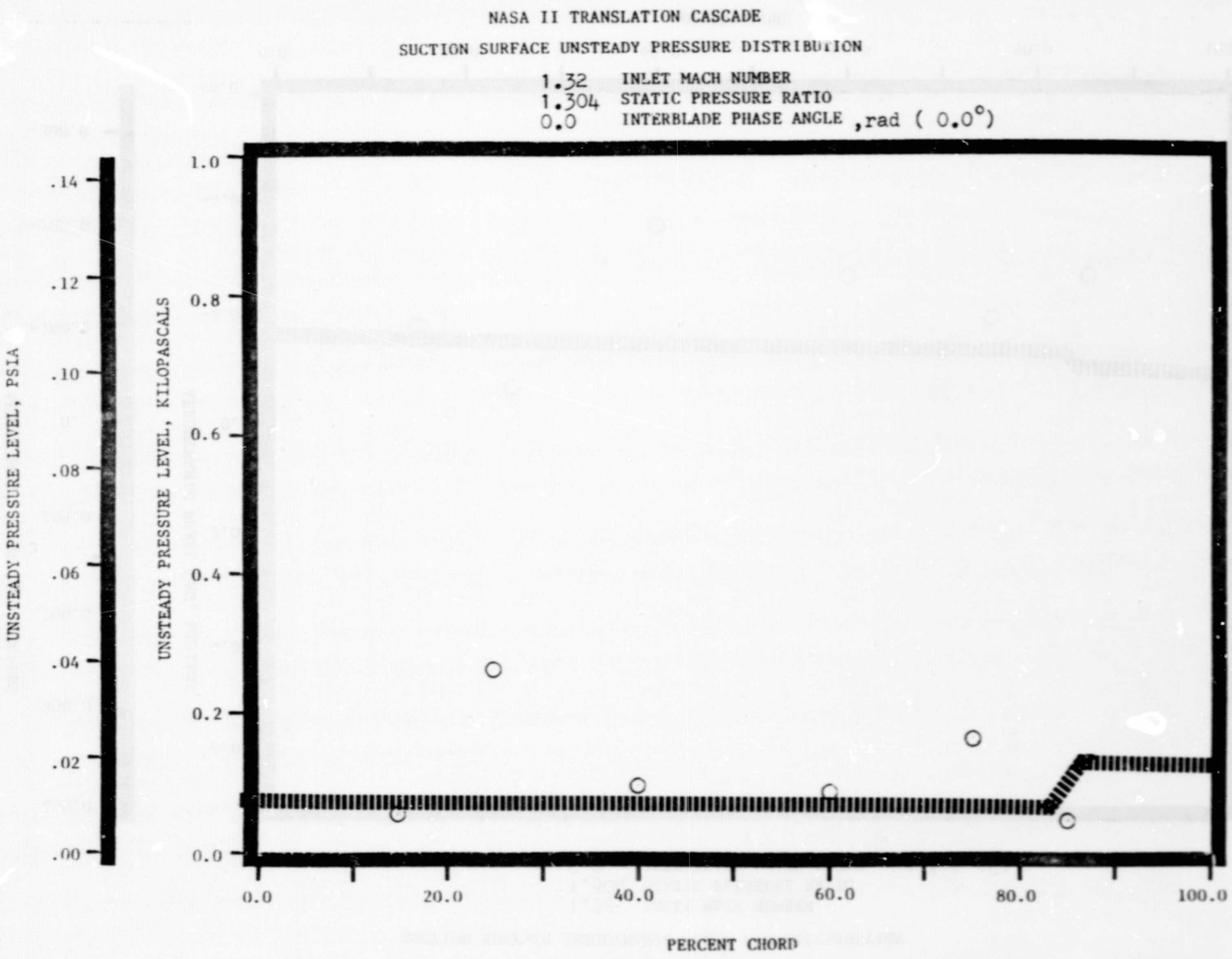
NASA II TRANSLATION CASCADE
SUCTION SURFACE UNSTEADY PRESSURE DISTRIBUTION
1.32 INLET MACH NUMBER
1.304 STATIC PRESSURE RATIO
0.0 INTERBLADE PHASE ANGLE ,rad (0.0°)
UNSTEADY PRESSURE LEVEL, PSIA
.14
.12
.10
.08
.06
.04
.02
.00
UNSTEADY PRESSURE LEVEL, KILOPASCALS
1.0
0.8
0.6
0.4
0.2
0.0
0.0
20.0
40.0
60.0
80.0
100.0
PERCENT CHORD

NASA II TRANSLATION CASCADE

PRESSURE SURFACE AERODYNAMIC PHASE LAG DISTRIBUTION

1.32 INLET MACH NUMBER
1.304 STATIC PRESSURE RATIO
-0.52 INTERBLADE PHASE ANGLE ,rad (-30°)

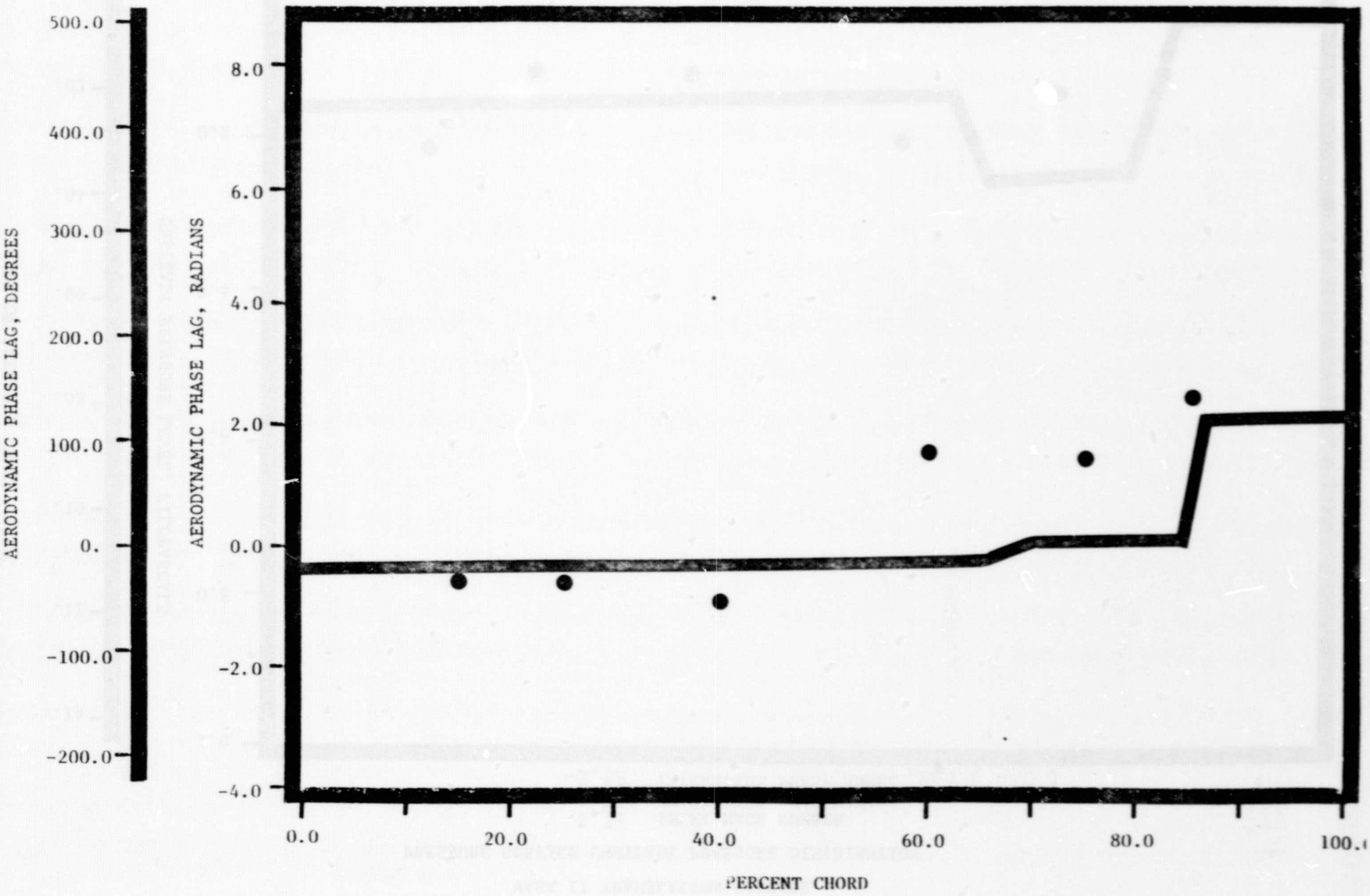

NASA II TRANSLATION CASCADE

PRESSURE SURFACE UNSTEADY PRESSURE DISTRIBUTION

1.32 INLET MACH NUMBER
1.304 STATIC PRESSURE RATIO
-0.52 INTERBLADE PHASE ANGLE ,rad (-30°)

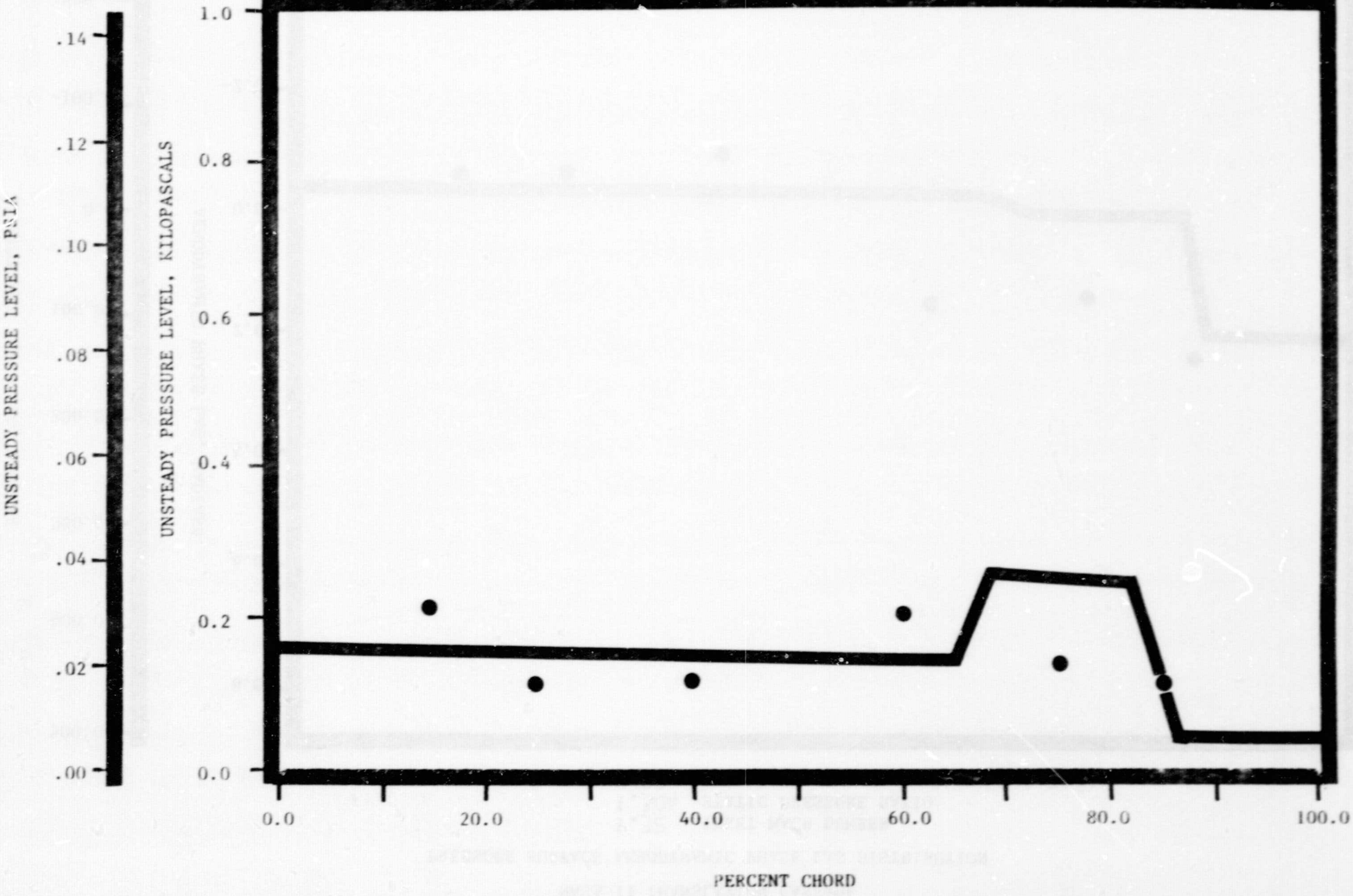

NASA II TRANSLATION CASCADE

SUCTION SURFACE AERODYNAMIC PHASE LAG DISTRIBUTION

1.32 INLET MACH NUMBER
1.304 STATIC PRESSURE RATIO
-0.52 INTERBLADE PHASE ANGLE, rad (-30°)

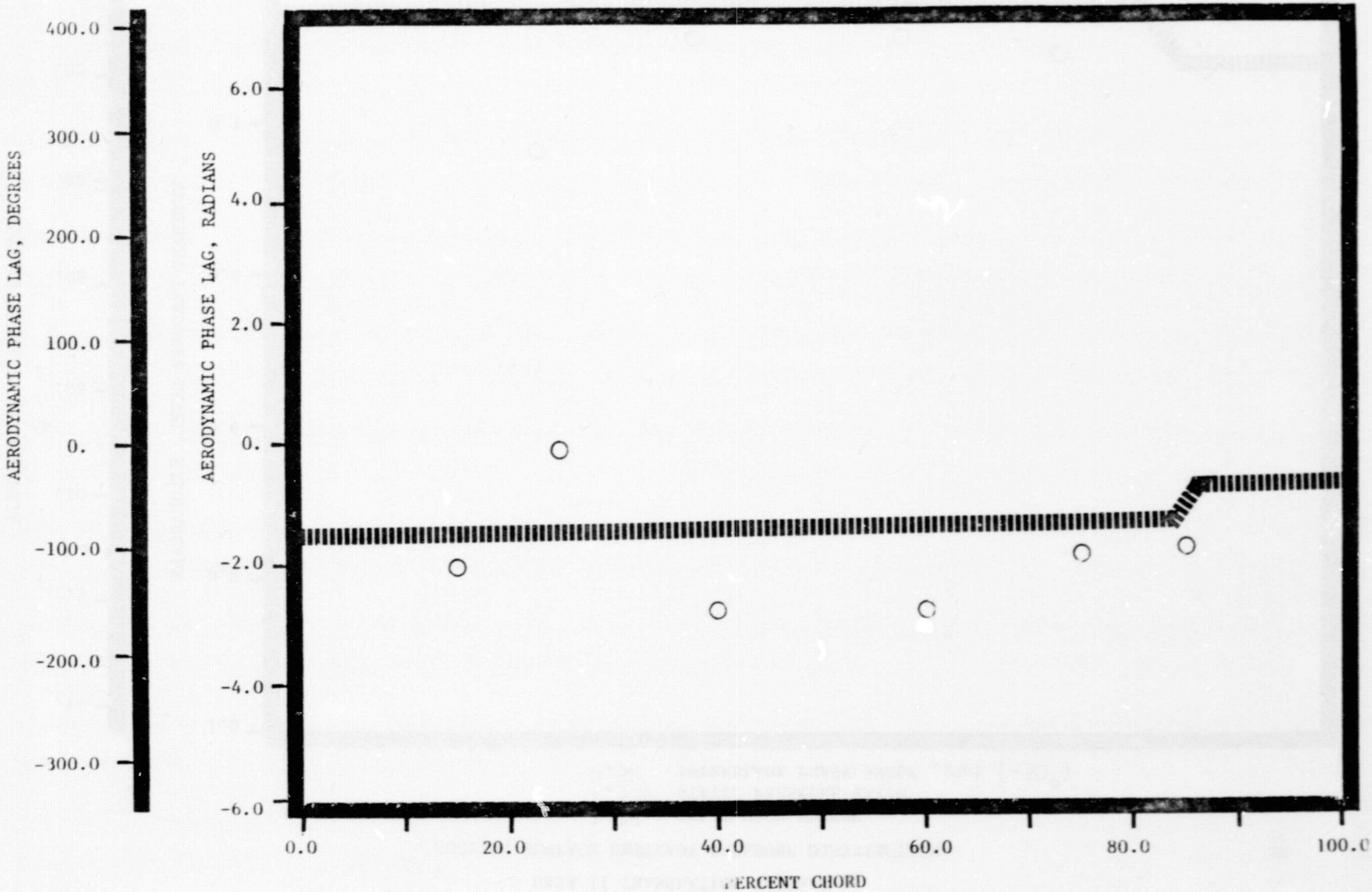

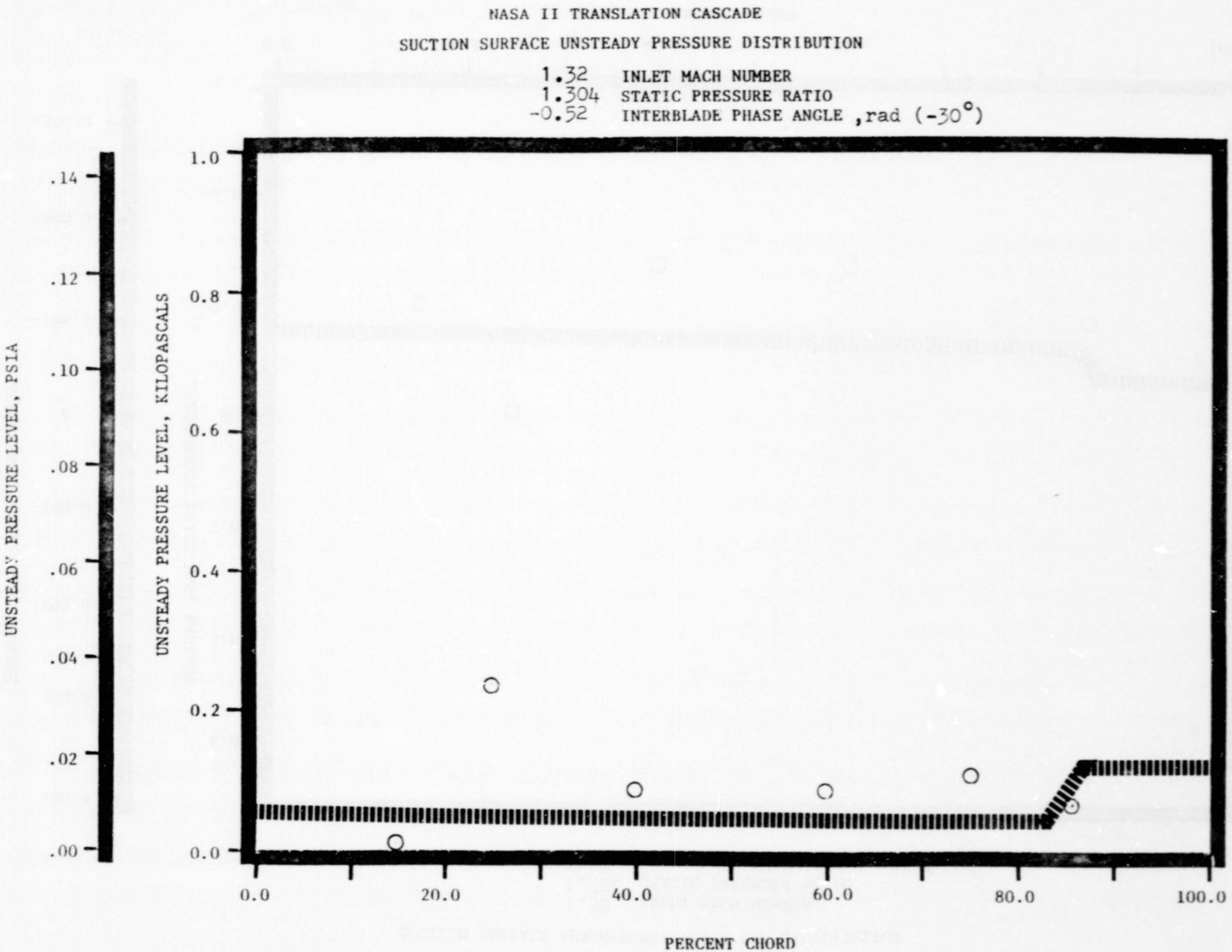
NASA II TRANSLATION CASCADE
SUCTION SURFACE UNSTEADY PRESSURE DISTRIBUTION
1.32 INLET MACH NUMBER
1.304 STATIC PRESSURE RATIO
-0.52 INTERBLADE PHASE ANGLE ,rad (-30°)
UNSTEADY PRESSURE LEVEL, PSIA
.14
.12
.10
.08
.06
.04
.02
.00
UNSTEADY PRESSURE LEVEL, KILOPASCALS
1.0
0.8
0.6
0.4
0.2
0.0
0.0
20.0
40.0
60.0
80.0
100.0
PERCENT CHORD

NASA II TRANSLATION CASCADE

PRESSURE SURFACE AERODYNAMIC PHASE LAG DISTRIBUTION

1.32 INLET MACH NUMBER
1.304 STATIC PRESSURE RATIO
-1.05 INTERBLADE PHASE ANGLE ,rad (-60°)

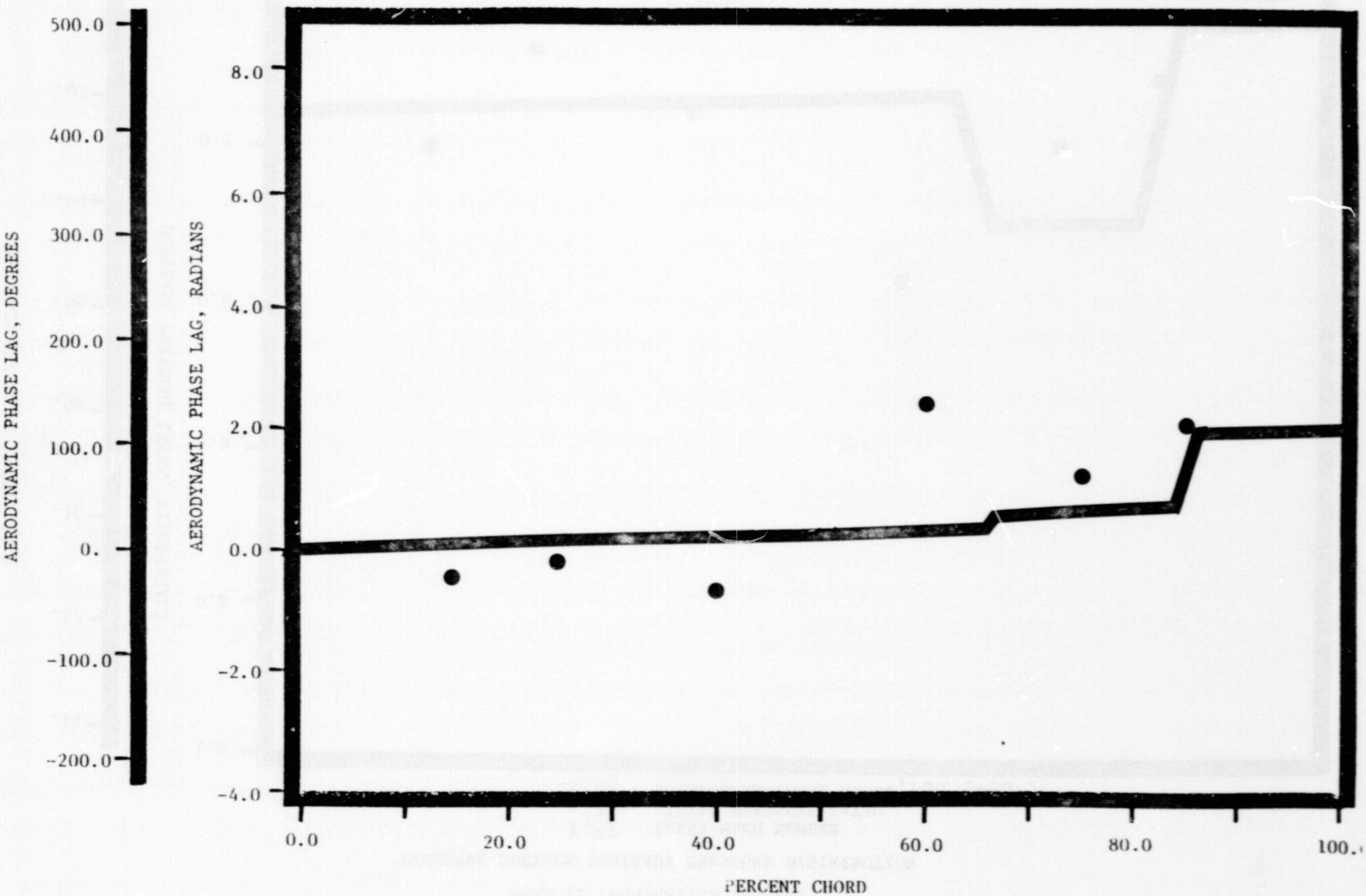

NASA II TRANSLATION CASCADE

PRESSURE SURFACE UNSTEADY PRESSURE DISTRIBUTION

1.32 INLET MACH NUMBER
1.304 STATIC PRESSURE RATIO
-1.05 INTERBLADE PHASE ANGLE, rad (-60°)

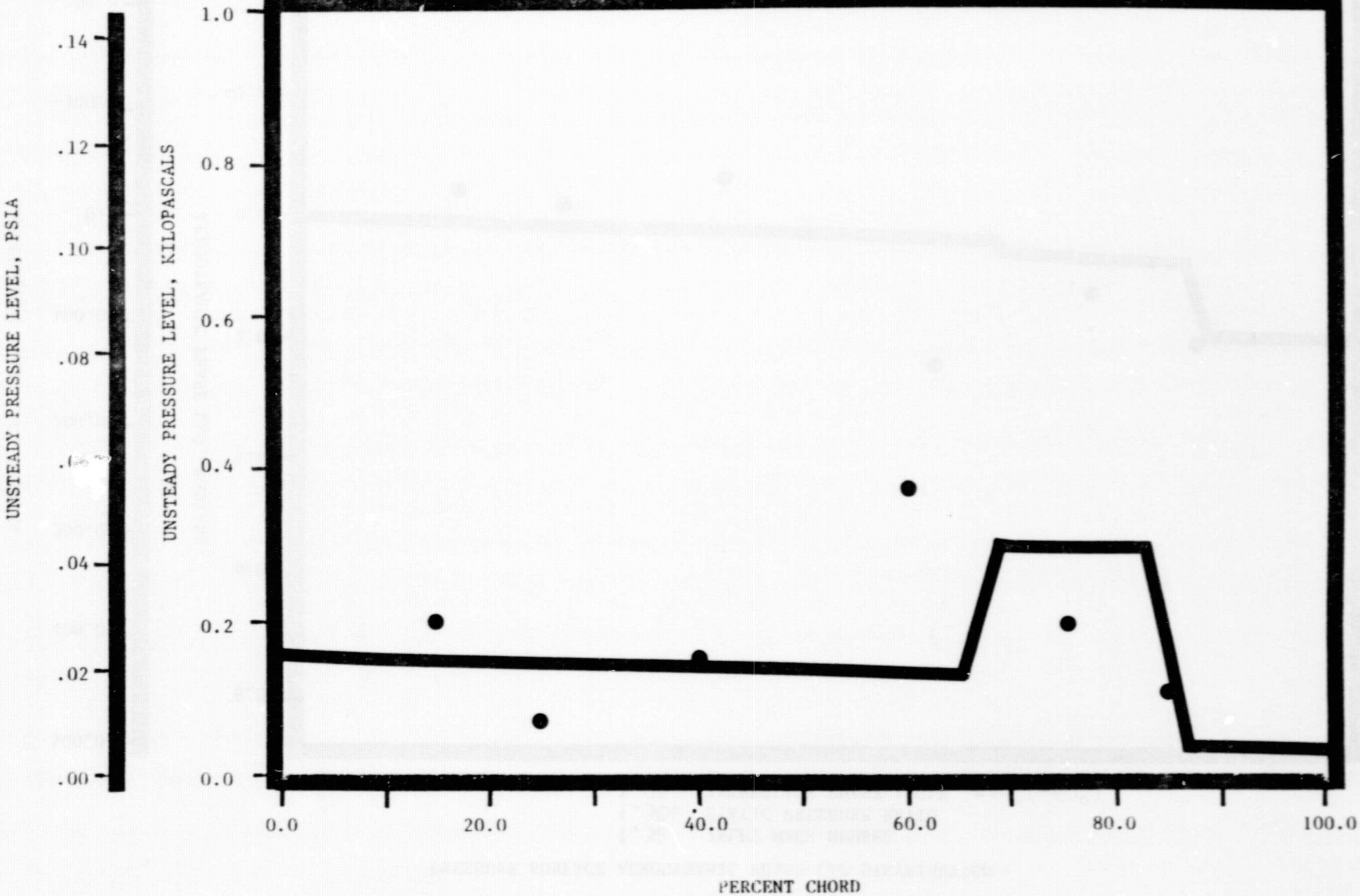

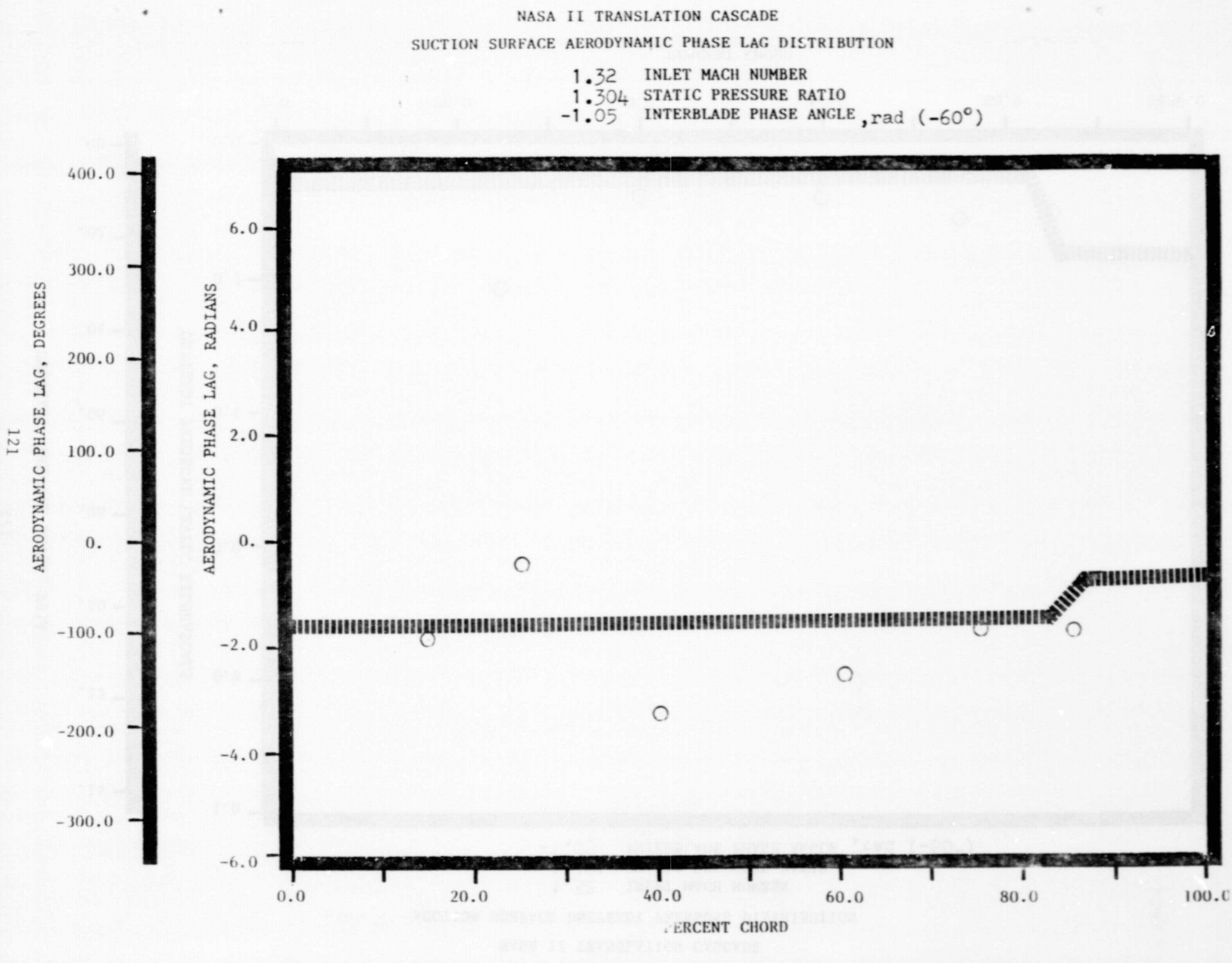
NASA II TRANSLATION CASCADE
SUCTION SURFACE AERODYNAMIC PHASE LAG DISTRIBUTION
1.32 INLET MACH NUMBER
1.304 STATIC PRESSURE RATIO
-1.05 INTERBLADE PHASE ANGLE ,rad (-60°)
AERODYNAMIC PHASE LAG, DEGREES
400.0
300.0
200.0
100.0
0.
-100.0
-200.0
-300.0
AERODYNAMIC PHASE LAG, RADIANS
6.0
4.0
2.0
0.
-2.0
-4.0
-6.0
0.0
20.0
40.0
60.0
80.0
100.0
PERCENT CHORD

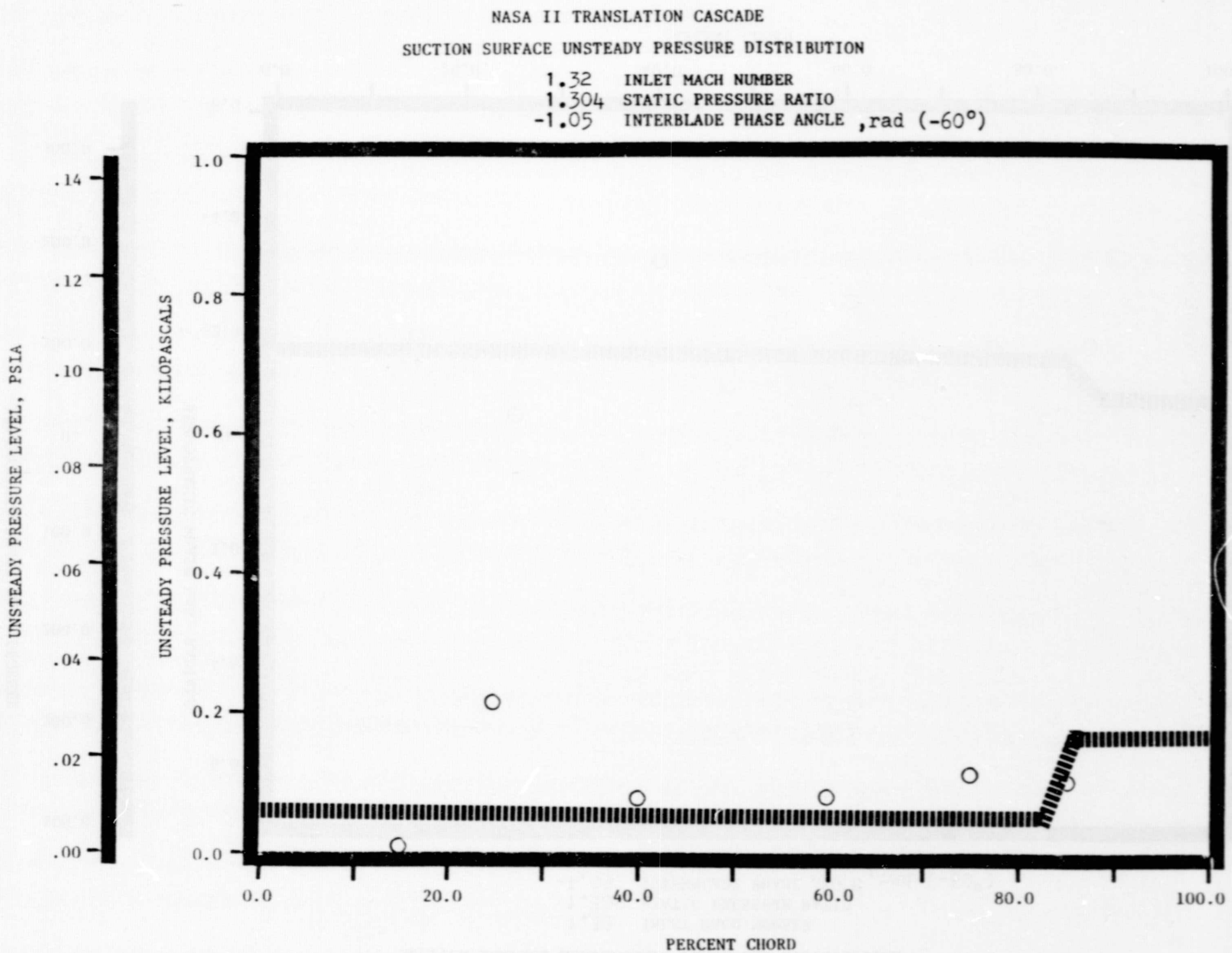
NASA II TRANSLATION CASCADE
SUCTION SURFACE UNSTEADY PRESSURE DISTRIBUTION
1.32 INLET MACH NUMBER
1.304 STATIC PRESSURE RATIO
-1.05 INTERBLADE PHASE ANGLE ,rad (-60°)
UNSTEADY PRESSURE LEVEL, PSIA
.14
.12
.10
.08
.06
.04
.02
.00
UNSTEADY PRESSURE LEVEL, KILOPASCALS
1.0
0.8
0.6
0.4
0.2
0.0
0.0
20.0
40.0
60.0
80.0
100.0
PERCENT CHORD

NASA II TRANSLATION CASCADE

PRESSURE SURFACE AERODYNAMIC PHASE LAG DISTRIBUTION

1.32 INLET MACH NUMBER
1.304 STATIC PRESSURE RATIO
-1.57 INTERBLADE PHASE ANGLE ,rad (-90°)

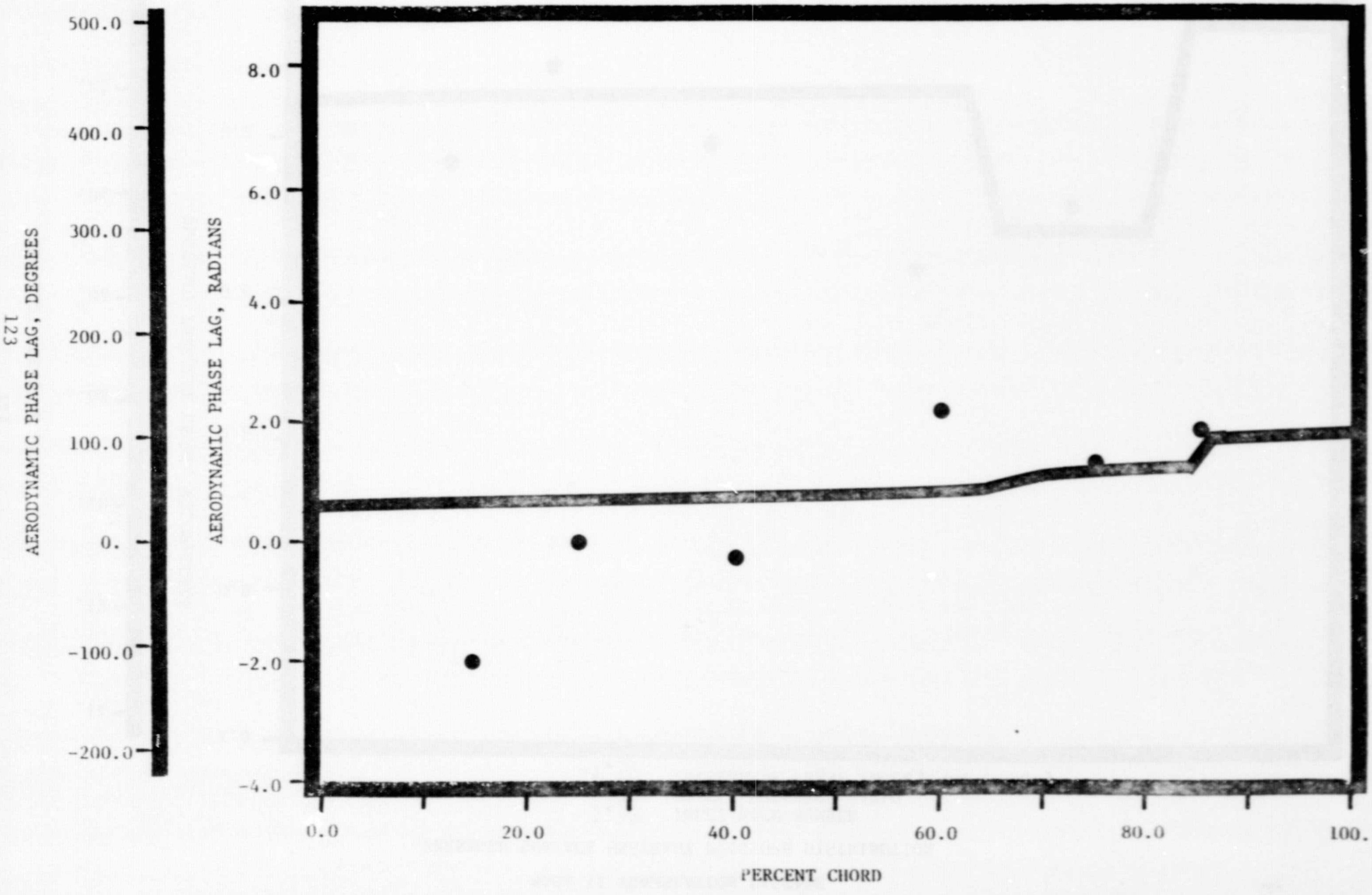

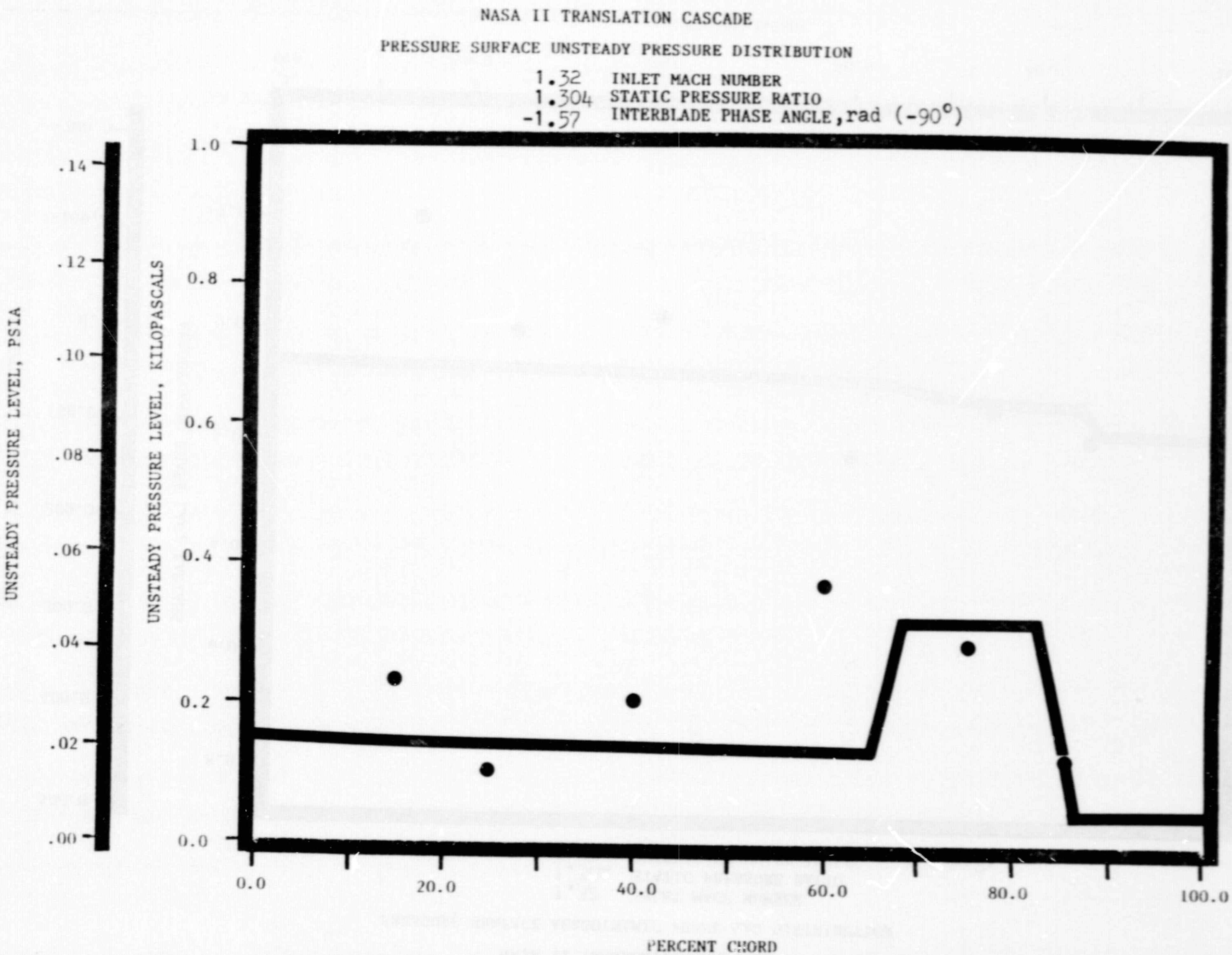
NASA II TRANSLATION CASCADE
PRESSURE SURFACE UNSTEADY PRESSURE DISTRIBUTION
1.32 INLET MACH NUMBER
1.304 STATIC PRESSURE RATIO
-1.57 INTERBLADE PHASE ANGLE, rad (-90°)
UNSTEADY PRESSURE LEVEL, PSIA
.14
.12
.10
.08
.06
.04
.02
.00
UNSTEADY PRESSURE LEVEL, KILOPASCALS
1.0
0.8
0.6
0.4
0.2
0.0
0.0
20.0
40.0
60.0
80.0
100.0
PERCENT CHORD

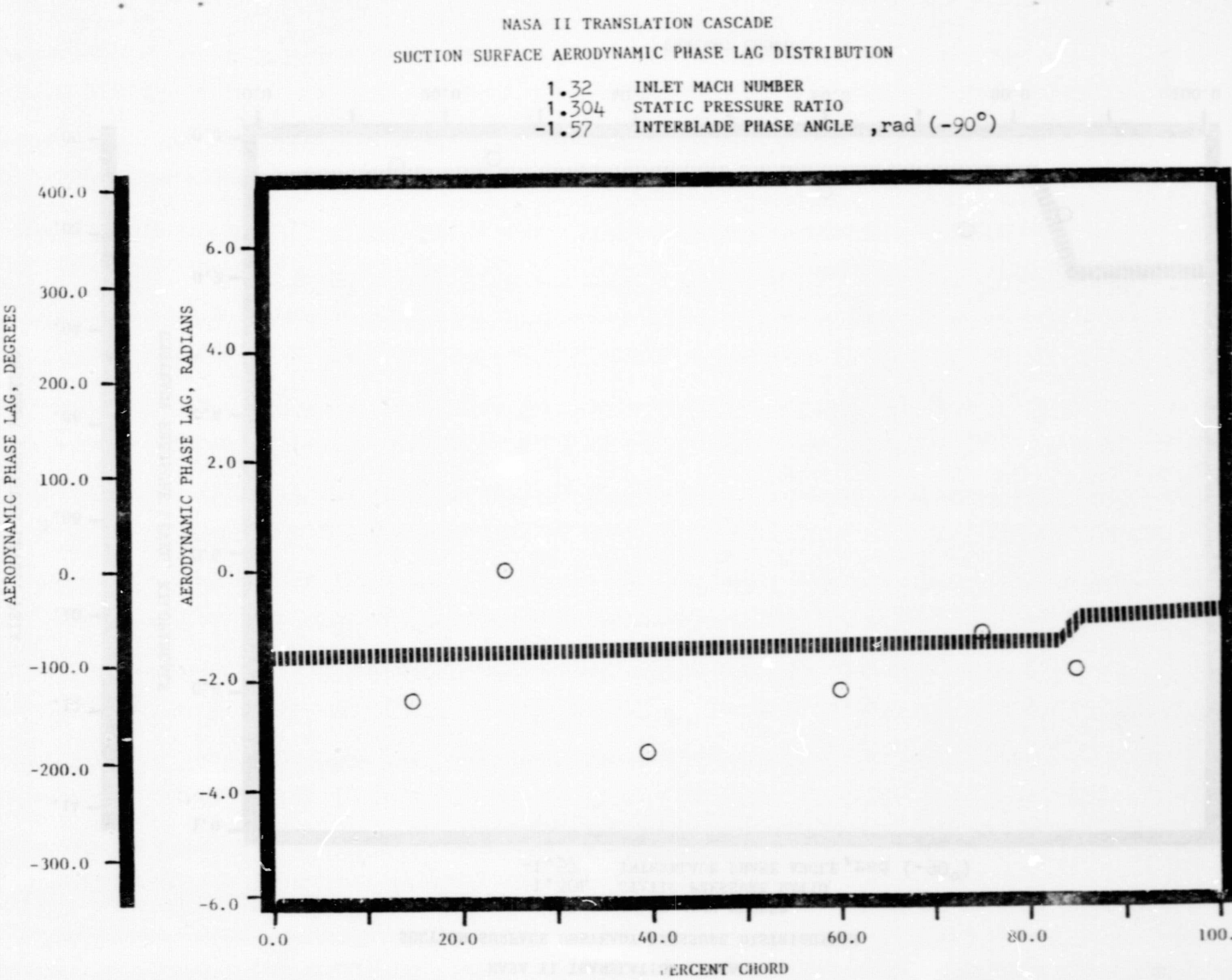
NASA II TRANSLATION CASCADE
SUCTION SURFACE AERODYNAMIC PHASE LAG DISTRIBUTION
1.32 INLET MACH NUMBER
1.304 STATIC PRESSURE RATIO
-1.57 INTERBLADE PHASE ANGLE ,rad (-90°)
AERODYNAMIC PHASE LAG, DEGREES
400.0
300.0
200.0
100.0
0.
-100.0
-200.0
-300.0
AERODYNAMIC PHASE LAG, RADIANS
6.0
4.0
2.0
0.
-2.0
-4.0
-6.0
0.0
20.0
40.0
60.0
80.0
100.0
PERCENT CHORD

NASA II TRANSLATION CASCADE

SUCTION SURFACE UNSTEADY PRESSURE DISTRIBUTION

1.32 INLET MACH NUMBER
1.304 STATIC PRESSURE RATIO
-1.57 INTERBLADE PHASE ANGLE, rad (-90°)

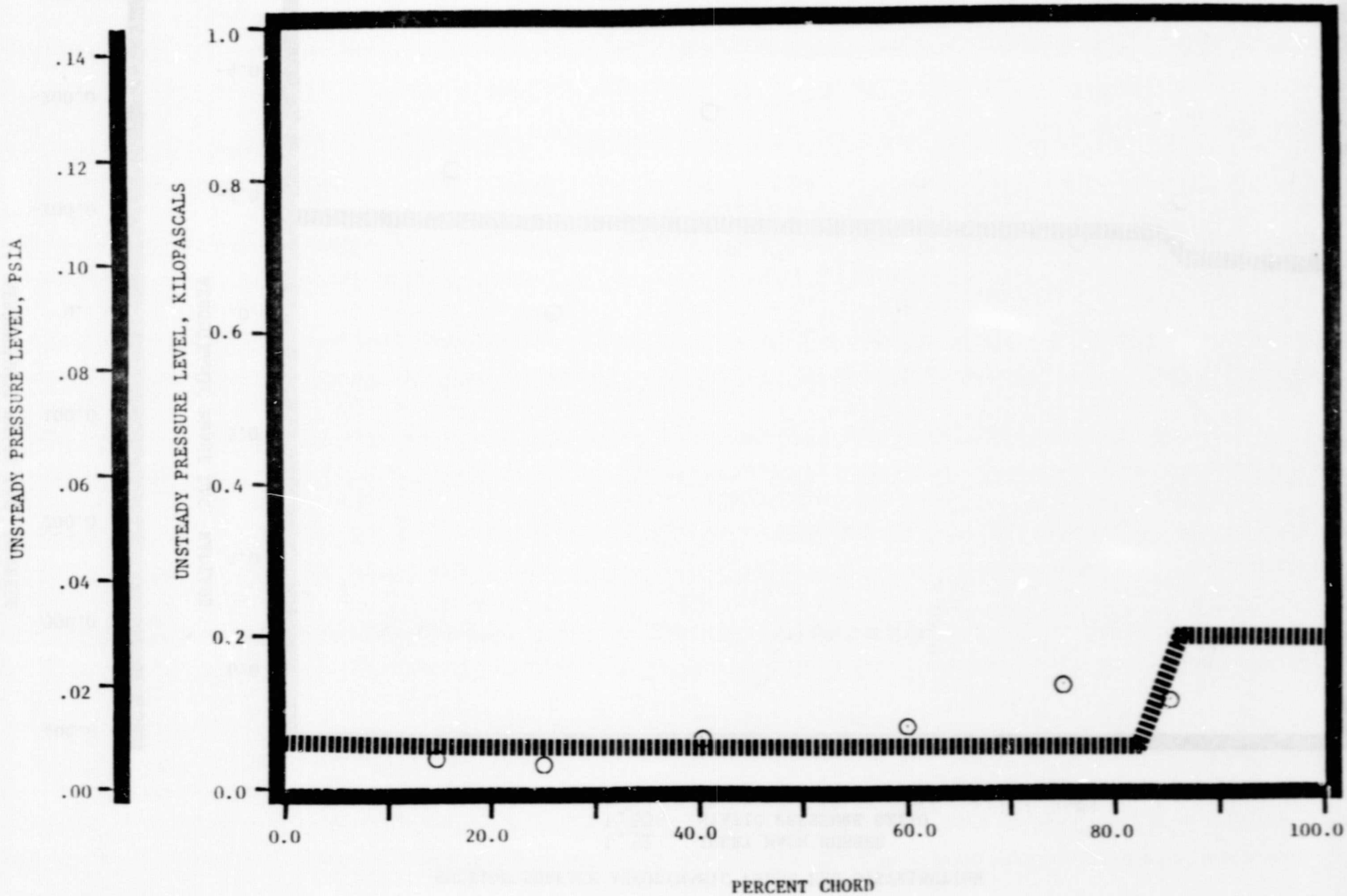

NASA II TRANSLATION CASCADE

PRESSURE SURFACE AERODYNAMIC PHASE LAG DISTRIBUTION

1.32 INLET MACH NUMBER
1.475 STATIC PRESSURE RATIO
3.14 INTERBLADE PHASE ANGLE .rad (180°)

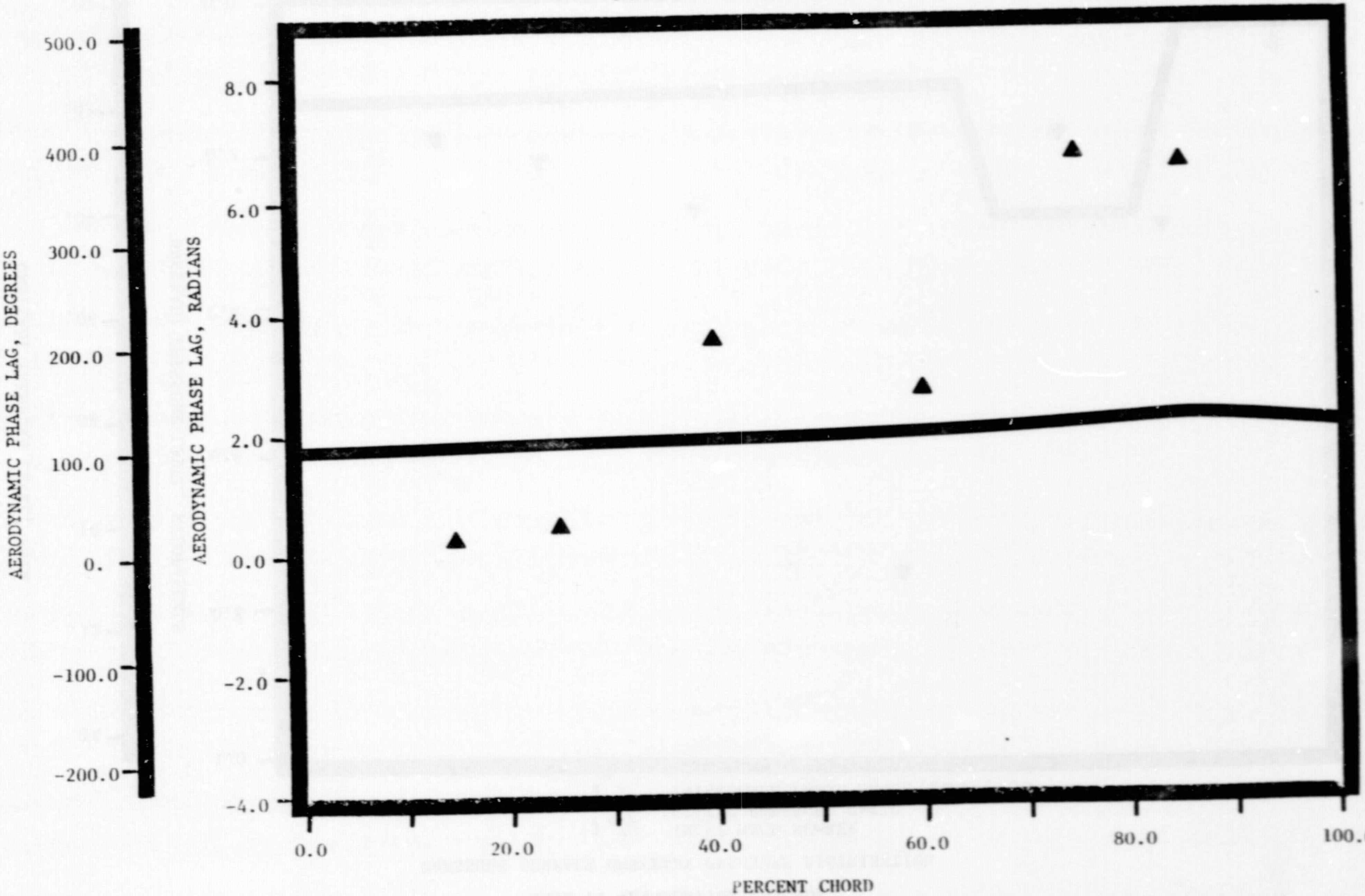

NASA II TRANSLATION CASCADE

PRESSURE SURFACE UNSTEADY PRESSURE DISTRIBUTION

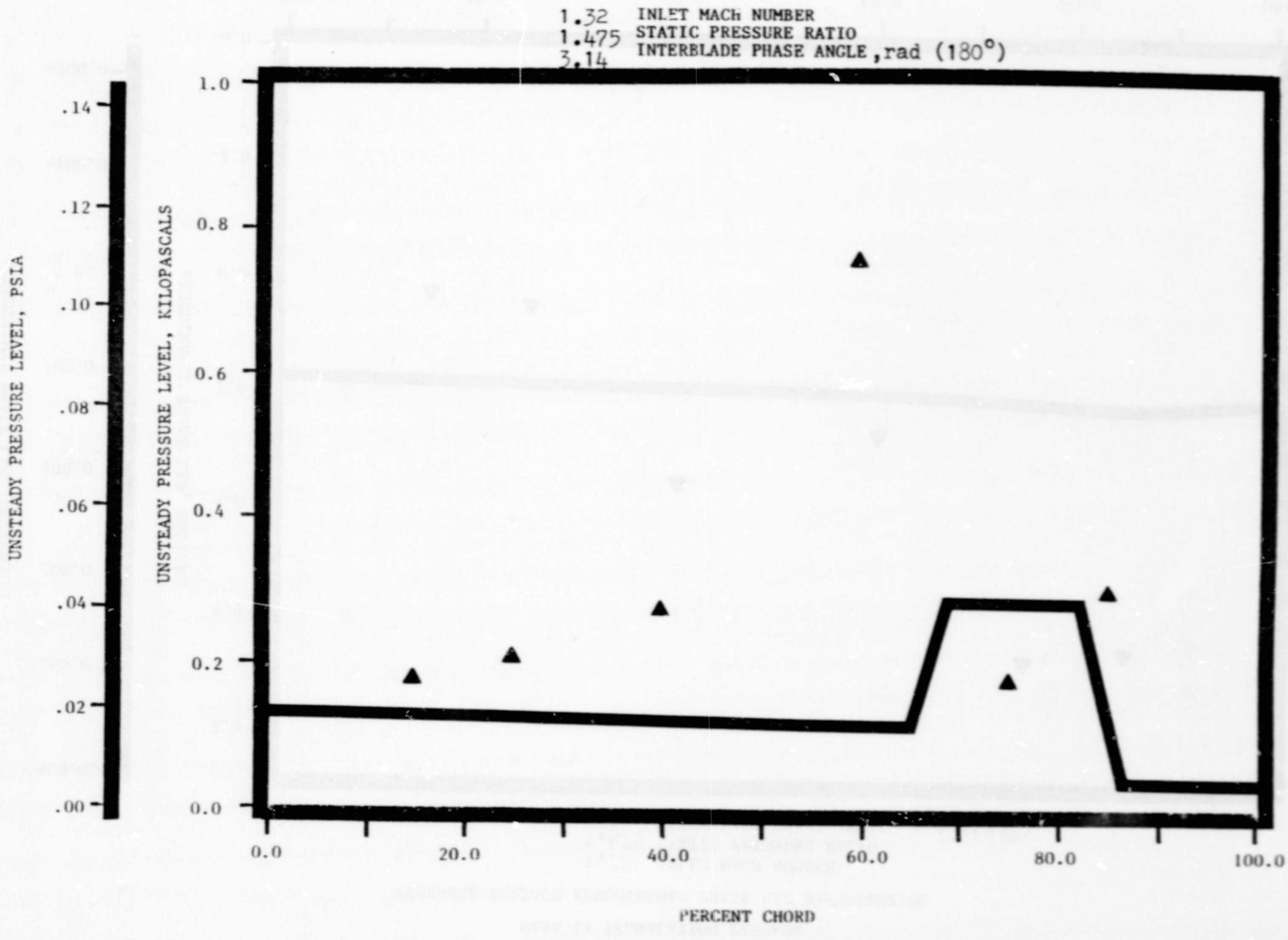

NASA II TRANSLATION CASCADE

SUCTION SURFACE AERODYNAMIC PHASE LAG DISTRIBUTION

1.32 INLET MACH NUMBER
1.475 STATIC PRESSURE RATIO
3.14 INTERBLADE PHASE ANGLE ,rad (180°)

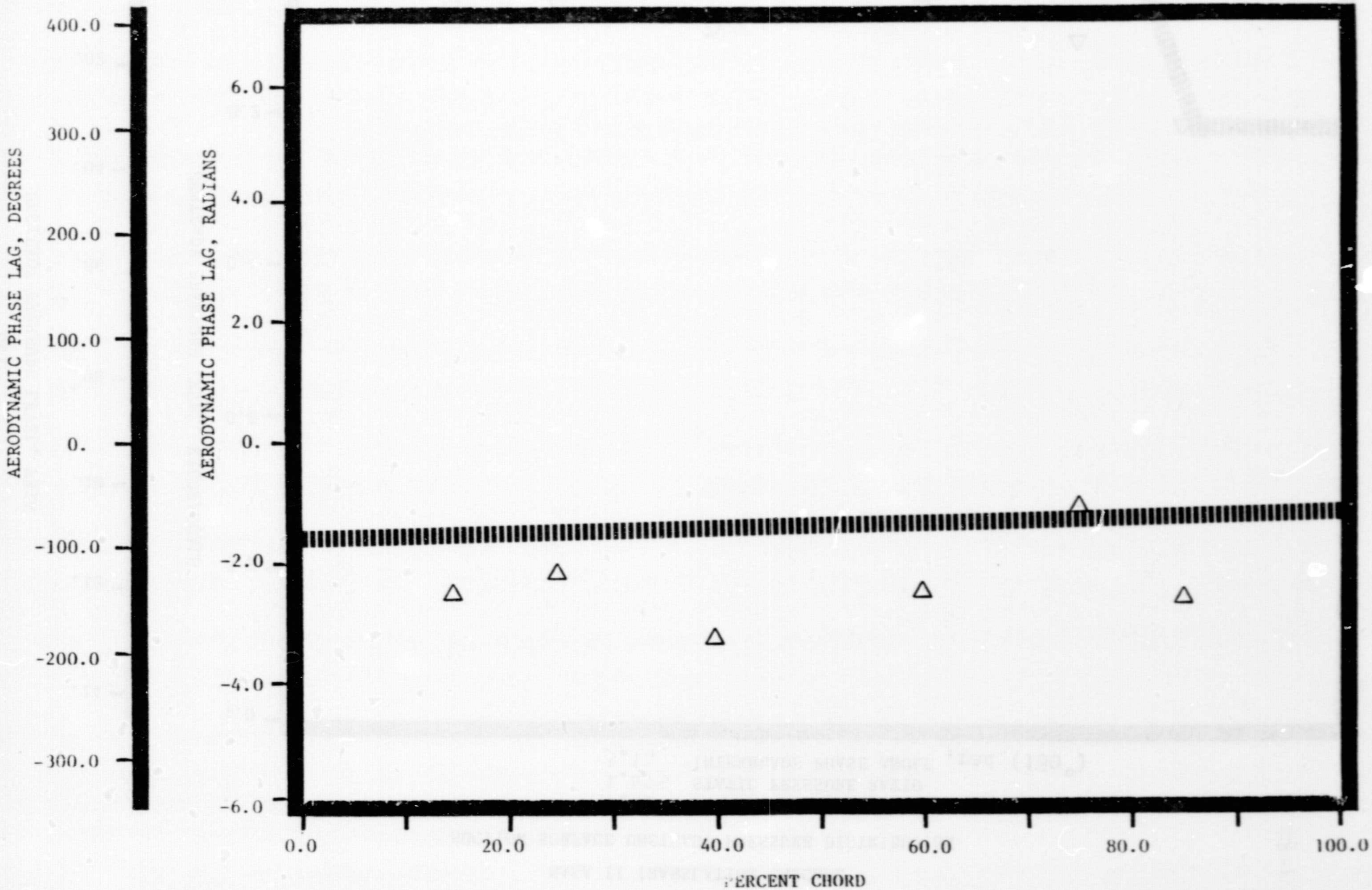

NASA II TRANSLATION CASCADE

SUCTION SURFACE UNSTEADY PRESSURE DISTRIBUTION

1.32 INLET MACH NUMBER
1.475 STATIC PRESSURE RATIO
3.14 INTERBLADE PHASE ANGLE ,rad (180°)

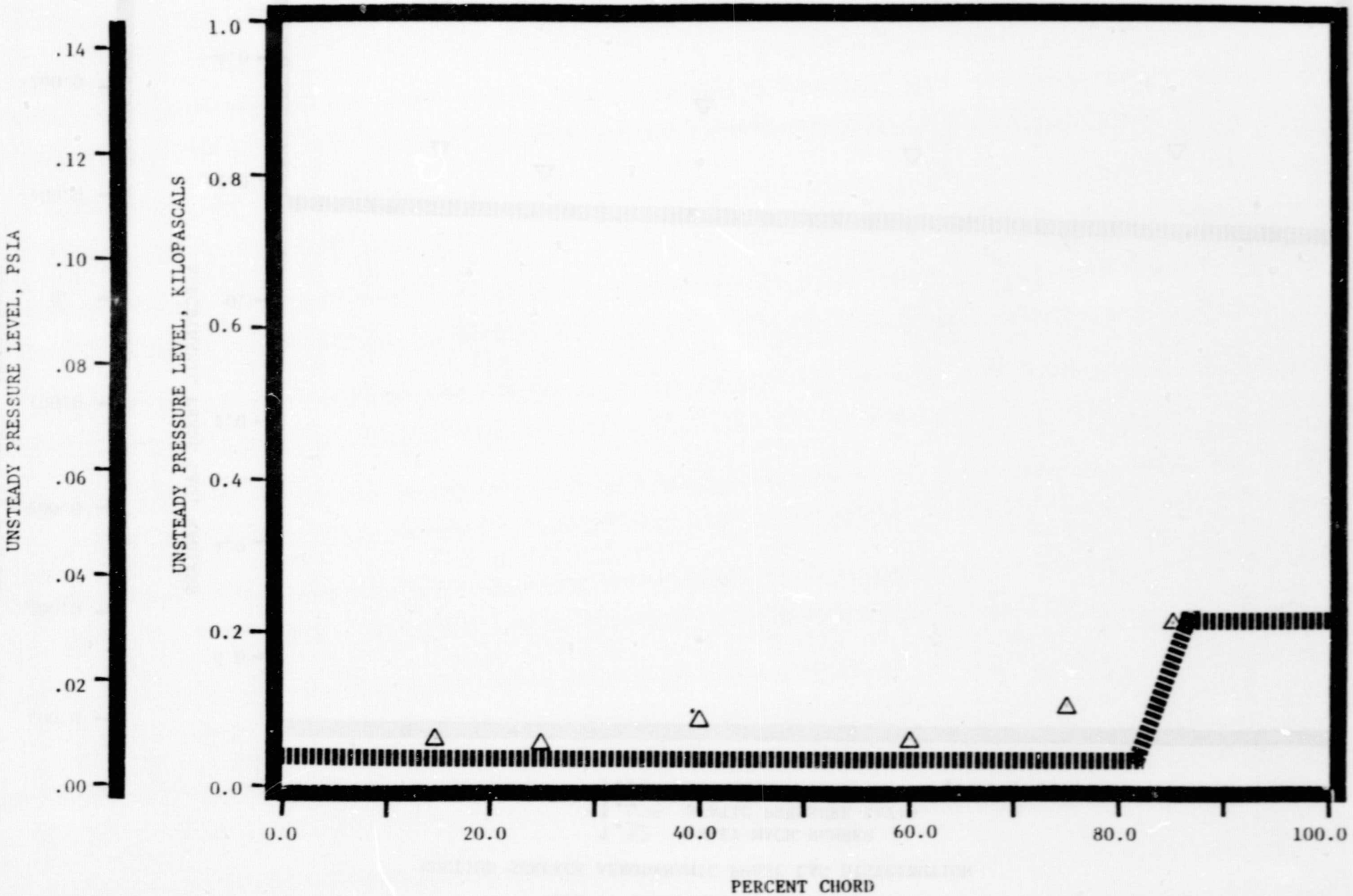

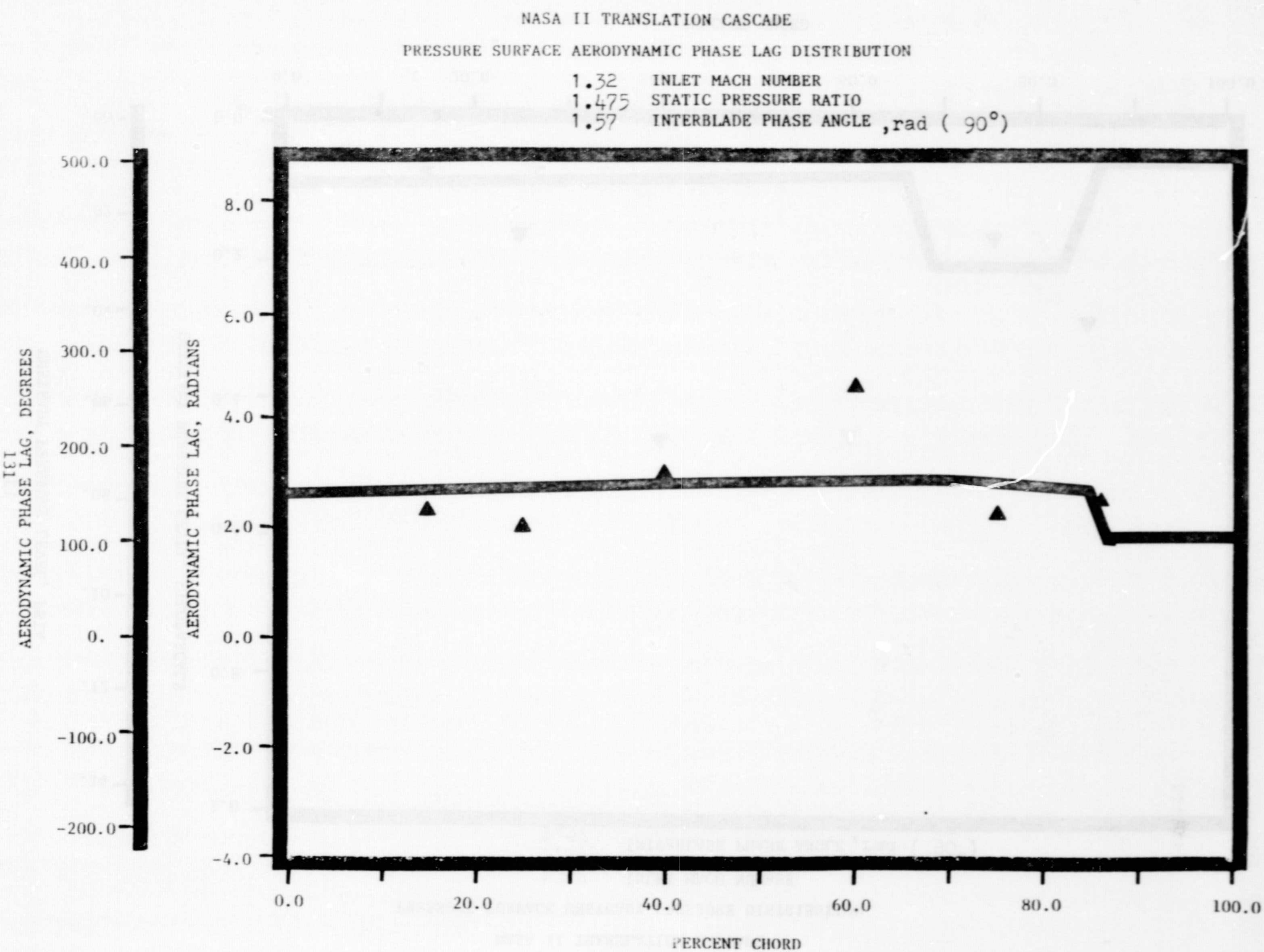
NASA II TRANSLATION CASCADE
PRESSURE SURFACE AERODYNAMIC PHASE LAG DISTRIBUTION
1.32 INLET MACH NUMBER
1.475 STATIC PRESSURE RATIO
1.57 INTERBLADE PHASE ANGLE ,rad (90°)
AERODYNAMIC PHASE LAG, DEGREES
500.0
400.0
300.0
200.0
100.0
0.
-100.0
-200.0
AERODYNAMIC PHASE LAG, RADIANS
8.0
6.0
4.0
2.0
0.0
-2.0
-4.0
0.0
20.0
40.0
60.0
80.0
100.0
PERCENT CHORD

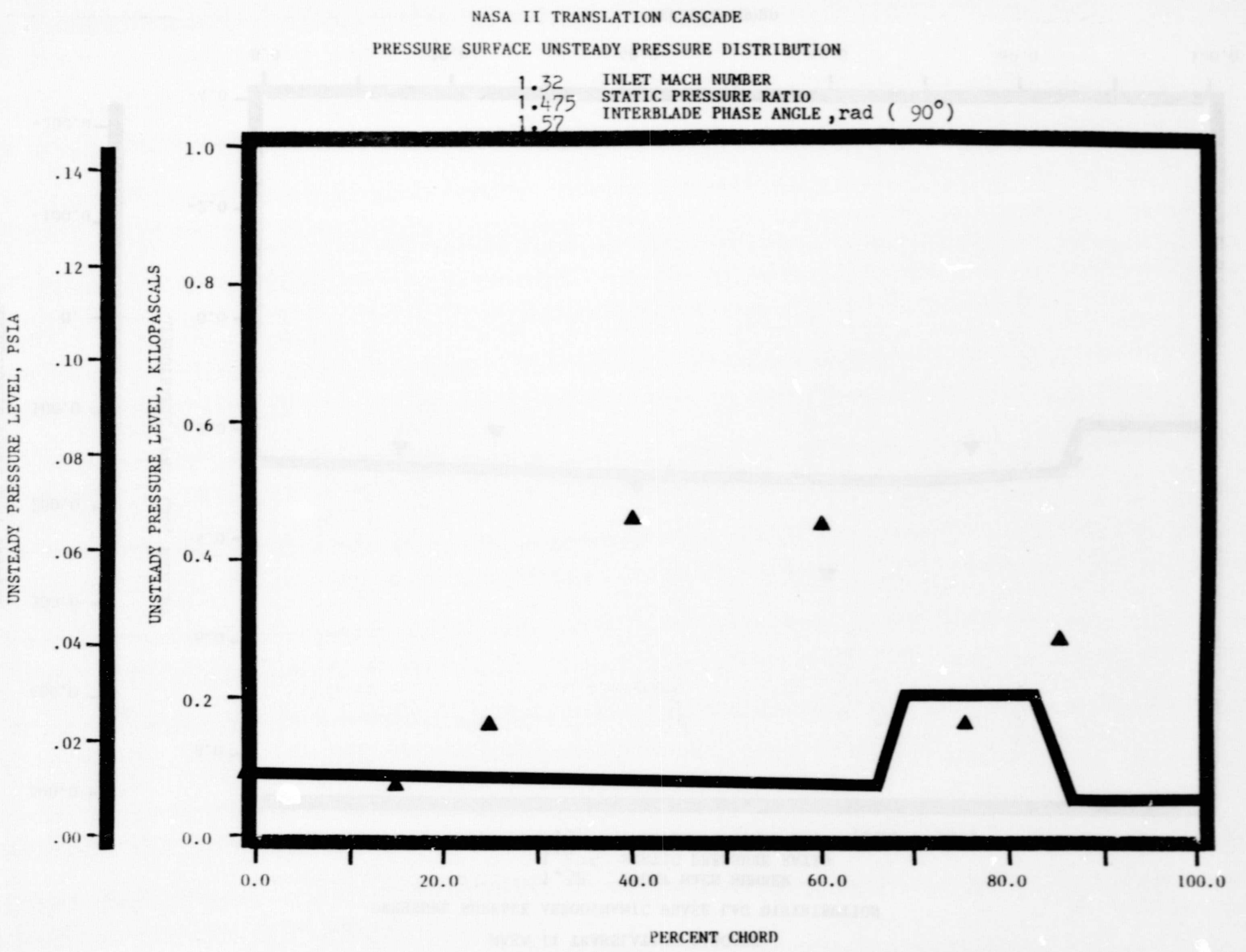
NASA II TRANSLATION CASCADE
PRESSURE SURFACE UNSTEADY PRESSURE DISTRIBUTION
1.32 INLET MACH NUMBER
1.475 STATIC PRESSURE RATIO
1.57 INTERBLADE PHASE ANGLE ,rad (90°)
UNSTEADY PRESSURE LEVEL, PSIA
.14
.12
.10
.08
.06
.04
.02
.00
UNSTEADY PRESSURE LEVEL, KILOPASCALS
1.0
0.8
0.6
0.4
0.2
0.0
0.0
20.0
40.0
60.0
80.0
100.0
PERCENT CHORD

NASA II TRANSLATION CASCADE

SUCTION SURFACE AERODYNAMIC PHASE LAG DISTRIBUTION

1.32 INLET MACH NUMBER
1.475 STATIC PRESSURE RATIO
1.57 INTERBLADE PHASE ANGLE, rad (90°)

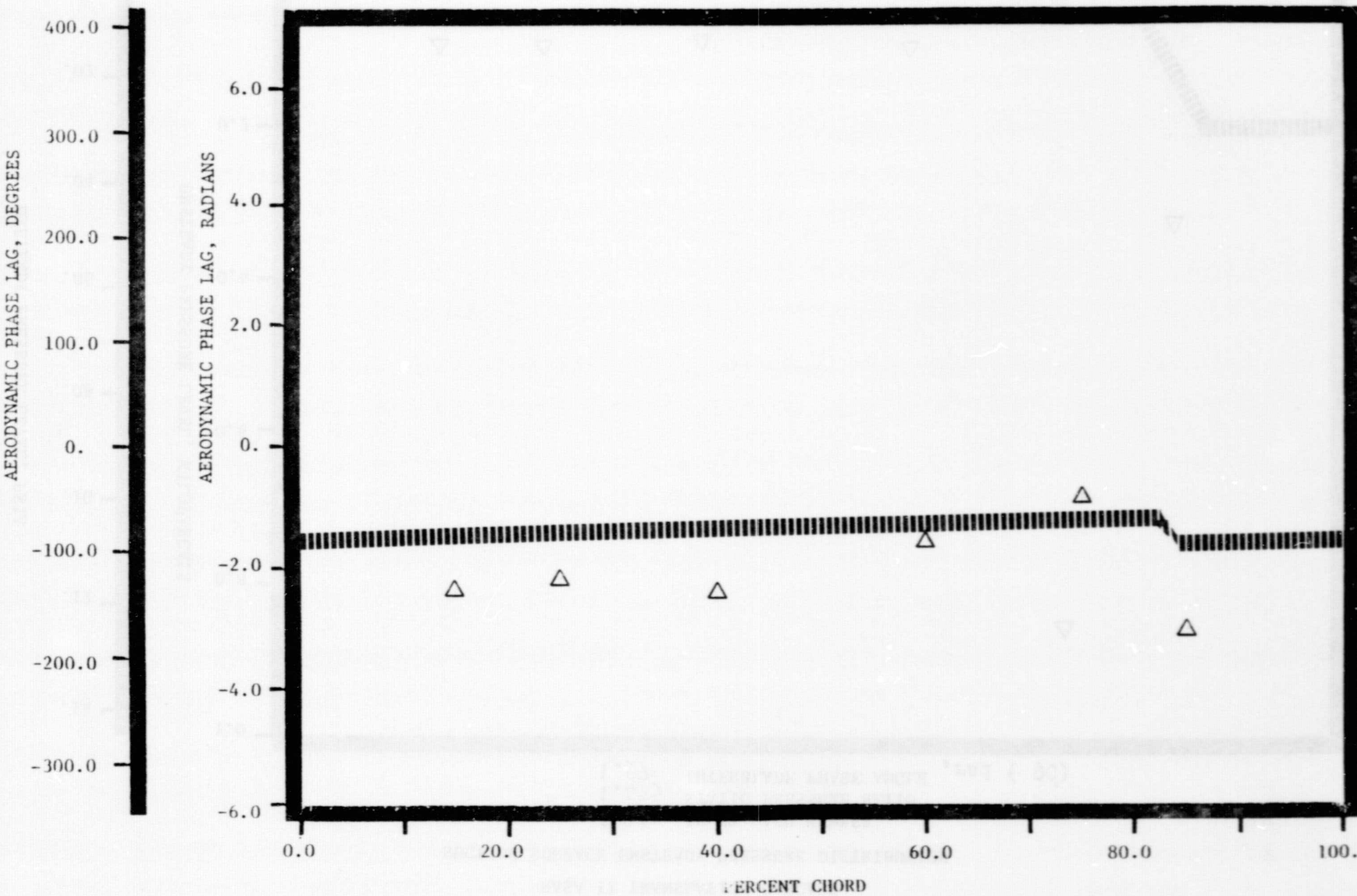

NASA II TRANSLATION CASCADE

SUCTION SURFACE UNSTEADY PRESSURE DISTRIBUTION

1.32 INLET MACH NUMBER
1.475 STATIC PRESSURE RATIO
1.57 INTERBLADE PHASE ANGLE ,rad (90°)

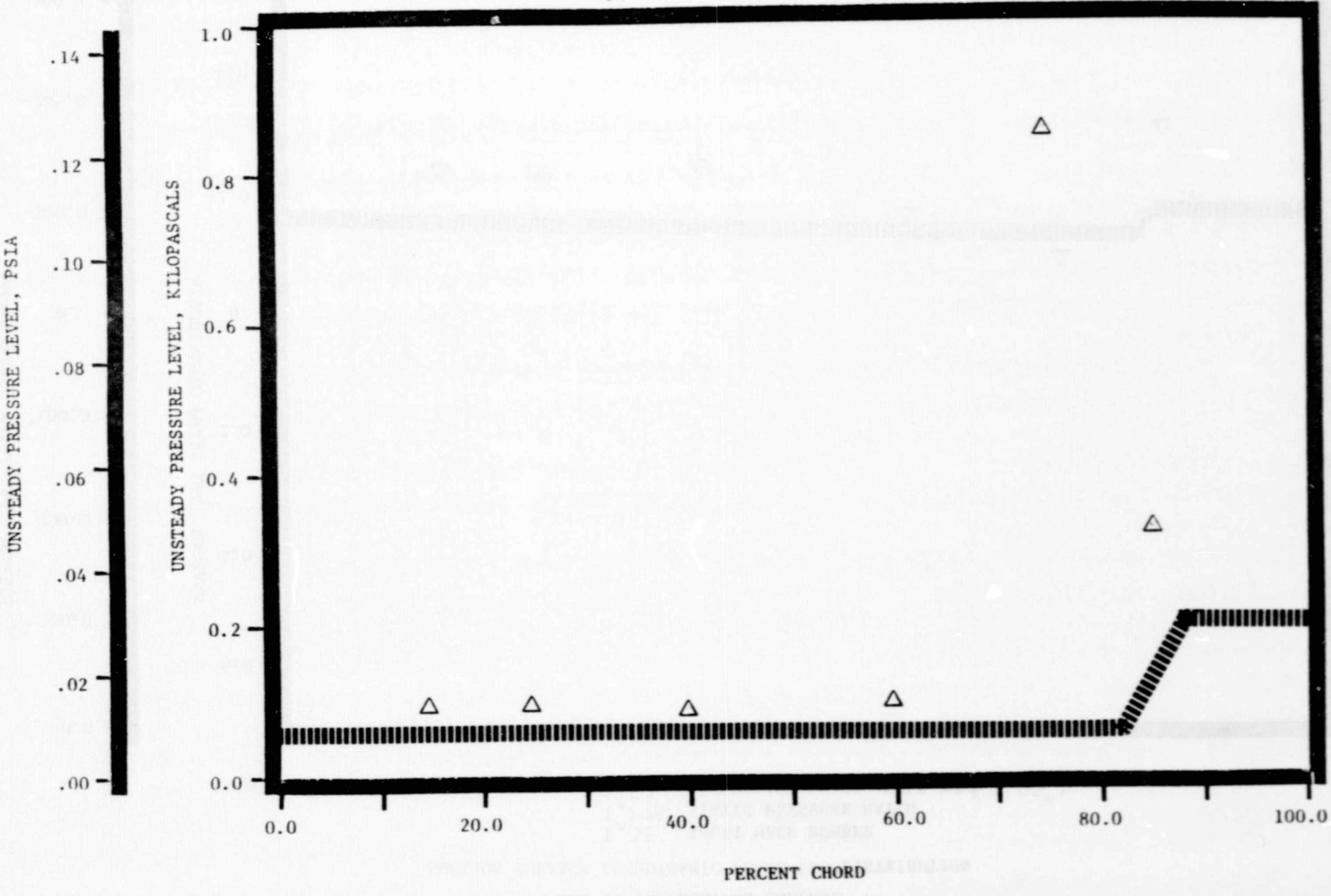

NASA II TRANSLATION CASCADE

PRESSURE SURFACE AERODYNAMIC PHASE LAG DISTRIBUTION

1.32 INLET MACH NUMBER
1.475 STATIC PRESSURE RATIO
1.05 INTERBLADE PHASE ANGLE ,rad (60°)

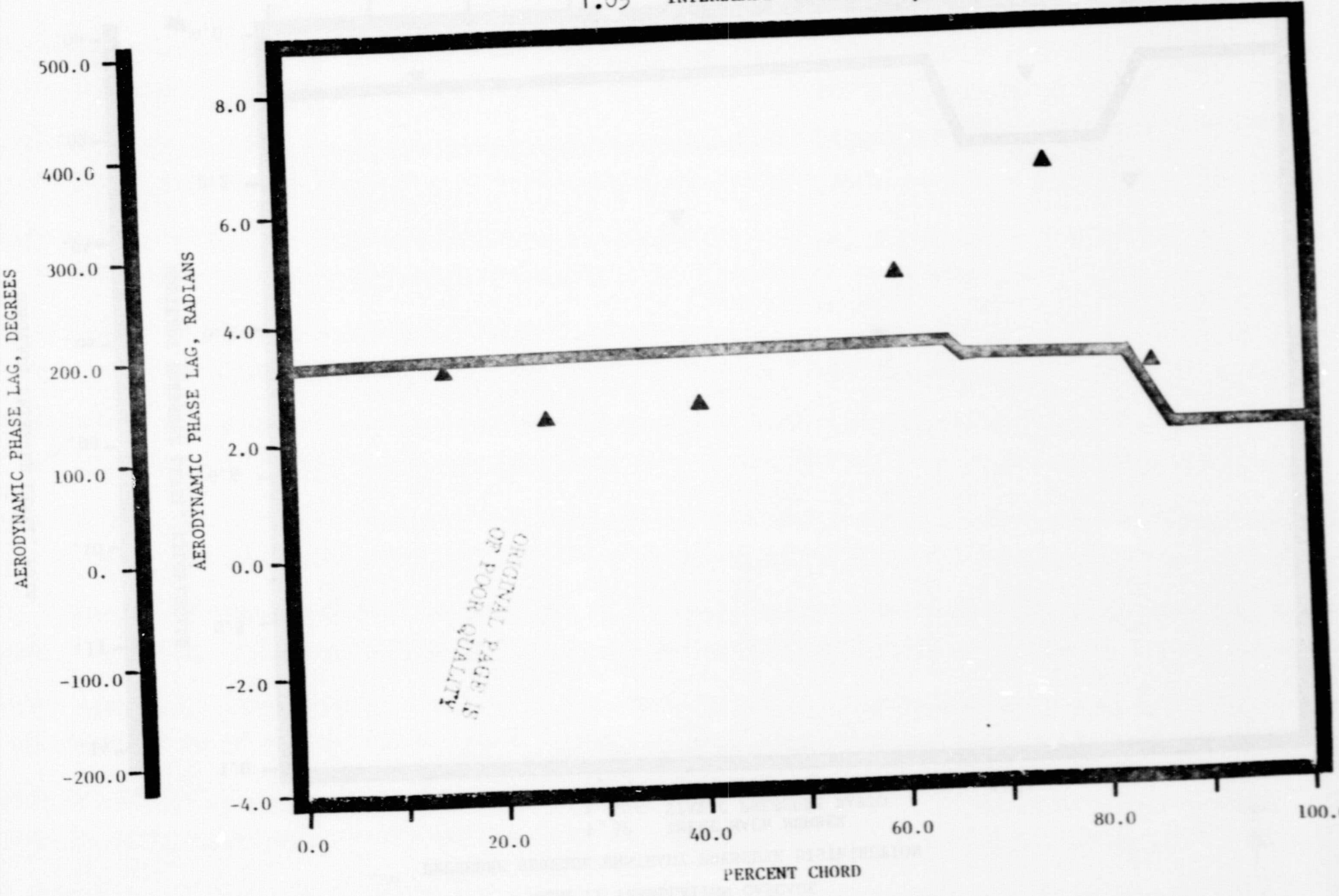

NASA II TRANSLATION CASCADE

PRESSURE SURFACE UNSTEADY PRESSURE DISTRIBUTION

1.32 INLET MACH NUMBER
1.475 STATIC PRESSURE RATIO
1.05 INTERBLADE PHASE ANGLE, rad (60°)

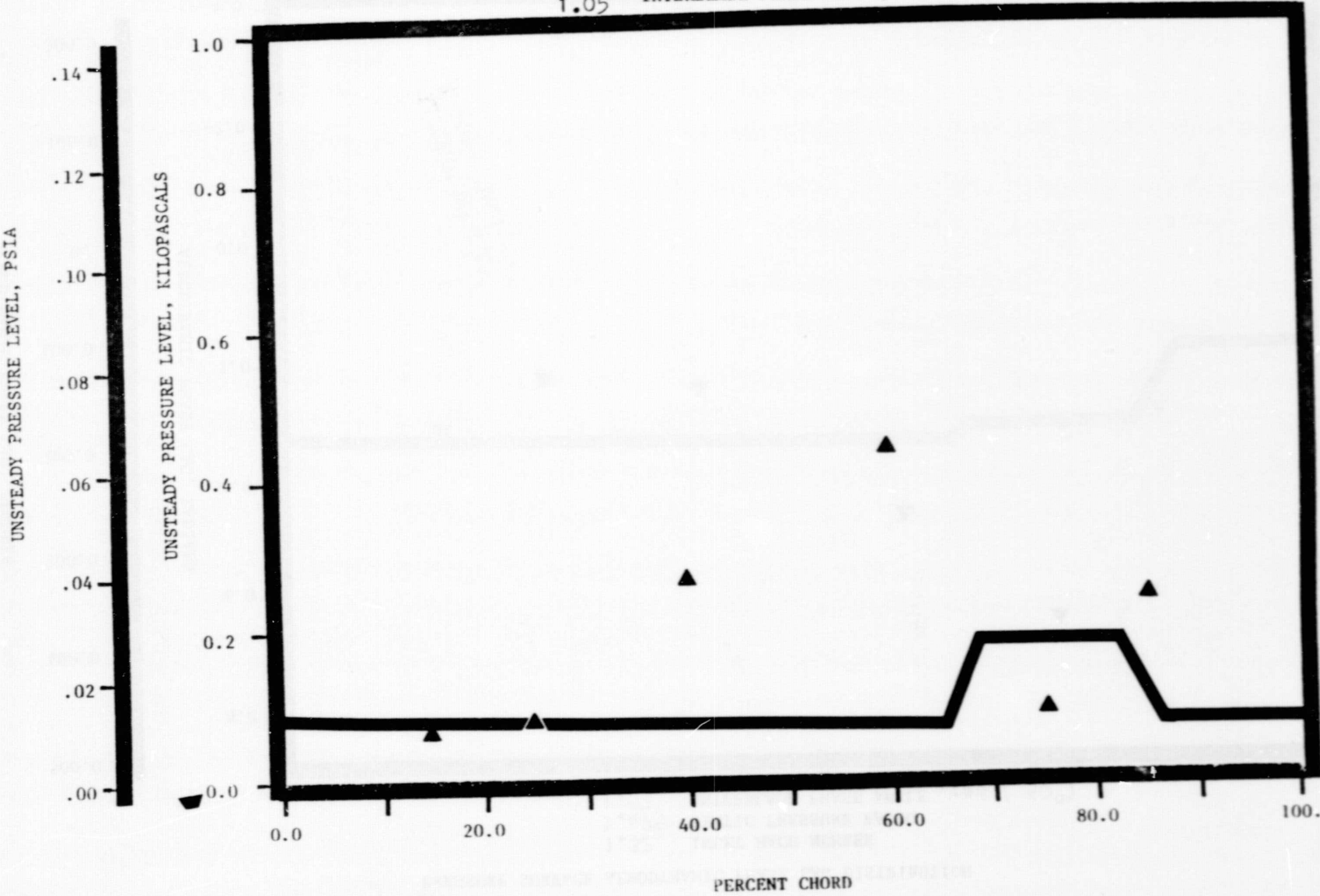

NASA II TRANSLATION CASCADE

SUCTION SURFACE AERODYNAMIC PHASE LAG DISTRIBUTION

1.32 INLET MACH NUMBER
1.475 STATIC PRESSURE RATIO
1.05 INTERBLADE PHASE ANGLE ,rad (60°)

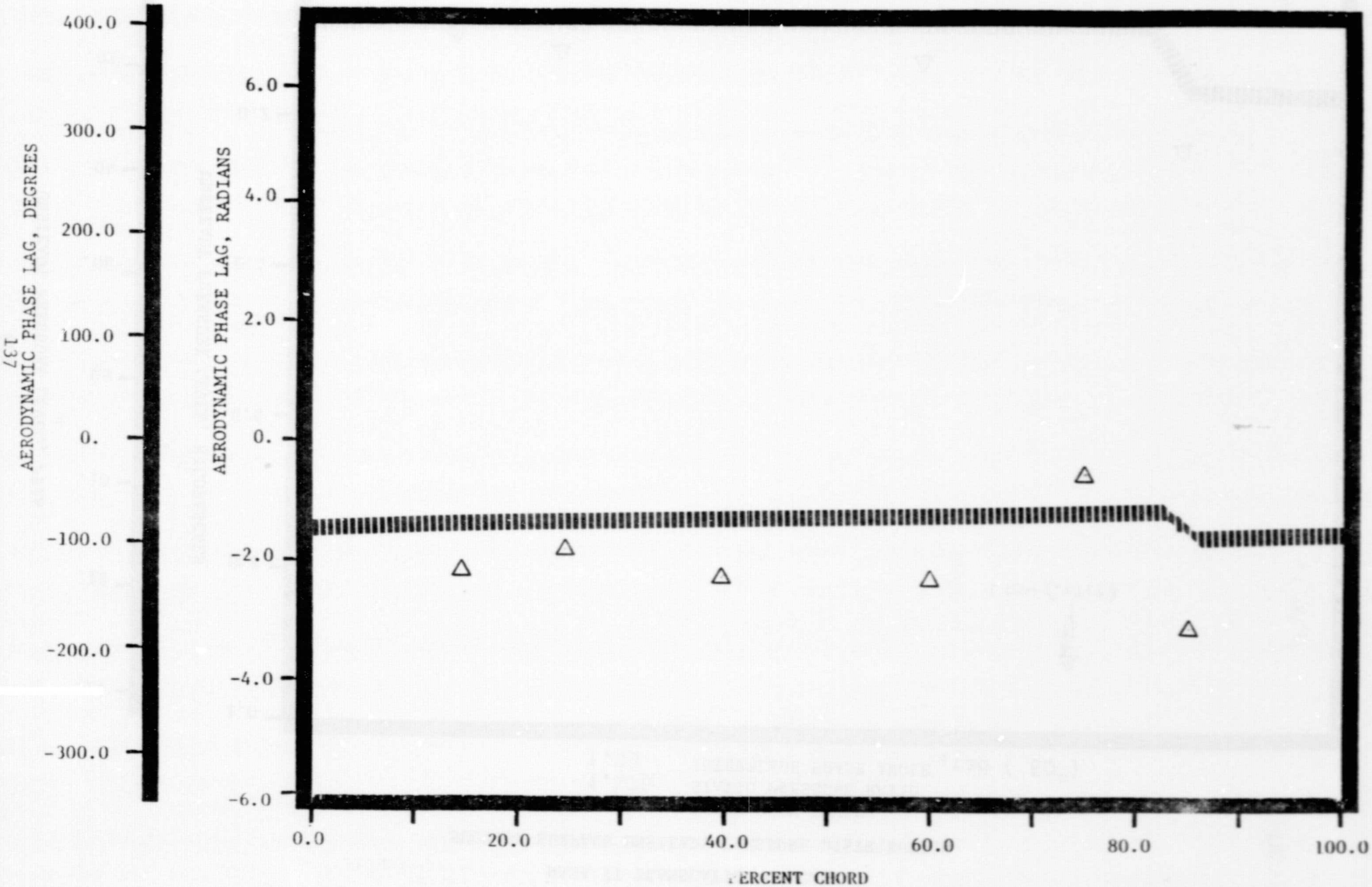

NASA II TRANSLATION CASCADE

SUCTION SURFACE UNSTEADY PRESSURE DISTRIBUTION

1.32 INLET MACH NUMBER
1.475 STATIC PRESSURE RATIO
1.05 INTERBLADE PHASE ANGLE ,rad (60°)

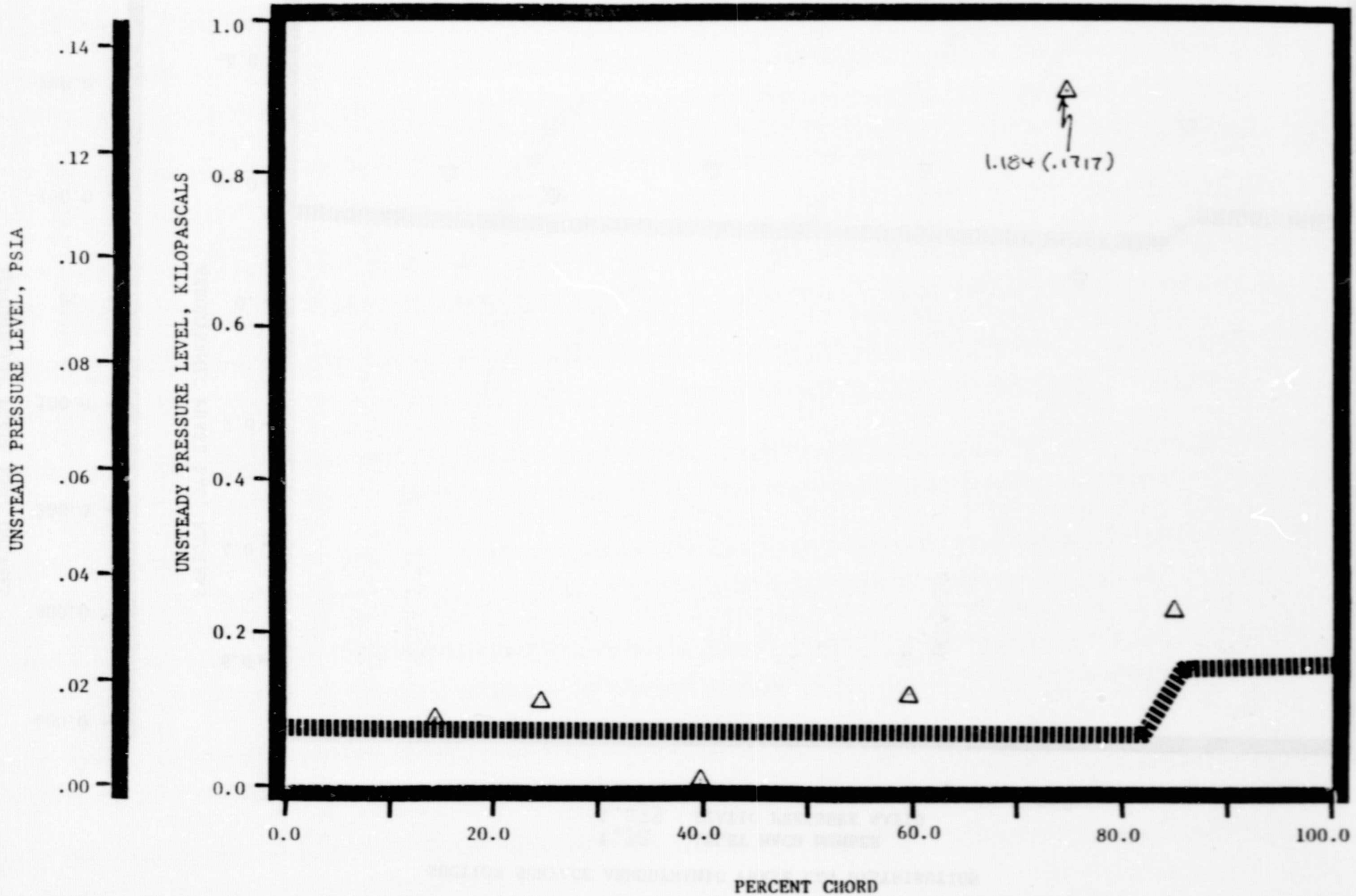

NASA II TRANSLATION CASCADE

PRESSURE SURFACE AERODYNAMIC PHASE LAG DISTRIBUTION

1.32 INLET MACH NUMBER
1.475 STATIC PRESSURE RATIO
0.0 INTERBLADE PHASE ANGLE ,rad (0.0°)

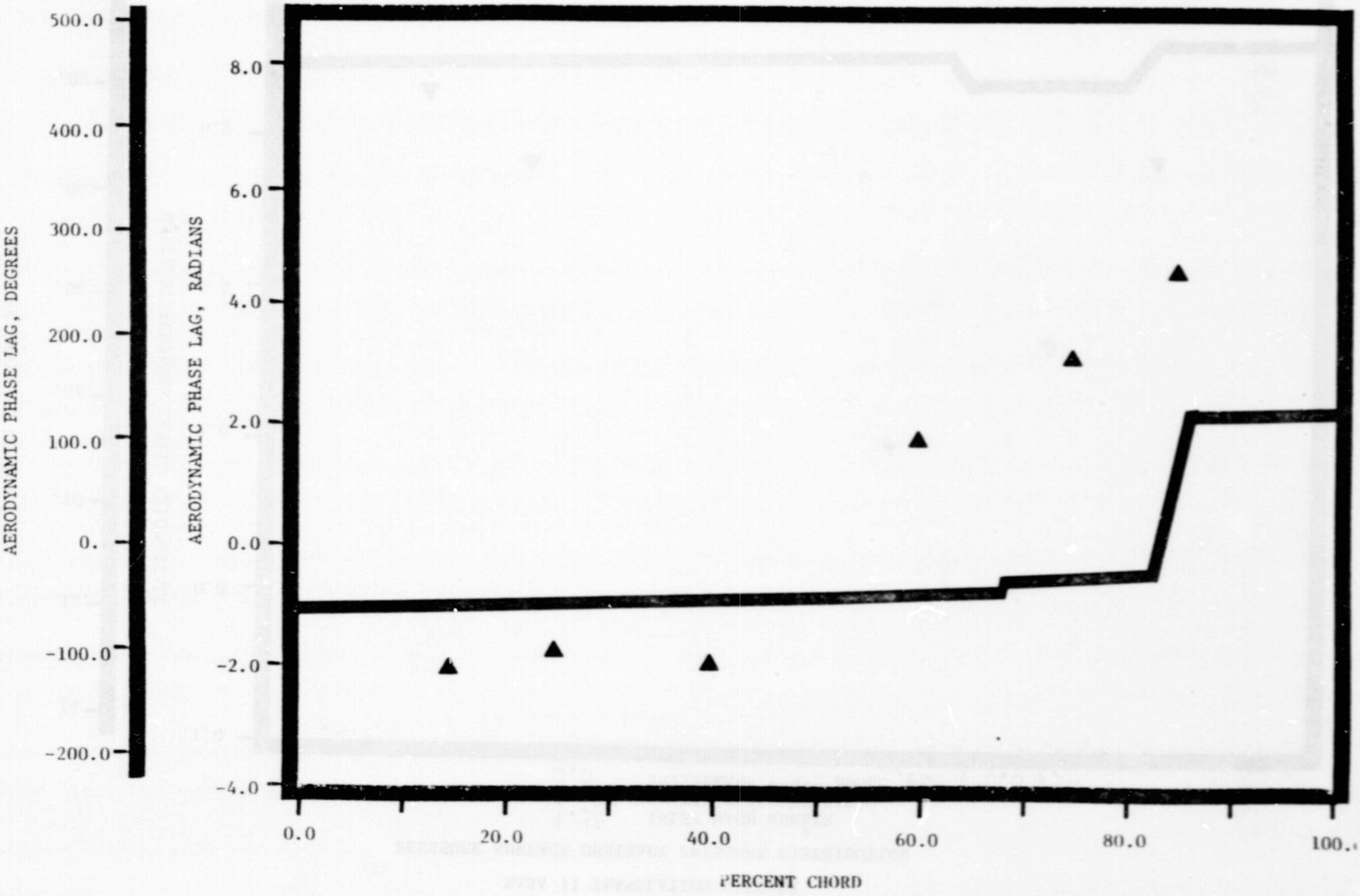

NASA II TRANSLATION CASCADE

PRESSURE SURFACE UNSTEADY PRESSURE DISTRIBUTION

1.32 INLET MACH NUMBER
1.475 STATIC PRESSURE RATIO
0.0 INTERBLADE PHASE ANGLE ,rad (0.0°)

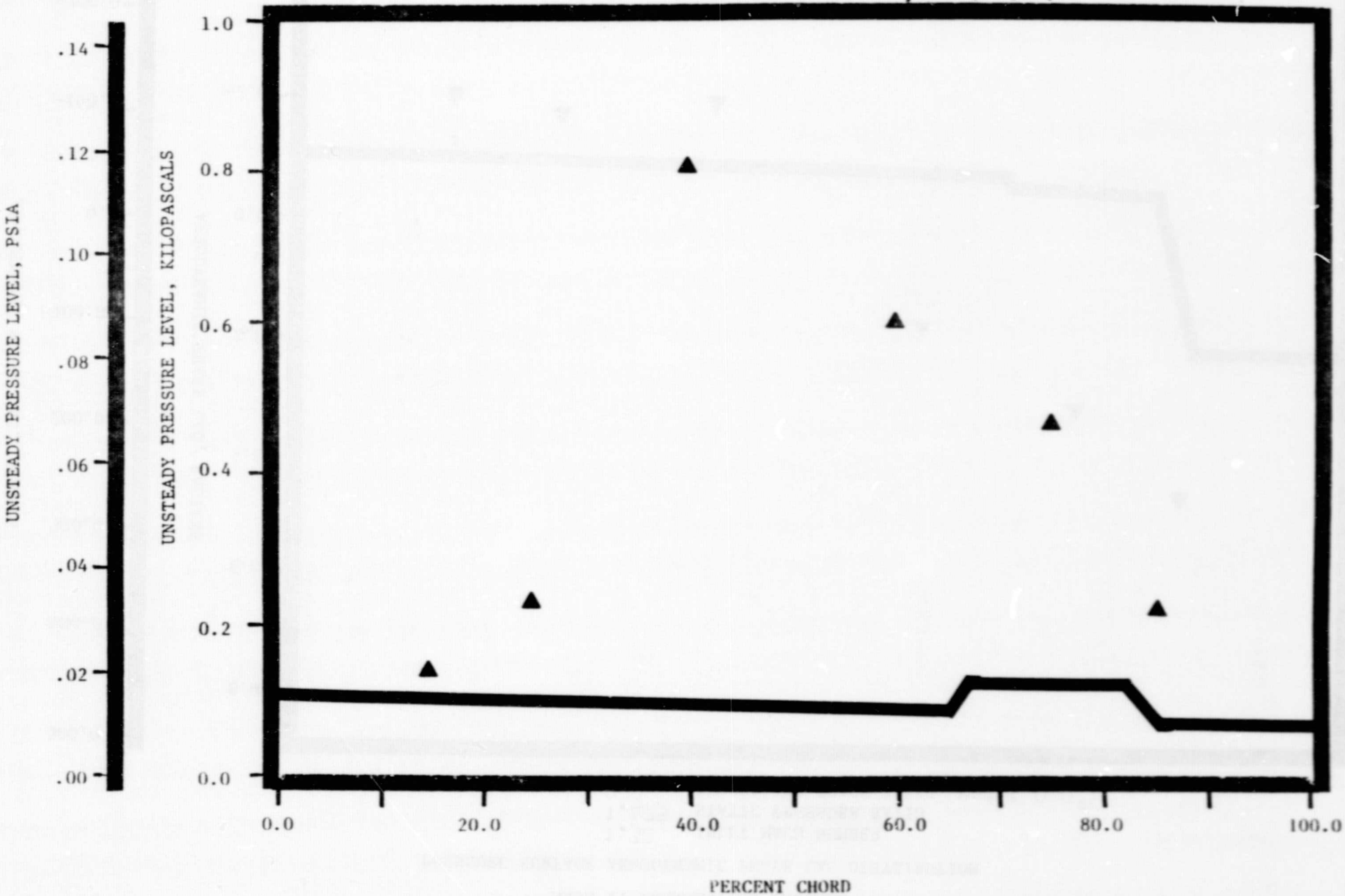

NASA II TRANSLATION CASCADE

SUCTION SURFACE AERODYNAMIC PHASE LAG DISTRIBUTION

1.32 INLET MACH NUMBER
1.475 STATIC PRESSURE RATIO
0.0 INTERBLADE PHASE ANGLE ,rad (0.0°)

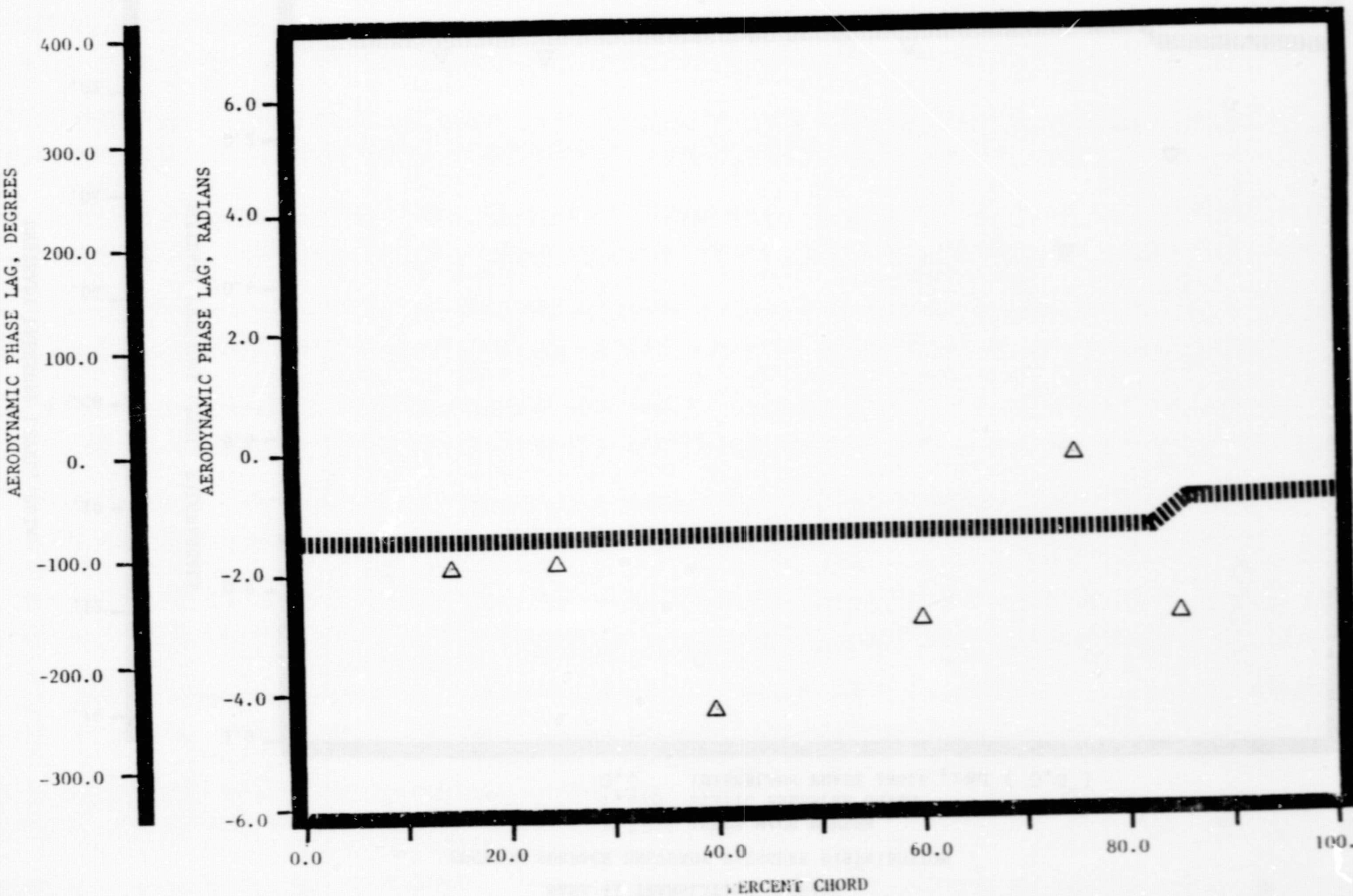

NASA II TRANSLATION CASCADE

SUCTION SURFACE UNSTEADY PRESSURE DISTRIBUTION

1.32 INLET MACH NUMBER
1.475 STATIC PRESSURE RATIO
0.0 INTERBLADE PHASE ANGLE ,rad (0.0°)

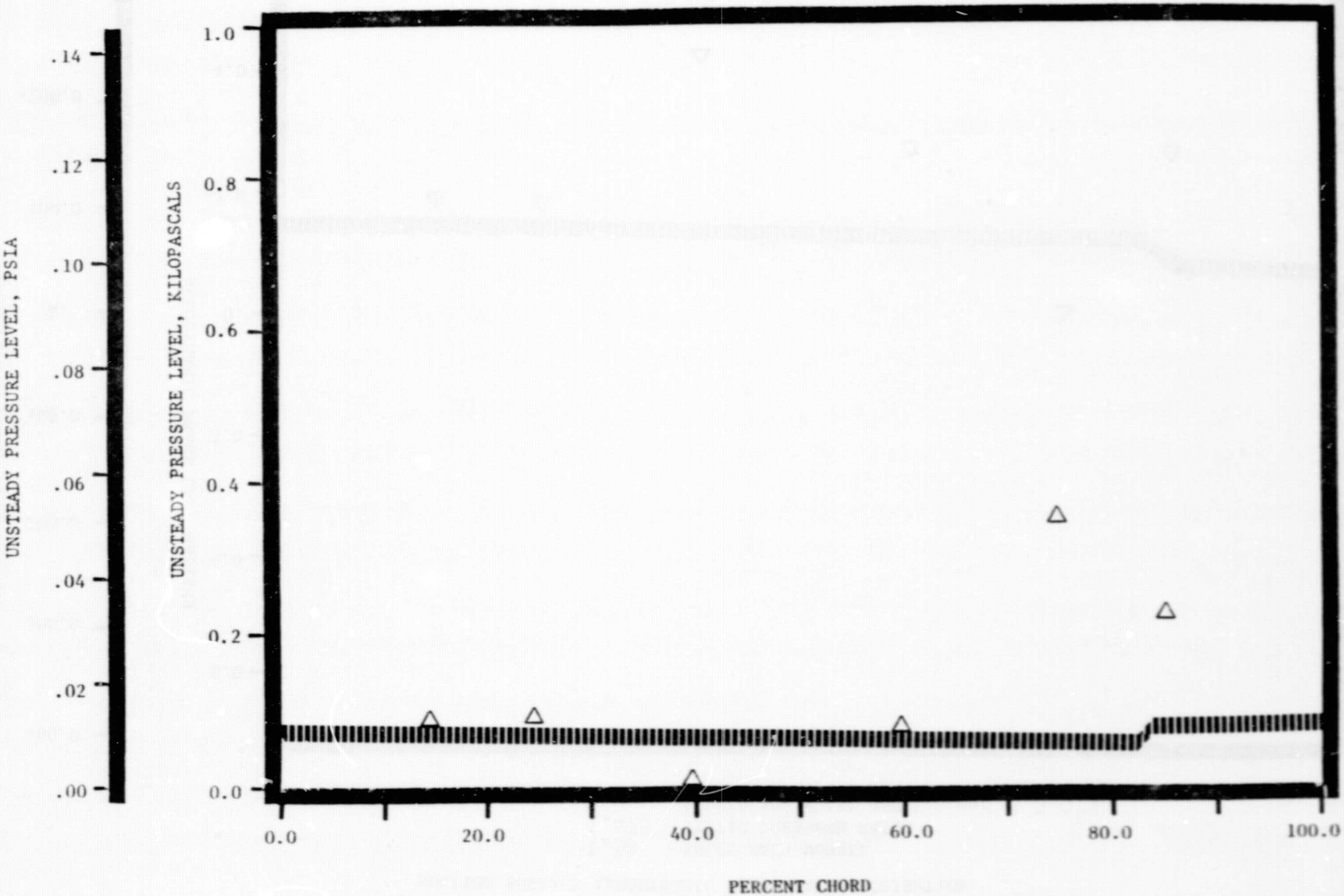

NASA II TRANSLATION CASCADE

PRESSURE SURFACE AERODYNAMIC PHASE LAG DISTRIBUTION

1.32 INLET MACH NUMBER
1.475 STATIC PRESSURE RATIO
-1.05 INTERBLADE PHASE ANGLE ,rad (-60°)

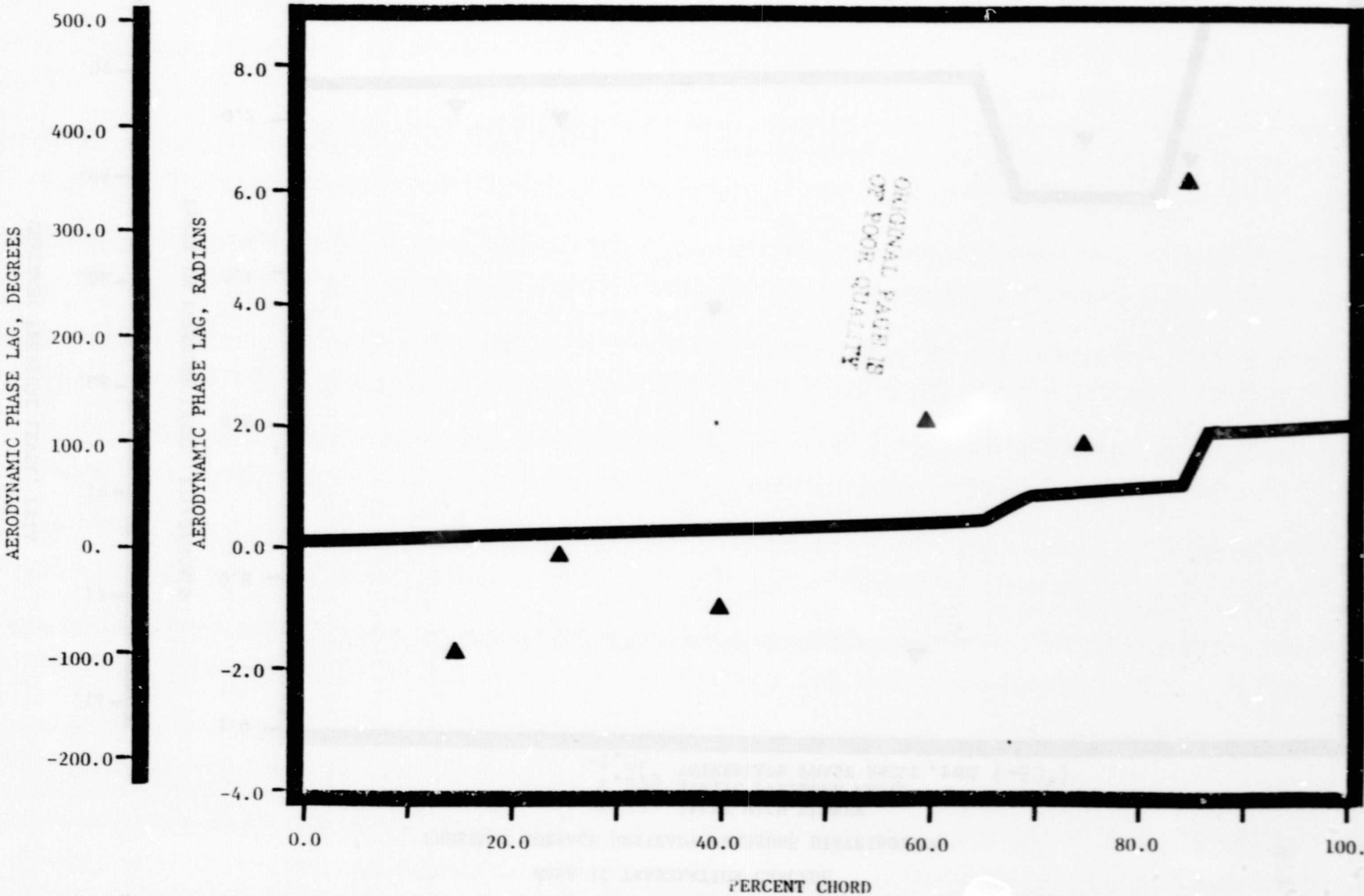

NASA II TRANSLATION CASCADE

PRESSURE SURFACE UNSTEADY PRESSURE DISTRIBUTION

1.32 INLET MACH NUMBER
1.475 STATIC PRESSURE RATIO
-1.05 INTERBLADE PHASE ANGLE ,rad (-60°)

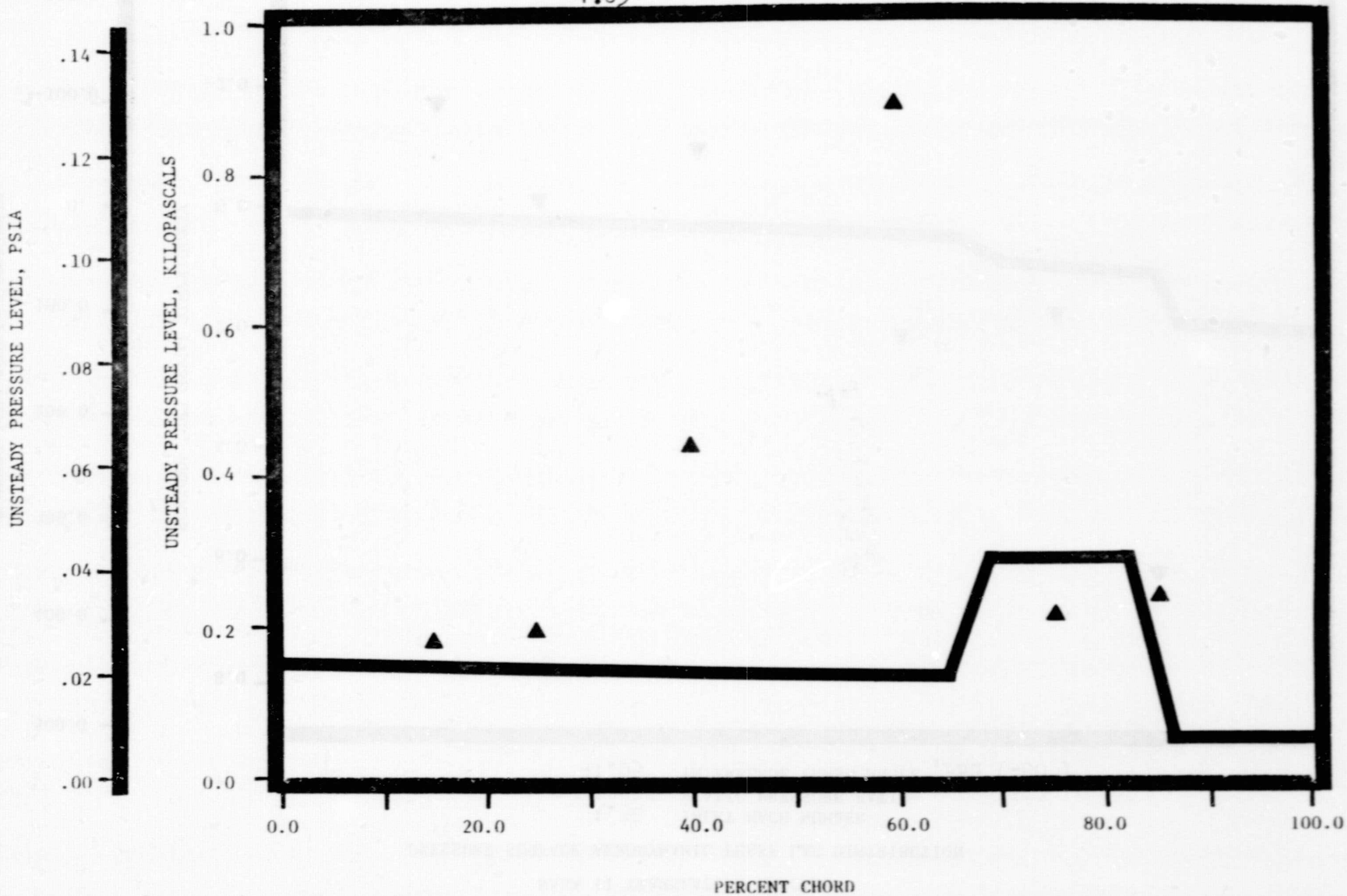

NASA II TRANSLATION CASCADE

SUCTION SURFACE AERODYNAMIC PHASE LAG DISTRIBUTION

1.32 INLET MACH NUMBER
1.475 STATIC PRESSURE RATIO
-1.05 INTERBLADE PHASE ANGLE ,rad (-60°)

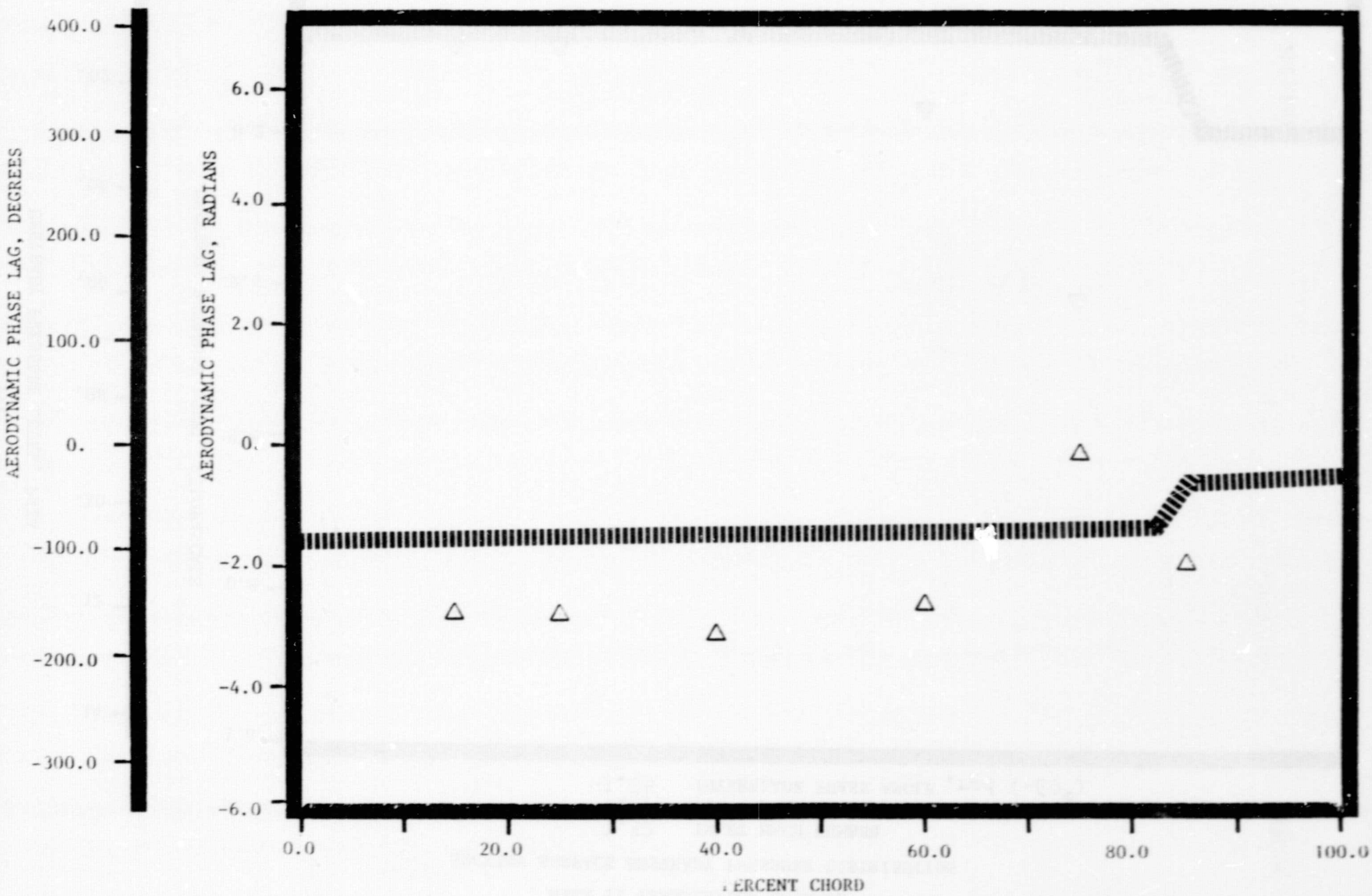

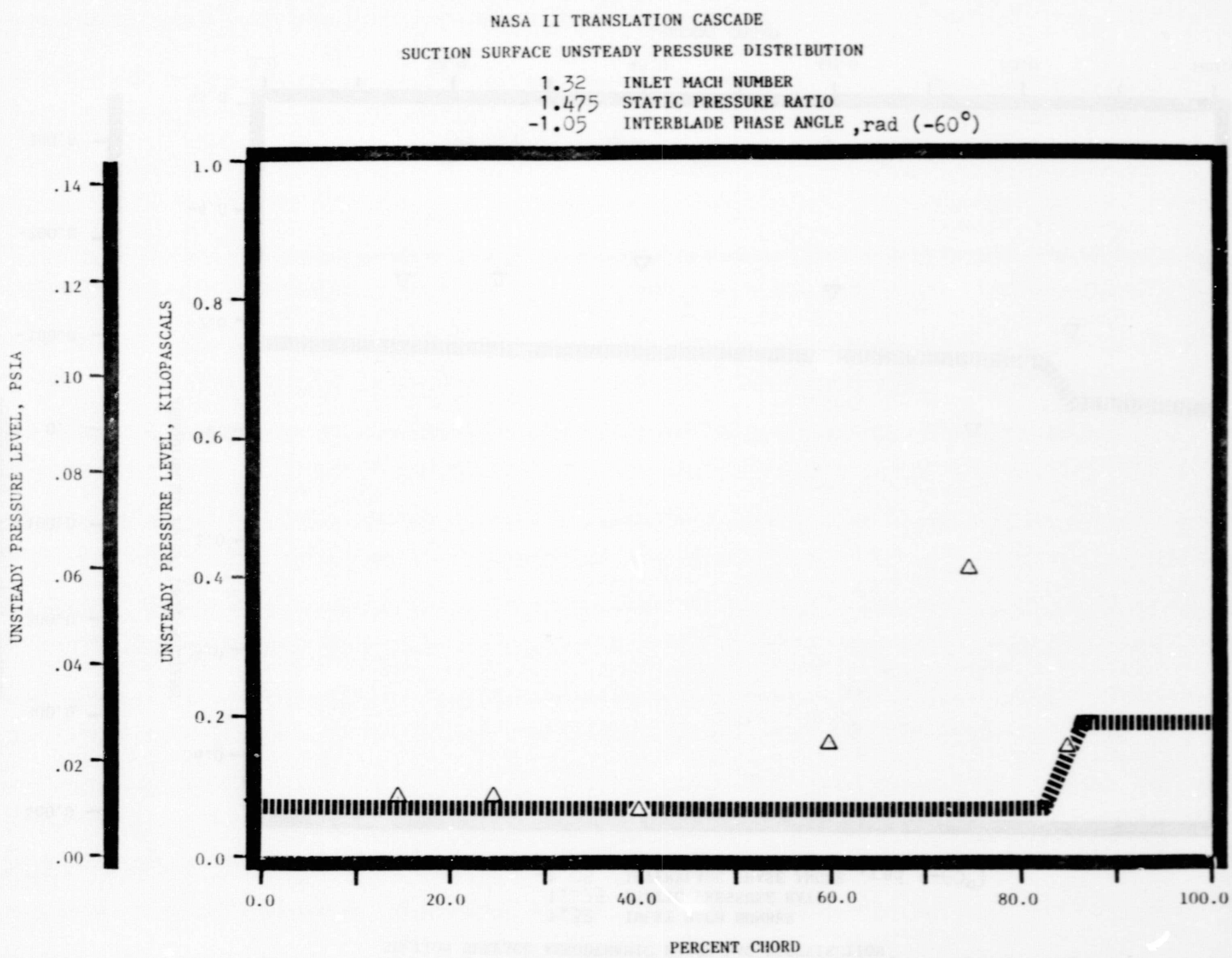
NASA II TRANSLATION CASCADE
SUCTION SURFACE UNSTEADY PRESSURE DISTRIBUTION
1.32 INLET MACH NUMBER
1.475 STATIC PRESSURE RATIO
-1.05 INTERBLADE PHASE ANGLE ,rad (-60°)
UNSTEADY PRESSURE LEVEL, PSIA
.14
.12
.10
.08
.06
.04
.02
.00
UNSTEADY PRESSURE LEVEL, KILOPASCALS
1.0
0.8
0.6
0.4
0.2
0.0
0.0
20.0
40.0
60.0
80.0
100.0
PERCENT CHORD

NASA II TRANSLATION CASCADE

PRESSURE SURFACE AERODYNAMIC PHASE LAG DISTRIBUTION

1.32 INLET MACH NUMBER
1.475 STATIC PRESSURE RATIO
-1.57 INTERBLADE PHASE ANGLE, rad (-90°)

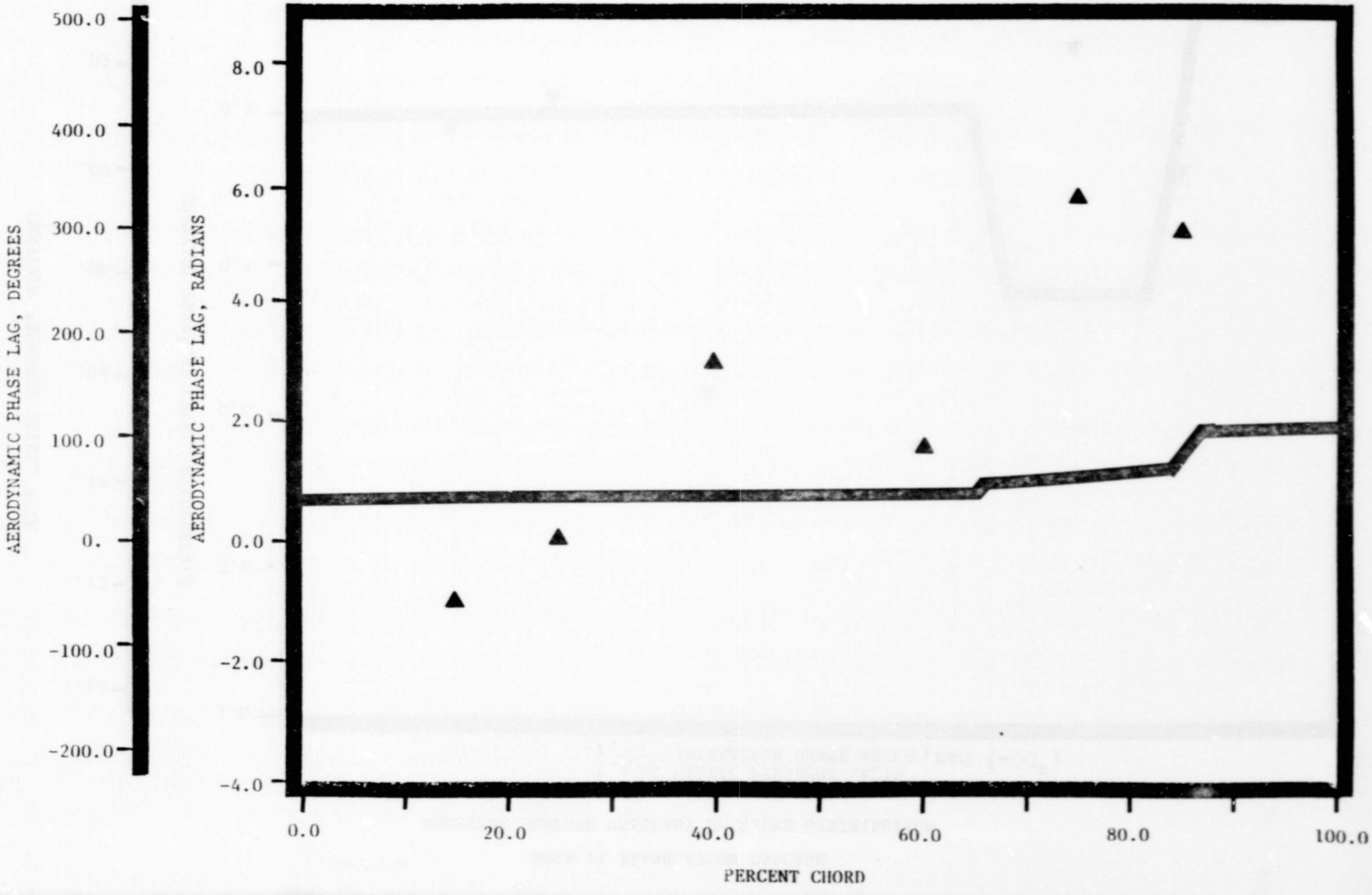

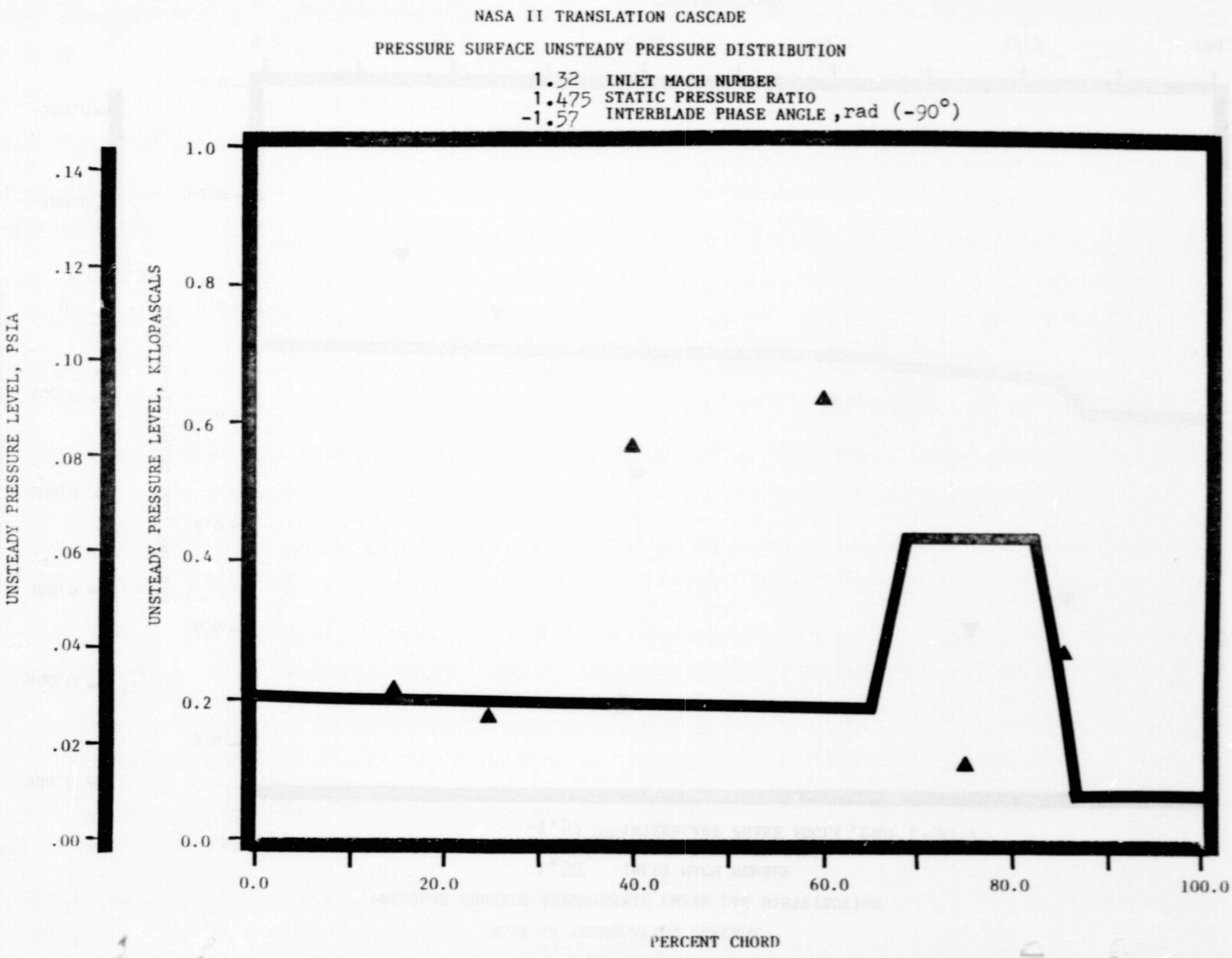

NASA II TRANSLATION CASCADE
PRESSURE SURFACE UNSTEADY PRESSURE DISTRIBUTION
1.32 INLET MACH NUMBER
1.475 STATIC PRESSURE RATIO
-1.57 INTERBLADE PHASE ANGLE ,rad (-90°)
UNSTEADY PRESSURE LEVEL, PSIA
.14
.12
.10
.08
.06
.04
.02
.00
UNSTEADY PRESSURE LEVEL, KILOPASCALS
1.0
0.8
0.6
0.4
0.2
0.0
0.0
20.0
40.0
60.0
80.0
100.0
PERCENT CHORD

NASA II TRANSLATION CASCADE

SUCTION SURFACE AERODYNAMIC PHASE LAG DISTRIBUTION

1.32 INLET MACH NUMBER
1.475 STATIC PRESSURE RATIO
-1.57 INTERBLADE PHASE ANGLE ,rad (-90°)

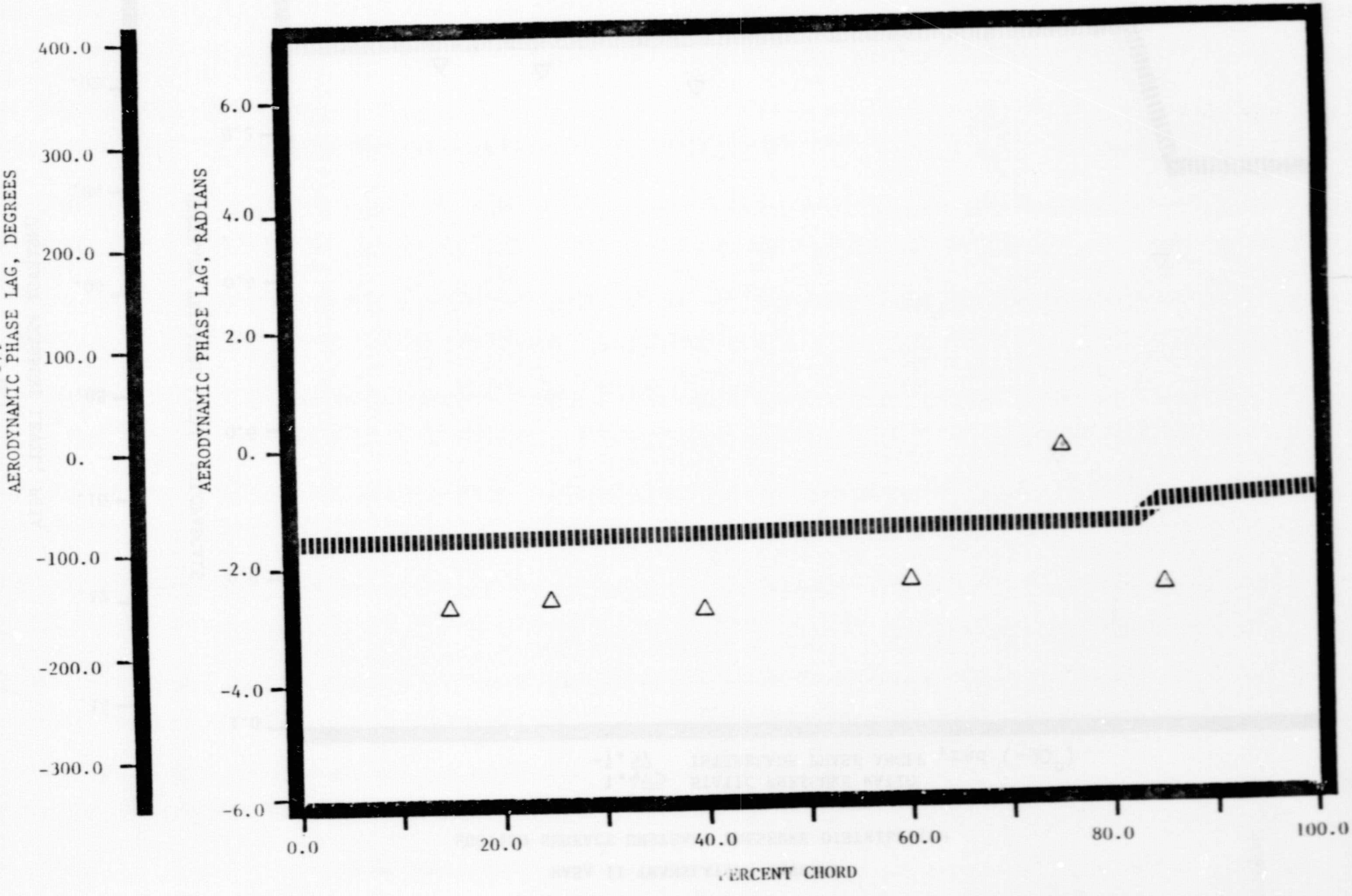

NASA II TRANSLATION CASCADE

SUCTION SURFACE UNSTEADY PRESSURE DISTRIBUTION

1.32 INLET MACH NUMBER
1.475 STATIC PRESSURE RATIO
-1.57 INTERBLADE PHASE ANGLE ,rad (-90°)

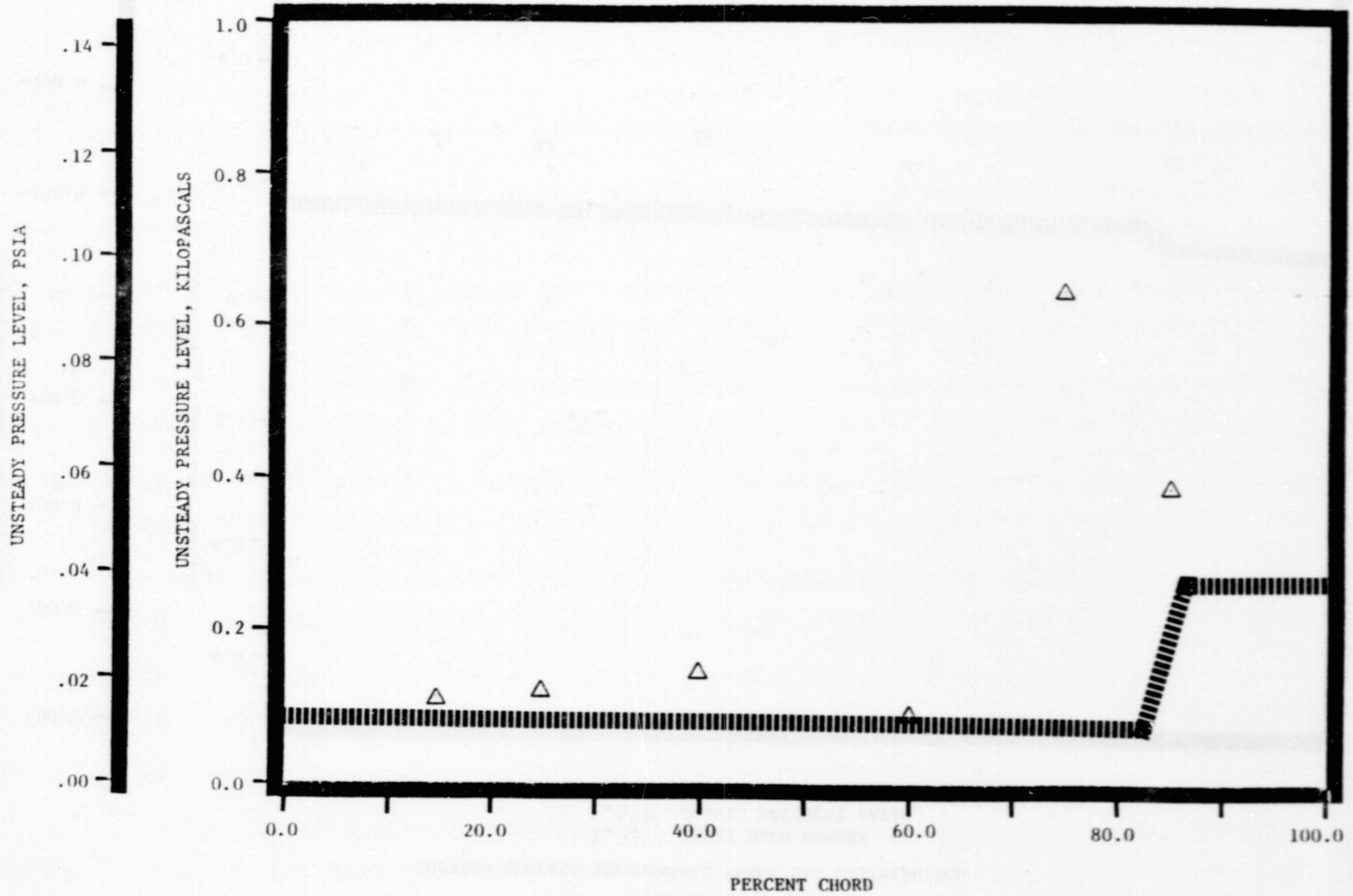

NASA II TRANSLATION CASCADE

PRESSURE SURFACE AERODYNAMIC PHASE LAG DISTRIBUTION

1.32 INLET MACH NUMBER
1.68 STATIC PRESSURE RATIO
3.14 INTERBLADE PHASE ANGLE ,rad (180°)

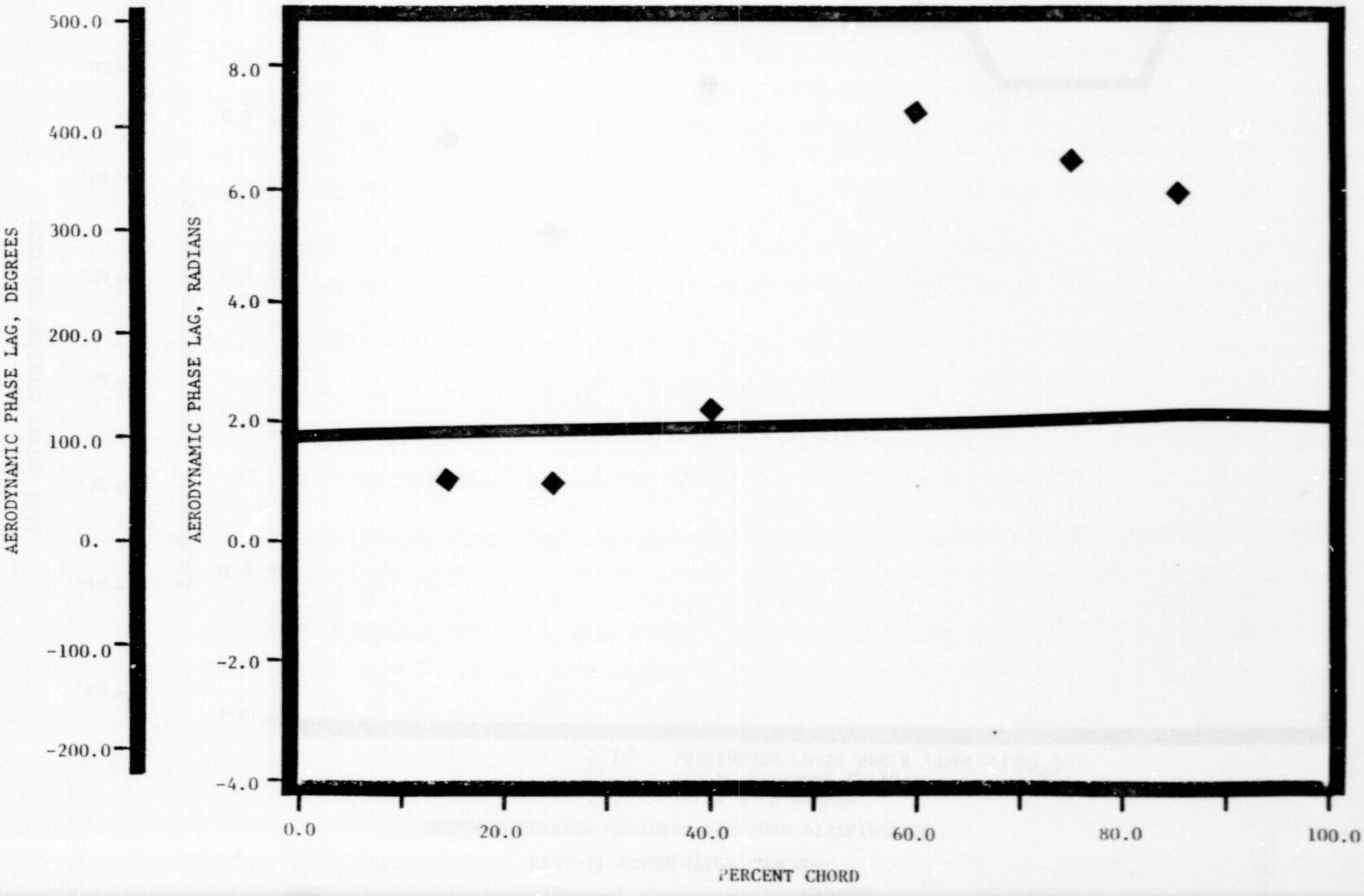

NASA II TRANSLATION CASCADE

PRESSURE SURFACE UNSTEADY PRESSURE DISTRIBUTION

1.32 INLET MACH NUMBER
1.68 STATIC PRESSURE RATIO
3.14 INTERBLADE PHASE ANGLE ,rad (180°)

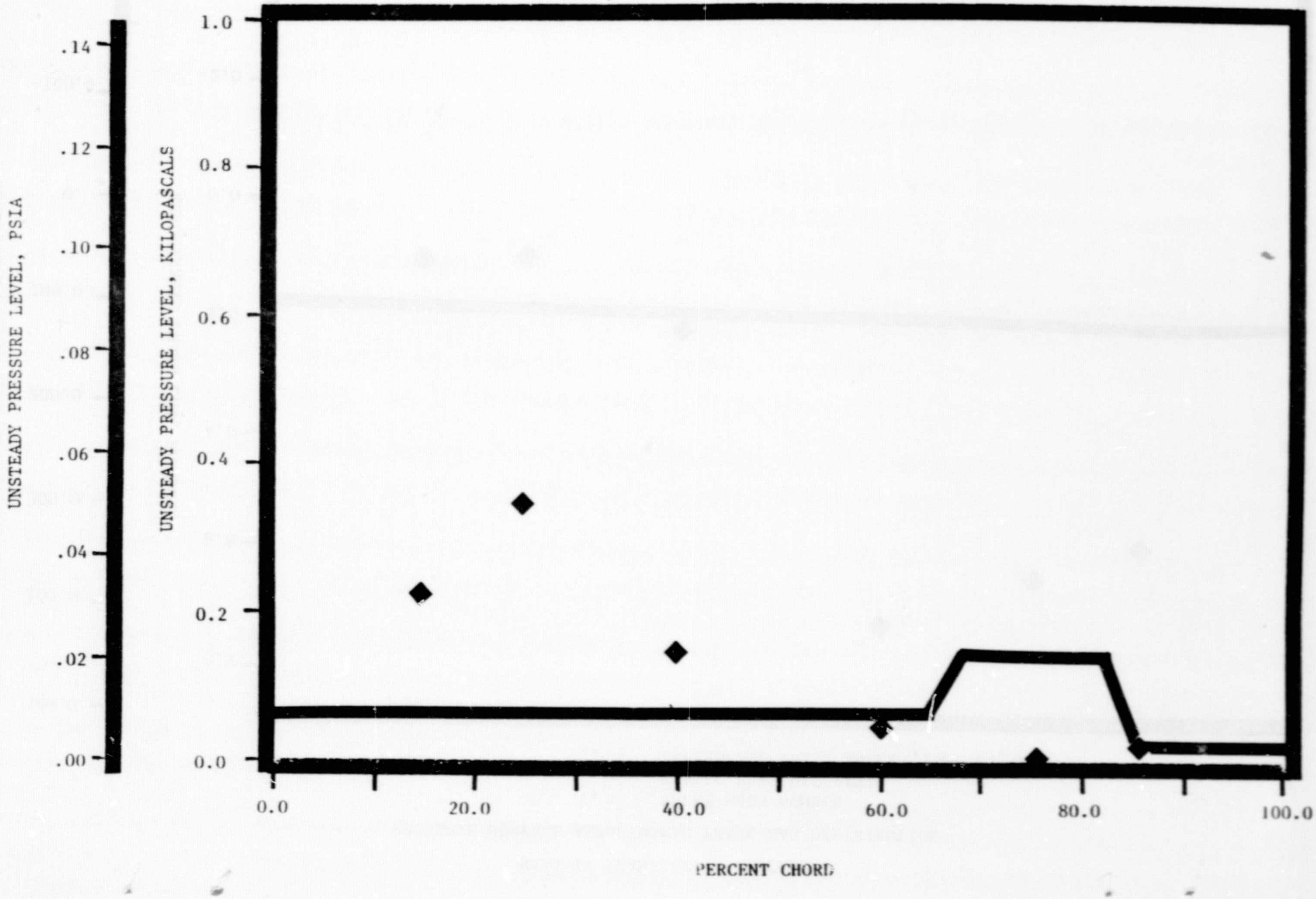

NASA II TRANSLATION CASCADE

SUCTION SURFACE AERODYNAMIC PHASE LAG DISTRIBUTION

1.32	INLET MACH NUMBER
1.68	STATIC PRESSURE RATIO
3.14	INTERBLADE PHASE ANGLE, rad (180°)

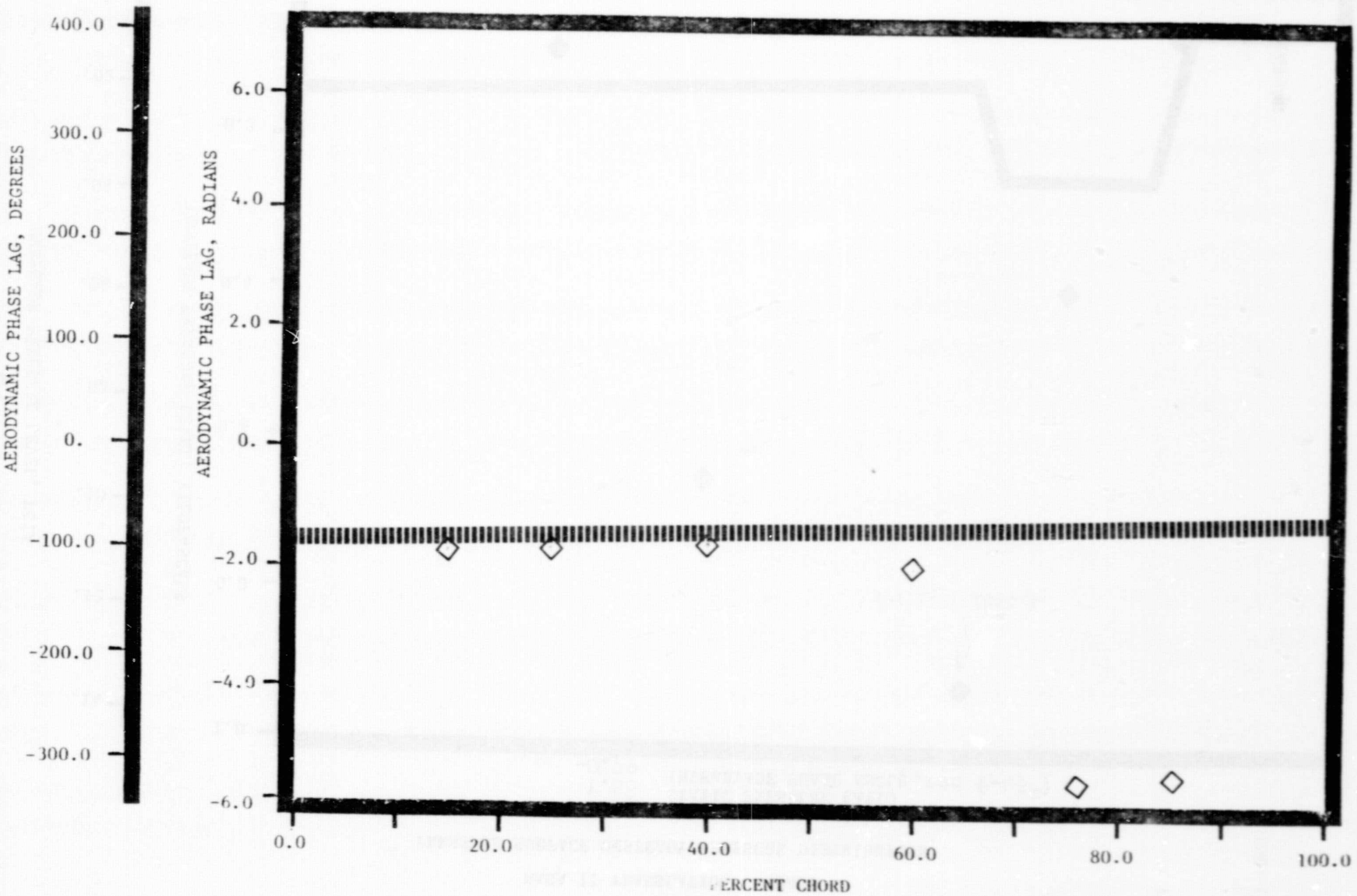

NASA II TRANSLATION CASCADE

PRESSURE SURFACE UNSTEADY PRESSURE DISTRIBUTION

1.32 INLET MACH NUMBER
1.68 STATIC PRESSURE RATIO
-0.79 INTERBLADE PHASE ANGLE, rad (-45°)

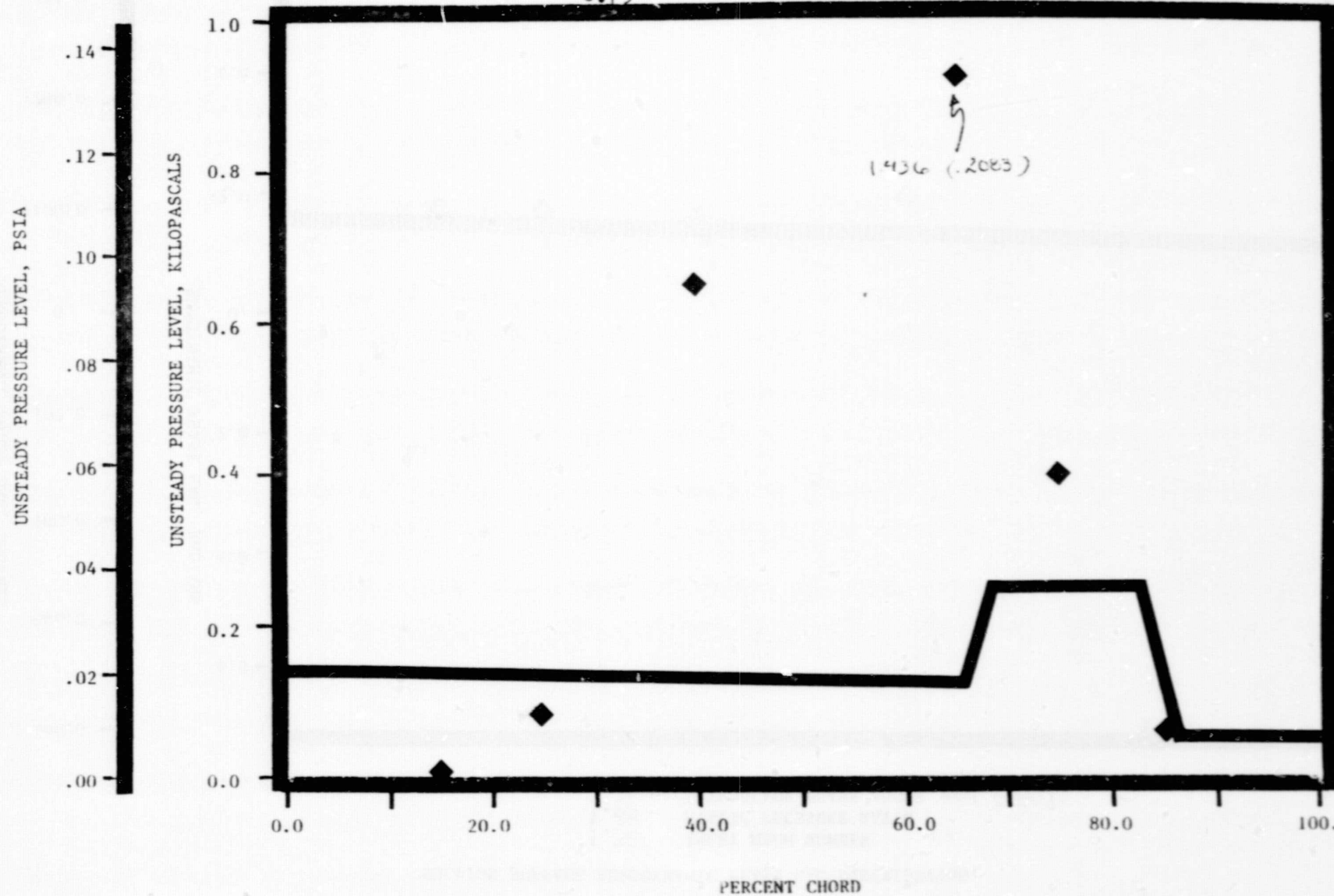

NASA II TRANSLATION CASCADE

SUCTION SURFACE AERODYNAMIC PHASE LAG DISTRIBUTION

1.32 INLET MACH NUMBER
1.68 STATIC PRESSURE RATIO
-0.79 INTERBLADE PHASE ANGLE, rad (-45°)

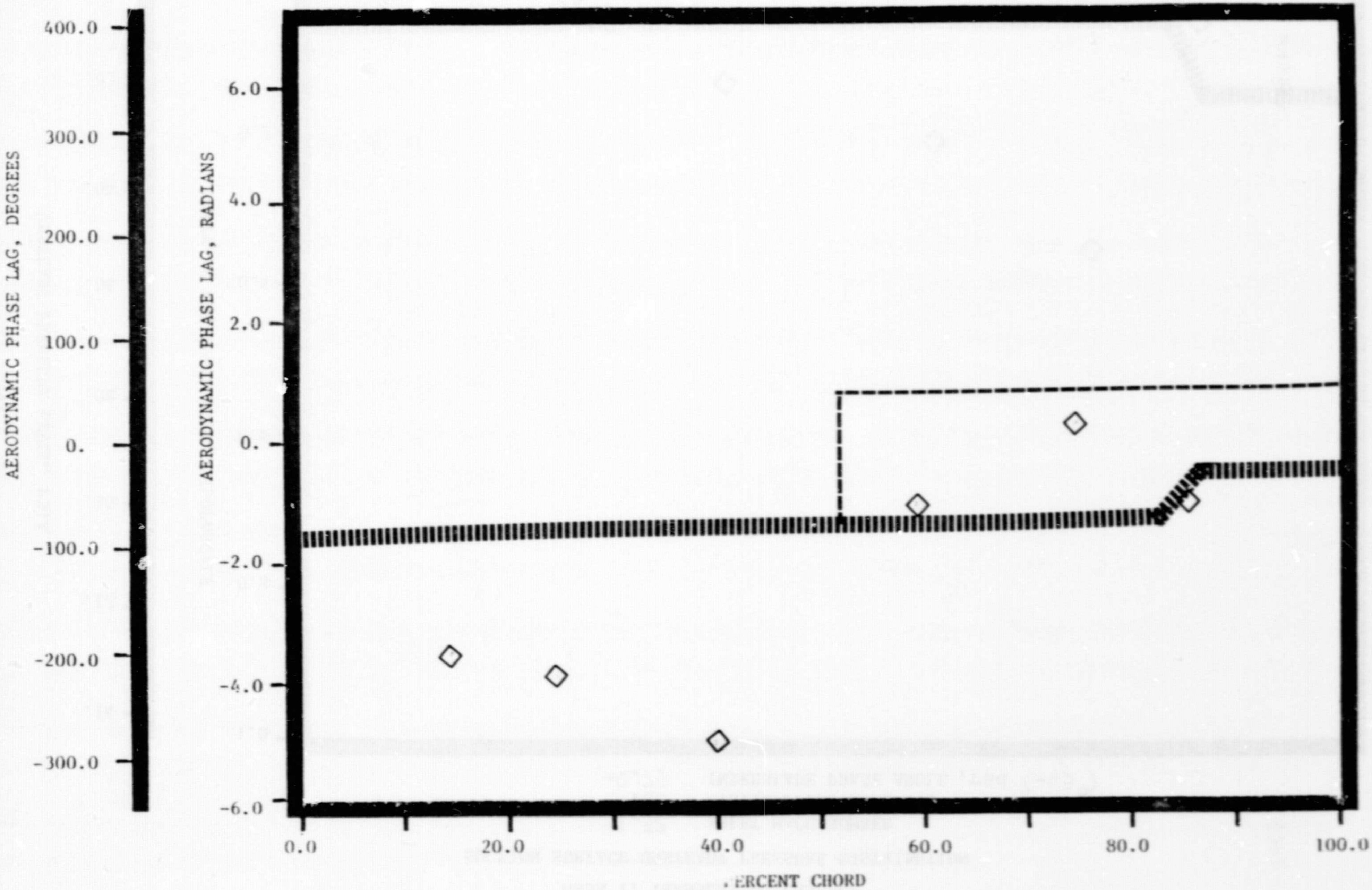

NASA II TRANSLATION CASCADE

SUCTION SURFACE UNSTEADY PRESSURE DISTRIBUTION

1.32 INLET MACH NUMBER
1.68 STATIC PRESSURE RATIO
-0.79 INTERBLADE PHASE ANGLE ,rad (-45°)

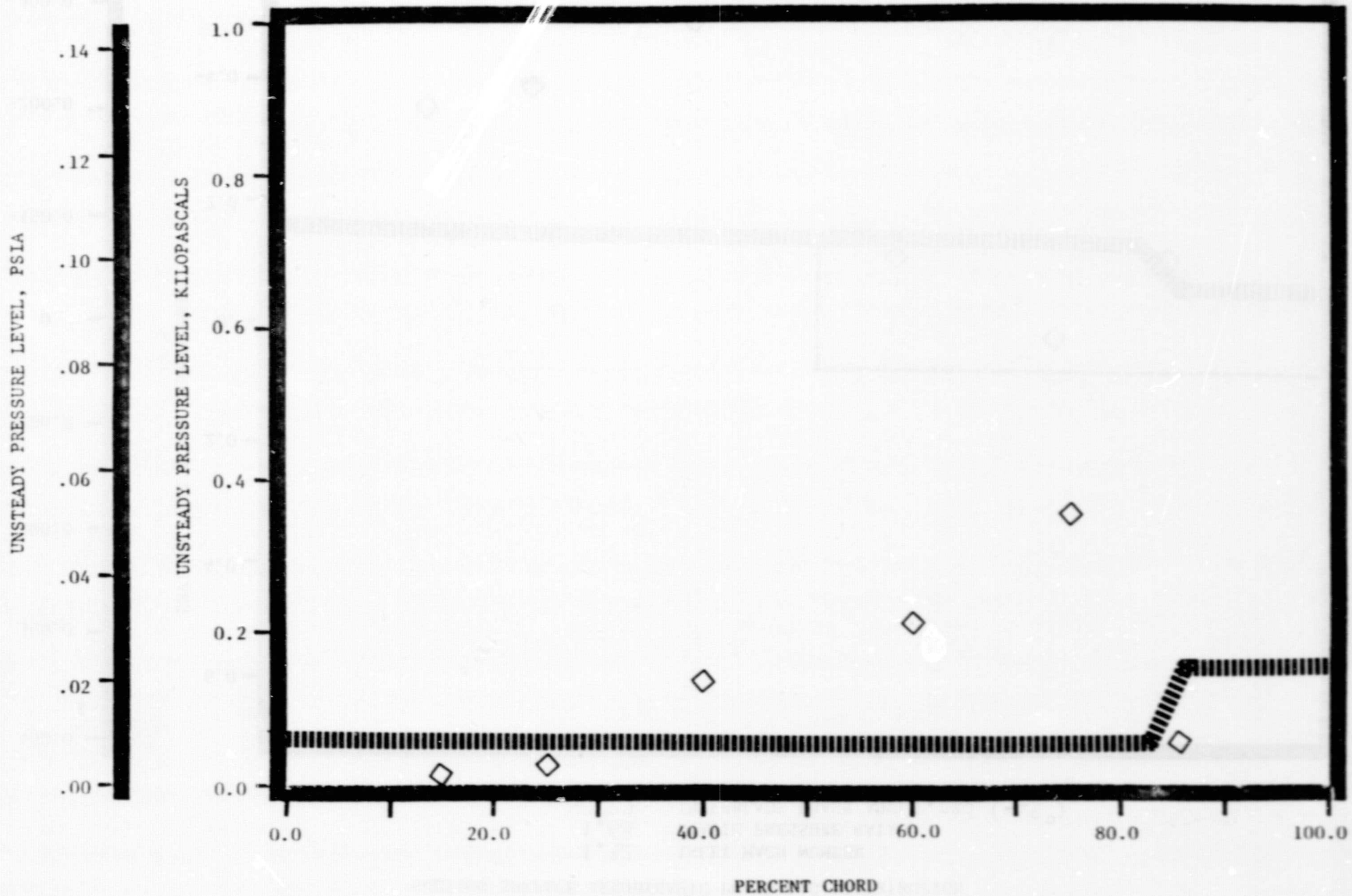

NASA II TRANSLATION CASCADE

PRESSURE SURFACE AERODYNAMIC PHASE LAG DISTRIBUTION

1.32 INLET MACH NUMBER
1.68 STATIC PRESSURE RATIO
-1.57 INTERBLADE PHASE ANGLE ,rad (-90°)

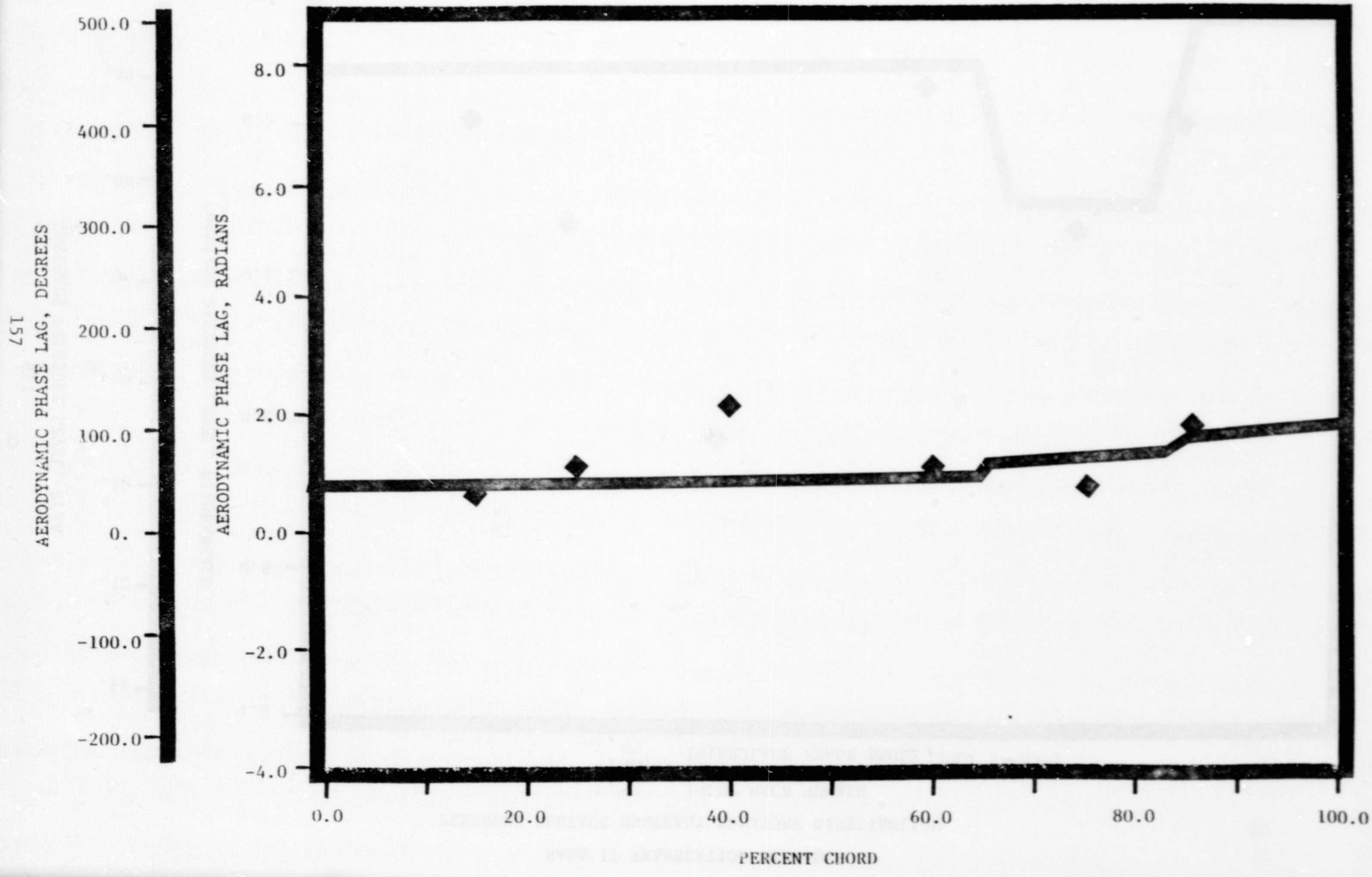

NASA II TRANSLATION CASCADE

PRESSURE SURFACE UNSTEADY PRESSURE DISTRIBUTION

1.32	INLET MACH NUMBER
1.68	STATIC PRESSURE RATIO
-1.57	INTERBLADE PHASE ANGLE, rad (-90°)

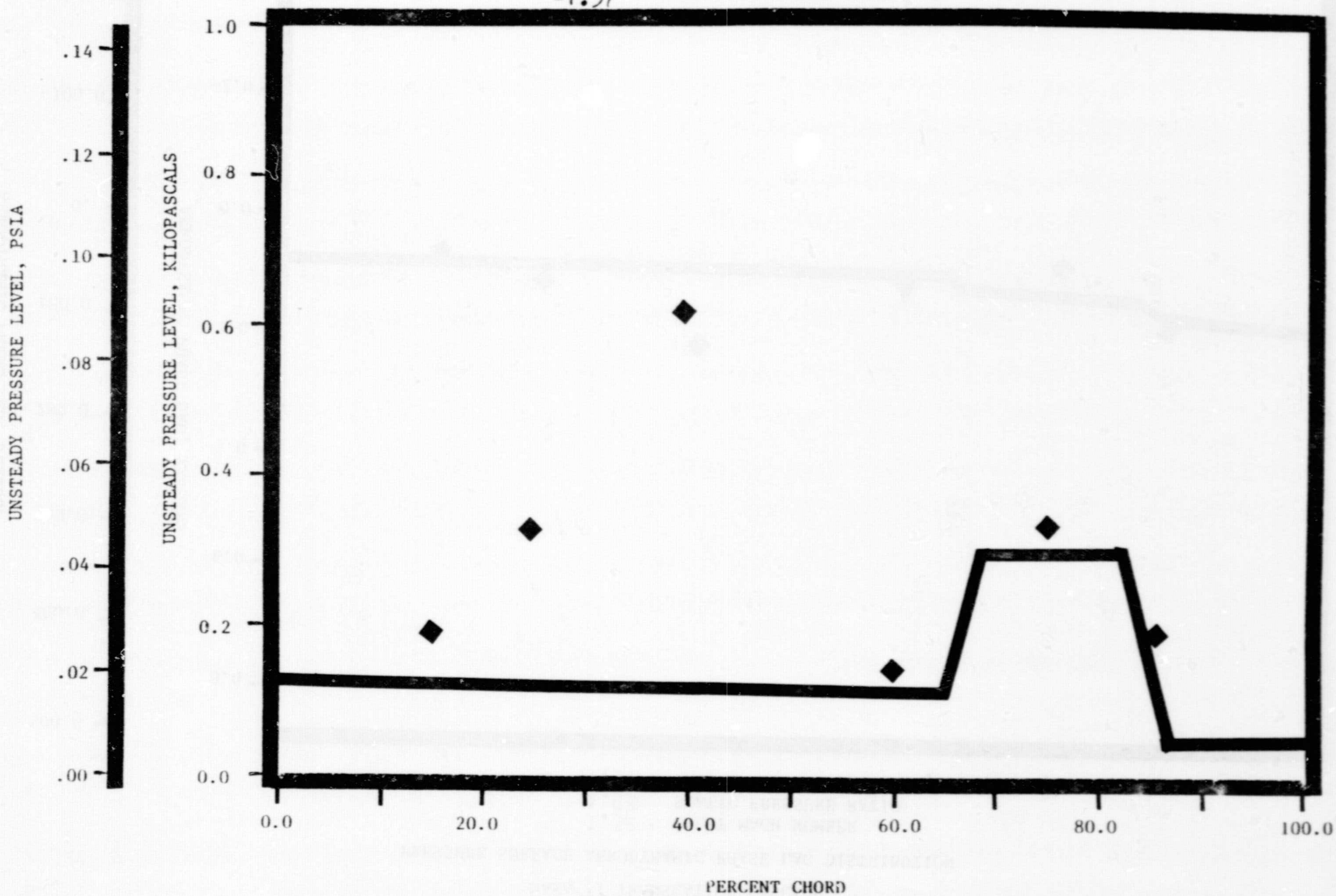

NASA II TRANSLATION CASCADE

SUCTION SURFACE AERODYNAMIC PHASE LAG DISTRIBUTION

1.32 INLET MACH NUMBER
1.68 STATIC PRESSURE RATIO
-1.57 INTERBLADE PHASE ANGLE, rad (-90°)

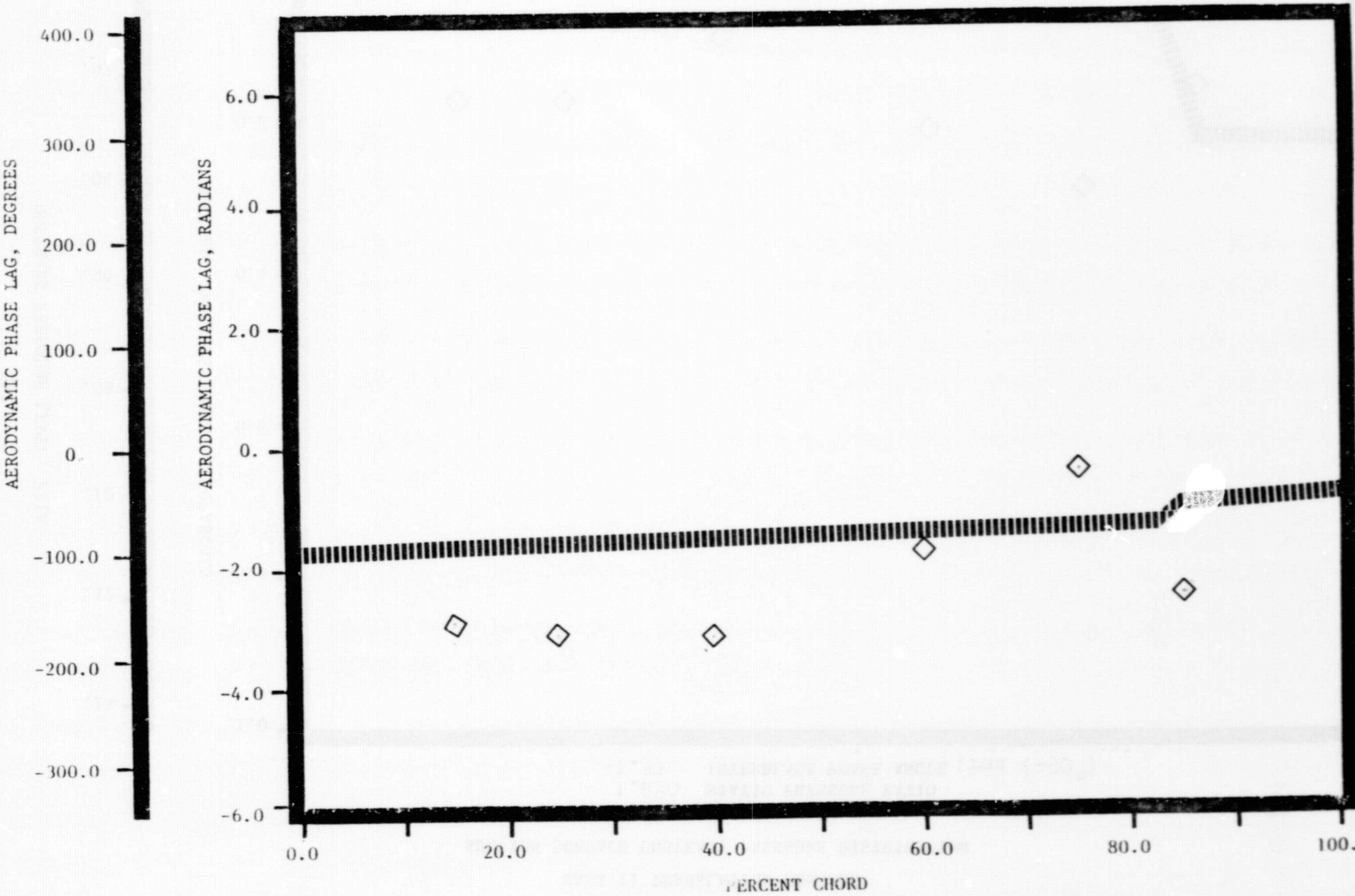

NASA II TRANSLATION CASCADE

SUCTION SURFACE UNSTEADY PRESSURE DISTRIBUTION

1.32	INLET MACH NUMBER
1.680	STATIC PRESSURE RATIO
-1.57	INTERBLADE PHASE ANGLE ,rad (-90°)

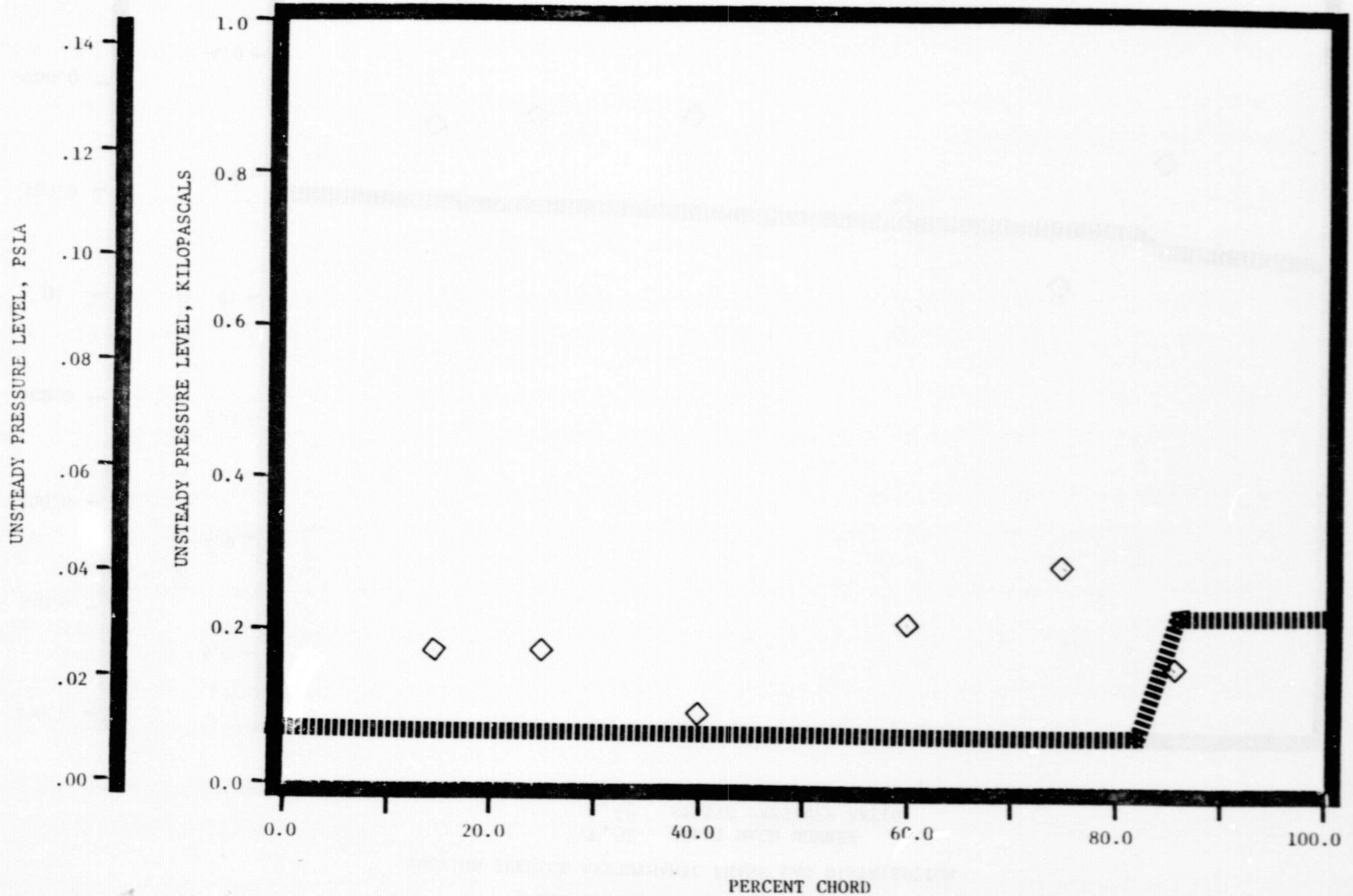

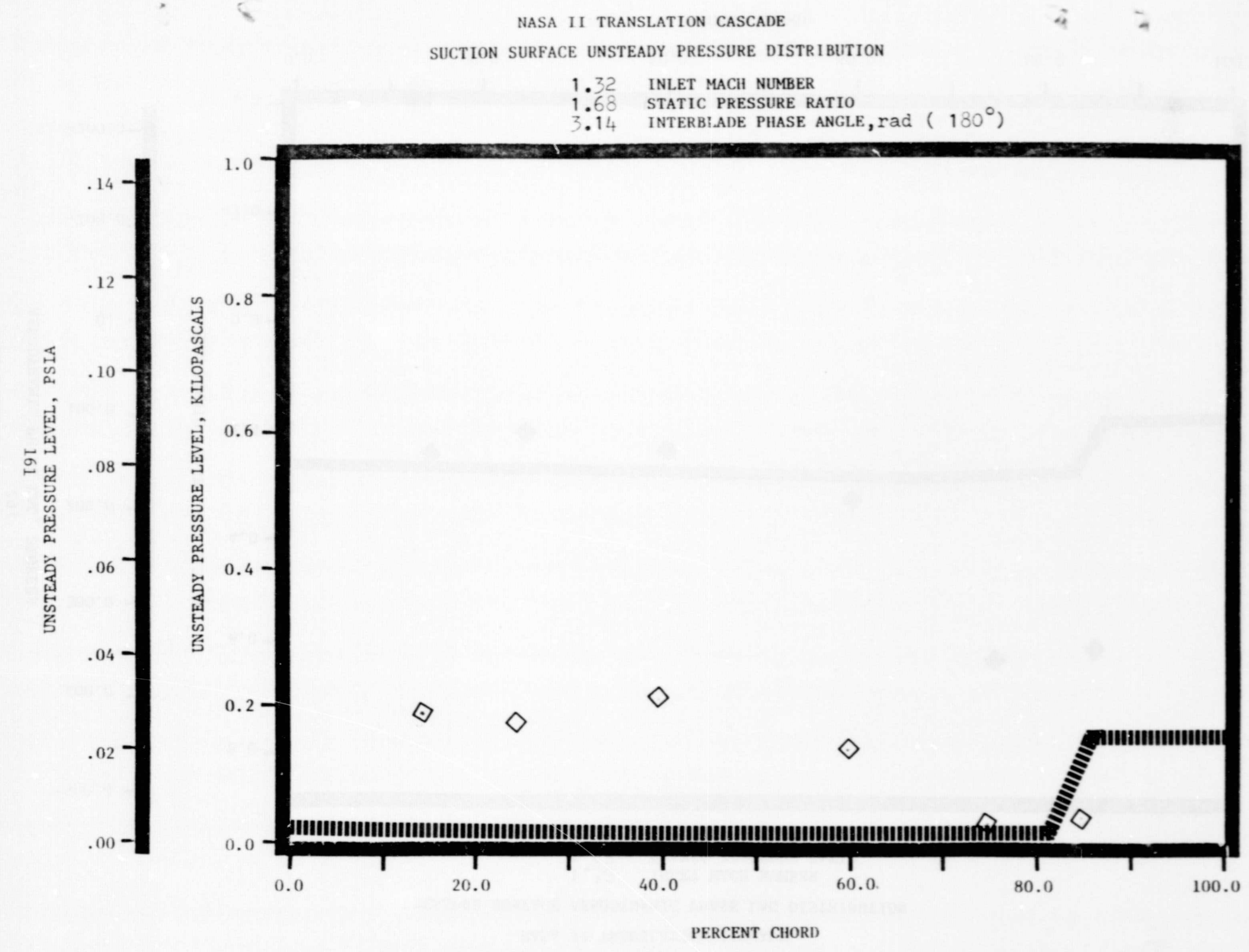
NASA II TRANSLATION CASCADE
SUCTION SURFACE UNSTEADY PRESSURE DISTRIBUTION
1.32 INLET MACH NUMBER
1.68 STATIC PRESSURE RATIO
3.14 INTERBLADE PHASE ANGLE, rad (180°)
UNSTEADY PRESSURE LEVEL, PSIA
.14
.12
.10
.08
.06
.04
.02
.00
UNSTEADY PRESSURE LEVEL, KILOPASCALS
1.0
0.8
0.6
0.4
0.2
0.0
0.0
20.0
40.0
60.0
80.0
100.0
PERCENT CHORD

NASA II TRANSLATION CASCADE

PRESSURE SURFACE AERODYNAMIC PHASE LAG DISTRIBUTION

1.32 INLET MACH NUMBER
1.68 STATIC PRESSURE RATIO
1.57 INTERBLADE PHASE ANGLE ,rad (90°)

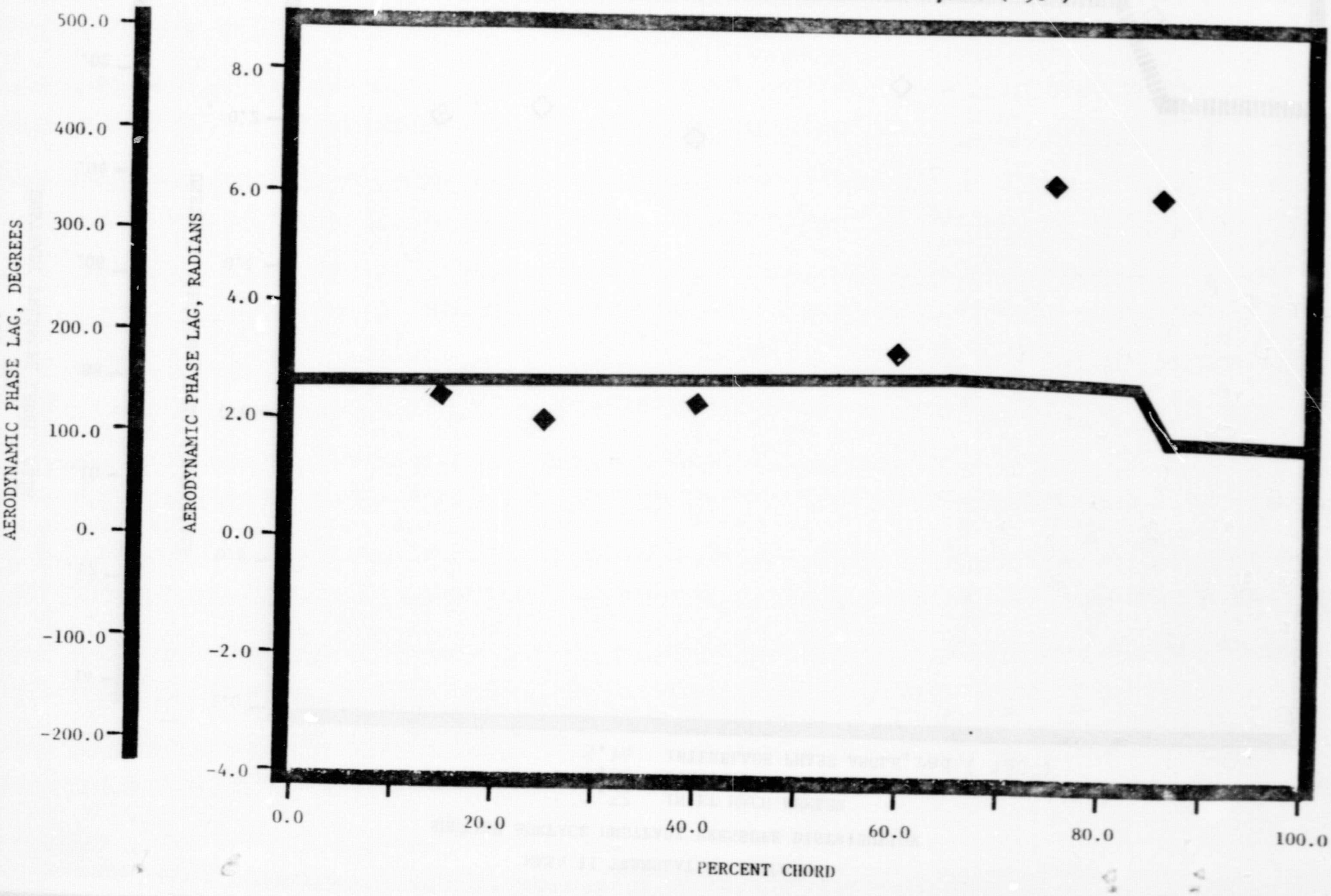

NASA II TRANSLATION CASCADE

PRESSURE SURFACE UNSTEADY PRESSURE DISTRIBUTION

1.32 INLET MACH NUMBER
1.68 STATIC PRESSURE RATIO
1.57 INTERBLADE PHASE ANGLE ,rad (90 °)

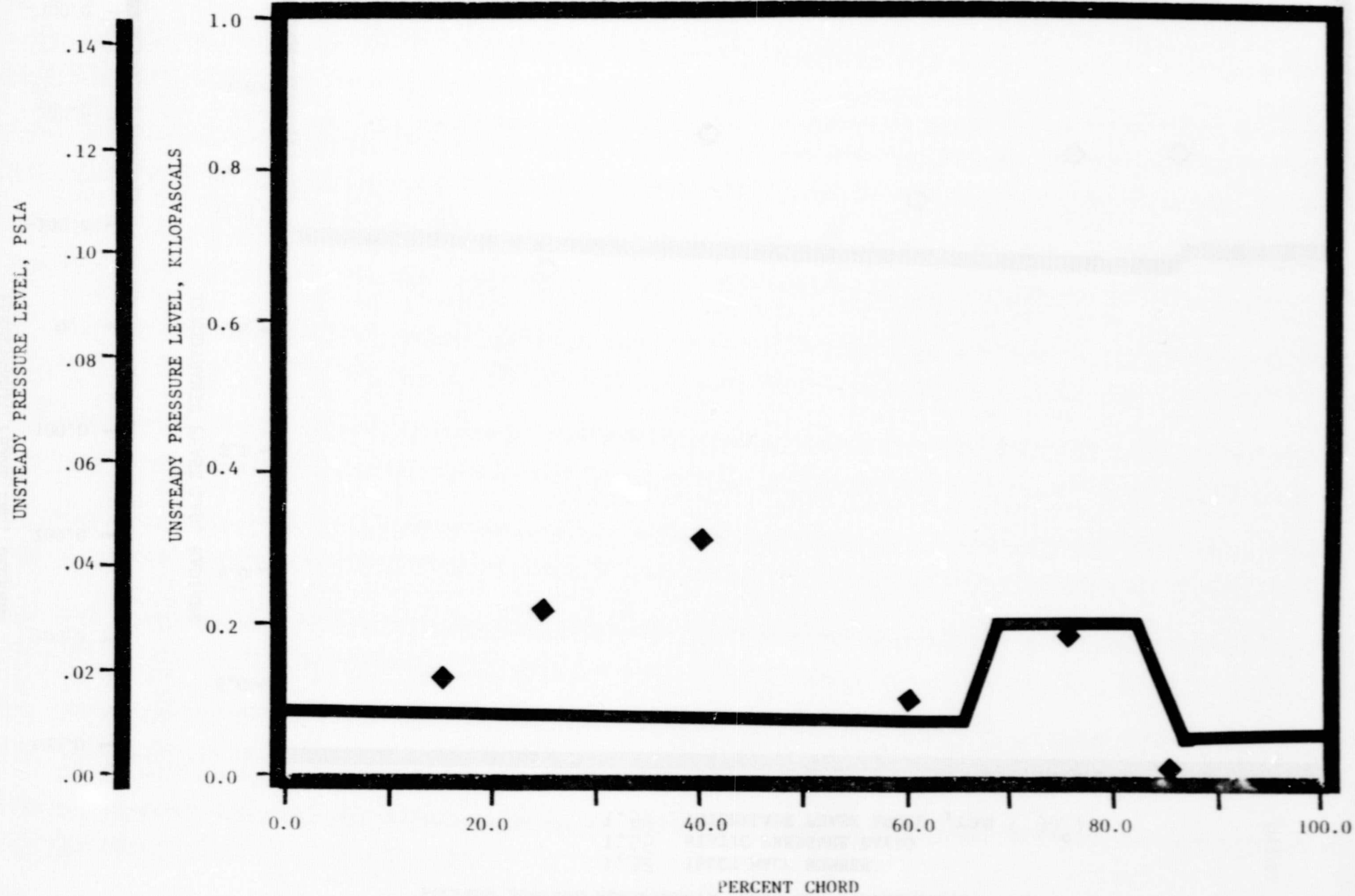

NASA II TRANSLATION CASCADE

SUCTION SURFACE AERODYNAMIC PHASE LAG DISTRIBUTION

1.32 INLET MACH NUMBER
1.68 STATIC PRESSURE RATIO
1.57 INTERBLADE PHASE ANGLE ,rad (90°)

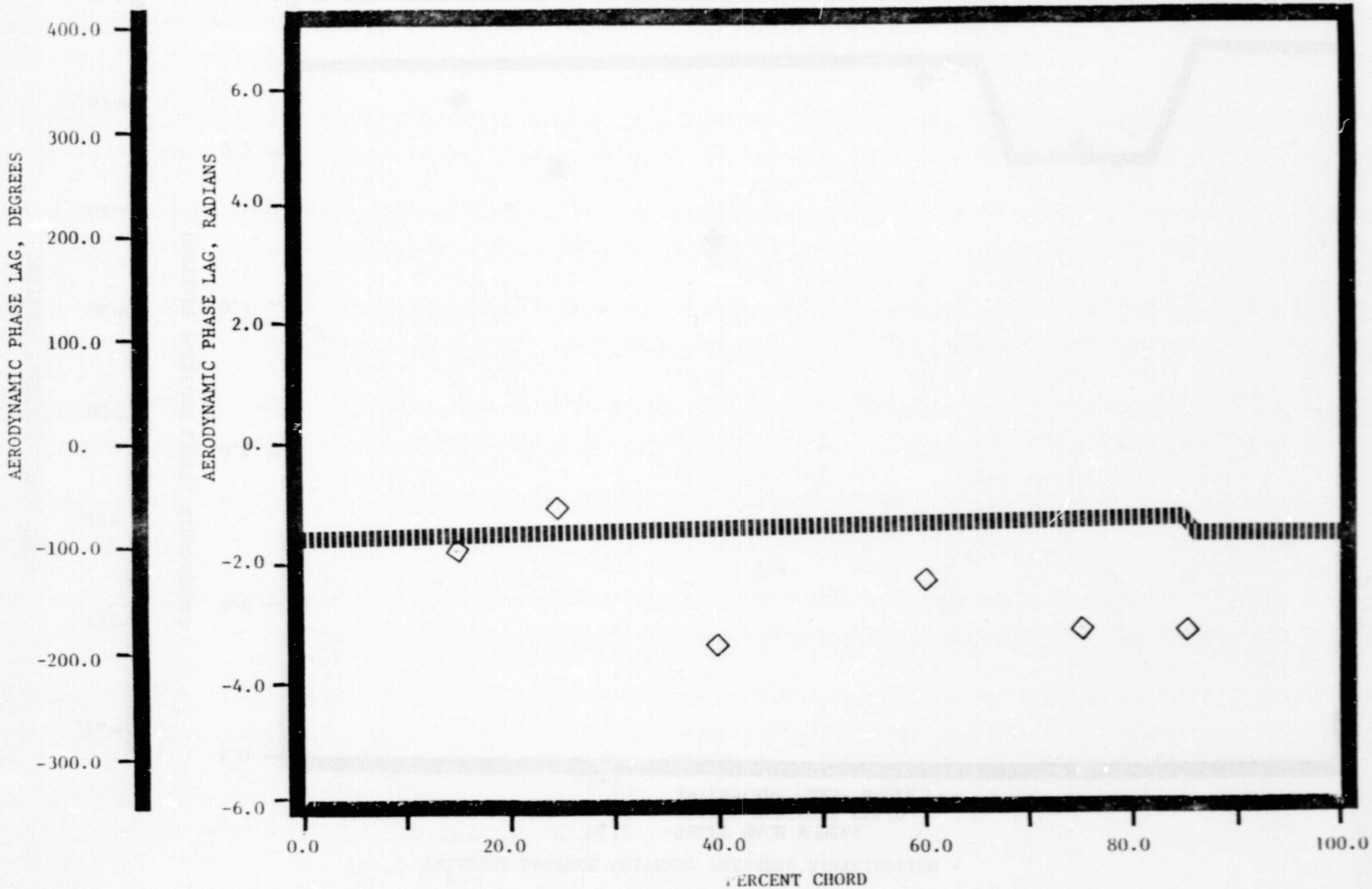

NASA II TRANSLATION CASCADE

SUCTION SURFACE UNSTEADY PRESSURE DISTRIBUTION

1.32 INLET MACH NUMBER
1.68 STATIC PRESSURE RATIO
1.57 INTERBLADE PHASE ANGLE ,rad (90°)

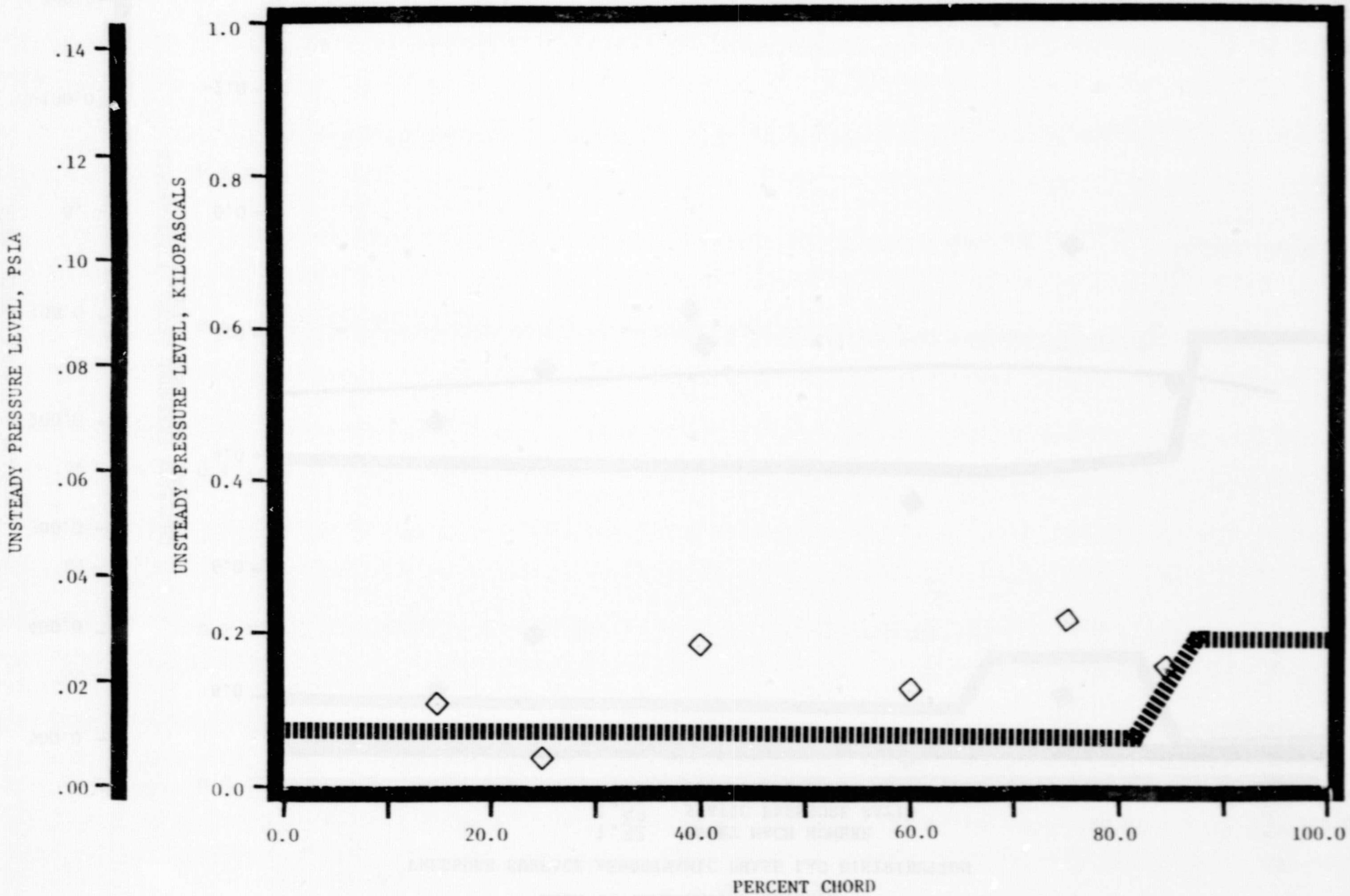

NASA II TRANSLATION CASCADE

PRESSURE SURFACE AERODYNAMIC PHASE LAG DISTRIBUTION

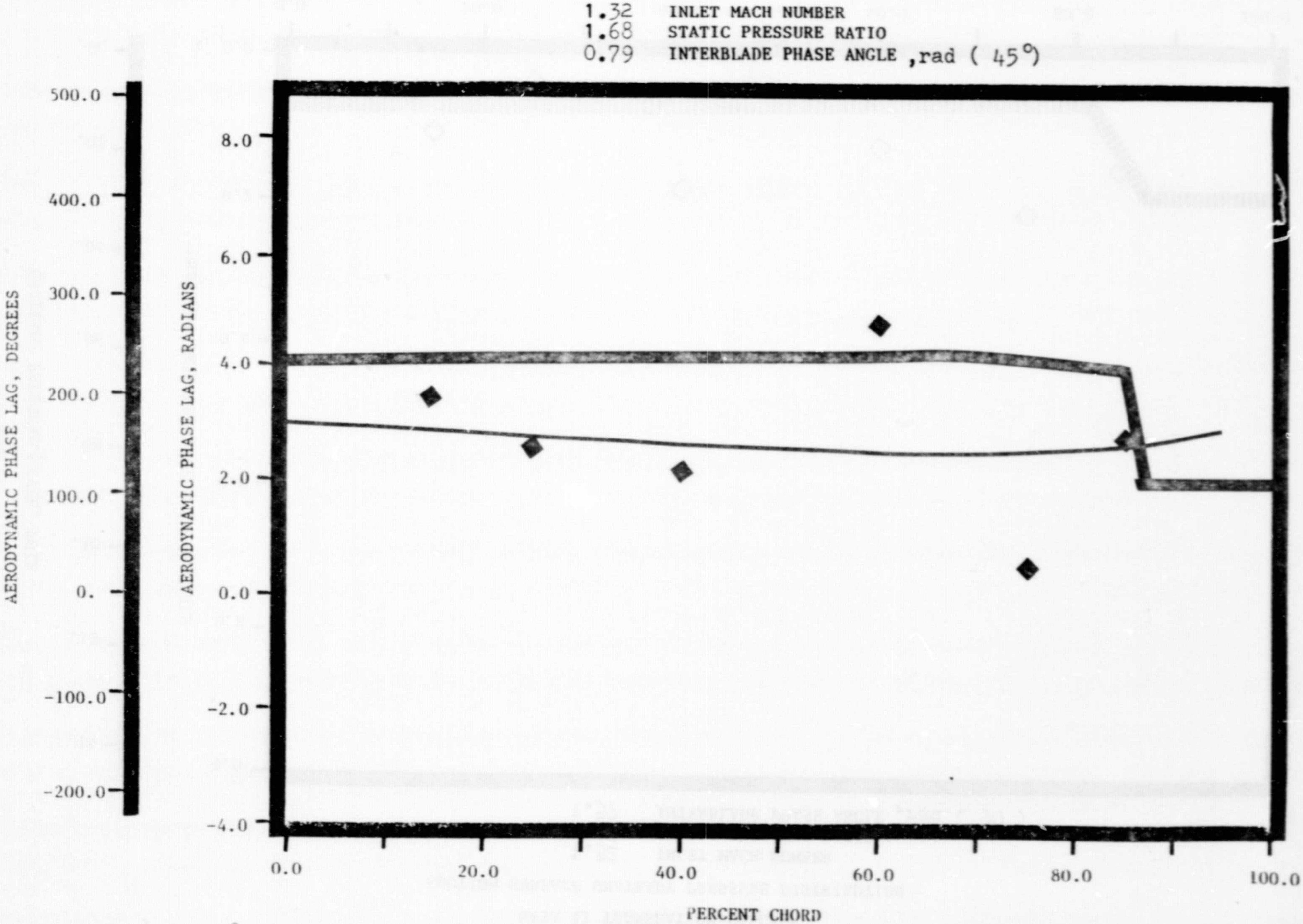

NASA II TRANSLATION CASCADE

PRESSURE SURFACE UNSTEADY PRESSURE DISTRIBUTION

1.32 INLET MACH NUMBER
1.68 STATIC PRESSURE RATIO
0.79 INTERBLADE PHASE ANGLE, rad (45°)

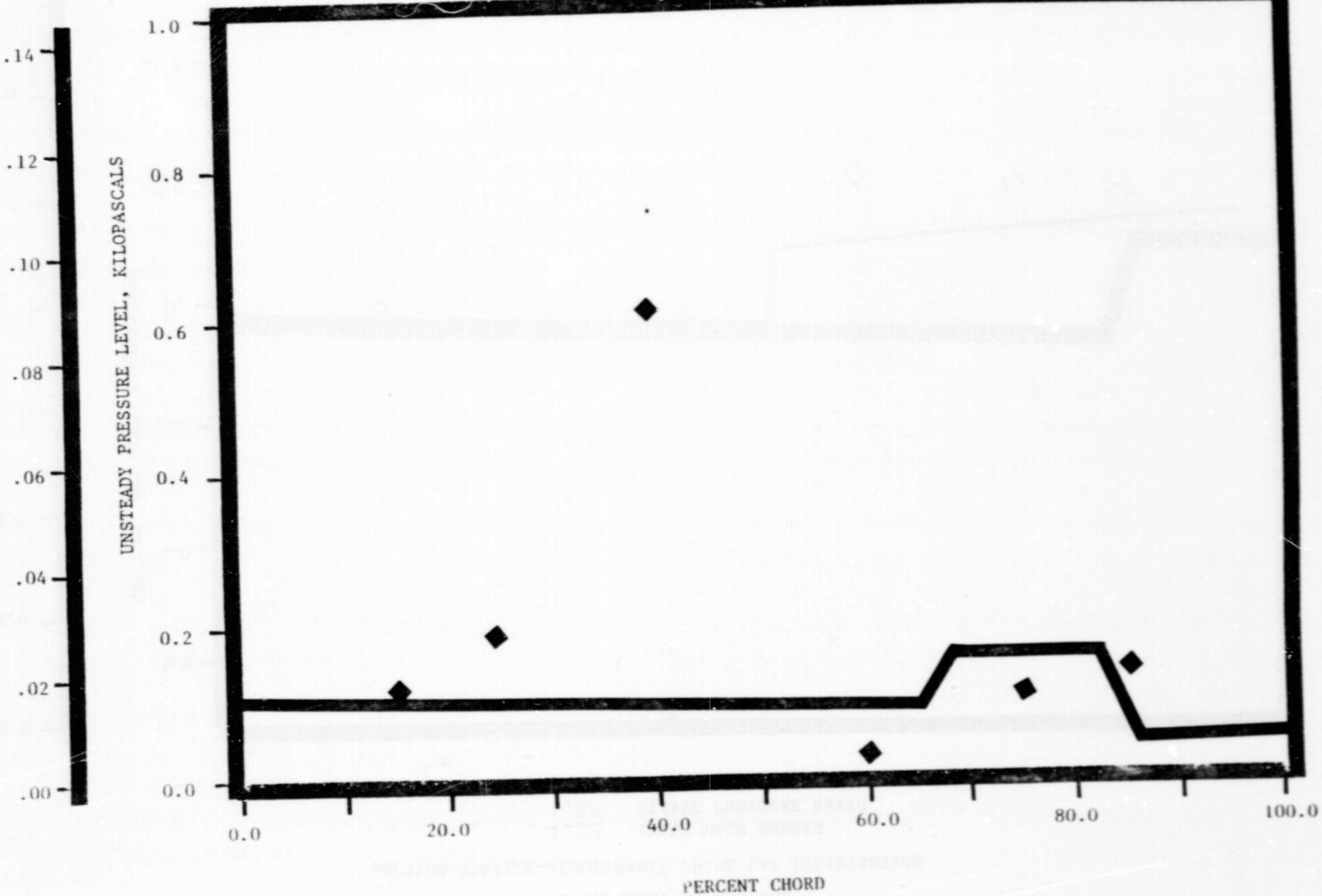

NASA II TRANSLATION CASCADE

SUCTION SURFACE AERODYNAMIC PHASE LAG DISTRIBUTION

1.32 INLET MACH NUMBER
1.68 STATIC PRESSURE RATIO
0.79 INTERBLADE PHASE ANGLE ,rad (45°)

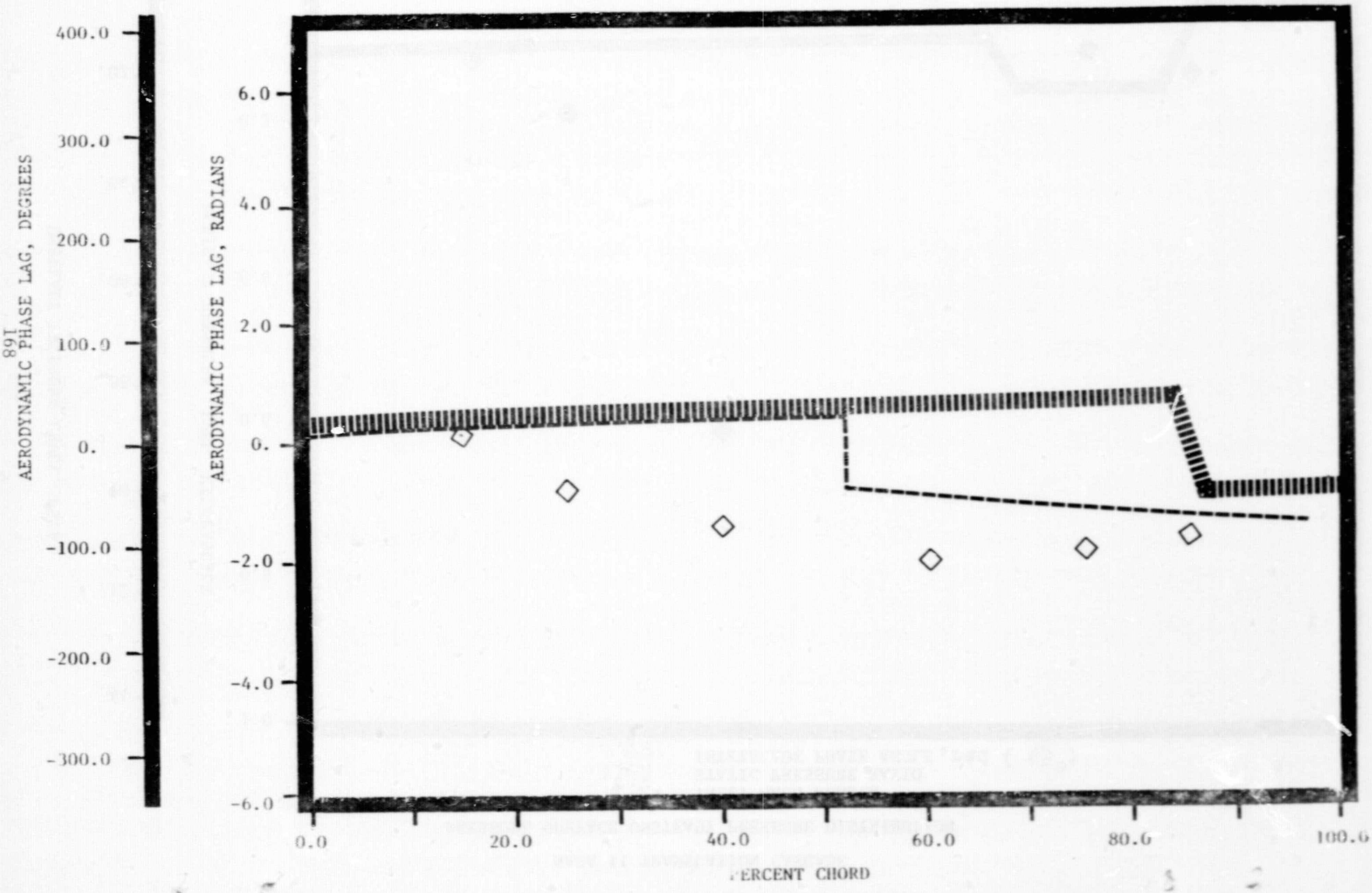

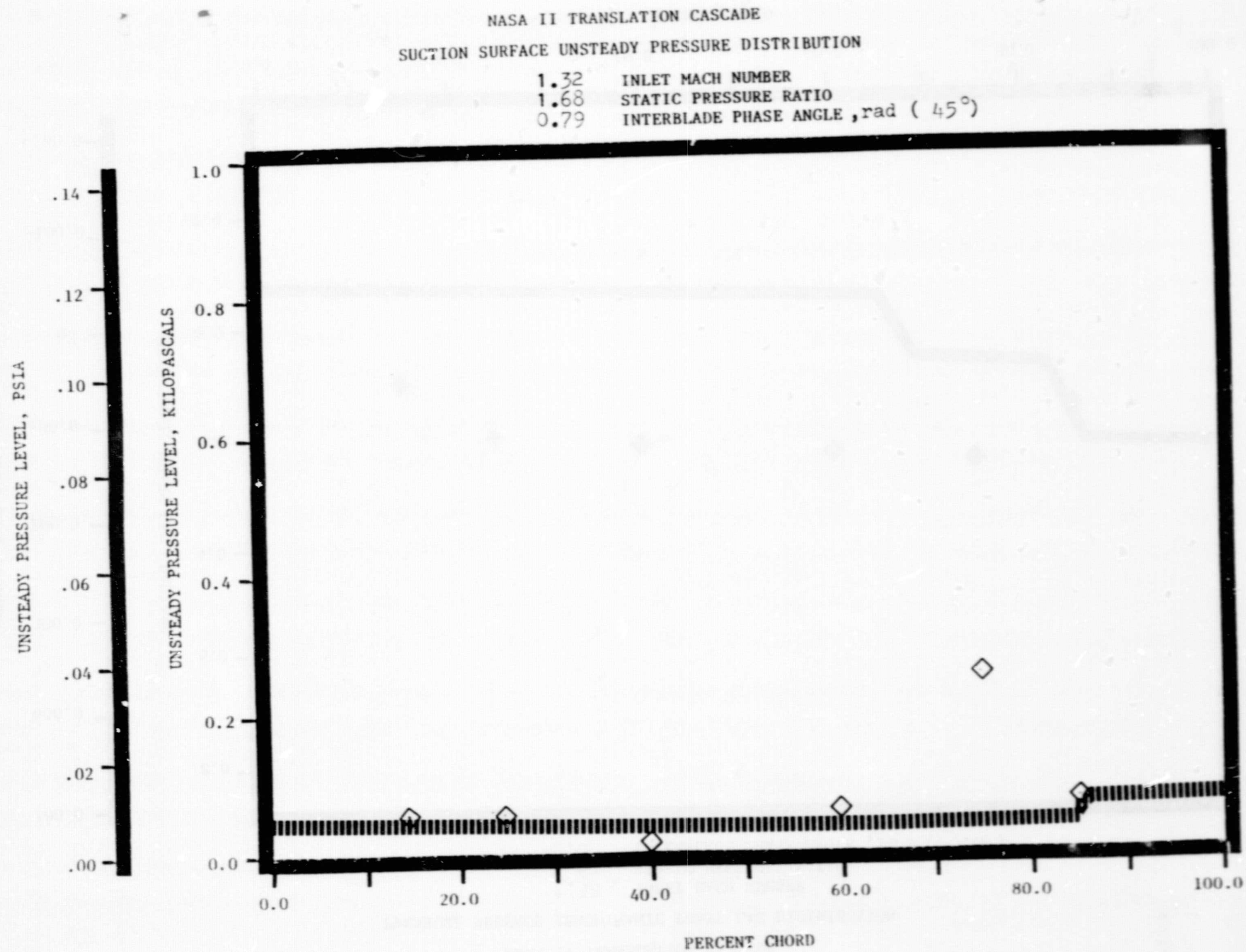
NASA II TRANSLATION CASCADE
SUCTION SURFACE UNSTEADY PRESSURE DISTRIBUTION
1.32 INLET MACH NUMBER
1.68 STATIC PRESSURE RATIO
0.79 INTERBLADE PHASE ANGLE ,rad (45°)
UNSTEADY PRESSURE LEVEL, PSIA
.14
.12
.10
.08
.06
.04
.02
.00
UNSTEADY PRESSURE LEVEL, KILOPASCALS
1.0
0.8
0.6
0.4
0.2
0.0
0.0
20.0
40.0
60.0
80.0
100.0
PERCENT CHORD

NASA II TRANSLATION CASCADE

PRESSURE SURFACE AERODYNAMIC PHASE LAG DISTRIBUTION

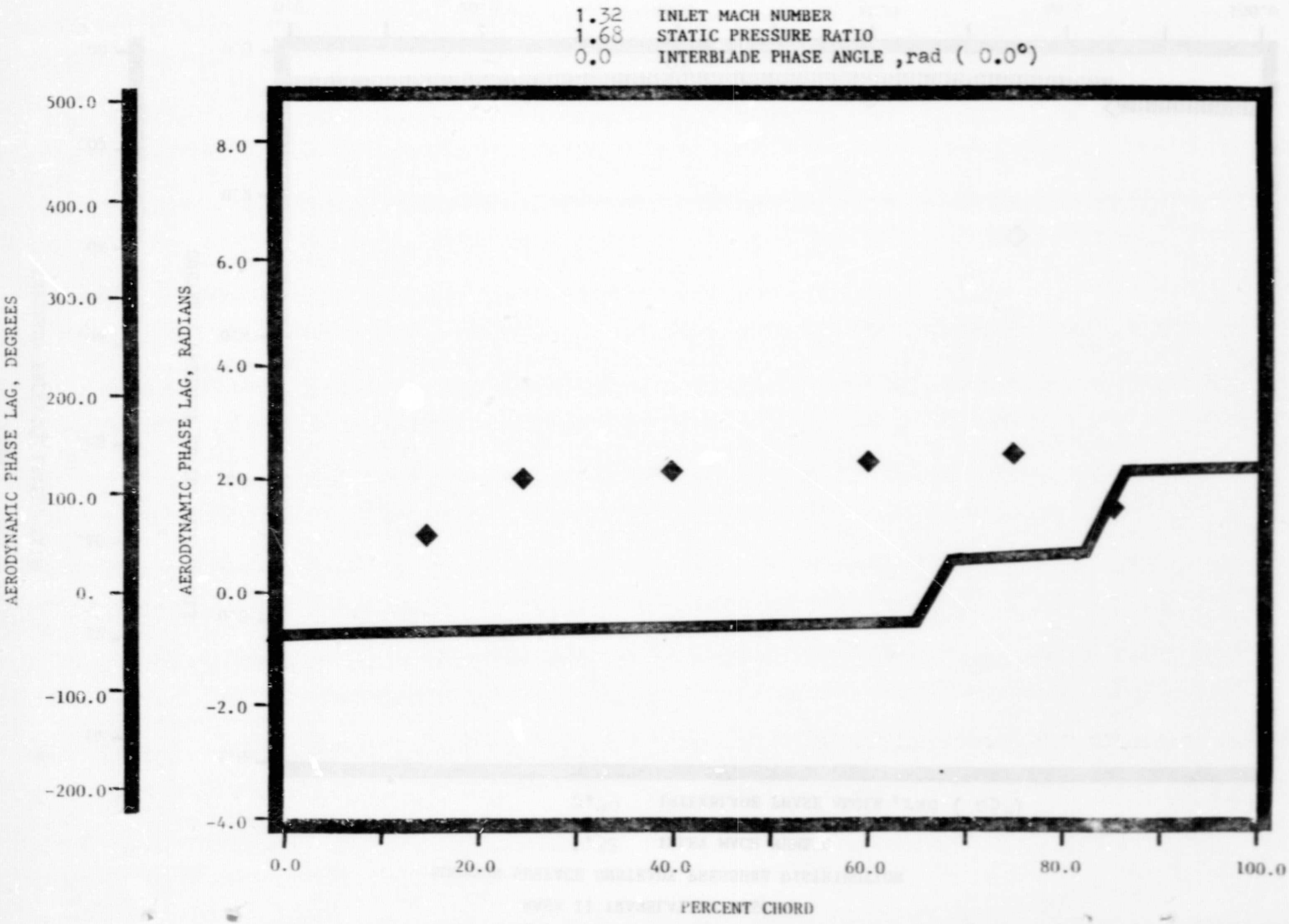

NASA II TRANSLATION CASCADE

PRESSURE SURFACE UNSTEADY PRESSURE DISTRIBUTION

1.32 INLET MACH NUMBER
1.68 STATIC PRESSURE RATIO
0.0 INTERBLADE PHASE ANGLE ,rad (0.0°)

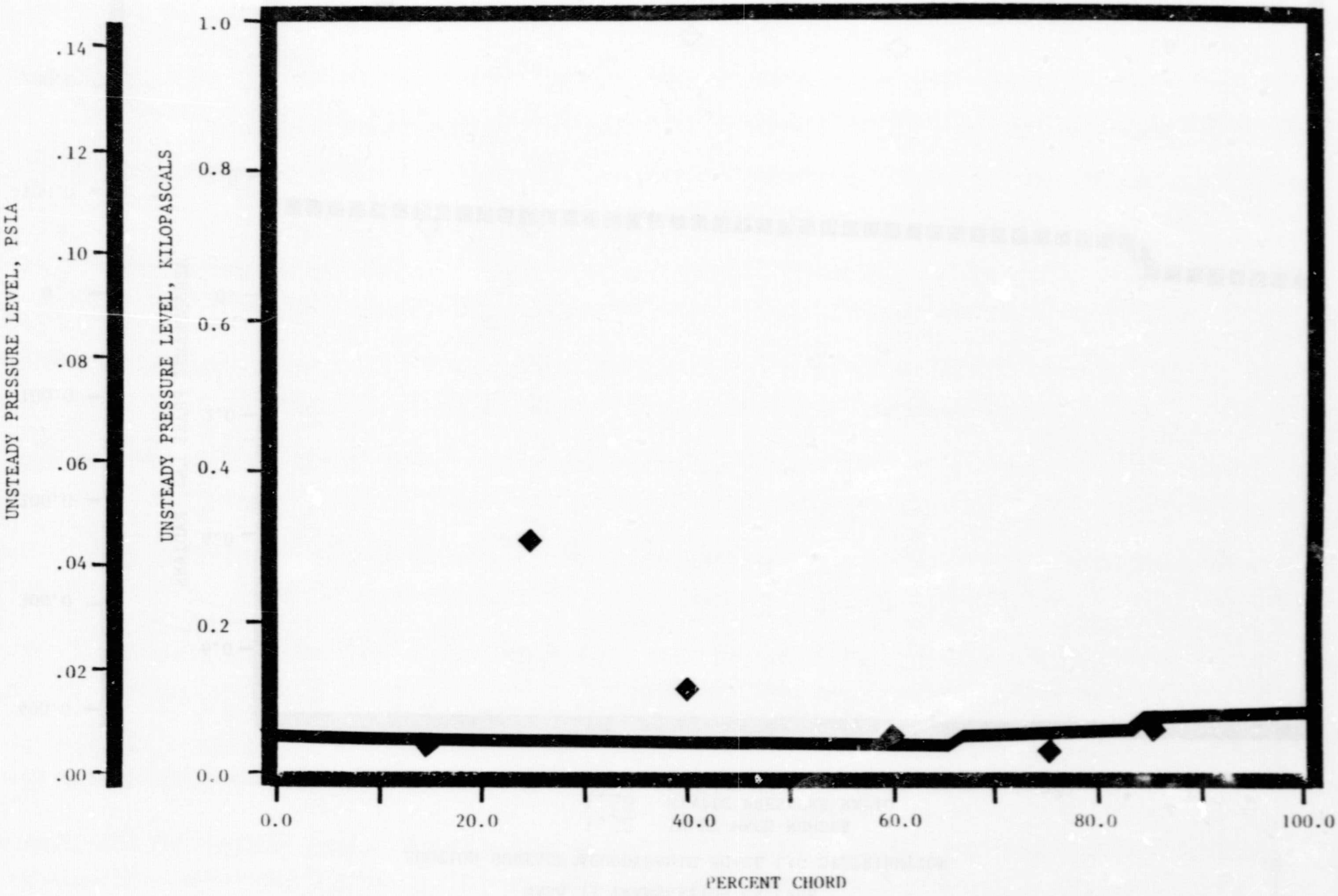

NASA II TRANSLATION CASCADE

SUCTION SURFACE AERODYNAMIC PHASE LAG DISTRIBUTION

1.32 INLET MACH NUMBER
1.68 STATIC PRESSURE RATIO
0.0 INTERBLADE PHASE ANGLE ,rad (0.0°)

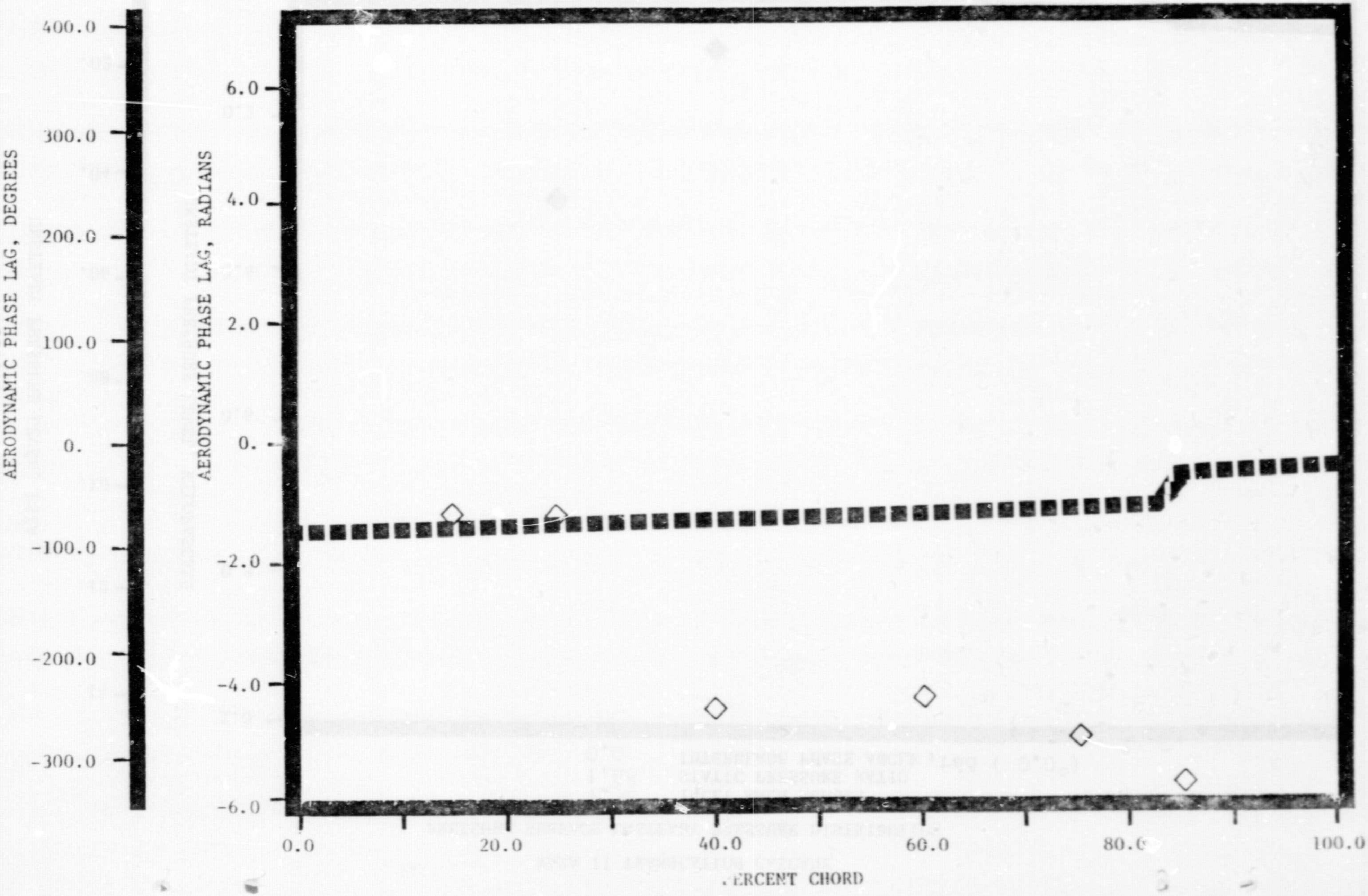

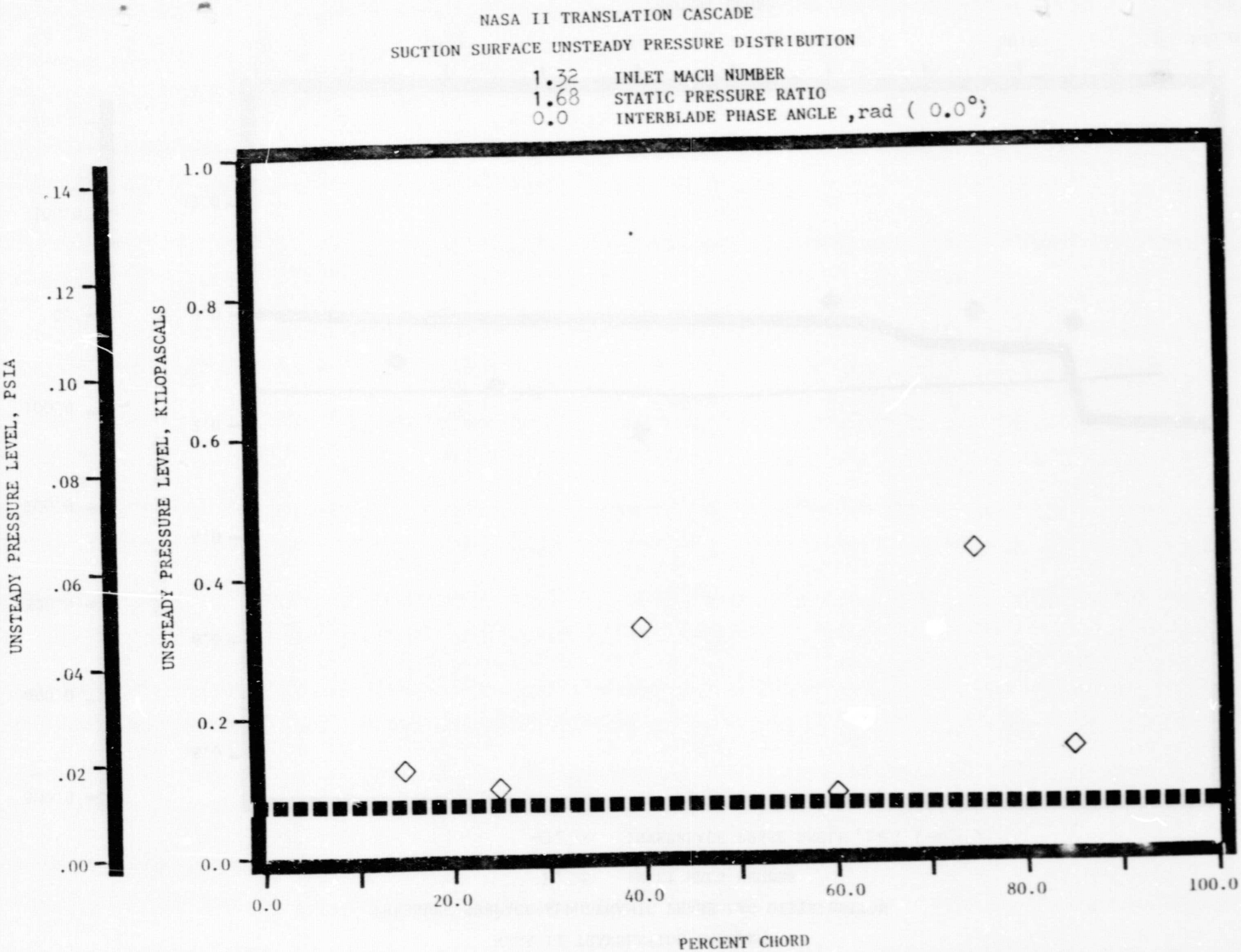
NASA II TRANSLATION CASCADE
SUCTION SURFACE UNSTEADY PRESSURE DISTRIBUTION
1.32 INLET MACH NUMBER
1.68 STATIC PRESSURE RATIO
0.0 INTERBLADE PHASE ANGLE ,rad (0.0°)
UNSTEADY PRESSURE LEVEL, PSIA
.14
.12
.10
.08
.06
.04
.02
.00
UNSTEADY PRESSURE LEVEL, KILOPASCALS
1.0
0.8
0.6
0.4
0.2
0.0
0.0
20.0
40.0
60.0
80.0
100.0
PERCENT CHORD

NASA II TRANSLATION CASCADE

PRESSURE SURFACE AERODYNAMIC PHASE LAG DISTRIBUTION

1.32 INLET MACH NUMBER
1.68 STATIC PRESSURE RATIO
-0.79 INTERBLADE PHASE ANGLE ,rad (-45°)

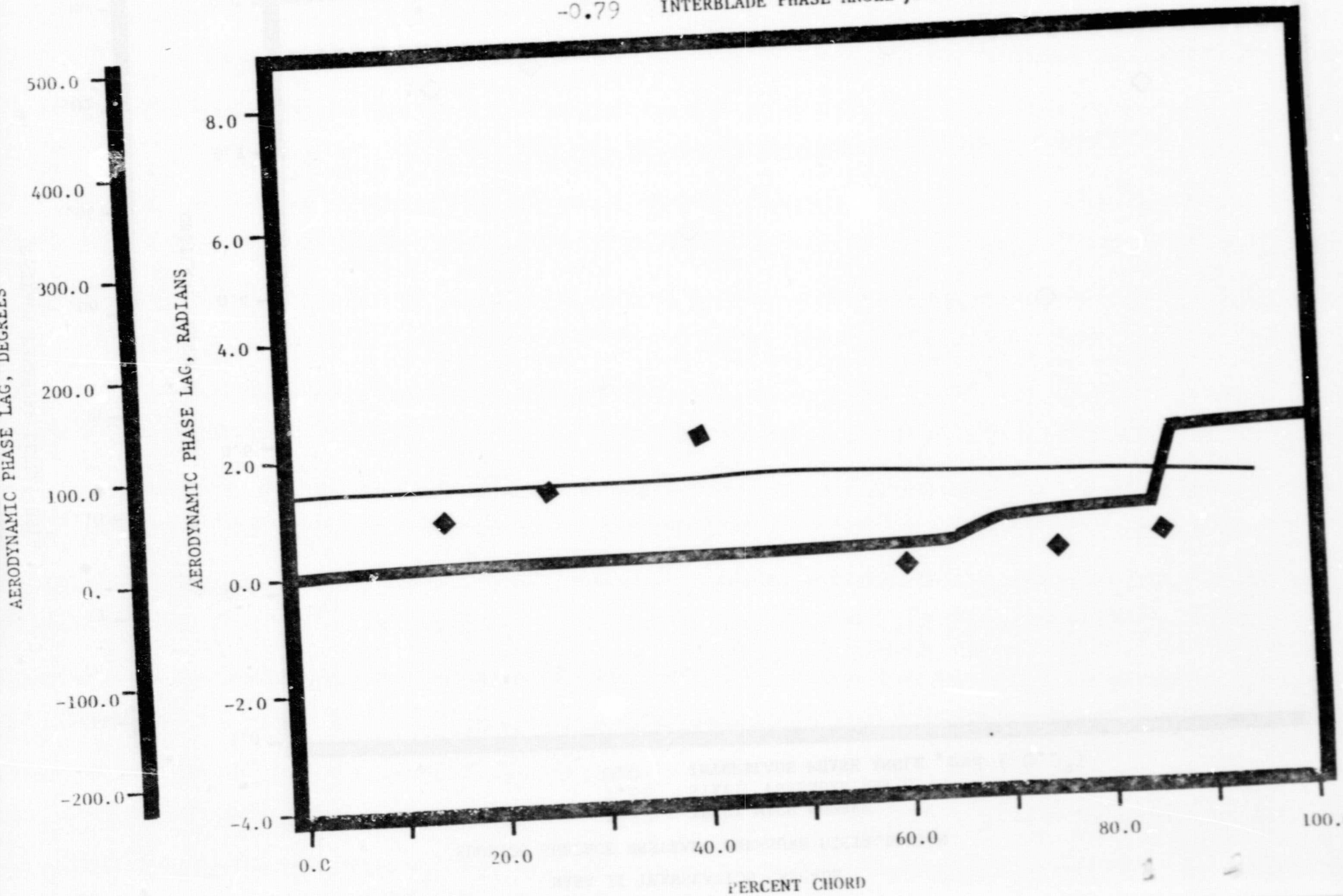

REFERENCES

1. Messenger, H. E. and Kennedy, E. E., "Two-Stage Fan Aerodynamic and Mechanical Design" (NASA CR-120859, January 1972.

2. Riffel, R. E., and Rothrock, M. D., "Experimental Determination of Unsteady Blade Element Aerodynamics in Cascades - Torsion Mode Cascade Final Report" NASA CR-159831, June 1980.

3. Caruthers, J. E. and Riffel, R. E., "Aerodynamic Analysis of a Supersonic Cascade Vibrating in a Complex Mode." Journal of Sound and Vibration, Vol 71, No. 2, July 22, 1980.

4. Garrick, J. E., and Rubinow, S. J., "Flutter and Oscillating Air Force Calculations for an Airfoil in Two-Dimensional Supersonic Flow." NACA Report 846, 1946.

5. Chalkley, H. G., "A Study of Supersonic Cascade Flutter." Aeronautical Engineers Thesis, Naval Post-graduate School, Monterey, California, June, 1972.

6. Verdon, J. M. and McCune, J. E., "The Unsteady Supersonic Cascade in Subsonic Axial Flow." AIAA Paper No. 75-22, presented at the AIAA 13th Aerospace Sciences Meeting, Pasadena, California, January 20-22, 1975.

7. Brix, C. W. and Platzer, M. F., "Theoretical Investigation of Supersonic Flow Past Oscillating Cascades with Subsonic Leading Edge Locus." AIAA Paper No. 74-14 presented at the AIAA 12th Aerospace Sciences Meeting, Washington, D. C., January 1974.

8. Caruthers, J. E., "Theoretical Analysis of Unsteady Supersonic Flow Through Harmonically Oscillating Turbofan Cascades." PhD thesis, Georgia Institute of Technology, June 1976 (to be published).

9. Goldstein, M. E., Braun, W. and Adamczyk, J. J., "Unsteady Flow in a Supersonic Cascade with Strong In-Passage Shocks. J. Fluid Mech., Vol 83, Part III, 1977